

**Investigating the Genetic Interaction of
dLRRK/LRRK2 with the Visual System and the
Stability of LRRK2 Protein in a *Drosophila*
model of Parkinson's Disease**

Khalid Jambi

PhD

University of York

Biology

May 2022

Abstract

The *G2019S* mutation within the kinase domain of *Leucine-rich repeat kinase 2* (*LRRK2*) is the most common reported and studied cause of familial Parkinson's Disease (PD). *LRRK2* has been associated with many cellular pathways, but its exact role is still to be elucidated. Using *Drosophila* as a model for PD, the role of the protein is examined.

In this project, we found that *dLRRK* loss-of-function (*dLRRK^{LOF}*) flies had an age-dependent visual deficit that was rescued with the expression of the native gene (*dLRRK*) in non-neuronal cells (fat body and pigment cells) bolstering the suggestion of protein's ability to transport cell-cell. Furthermore, placing mutations of different eye colour genes encoding proteins normally involved in vesicle trafficking in the *dLRRK^{LOF}* background caused a loss of viability in combination which suggests a role for *dLRRK* in regulating pigment granules specifically and in the lysosomal pathway in general.

In a gain-of-function approach, young flies expressing *LRRK2-G2019S* in dopaminergic (DA) neurons and pigment cells demonstrated an aberrant electroretinogram (ERG) indicating a failure in their ability to adapt to light. This was partially complemented by anatomical assessment where expressing *LRRK2-G2019S* in pigment cell caused flies to have larger deep pseudopupil (DPP) than the controls indicating defective eye function.

Finally, mutations in *LRRK2* are thought to potentially affect the stability of the protein in fly model as well as in cells. We used two kinase inhibitors (vitamin B₁₂ and MLI-2) with different mode of actions to test their effect on *LRRK2* stability. We showed that these two inhibitors might variably affect *LRRK2* stability dependent on the mutation on the protein.

Table of Contents

Abstract	2
Table of Contents.....	3
List of Tables.....	7
List of Figures	8
Acknowledgments	11
Declaration	12
List of Abbreviations	13
1 Introduction.....	17
1.1 Parkinson’s Disease (PD).....	17
1.1.1 Clinical manifestations.....	17
1.1.2 Neuropathology.....	18
1.1.3 Aetiology.....	21
1.1.4 Pathogenesis.....	25
1.1.5 Treatment	28
1.2 Leucine-rich repeat kinase 2 (LRRK2).....	29
1.2.1 LRRK2 structure and localisation.....	29
1.2.2 <i>LRRK2</i> Mutations.....	31
1.2.3 LRRK2 Interactors	32
1.2.4 LRRK2 and cell biological functions.....	33
1.2.4.1 Autophagy.....	33
1.2.4.2 Mitochondria.....	34
1.2.4.3 Endocytosis.....	35
1.2.4.4 LRRK2 function and Trans-Golgi network (TGN) and endoplasmic reticulum (ER).....	35
1.2.4.5 Microtubules and ribosomes.....	36
1.3 Modelling PD	37
1.3.1 Cellular models	38
1.3.2 Animal models	39
1.3.2.1 Toxin-treated models	40
1.3.2.2 Genetic models	41

1.4	<i>Drosophila</i> as a powerful model organism	43
1.4.1	The genetic toolbox of <i>Drosophila</i>	43
1.4.1.1	The Gal4/UAS system	44
1.4.1.2	Balancer chromosomes	46
1.4.2	<i>Drosophila</i> as a model for neurodegenerative disease	47
1.4.3	<i>Drosophila</i> models of PD	48
1.4.3.1	<i>LRRK2</i> <i>Drosophila</i> models of PD	49
1.5	Investigating PD through <i>Drosophila</i> eyes	51
1.5.1	The retina	51
1.5.2	Visual dysfunctions in PD	53
1.5.3	The structure of the <i>Drosophila</i> visual system	54
1.5.4	Similarities between the <i>Drosophila</i> and human visual systems	56
1.6	Aims	60
2	Materials and Methods	61
2.1	<i>Drosophila</i> husbandry and genetics	61
2.1.1	<i>Drosophila</i> stocks	61
2.1.2	<i>Drosophila</i> media	62
2.1.3	<i>Drosophila</i> anaesthesia	63
2.1.4	<i>Drosophila</i> crossing techniques	63
2.1.5	Recombination	64
2.2	Cell culture	65
2.2.1	Cell lines	65
2.2.2	Growth and maintenance of cells	66
2.2.3	Counting and plating of cells	67
2.3	Physiological and anatomical analyses	68
2.3.1	Flash Electroretinogram (fERG)	68
2.3.2	Deep Pseudopupil (DPP) and Pseudopupil Analysis (PPA)	69
2.4	Molecular Biology	70
2.4.1	Genomic DNA isolation	70
2.4.2	Polymerase Chain Reaction (PCR)	70
2.4.3	DNA agarose gel electrophoresis	71
2.5	Western blotting	72
2.5.1	Protein extraction	72
2.5.2	Quantification of protein concentration	73

2.5.3	Sodium Dodecyl Sulphate Polyacrylamide Gel Electrophoresis (SDS-PAGE)	73
2.5.4	Protein transfer to polyvinylidene fluoride (PVDF) membrane	74
2.5.5	Probing of PVDF membrane	74
2.6	Statistical analysis and bioinformatics	75
3	The effects of <i>dLRRK^{e03680}</i> on eye physiology and eye pigment	77
3.1	Introduction	77
3.1.1	<i>Drosophila LRRK (dLRRK)</i>	77
3.1.2	Vision and <i>dLRRK</i>	78
3.1.3	<i>Drosophila</i> eye pigments biosynthesis	80
3.2	Aims	83
3.3	Results	83
3.3.1	Investigating the ability of <i>dLRRK</i> to rescue the visual dysfunction in <i>dLRRK^{LOF}</i> old flies when expressed in non-neural tissues	83
3.3.1.1	A possible rescue of visual function in <i>dLRRK^{LOF}</i> flies when <i>dLRRK</i> is expressed in non-neuronal tissues	84
3.3.1.2	Does <i>dLRRK</i> leak to other tissues?	88
3.3.2	<i>dLRRK^{LOF}</i> interaction with eye pigments	91
3.3.2.1	The combination of <i>dLRRK^{LOF}</i> with <i>pr^J</i> showed no synthetic lethality.	91
3.3.2.2	The combination of <i>dLRRK^{LOF}</i> with <i>cn^{35k}</i> showed no synthetic lethality.	92
3.3.2.3	The effect of overexpressing of <i>se</i> , <i>sptr</i> , and <i>pu</i> in the DA neurons on visual function	93
3.4	Discussion	96
4	The effect of dopaminergic <i>LRRK2-G2019S</i> expression on eye adaptation to light	100
4.1	Introduction	100
4.2	Aim	102
4.3	Results	102
4.3.1	Investigating the effect of expressing <i>LRRK2-G2019S</i> in components of the visual circuit on eye adaptation using ERG	102
4.3.1.1	The effect of expressing <i>LRRK2-G2019S</i> in the photoreceptors	103
4.3.1.2	The effect of expressing <i>LRRK2-G2019S</i> in DA neurons	105
4.3.1.3	The effect on visual responses of expressing <i>LRRK2-G2019S</i> in pigment cells	107

4.3.2	Investigating the effect of expressing <i>LRRK2-G2019S</i> on eye adaptation using Deep Pseudo-Pupil (DPP) analysis	110
4.3.2.1	The effect of expressing <i>LRRK2-G2019S</i> in photoreceptors on DPP development	110
4.3.2.2	The effect on DPP of expressing <i>LRRK2-G2019S</i> in DA neurons.....	112
4.3.2.3	The effect on DPP of expressing <i>LRRK2-G2019S</i> in pigment cells.....	113
4.4	Discussion.....	115
5	Stability of LRRK2 Mutants Proteins <i>in vitro</i> and <i>in vivo</i>	118
5.1	Introduction	118
5.2	Aims	120
5.3	Results	120
5.3.1	<i>In vitro</i> evaluation of LRRK2 stability	121
5.3.1.1	No evident leak of expression was detected in the tested cell lines	121
5.3.1.2	Stability of LRRK2 protein <i>in vitro</i>	122
5.3.1.3	Kinase inhibitors effects on protein stability <i>in vitro</i>	124
5.3.2	<i>In vivo</i> evaluation of LRRK2 stability	128
5.3.2.1	Testing for leak of expression of LRRK2 in uninduced transgenic flies .	128
5.3.2.2	Stability of LRRK2 protein <i>in vivo</i>	129
5.3.2.3	Kinase inhibitors effects on protein stability <i>in vivo</i>	130
5.3.3	Examining LRRK2 stability via Rab10 and phosphorylated Rab10 expression.....	134
5.4	Discussion.....	134
6	General discussion and future works.....	138
6.1	Introduction	138
6.2	dLRRK/LRRK2 mode of action	138
6.3	LRRK2 and non-motor deficits in PD.....	140
6.4	LRRK2 stability and kinase inhibitors	141
6.5	Future works.....	142
6.6	Conclusion.....	143
	References.....	145

List of Tables

Table 1.1 List of monogenic PD	23
Table 2.1 Fly Stocks.....	61
Table 2.2. Primer sequences.....	71
Table 2.3. List of antibodies used in western blot.....	75

List of Figures

Figure 1.1 PD non-motor symptoms.....	18
Figure 1.2 PD neuropathology in the substantia nigra.....	20
Figure 1.3 Molecular mechanisms implicated in PD according to the genetic findings	24
Figure 1.4 Braak staging system of PD pathology.....	26
Figure 1.5 Multiple roles of mitochondria in Parkinson’s disease.....	27
Figure 1.6. LRRK2 structure, mutations, and interactors	30
Figure 1.7. The involvement of LRRK2 in different organelles and cellular mechanisms.	37
Figure 1.8. The Gal4/UAS system in <i>Drosophila</i>	45
Figure 1.9. The Gal4/UAS system (GeneSwitch) in <i>Drosophila</i>	46
Figure 1.10. An illustration of a balancer chromosome used in a crossing scheme	47
Figure 1.11. The structure of the eye and retina	53
Figure 1.12. <i>Drosophila</i> eye with a schematic structure of the ommatidium.	55
Figure 1.13. The anatomy of <i>Drosophila</i> visual system	56
Figure 1.14. Cajal’s drawing of fly and vertebrate visual systems	57
Figure 1.15. Similarities between vertebrate and fly visual systems	58
Figure 1.16 Phototransduction cascades in vertebrates and <i>Drosophila</i>	59
Figure 2.1 Selection criteria for <i>Drosophila</i> crossing.....	64
Figure 2.2. Recombination scheme in a <i>Drosophila</i> to allow the use of 2 desired elements on the same chromosome.....	65
Figure 2.3. Flp-In T-REx system mechanism	66
Figure 2.4. Haemocytometer gridlines.....	67
Figure 2.5. Recording the visual response of <i>Drosophila</i> using the flash ERG	69
Figure 2.6. Schematic of the microscope setup for PPA.....	70
Figure 2.7. PCR of Mutant <i>dLRRK^{e03680}</i> recombinants.....	72

Figure 3.1 Comparison of the domain structure of LRRK proteins in human and <i>Drosophila</i>	77
Figure 3.2 Age dependant loss of visual function in flies expressing human <i>LRRK2-G2019S</i> in DA neurons and <i>dLRRK^{e03680}</i> flies.	79
Figure 3.3 <i>dLRRK</i> expression in the lamina neurons, DA neurons or photoreceptors in <i>dLRRK^{LOF}</i> background rescues the age-dependant loss of visual function.....	80
Figure 3.4 An illustration of the pathways involved in the biosynthesis of pigment granules	83
Figure 3.5 A reduction in ERG amplitude in <i>dLRRK^{LOF}</i> old flies (21 days) compared to control.	84
Figure 3.6 Crossing summary of flies expressing <i>dLRRK</i> gene in non-neural tissues using Gal4/UAS system for the assessment of visual system rescue.....	85
Figure 3.7 <i>dLRRK</i> expression in the fat body or pigment cells in <i>dLRRK^{LOF}</i> background revealed a possible rescues of the age-dependent loss of visual function.....	88
Figure 3.8 A possible leak of dLRRK is detected in pigment cells Gal4 flies when only one component of the UAS/GAL4 system is expressed in <i>dLRRK^{LOF}</i> flies background	90
Figure 3.9 Homozygous or hetrozygous <i>pr^l</i> mutation is NOT synthetically lethal with homozygous <i>dLRRK^{LOF}</i> mutation	92
Figure 3.10 Homozygous or hetrozygous <i>cn^{35k}</i> mutation is NOT synthetically lethal with homozygous <i>dLRRK^{LOF}</i> mutation	93
Figure 3.11 Crossing summary of flies over-expressing <i>sptr</i> , <i>se</i> , and <i>pu</i> in DA neurons in <i>dLRRK^{LOF}</i> background.....	94
Figure 3.12 Over-expression of <i>sptr</i> , <i>se</i> , and <i>pu</i> had no effect on restoring normal ERG in old flies.....	96
Figure 4.1 An example of a recorded ERG for eye adaptation to light test.....	103
Figure 4.2 No changes in ERG amplitude is observed in flies expressing <i>LRRK2-G2019S</i> in the photoreceptors	104
Figure 4.3 A failure in adaptation is observed in ERG amplitude in young flies expressing <i>G2019S</i> in DA neurons indicated by the decline in ERG amplitude in light adapted condition	106

Figure 4.4 A failure in adaptation is observed in young flies expressing <i>LRRK2-G2019S</i> in pigment cells indicated by the decline in ERG amplitude in light adapted condition	108
Figure 4.5 A significant difference in ERG amplitude is observed when <i>LRRK2-G2019S</i> is expressed in DA neurons and pigment cells in 3 days old flies	109
Figure 4.6 A larger DPP is formed in flies expressing <i>LRRK2-G2019S</i> in photoreceptors	111
Figure 4.7 Inconclusive results for DPP formation in flies expressing <i>LRRK2-G2019S</i> in DA neurons	112
Figure 4.8 No degeneration of ommatidia observed in flies expressing <i>LRRK2-G2019S</i> in DA neurons	113
Figure 4.9 A larger DPP formed in young flies expressing <i>LRRK2-G2019S</i> in pigment cells	114
Figure 4.10 No degeneration of ommatidia observed in flies expressing <i>LRRK2-G2019S</i> in pigment cells	115
Figure 5.1 The timeline of LRRK2 stability experiment	121
Figure 5.2 In the absence of inducing agent, no LRRK2 protein is expressed by the FLP-In T-REx system	121
Figure 5.3 LRRK-R1441C appears to be potentially the least stable PD associated LRRK2 protein variant when expressed in cell culture	123
Figure 5.4 Vitamin B ₁₂ appears to affect LRRK2-D2017A protein stability	125
Figure 5.5 MLi-2 appears to have no effect on LRRK2 stability	127
Figure 5.6 No <i>LRRK2</i> expression from transgenes is observed in uninduced animals indicating absence of expression except for the <i>LRRK2-I2020T</i> transgene.....	128
Figure 5.7 R1441C is potentially the least stable of LRRK2 protein variants.....	130
Figure 5.8 Vitamin B ₁₂ might affect LRRK2 stability of LRRK2-I1122V	132
Figure 5.9 MLi-2 might effect LRRK2 stability for LRRK2-WT and LRRK2-I1122V	134

Acknowledgments

قال صلى الله عليه وسلم: "لا يشكرُ الله من لا يشكرُ الناس"

“He who does not thank people does not thank Allah”

I would like to express my deepest appreciation to my supervisor Dr. Chris Elliott for everything that he has done for me throughout my PhD journey. Thank you for your invaluable advice, kindness, continuous support, patience, and keeping your door open all the time (literally & figuratively). I would also like to thank my second supervisor Dr. Sean Sweeney who was always there for guidance and advice. Christmas’s dinner at your house was always a highlight.

My appreciation goes to D1 corridor and all members of both the Elliott and Sweeney labs, past and present. Thank you to Alison, Laura, Dr. Laura Fort Aznar (my coffee buddy), Dr. Chris Ugbo, Dr. Ryan West, Dr. Nathan Garnham, Egle, Katy, Adam, and Dr. Jack Munns for keeping the fly lab tidy and giving me a hand when needed. I would also like to thank my TAP members, Dr. Sangeeta Chawla, Dr. Gareth Evans, and Dr. Miles Whittington for their constructive advice and discussions during our meetings. Thank you to Dr. Dario Alessi lab for providing me with the cell lines and Dr. Carlo Breda from the University of Leicester for teaching me how to perform pseudopupil analysis.

I am grateful to my sponsor, Taif University, and their representative in the UK, the Saudi Arabian Cultural Bureau in the UK (UKSACB), for all their support. This scholarship was indeed a life changing experience.

Thank you to my friends back home and especially here in the UK. Thank you to Adil, Sultan, Mohammad, Ahmad, Abdullah, Abdulelah, Raed and the people I have met via the Saudi student club in York for accompanying me over the past few years and providing me with an escape outside the PhD.

I am very grateful to my family, my mother, Rusmati, my brothers, Ahmad and Ihsan, my sisters, Amnah, Amani, Isra and Ikram. Thank you for your support and encouragement throughout the years. Lastly, I would like to dedicate this work to the memory of my father, Muhammad. Despite not completing his primary education, he had always put our education as a priority. I know he would be very proud.

Declaration

I hereby declare that, unless explicitly stated, all of the work presented within this thesis is a presentation of original work and I am the sole author. This work has not previously been presented for an award at this, or any other, University. All sources are acknowledged as References.

List of Abbreviations

♀	Female
♂	Male
3-HK	3-hydroxykynurenine
4E-BP	4E-binding protein
6-OHDA	6-hydroxydopamine
6-PTP	6- pyruvoyltetrahydropterin
a.u.	arbitrary unit
AC	Alternating Current
AD	Alzheimer Disease
ALS	Amyotrophic Lateral Sclerosis
ANK	ankyrin repeat
ANOVA	Analysis Of Variance
AP3	Adaptor Protein 3
ApoE	Apolipoprotein E
ARM	Armadillo-like Repeat
ATP	Adenosine Triphosphate
BBB	Blood Brain Barrier
BCA	Bicinchoninic Acid
BDSC	Bloomington Drosophila Stock Center
BH4	Tetrahydrobiopterin
BLOC	Biogenesis of Lysosome-related Organelles Complex
BMP	Bone Morphogenetic protein
BSA	Bovine Serum Albumin
<i>bw</i>	<i>brown</i>
C	Celsius
CD	Crohn's Disease
CHIP	C-terminus of Hsp70-Interacting Protein
CK1	Casein Kinase 1
<i>cm</i>	<i>carmine</i>
CMA	Chaperone-Mediated Autophagy
<i>cn</i>	<i>cinnabar</i>
CNS	Central Nervous System
COR	C-terminal of Roc
CRISPR	Clustered Regularly Interspaced Short Palindromic Repeats
CSF	Cerebrospinal Fluid
DA	Dopaminergic
DBS	Deep Brain Stimulation
DC	Direct Current
dH ₂ O	Distilled Water
<i>dLRRK</i>	<i>drosophila</i> Leucine Rich Repeat Kinase
DMEM	Dulbecco's Modified Eagle Media
DNA	Deoxyribonucleic Acid

Doxy	Doxycycline
DPP	Deep Pseudopupil
EDTA	Ethylenediaminetetraacetic Acid
EMS	Ethyl Methane Sulphate
ER	Endoplasmic Reticulum
ERES	Endoplasmic Reticulum Exit Sites
ERG	Electroretinogram
EtOH	Ethanol
FBS	Foetal Bovine Serum
fERG	Flash Electroretinogram
<i>g</i>	<i>garnet</i>
GAPDH	Glyceraldehyde 3-Phosphate Dehydrogenase
GBA	Glucosylceramidase beta
Gcase	Glucocerebrosidase
GCL	Ganglion Cell Layer
GFP	Green Fluorescent Protein
GTP	Guanosine Triphosphate
GTPCH I	GTP Cyclohydrolase I
H2-NTP	7,8-dihydroneopterin triphosphate
H ₂ O	Water
H4	Human Neuroglioma
HD	Huntington Disease
HD CAV-2	Helper-Dependent Canine Adenovirus Type 2
HEK 293	Human Embryonic Kidney 293
<i>hLRRK1</i>	human Leucine Rich Repeat Kinase 1
<i>hLRRK2</i>	human Leucine Rich Repeat Kinase 2
HRP	Horseradish Peroxide
hMOs	human Midbrain Organoids
IBD	Inflammatory bowel disease
IKK	Ikappa B Kinase
INL	Inner Nuclear Layer
IPL	Inner Plexiform Layer
iPSCs	induced Pluripotent Stem Cells
K	Lysine
kDa	kilo Dalton
LBs	Lew Bodies
LED	Light Emitting Diode
L-DOPA	Levodopa
LOF	Loss Of Function
LRO	Lysosome-Related Organelle
LRR	Leucine Rich Repeat
LUHMES	Lund Human Mesencephalic
MAO-B	Monoamine Oxidase B
MLi-2	cis-2,6-dimethyl-4-6-5-1-methylcyclopropoxy
MPP+	1-methyl-4-phenylpyridinium

MPTP	1-methyl-4-phenyl-1,2,3,6-tetrahydropyridine
ms	milliseconds
mV	millivolt
MW	Molecular Weight
NHP	Non-Human Primate
NM	Neuromelanin
NSAIDs	Non-Steroidal Anti-Inflammatory Drugs
NSF	N-ethylmaleimide Sensitive Fusion
OMIM	Online Mendelian Inheritance in Man
ONL	Outer Nuclear Layer
OPL	Outer Plexiform Layer
<i>or</i>	<i>orange</i>
PBS	Phosphate Buffered Saline
PCR	Polymerase Chain Reaction
PD	Parkinson's Disease
PDA	Pyrimidodiazepine
<i>PINK1</i>	<i>PTEN Induced Kinase 1</i>
PKA	Protein Kinase A
PPA	Pseudopupil Analysis
<i>pr</i>	<i>purple</i>
PRDX-3	Peroxiredoxin-3
<i>pu</i>	<i>punch</i>
PVDF	Polyvinylidene Fluoride
R	Photoreceptors
<i>rb</i>	<i>ruby</i>
RGCs	Retina Ganglion Cells
Rh	Rhodopsin
RIPA	Radioimmunoprecipitation Assay
RNA	Ribonucleic Acid
RNAi	RNA interference
ROC	Ras of Complex Proteins
ROS	Reactive Oxygen Species
RPE	Retinal Pigment Epithelium
RT	Room Temperature
RU486	Mifepristone (Roussel-Uclaf 486)
<i>s</i>	<i>scarlet</i>
SDS-PAGE	Sodium Dodecyl Sulfate-Polyacrylamide Gel Electrophoresis
<i>se</i>	<i>sepia</i>
SEM	Standard Error of the Mean
<i>SNCA</i>	<i>α-synuclein</i>
<i>SNpc</i>	Substantia Nigra pars compacta
<i>sptr</i>	<i>sepiapterin reductase</i>
STN	Subthalamic Nucleus
$t_{1/2}$	half-life

TAE	Tris-Acetate-EDTA
TBS-T	Tris Buffered Saline-Tween
TC	Tetracycline
TGFbeta	Transforming Growth Factor beta
TGN	Trans-Golgi Network
TH	Tyrosine Hydroxylase
T _m	Melting Temperature
TRIM1	Tripartite Motif Family 1
UAS	Upstream Activated Sequence
UCA	Ursocholic Acid
UDCA	Ursodeoxycholic Acid
<i>v</i>	<i>vermilion</i>
<i>w</i>	<i>white</i>
WB	Western Blot
WT	Wild Type

1 Introduction

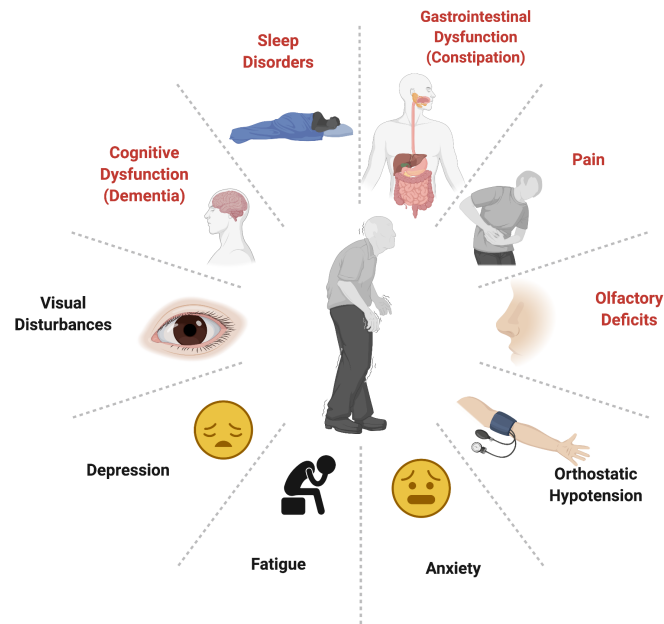
1.1 Parkinson's Disease (PD)

PD was first described by James Parkinson, an English physician, in his 66-page monograph "*An Essay on the Shaking Palsy*" published in 1817. The disease was later named after him in respect of his pioneering work by Jean-Martin Charcot who added more details to Parkinson's observations and established it as a neurological disorder distinctive from palsy or paralysis (Goetz, 1986).

PD is the second most common neurodegenerative disorder after Alzheimer's disease (AD). It affects around 145,000 people in the UK (Parkinson'sUK, 2018) and around 6 million globally (Dorsey *et al.*, 2018). Age is the main risk factor and disease prevalence increases by up to 4% in people aged 60 and older. Males are more prone to develop PD than females with no clear explanation; however, some reports suggest a neuroprotective effect for oestrogen (de Lau and Breteler, 2006).

1.1.1 Clinical manifestations

PD is still being diagnosed by the subject manifesting what is known as classical motor features that were defined over 200 years ago. These are bradykinesia (slowing of movement), resting tremor and rigidity. The first symptom is present in all patients while the latter two are present in the majority. Other features might include postural reflex disturbances and postural instability (Obeso *et al.*, 2017). Although PD is considered a motor disorder, surprisingly, almost all patients report at least one non-motor symptoms (e.g., visual and/or olfactory dysfunction) and currently these symptoms contribute toward the certainty of the diagnosis (Kim *et al.*, 2013b) (Figure 1.1). In theory, these symptoms can help in predicting the probability of an individual developing PD because some of them (e.g., alterations in olfactory acuity) appear years before the manifestation of the motor symptoms and such symptoms can help as well in the possibility of discovering biomarkers for PD. However, the difficulty is in distinguishing PD-related symptoms from normal individuals that have them as a normal part of aging (Krishnan *et al.*, 2011). The range of reported non-motor symptoms vary from as high as 90% such as those observed with sleep disorders, constipations and olfactory deficits to as low as 20% - 40% in depression, anxiety and visual disturbances (Pfeiffer, 2016).



reported in over 70% of cases

Figure 1.1 PD non-motor symptoms

Some of the non-motor symptoms reported in PD patients with the red symptoms indicating higher incidence than others. Data obtained from (Davidsdottir *et al.*, 2005, Fasano *et al.*, 2015, Pfeiffer, 2016).

1.1.2 Neuropathology

Underlying the motor symptoms of PD is a progressive selective moderate to severe loss of dopaminergic (DA) pigmented neurons in the substantia nigra pars compacta (*SNpc*) in the midbrain region. The substantia nigra connects to the striatum, which is part of the basal ganglia and includes the caudate and putamen. In doing so, they establish the nigrostriatal dopamine pathway, which is hypothesized to be important in movement facilitation. Moreover, the substantia nigra performs activities other than motor control. It is also thought to be involved in a variety of other activities and behaviours, such as learning, drug addiction, and emotion (Kandel *et al.*, 2014). The cause of this loss is still under investigation but it is the most consistent neuropathological observation found in all individuals diagnosed clinically with PD and can be examined clearly macroscopically or microscopically post mortem. Interestingly, the ventral tegmental region (VTA), where the cell bodies of the mesolimbic DA neurons are located next to the *SNpc*, is significantly less impacted in PD (Uhl *et al.*,

1985). Another diagnostic feature reported in PD, though with less frequency than neuronal degeneration, is the presence of neuronal inclusions called Lewy bodies (LBs). These consists of misfolded protein aggregates with α -synuclein making up the majority of the aggregate. The case for LBs as a major cellular pathology in PD is a little controversial. On one hand, (Braak *et al.*, 2003) has developed a staging method for PD progression based on the spread of LB lesions in different parts of the brain and this is very helpful in diagnosis. On the other hand, LB is not specific for PD because it can be seen in other neurodegenerative disorders and normal individuals. Interestingly, the majority of individuals with Lewy pathologies in their brains are Alzheimer's patients, where up to 60% have these inclusions (Dickson *et al.*, 2009, Halliday *et al.*, 2011). (Figure 1.2) illustrates the difference in DA neurons loss in *SNpc* in healthy and PD patients. Nonetheless, mis-sense mutations in α -synuclein that pre-dispose the protein to aggregation, or mutations that increase the concentration of α -synuclein via gene duplication or triplication cause PD (reviewed in (Waxman and Giasson, 2009)).

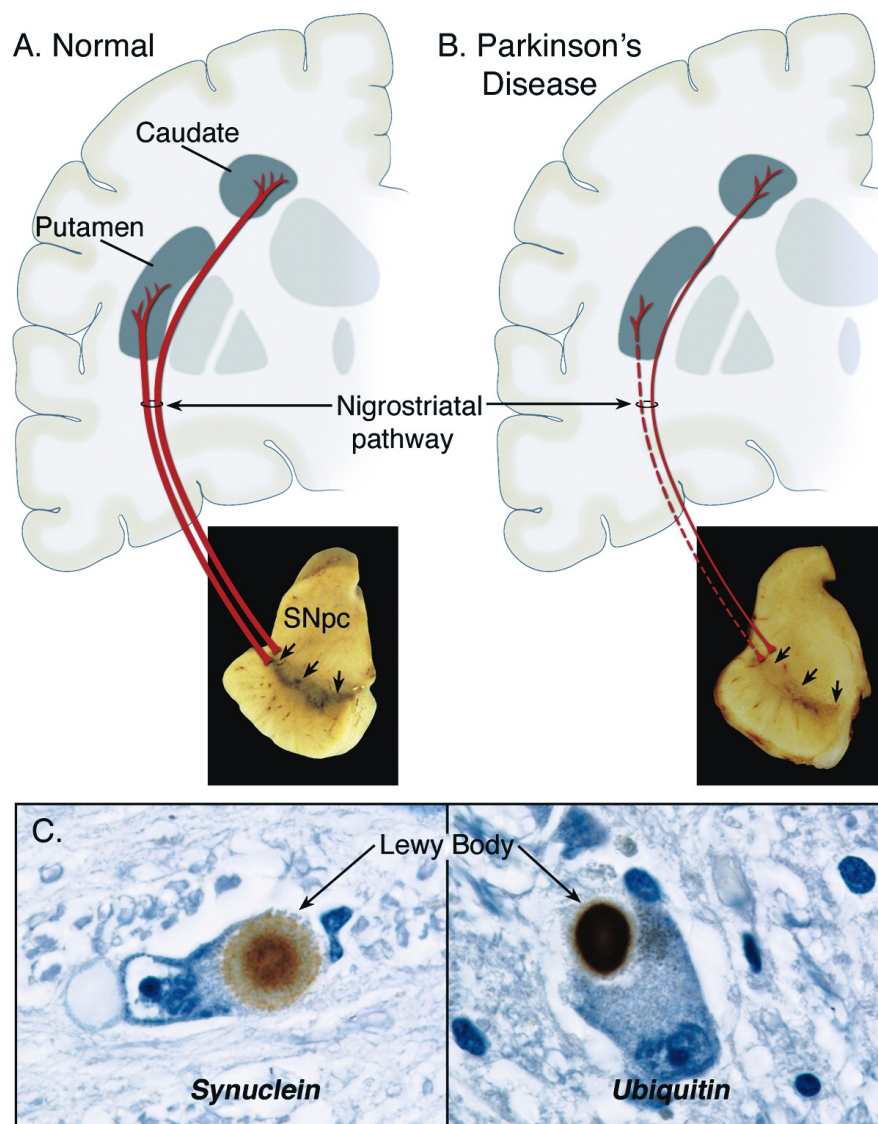


Figure 1.2 PD neuropathology in the substantia nigra

Schematic representation of a normal nigrostriatal pathway (A) and a PD one (B). The substantia nigra pars compacta (*SNpc*) contain DA neurons that extend to the basal ganglia and synapse in the striatum i.e., putamen and caudate nucleus. Transverse brain sections indicate that the *SNpc* is normally pigmented in control brains while the loss of the dark-brown pigment neuromelanin is seen in PD brains. (C) Immunohistochemical labelling of midbrain dopaminergic neurons for α -synuclein and ubiquitin, identifying Lewy bodies. Taken from (Dauer and Przedborski, 2003).

An important question that the PD community is still looking for an answer to is why DA neurons, particularly in the *SNpc*, are more prone to insult than other neurons in PD? One hypothesis suggests that their anatomy could be the reason. A lengthy and heavily branched unmyelinated axon with an unusual number of transmitter release sites distinguishes DA neurons in the *SNpc*. In rodents, *SNpc* DA neurons contain axons that branch abundantly in the striatum and up to 200 000 vesicular release sites (Matsuda *et*

al., 2009). This unique morphology put them at a disadvantage in that they simply have “too many mouths to feed” and thus making them especially vulnerable to stressors of any sort, including environmental and genetic factors (Bolam and Pissadaki, 2012). For example, mitochondrial oxidant stress, one of the potential driver of neurodegeneration, is increased in the axon of *SNpc* DA neurons and this stress is alleviated by reducing the size of the axonal arborization (Pacelli *et al.*, 2015). In addition, α -synuclein is primarily a synaptic protein, the extraordinarily extensive axonal arborization of *SNpc* DA neurons is extremely likely to increase its expression, increasing the risk of α -synuclein aggregation and incidence of disease such as PD (Zharikov *et al.*, 2015). However, some additional factors may be at play as not all neurons with long, branching axons are sensitive in PD, such as striatal cholinergic interneurons (Zhou *et al.*, 2002). Another potential cause of the selective degeneration of *SNpc* DA neurons might be the surrounding environment around their cell bodies. The substantia nigra neuropil, which is made up of axon projections from the striatum and globus pallidus, stains highly for calbindin D_{28K}, and most dopaminergic cell bodies are found inside this calbindin-rich neuropil. However, in PD, vulnerable neurons tend to be in calbindin-poor portions of the substantia nigra (Dauer and Przedborski, 2003). Other suggested cause of this selectivity might include dopamine toxicity, iron content, and autonomus pacemaking (Giguère *et al.*, 2018).

1.1.3 Aetiology

PD is a complex disorder with less than 10% of cases attributed to hereditary origin while the majority of cases are sporadic (Thomas and Beal, 2007). Although aging could be the greatest risk to eventually developing PD, at present, the evidence supports an interplay of environmental and genetic factors in disease development. Many environmental and genetic factors have been linked to PD since the accidental discovery of a PD-like illness caused by 1-methyl-4-phenyl-1,2,3,6-tetrahydropyridine (MPTP) in 1983 (Langston *et al.*, 1983) and the discovery of the first gene causing a familial form of PD which is *α -synuclein (SNCA)* in 1997 (Polymeropoulos *et al.*, 1997). MPTP itself is not toxic but when it enters the brain it is converted into 1-methyl-4-phenylpyridinium (MPP⁺) which is taken up by the DA neurons. In the DA neurons, MPP⁺ is toxically concentrated in the mitochondria which leads to cell death, eventually (Langston, 2017). Exposure to pesticides such as paraquat and rotenone have been reported to increase PD risk. This is not surprising since good animal models were produced using paraquat and rotenone but this increased risk has not been reported in all studies. Additionally, head

injury (especially in those with repeated injury) and those involved in farming and living in rural areas which might increase the likelihood of pesticide exposure have been found to have an increased PD risk. Interestingly, drinking coffee and alcohol and cigarette smoking reduce the risk of PD. This could be due to the presence of caffeine in coffee and nicotine in cigarette which were found to be neuroprotective in animal models (Goldman, 2014, Hernán *et al.*, 2002, Noyce *et al.*, 2012).

Since the discovery of the first gene associated with PD i.e., *SNCA*, more genes and loci have been discovered and associated with PD. They have been designated with the names PARK genes and were numbered in chronological order of discovery. For example, *SNCA* is called PARK1; however, this naming scheme is a bit misleading because PARK4 refers to *SNCA* as well but with different type of mutation. Furthermore, some of the PARK genes have an unconfirmed link to PD like PARK2, 5, 11, 13, 18, 21. Hence, the Movement disorder Society Task Force for the Nomenclature Genetic Movement Disorders have recommended a new naming scheme based on clinical grounds into i) classical PD, ii) early-onset PD with similarity to classical PD and iii) atypical parkinsonism (Marras *et al.*, 2016) to alleviate some of the confusion that might rise due the old system (Table 1.1).

Table 1.1 List of monogenic PD causes

	Old Name	New Name	Inheritance	OMIM*	Clinical clues
Classical parkinsonism	PARK1 & 4	PARK- <i>SNCA</i>	Autosomal Dominant	168601	Missense mutations cause classical parkinsonism. Duplication or triplication of this gene cause early onset parkinsonism with prominent dementia.
	PARK8	PARK- <i>LRRK2</i>		607060	Clinically typical PD
	PARK17	PARK- <i>VPS35</i>		614203	Clinically typical PD
Early onset parkinsonism	PARK2	PARK- <i>PARKIN</i>	Autosomal Recessive	600116	Often presents with dystonia, often in a leg.
	PARK6	PARKI- <i>PINK1</i>		605909	Psychiatric features common.
	PARK7	PARK- <i>DJI</i>		606324	
Atypical Parkinsonism	PARK9	PARK- <i>ATP13A2</i>		606693	Kufor-Rakeb syndrome with parkinsonism and dystonia.
	PARK14	PARK- <i>PLA2G6</i>		612953	<i>PLA2G6</i> -associated neurodegeneration (PLAN): dystonia, parkinsonism, cognitive decline, pyramidal signs, psychiatric symptoms (adult phenotype), ataxia (childhood phenotype)
	PARK15	PARK- <i>FBXO7</i>		260300	Early onset parkinsonism with pyramidal signs.
	PARK19	PARK- <i>DNAJC6</i>		615528	Occasional mental retardation and seizures.
	PARK20	PARK- <i>SYNJ1</i>		615530	May have seizures, cognitive decline, abnormal eye movements, and dystonia.

Adapted from (Marras *et al.*, 2016). *Online Mendelian Inheritance in Man

Genome-wide association studies (GWAS) have detected risk genes for PD, demonstrating that monogenic and sporadic PD are not distinct entities, and that many genes may cooperate to influence downstream shared targets. Variation in the glucocerebrosidase gene (*GBA1*) is the prototypic genetic risk factor for PD. The gene was originally linked to autosomal recessive Gaucher's disease, a lysosomal storage disorder. This was discovered because family members of Gaucher's disease patients had an elevated risk of PD, and many were found to be heterozygous *GBA1* variant carriers (Halperin *et al.*, 2006, Tayebi *et al.*, 2001). Adaptive immune system genes, mitochondrial genes, and genes involved in dopamine metabolism are among the other routes for PD that have been discovered by genetic study. Five genes make up the

PARK16 locus, but RAB7L1 has received the most attention due to its expression in the brain and PD susceptibility. It has been demonstrated that RAB7L1 interacts with LRRK2 and VPS35, and it appears to be involved in endosomal-lysosomal trafficking (MacLeod *et al.*, 2013). The genetic variation of the microtubule-associated protein tau (MAPT) and idiopathic PD have been linked, according to many genome-wide association studies of PD (Pankratz *et al.*, 2012, Skipper *et al.*, 2004). Figure 1.3 shows the molecular function of PD-associated genes and their neuronal subcellular locations.

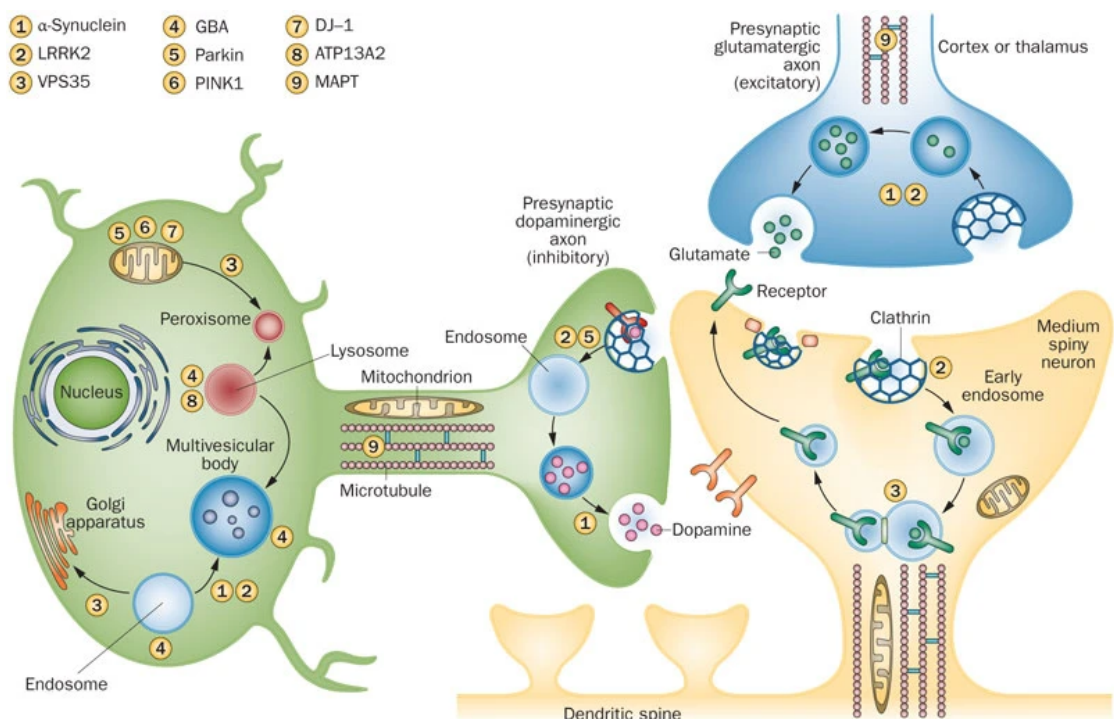


Figure 1.3 Molecular mechanisms implicated in PD according to the genetic findings

This figure shows a DA neuron (green), an axon of a presynaptic glutamatergic cortical neuron (blue), and a dendritic spine of a medium spiny neuron (yellow). The subcellular locations of genes reported to be associated in sporadic PD and associated pathogenic models. Genes linked to sporadic PD are most frequently found in the mitochondria, vesicular trafficking organelles, the Golgi network, and lysosomes and endosomes. Taken from (Trinh and Farrer, 2013).

1.1.4 Pathogenesis

There has been a number of mechanisms implicated in PD pathogenesis such as protein misfolding, mitochondrial dysfunction, and neuroinflammation. α -synuclein misfolding and aggregation which lead to the formation of LBs is a pathological feature found in most PD. The mechanism of this misfolding and aggregation is elusive but perhaps the native structure of α -synuclein in brains, that is largely an unstructured monomer, make it more liable to aggregate than a protein with defined stable structure (Burré *et al.*, 2013). Moreover, α -synuclein has been shown to act in a prion-like manner capable of spreading from cell to cell and cause toxicity (Ma *et al.*, 2019). As the illness advances, the PD-brain experiences progressive modifications, with LBs impacting susceptible neural circuits, according to research done in 2003 by Braak and colleagues (Braak *et al.*, 2003). Based on the progression of neuropathological alterations they noticed, they developed a staging system, arguing that neuronal damage doesn't occur randomly but rather develops after a predefined chain of pathological incidents. They classified the pathological evolution associated with PD into six phases (Figure 1.4), stage 1 includes the regions afflicted at the onset of the illness. Stage 1 lesions begin in the anterior olfactory nucleus and dorsal motor nucleus of the glossopharyngeal and vagal nerves (lower brainstem). The illness then advances stepwise in an upward direction toward the midbrain and forebrain nuclei, eventually impacting the neocortex in its latter stages (Braak *et al.*, 2003).

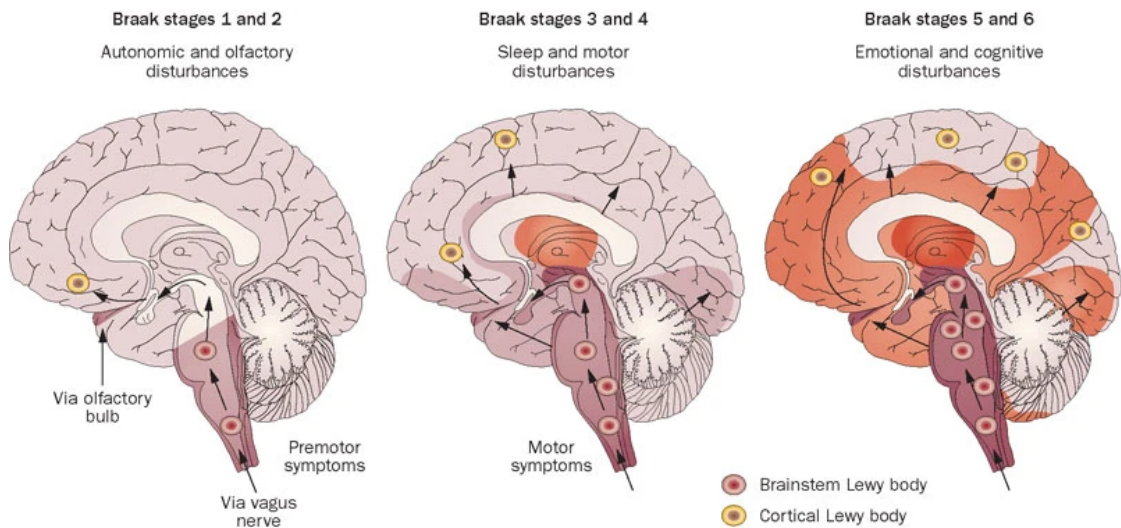


Figure 1.4 Braak staging system of PD pathology

The staging suggests that α -synuclein pathology starts in the olfactory bulb and brainstem regions (Braak stages 1 and 2) and, subsequently, the Lewy pathology spreads into the midbrain and the basal forebrain (Braak stages 3 and 4) before finally reaching cortical regions (Braak stages 5 and 6). Taken from (Doty, 2012).

Mitochondrial dysfunction is a recurrent theme in sporadic and familial PD pathology and has been linked to genetic and environmental risk factors (Figure 1.5). A defect in the mitochondrial complex-I has been shown in studies of MPTP, paraquat, and rotenone exposure and has given a clue to the association of mitochondrial dysfunction with PD. Also, mitochondrial complex-I abundance has been reported to be reduced in post-mortem PD patients' brain. Death in DA neurons due to energy depletion caused by this dysfunction could explain this link (Moon and Paek, 2015). Additionally, the discovery of PTEN induced kinase 1 (*PINK1*) and the *PRKN* involvement in mitophagy gave another clue of mitochondrial dysfunction theme in PD. A loss of function mutation in either genes have led to impaired mitochondria production and degradation which might lead to developing PD (Pickrell and Youle, 2015).

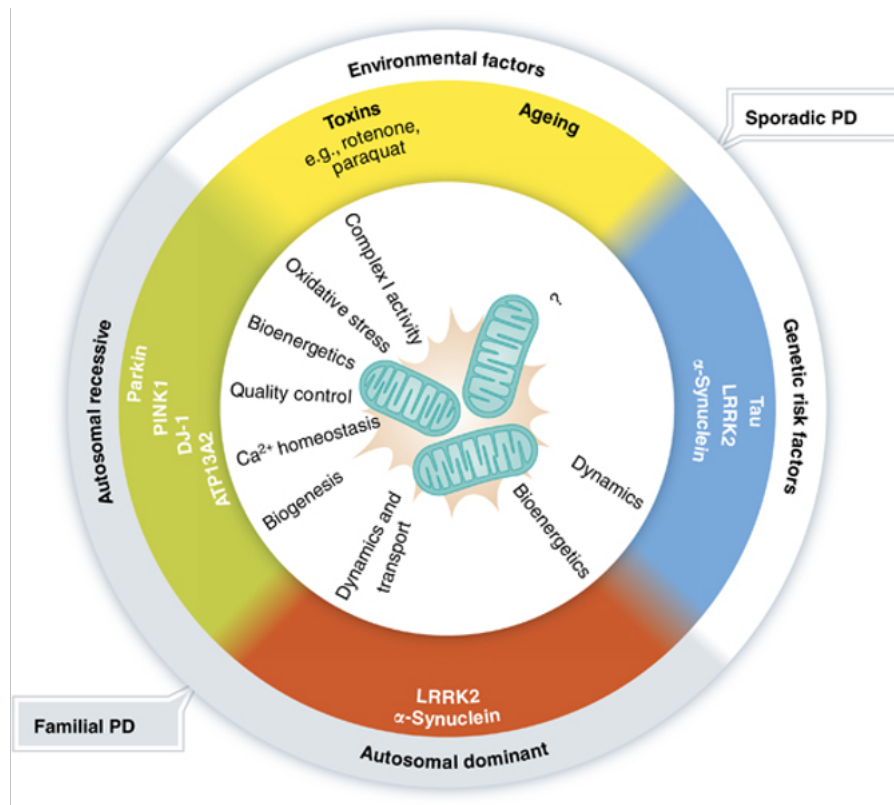


Figure 1.5 Multiple roles of mitochondria in Parkinson's disease

Mitochondrial integrity may change as a result of familial PD genes (autosomal recessive or dominant). Through various mitochondrial functions like bioenergetics, dynamics, transport, and quality control, genetic and environmental factors may be involved in the pathogenesis as well. Taken from (Exner *et al.*, 2012).

An interesting mechanism that could be involved in PD is neuroinflammation. Studies of PD risk factors and in patients pre and post-mortem have suggested an involvement of neuroinflammatory process in PD pathology either directly in neurons damage or indirectly in respond to the damage (Hirsch and Hunot, 2009). For example, an outbreak can occur within the brain, then stressed neurons activate glial cells (neurons immune cells) which would cause an upregulation of neuroinflammatory processes with subsequent neurodegeneration as a result or systemic inflammation could propagate into the brain and activate on site inflammatory events, which in the end will lead to neurodegenerative processes (Tansey and Goldberg, 2010). Interestingly, the density of microglial cells is very high in the region of the substantia nigra which makes the neuroinflammation mechanism even more plausible (Kim *et al.*, 2000). Having said that, neuroinflammation is commonly reported in other neurodegenerative disorders such AD (Hirsch and Hunot, 2009) so it is not a mechanism exclusive to PD. Another mechanism that might be implicated in PD includes dysfunction in protein degradation

systems either via the ubiquitin-proteasome system (UPS) or lysosome system where failure to clear misfolded α -synuclein or defective mitochondria leads to the possibility of LBs formation (Kouli *et al.*, 2018).

1.1.5 Treatment

To date, there is no cure for PD; however, management and treatment have improved significantly. Pharmacologically, Levodopa (L-DOPA) is still the standard to treat PD for more than 50 years since it was first used in 1967 (Cotzias *et al.*, 1967). L-DOPA, a dopamine precursor, and unlike dopamine, is able to cross the blood-brain barrier (BBB) can then convert into dopamine by DOPA decarboxylase to replenish the depleted neurotransmitter lost due to the disease. Despite its clear effectiveness, it comes with significant side effects. Some of the early treatment side effects include nausea and drowsiness while chronic treatment includes motor fluctuations, dyskinesia, hallucinations, and other psychiatric side effects. These side effects could be managed with dose control and a change in route of administration such as injection instead of oral (Zahoor *et al.*, 2018). Beside the side effects, another major issue with L-DOPA that has been reported is the possibility of being neurotoxic itself (Zahoor *et al.*, 2018). Other drugs used to treat PD, mostly in the early stages, include dopamine agonists which work by simulating the activity of the dopamine system without the need to be converted into dopamine. These include monoamine oxidase B (MAO-B) and Catechol-O-methyl transferase inhibitors which work by stabilising the level of endogenous dopamine, and anticholinergics which work by restoring the normal balance between dopamine and acetylcholine (Zahoor *et al.*, 2018). Apart from using drugs, neurosurgery and cell therapy could offer good options to treat PD. Deep brain stimulation (DBS) is the most used surgical tool to treat PD and it had been used to treat a number of disorders since the 1960s (Bishop *et al.*, 1963) and used in PD treatment in the 1990s by stimulating the subthalamic nucleus (STN) (Pollak *et al.*, 1993). Despite its effectiveness, the mechanism of action is still not clear (Lozano and Lipsman, 2013).

In summary, PD is a very complex neurodegenerative disorder that has an effect on a selective part of the brain which manifest mainly as an impaired locomotor activity in patients. The disease is heterogenous with multiple non-motor symptoms and different risk factors reported and other than symptoms modifying treatments, no cure has been found.

1.2 Leucine-rich repeat kinase 2 (LRRK2)

The first clue of *LRRK2* association to PD was discovered in 2002 via a genome-wide linkage analysis of a Japanese family which displayed a phenotype similar to sporadic PD (Funayama *et al.*, 2002). Later, more studies have confirmed this pathogenic link and found it to cause a late onset autosomal dominant PD (Paisán-Ruíz *et al.*, 2004, Zimprich *et al.*, 2004a). At that time, dardarin (from the Basque word dardara which means tremor) was the name given by (Paisán-Ruíz *et al.*, 2004) to the encoded protein but today it is mostly referred to as LRRK2 for Leucine-Rich Repeat Kinase 2. Mutations in *LRRK2* are reported to cause 5-13% of familial and 1-5% of sporadic PD cases (Kumari and Tan, 2009).

1.2.1 LRRK2 structure and localisation

LRRK2 gene is located on chromosome 12 and encodes a large multifunctional protein of 2527 amino acids with a molecular weight of approximately 280 kDa. LRRK2 protein harbours presumably four domains for protein-protein interactions, two GTPase domains, and one kinase domain (Figure 1.6). The protein-protein interaction domains are located at the ends of protein terminals while the enzymatic domains are in the core. On the N-terminal of the protein there are armadillo repeats (ARM), ankyrin repeats (ANK), and leucine-rich repeats (LRR) domains while the tryptophan-aspartic acid 40 repeat (WD40) domain is present on the C-terminal. These domains are mostly involved in protein structure and signalling. For example, the WD40 domain has been shown to be involved in membrane binding and protein localization while LRR domain was involved in inter/intramolecular interactions (Gilsbach and Kortholt, 2014). The core domains of LRRK2 are the functional enzymatic domains with multiple pathogenic mutations found linked to PD. The GTPase function is mediated by Ras of complex (ROC) and C-terminal of ROC (COR) domains. These domains throughout evolution have been always linked together and some consider them as one functional unit even though they are structurally different. A diagram of LRRK2 structure can be found in Figure 1.6. The kinase function of LRRK2 is mediated by a serine/threonine kinase domain which has the ability to phosphorylate many substrates and to autophosphorylate as well (Berwick *et al.*, 2019). The presence of these GTPase bi-domain and kinase domain classifies LRRK2 as a member of ROCO family proteins, review by (Marín *et al.*, 2008), which include among others a mammalian homologue LRRK1. Despite the great homology between the two proteins, no links to PD have yet been found in LRRK1 (Taylor *et al.*, 2007).

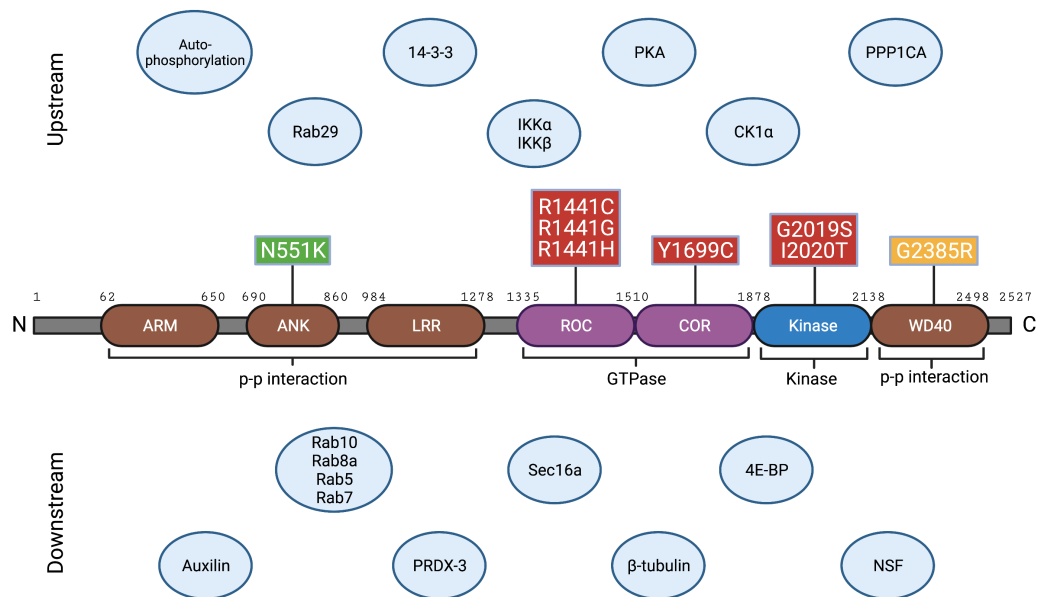


Figure 1.6. LRRK2 structure, mutations, and interactors

The structure of LRRK2 protein with different mutations sites and several upstream and downstream interactors. Domains implicated in protein-protein interactions are in brown, domains involved in GTPase function are in purple, and the kinase domain is in blue. *LRRK2* mutations are colour coded according to pathogenic (red), risk factor (yellow), and possibly neuroprotective (green) reports. The LRRK2 interactors are just a sample of many reported, for more see (Jeong and Lee, 2020, Marchand *et al.*, 2020).

LRRK2 is a cytosolic protein found mostly as a monomer with low kinase activity. While the activation mechanism is not completely understood, it is believed that membrane-recruitment and conformational activations reactions lead to LRRK2 dimerization and activation (Soliman *et al.*, 2020). The expression levels of *LRRK2* are variable throughout the body (Rideout *et al.*, 2020). It is highly expressed in the kidney, lung, and cells of the peripheral immune system. It is also found expressed in the intestine, multiple regions of the brain and extracellularly through exosomes (Rideout *et al.*, 2020). In the brain, the expression was detected in the neurons of cerebral cortex, caudate-putamen and *SNpc* regions (Higashi *et al.*, 2007). Inside cells, LRRK2 has been shown to colocalize with various cellular structures including endosomes, lysosomes, multivesicular bodies, the mitochondrial outer membrane, lipid rafts, microtubule-

associated vesicles, the Golgi apparatus and the endoplasmic reticulum (ER) (Hatano *et al.*, 2007). The association to a variety of membrane structure indicates multifunctional role in multiple cellular pathways for LRRK2.

1.2.2 *LRRK2* Mutations

Since its discovery in the early 21st century, many mutations have been reported throughout the *LRRK2* gene. The most well-studied PD-associated pathogenic mutations are missense mutations located within the enzymatic domains i.e., GTPase and kinase domains. For example, *LRRK2-R1441C/G/H* and *LRRK2-Y1699C* mutations were reported on domains ROC and COR respectively by (Mata *et al.*, 2005, Paisán-Ruíz *et al.*, 2004, Zimprich *et al.*, 2004b) in families with probable English and German origins. On the kinase domain, *LRRK2-G2019S* and *LRRK2-I2020T* were reported by (Di Fonzo *et al.*, 2005, Funayama *et al.*, 2005, Gilks *et al.*, 2005, Nichols *et al.*, 2005) and found in families of European, American, and Japanese origins. Moreover, many other mutations have been identified with various links to PD such as *LRRK2-G2385R* in the WD40 domain which is reported to be a risk factor (Jaleel *et al.*, 2007) and interestingly *LRRK2-N551K* and *LRRK2-R1398H* are reported to be neuroprotective in some cohorts (Ross *et al.*, 2011, Tan *et al.*, 2010).

The most common mutation reported and studied in *LRRK2* is *G2019S*. It accounts for 4% of familial and 1% of sporadic PD cases and it has been reported worldwide (Healy *et al.*, 2008) in many populations with some incidence of higher frequencies in populations such as in Ashkenazi Jewish and North African Berbers which accounts for 29% and 37% of familial cases of PD in these populations respectively (Lesage *et al.*, 2006, Ozelius *et al.*, 2006). The second most frequent mutation is *LRRK2-R1441C/G/H* and it is mostly reported in European populations. In fact, *LRRK2-R1441G* particularly has been found to be a founder mutation responsible for 46% of familial cases in the Basque population (Gorostidi *et al.*, 2008, Simón-Sánchez *et al.*, 2006).

The penetrance of *LRRK2* mutations vary depending on populations and age. For instance, *LRRK2-G2019S* has been found to cause 60% of PD cases in Tunisian people by age 60 whereas only 20% of Norwegians who carried the mutation developed PD (Hentati *et al.*, 2014). Furthermore, the penetrance in Basque population ranges from 13% at age 65 to 83% at age 80 for *LRRK2-R1441G* mutation (Ruiz-Martínez *et al.*, 2010).

1.2.3 LRRK2 Interactors

As mentioned earlier, LRRK2 is a large multi-domain protein expressed in many tissues with varying degree which makes elucidating its function very difficult. Despite this complexity, much research has been done and is still going to uncover the mysteries of this protein and which effectors it acts through. Not surprisingly, the majority of research was focused on the kinase activity because of the high prevalence of *G2019S* mutation which affects kinase activity and the reports of altered kinase level found in different pathogenic mutations.

In terms of phosphorylation of LRRK2, the protein is a highly phosphorylated one with at least 74 phosphorylation sites determined by phosphosite mapping studies and 60% of these sites have been identified as autophosphorylation sites (Marchand *et al.*, 2020). The autophosphorylation process is still a matter of investigation where the GTPase, kinase, and even WD40 domains were reported to play interactive roles in the process in addition to dimerization and phosphorylation of other substrates like Rab29 (Berwick *et al.*, 2019). Beside autophosphorylation, there are proteins that have been found to phosphorylate and dephosphorylate LRRK2. Protein kinase A (PKA) was the first protein reported to be able to phosphorylate LRRK2 on sites S910 and S935 with the latter one showing altered levels of phosphorylation reported in familial mutations *LRRK2-G2019S*, *LRRK2-R1441G* and *LRRK2-Y1699C* (Ito *et al.*, 2007, Li *et al.*, 2011, Muda *et al.*, 2014). Other kinases shown to be acting on the same phosphosites include Ikkappa B kinases (IKK α & β) and Casein Kinase 1-alpha (CK1 α) (Chia *et al.*, 2014, Dzamko *et al.*, 2012). On S910 and S935, only the alpha catalytic subunit of Protein Phosphatase 1 (PPP1CA) has been confirmed to be able to dephosphorylate LRRK2 in several types of cells (Lobbestael *et al.*, 2013). Moreover, 14-3-3 proteins have attracted attention due to their abundant presence in the brain, their binding ability to LRRK2 and the possible promotion of cell survival associated with them found in PD cellular models (Shimada *et al.*, 2013). The full interaction cascade is still not established but it is reported to be at sites S910 and S935. Dephosphorylation of these sites have shown disrupted binding of 14-3-3 with subsequent influence on LRRK2 cellular localization. This disruption was markedly demonstrated in five of the most common pathogenic mutations (*LRRK2-R1441C/G/H*, *LRRK2-Y1699C* and *LRRK2-I2020T*). Binding of 14-3-3 has also been shown to prevent the self-association of LRRK2 into dimers which might affect the kinase activity by reducing the amount of the dimerised activated kinase form of LRRK2 (Mamais *et al.*, 2014, Nichols *et al.*, 2010).

Downstream substrates of LRRK2, many substrates have been identified to be phosphorylated. The list includes proteins in different tissues and pathways such as moesin, β -tubulin, tau, Futsch, endophilin A1, a subset of Rab GTPases and many others (Jeong and Lee, 2020). Among these different LRRK2 substrates, Rab GTPases have been the focus of investigation recently perhaps because they have been validated to be phosphorylated *in vivo* by some groups compared to most of the others (Jeong *et al.*, 2018) and they have been found in abundance in CNS (D'Adamo *et al.*, 2014). Rab GTPases are key organizers of intracellular membrane trafficking and were initially discovered in brain tissue (Touchot *et al.*, 1987). Among more than 60 Rab GTPases that are encoded by the human genome, 24 are specific or enriched in CNS (Brighthouse *et al.*, 2010, Wilson *et al.*, 2014). Many of these have been implicated into neurodegenerative disorders either directly or indirectly (Steinert *et al.*, 2012, Wilson *et al.*, 2014); however, the exact mechanism by which LRRK2 regulates Rab GTPase function is still not clear.

1.2.4 LRRK2 and cell biological functions

LRRK2 has been reported to be involved in many cellular processes (Figure 1.7). In the next sections, we'll be discussing the role of LRRK2 in biological functions.

1.2.4.1 Autophagy

Autophagy is a crucial process to maintain protein homeostasis. It is a physiological process by which cells transport long-lived proteins or organelles such as mitochondria, that are unnecessary or even detrimental for cell survival to the lysosome for degradation. Autophagy is classified into three types: macroautophagy, microautophagy, and Chaperone-Mediated Autophagy (CMA). Macroautophagy is a nonselective process that targets macromolecules or subcellular organelles in bulk. Cytoplasmic material is sequestered into an autophagosome and delivered to the lysosome (or endolysosome) for degradation). Microautophagy involves the capture of cytoplasmic components through direct invagination of endolysosome membranes and can be nonspecific (in bulk) or highly specific. The CMA is a selective process of targeting proteins that contain a KFERQ pentapeptide-related motif by HSC70 and other co-chaperones such as HSP40 (Aman *et al.*, 2021).

Alterations in autophagy have been observed in brain tissue of PD patients as well as in different models. An analysis of macroautophagy protein markers, namely p62 and

LAMP1, in *LRRK2-G2019S*-PD patients' brains with LB pathology have shown significant low levels compared to sporadic PD brains suggestive of a divergence of effect in terms of autophagy between sporadic and *LRRK2* carriers (Mamais *et al.*, 2018). Furthermore, *LRRK2-G2019S* has been found to be poorly degraded by CMA than the wild-type *LRRK2* in cell culture, mouse and DA neurons of PD patients suggesting a disturbance of the typical CMA process caused by pathogenic mutations in *LRRK2* (Orenstein *et al.*, 2013). A knock-in mice with *LRRK2-R1441G* have shown marks of impaired CMA accompanied with accumulation of SNCA oligomers and increase in CMA markers like LAMP2a and HSPA8 in striatal tissue (Ho *et al.*, 2020). The previous observations point out to a physiological role to *LRRK2* in autophagy with a mechanism that is still needs to be investigated further.

1.2.4.2 Mitochondria

Impairment in mitochondrial functions and morphology is a recurrent theme in PD. This impairment is well-established prior to any discovery of a genetic link to PD where mitochondrial complex I was found to be deficient in *SNps* of PD patients (Schapira *et al.*, 1990). Observations have been reported of direct and indirect effect of *LRRK2* on mitochondrial function. Directly, an impairment of mitochondrial complexes III and IV was reported in primary human fibroblasts from manifesting and non-manifesting *LRRK2-G2019S* carriers (Mortiboys *et al.*, 2015). In addition, other studies have reported abnormalities in mitochondrial morphology caused by *LRRK2* mutations (Smith *et al.*, 2016, Yue *et al.*, 2015). Indirectly, *LRRK2-G2019S* has been reported to increase phosphorylation of peroxiredoxin-3 (PRDX-3), a scavenger of hydrogen peroxide produced by mitochondria, compared to the wild-type which leads to the increase of inhibition of endogenous peroxidase and promoting mitochondrial dysregulation and oxidative damage (Angeles *et al.*, 2011, Angeles *et al.*, 2014). Interestingly, *LRRK2* has been reported to be localised to the mitochondrial membrane (Biskup *et al.*, 2006) and this localisation might have an effect on mitochondrial biogenesis. For example, *LRRK2* has been reported to interact with an outer mitochondrial protein called Miro that is important in mitochondrial transportation. This interaction triggers the transport of damaged mitochondria along axonal microtubules which lead to mitophagy of damaged mitochondria and this response is lost in cells with the *LRRK2-G2019S* mutation (Hsieh *et al.*, 2016). Similar results have been reported for *R1441C* and *Y1699C* mutations as well (Godena *et al.*, 2014, Thomas *et al.*, 2016).

1.2.4.3 Endocytosis

Endocytosis is the process of engulfing and trafficking of plasma membrane associated proteins through a series of intracellular membrane-limited compartments that leads to degradation by lysosomes or recycling into other intracellular locations. LRRK2 has been reported to interact with different protein associated with endocytosis. The mechanism of this interaction is still to be explained; however, Rab GTPases have been associated with many of these interactions (Steger *et al.*, 2017, Steger *et al.*, 2016). Rab29, also known as Rab7L1, has been found to recruit LRRK2 to enlarged lysosomes in chloroquine stressed cells. This recruitment led to the phosphorylation of Rab8a and Rab10 by LRRK2 and eventually aided lysosomal function by promoting lysosomal secretion (Eguchi *et al.*, 2018). Similar results have been reported by (Herbst *et al.*, 2020, Lee *et al.*, 2020) on the effect of LRRK2 phosphorylation of Rab8a and Rab10 in stressed endosomes and lysosomes. Expressing *LRRK2-G2019S* and *LRRK2-R1441C/G* mutations in iPSC-derived DA neurons from PD patients have impaired lysosomal function (Ysselstein *et al.*, 2019) suggesting a crucial role for LRRK2 in regulating lysosomal functions.

Moreover, LRRK2 has been implicated in synaptic vesicle endocytosis. Overexpression of *LRRK2-G2019S* and *LRRK2-R1441G* in primary midbrain, primary hippocampal neurons, and iPSC-derived DA neurons from PD patients impaired endocytosis of synaptic vesicles (Matta *et al.*, 2012, Nguyen and Krainc, 2018, Pan *et al.*, 2017). Many proteins have been reported to interact with LRRK2 in regulating synaptic vesicle endocytosis that include auxilin, Dynamin GTPases, and synaptojanin-1 (Gad *et al.*, 2000, Stafa *et al.*, 2014, Yim *et al.*, 2010). In addition, Rab5 and Rab7 have been reported to be involved with LRRK2 in early and late endosome respectively (Dodson *et al.*, 2012, Shin *et al.*, 2008).

1.2.4.4 LRRK2 function and Trans-Golgi network (TGN) and endoplasmic reticulum (ER)

LRRK2 interacts with several proteins that reside at the Golgi body to regulate its integrity and function. For example, it has been found that Rab29, LRRK2, BAG5 and GAK proteins form a complex localised to TGN in cultured cells and mouse brain. Overexpression of pathogenic variants of *LRRK2* or any of these individual proteins causes Golgi fragmentation. This induced fragmentation can be blocked by the knockdown of any one of the other three proteins which indicates the importance of

these proteins in maintaining Golgi integrity (Beilina *et al.*, 2014). Additionally, LRRK2 has been reported to phosphorylate and form a complex with N-ethylmaleimide sensitive fusion (NSF) protein, which is an essential factor for vesicle trafficking in the Golgi body. NSF knockdown has shown similar results to *LRRK2* knockdown in terms of causing Golgi fragmentations and the formation of enlarged late endosomal structures. Disruption of plasma membrane receptor recycling pathways and trafficking of lysosomal hydrolyses from TGN to lysosomes were observed as well resulting in an impaired lysosomal degradation capacity (Lanning *et al.*, 2018).

Additionally, LRRK2 has been found to form a complex with Sec16a protein, a key protein in the formation of endoplasmic reticulum exit sites (ERES). The knockdown of *LRRK2* in primary hippocampal neurons led to the disruption of LRRK2-Sec16a complex and impaired the transport of vesicles to the Golgi. Similar results were found when a knock-in of *LRRK2-R1441C* was expressed (Cho *et al.*, 2014).

1.2.4.5 Microtubules and ribosomes

LRRK2 has been associated with the cytoskeleton, particularly microtubules. This interaction was identified first in 2006 and was shown to be an association of LRRK2 with β -tubulin (Biskup *et al.*, 2006). A post translational modification known to induce microtubule stability i.e. acetylation was reported to be increased in *LRRK2* knockout MEF cells and mouse kidney cells and associated with this is a strong localization of LRRK2 to microtubules that are dynamic i.e. not acetylated and less stable suggesting a negative effect of LRRK2 on microtubule stability (Law *et al.*, 2014, Pellegrini *et al.*, 2018). Interestingly, the activity of the association of LRRK2 with dynamic microtubules seems specific to the GTPase domain since it is only observed in *LRRK2-R1441C* and *LRRK2-Y1699C* but not in *LRRK2-G2019S* mutations (Godena *et al.*, 2014).

Furthermore, LRRK2 has been implicated in protein synthesis. This implication is a bit controversial because it was only replicated in fruit flies and weakly *in vitro* but not mammalian models (Imai *et al.*, 2008, Kumar *et al.*, 2010, Trancikova *et al.*, 2012). The eukaryotic initiation factor 4E binding protein (4E-BP), a repressor of translations, was found to be phosphorylated by the LRRK2 homologue in the *Drosophila* LRRK (dLRRK) and was able to inactivate 4E-BP (Imai *et al.*, 2008).

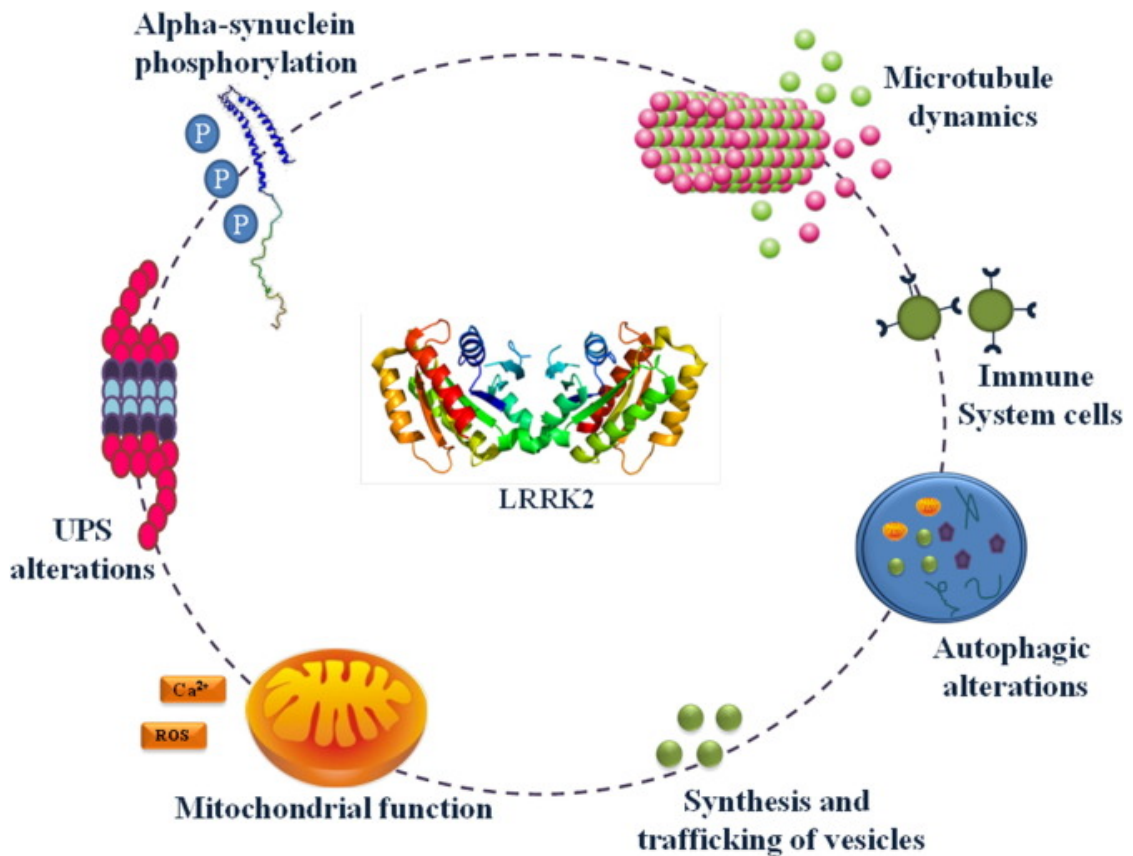


Figure 1.7. The involvement of LRRK2 in different organelles and cellular mechanisms.

LRRK2 is involved in the regulation of several biological processes, some of which are intertwined. Rab proteins are involved in several of these processes and potentially mediate some effects of LRRK2. Taken from (Esteves *et al.*, 2014).

In conclusion, LRRK2 is a large protein with several mutations discovered throughout the protein that are linked to PD. It has been found in many tissues and has been associated with many cellular processes. This introduces complexity to our understanding of the protein which makes it very difficult to elucidate its function and pathology in PD. Thus, further investigations are encouraged to uncover the mysteries of this protein.

1.3 Modelling PD

Potentially the best way to study human biology is to study it in humans themselves; however, the ethical and technical limitations are too significant to disregard. Thus, finding the best model that would recapitulate human biology is very crucial. Throughout the years, many models have been developed for PD, but none have been

able to fully recapitulate all disease characteristics. Nevertheless, the available models are still beneficial with different advantages and disadvantages.

1.3.1 Cellular models

Cellular models offer a controlled environment to simplify experimental variables compared to what is present in animal models. This type of modelling is very useful when investigating single cellular events or pathways; however, it fails to recapitulate non-cell autonomous effects that are essential in disease pathology. Compared to animal models, cellular models are fast and reproducible with the opportunity for specific genetic and environmental manipulations that are devoid of many ethical issues (Lazaro *et al.*, 2017).

Many cellular models have been developed to study PD. Human embryonic kidney 293 (HEK 293) and human neuroglioma (H4) cells are established cell lines that are commonly used as heterologous cellular models. These cell lines are quite useful because they are easy to maintain, provide unlimited supply of homogenous cells and grow rapidly which enable large scale studies, but being derived from cancer cells, many proteins are produced at abnormal (higher or lower) levels. HEK 293 and H4 cells have been used to study the effect of *SNCA* mutations (Lázaro *et al.*, 2016, Lazaro *et al.*, 2014) and *LRRK2* mutations (Nichols *et al.*, 2010) on different cellular events found in PD. The contributions of these cells are great; however, they lack the neuronal phenotype which limit their usefulness. This can be overcome by the use of cell lines that are capable of differentiating into neuronal-like cells, specifically, DA cells. For example, Lund Human Mesencephalic (LUHMES) cells are capable of differentiating into strong DA phenotype neuron-like cells (Scholz *et al.*, 2011). These cells have been used to study the different cytotoxic effects of α -synuclein (Tong *et al.*, 2017, Xiang *et al.*, 2013).

Recently, human induced pluripotent stem cells (iPSCs) have been instrumental in biomedical research since Shinya Yamanaka pioneered the technology of reprogramming somatic cells in 2006 (Takahashi and Yamanaka, 2006). Compared to the established cell lines, these cells are capable of being differentiated into DA neurons when taken from PD patients, which provide the best genetic background to study the disease. Over the past decade, many iPSCs models have been developed for neurodegenerative diseases including PD. Familial and sporadic PD have been modelled in these cells demonstrating the different pathological events of the disease such as

protein aggregation, mitochondrial dysfunction, and susceptibility to autophagy and oxidative stress. For more information see review by (Avazzadeh *et al.*, 2021). In addition to modelling PD to understand the pathway of the disease, the use of iPSCs has a great potential in drug discovery and cell therapy (Ke *et al.*, 2019). For example, an autologous transplant of DA progenitor cells in induced PD rhesus monkeys have shown alleviation of motor and depressive behaviours (Tao *et al.*, 2021). Moreover, the use of a DA progenitor cells (MSK-DA01) in PD patients is being assessed for its efficacy and safety after proving safe and effective in rats (Piao *et al.*, 2021).

A great advancement in cellular modelling of PD is the use of human organoids. These are small, self-organized, 3D tissue cultures that are derived from human stem cells. They have great potential in disease modelling, developmental biology and drug discovery. Compared to the traditional monolayered 2D cell cultures, human physiology is recapitulated better due to cellular heterogeneity. Additionally, they offer a better modelling for biological processes that are specific to the human body than animal models (Corro *et al.*, 2020, Kim *et al.*, 2020). In PD modelling, human midbrain organoids (hMOs), have shown a great potential to recapitulate many aspects of the disease and they have the capability to bridge the gap between cellular and animal models. Since their first introduction in 2014 (Tieng *et al.*, 2014), organoids have been successfully used to model PD genetically and phenotypically (Galet *et al.*, 2020).

1.3.2 Animal models

Although cellular models give great insights into the cellular pathology of PD, they lack the non-autonomous aspects of the disease progression. In addition, the physical and behavioural manifestations that occur in patients are impossible to demonstrate in cell culture. Thus, the next best option is animal models. They provide an excellent opportunity to understand the full picture of disease progression in a form mimicking human biology.

When looking for the ideal model for PD, one should look for what recapitulate or mimics the pathology of the disease such as a selective DA neurodegeneration, the presence of neuronal inclusions like LBs and a display of motor deficits. There have been two main types of animal models used in PD research, toxin treated and genetic models. The focus in the next sections will be on rodents, while the fruit fly will be discussed in later sections (section 1.4).

1.3.2.1 Toxin-treated models

This type of model utilises neurotoxins to induce the symptoms of PD. In 1968, Urban Ungerstedt injected 6-hydroxydopamine (6-OHDA) into rats' brains which led to the degeneration of neurons with high selectivity of DA neurodegeneration and marked motor deficits in these rats (Ungerstedt, 1968). Currently, 6-OHDA is a widely used neurotoxin to induce the symptoms of PD in animals. It demonstrates most of the known PD symptoms such as neurodegeneration and mitophagy; however, LBs seem to be absent, which may be a function of time (the injection of 6-OHDA may not allow time for aggregates to form). A drawback for this drug is its inability to cross the BBB which means it requires an injection into the brain to be administered (Hernandez-Baltazar *et al.*, 2017).

Another highly selectivity neurotoxin to DA neurons is MPTP. The parkinsonism effect of this drug was discovered by accident in 1983 in drug abusers (Langston *et al.*, 1983). Unlike 6-OHDA, MPTP can cross the BBB. MPTP itself is not toxic but when it enters the brain it is converted into 1-methyl-4-phenylpyridinium (MPP⁺) which is taken up by the DA neurons. In the DA neurons, MPP⁺ is toxically concentrated in the mitochondria which leads to cell death, eventually (Langston, 2017). Similar to 6-OHDA, MPTP treated brain fail to show LBs which is a cellular hallmark in PD.

The reports of increased risk of PD from environmental agents such as pesticides have resulted in the use of rotenone and paraquat as neurotoxin-based models (Tanner *et al.*, 2011). Rotenone and paraquat are similar to MPTP in that they are able to cross the BBB which enable them to be administered systemically. Additionally, they are able to mimic PD in terms of forming LBs unlike 6-OHDA and MPTP. Rotenone is a natural compound found in many plants and has been used as pesticide. Similar to MPTP, it causes DA neurons degeneration via mitochondrial dysfunction. The models produced are generally selective to the DA neurons but some reports showed multisystem degeneration (Hoglinger *et al.*, 2003) and the high mortality observed in some rat models (Fleming *et al.*, 2004) is a drawback. Paraquat was identified as a possible candidate to induce parkinsonism due to the structural similarity to MPP⁺. Unlike rotenone and MPTP, paraquat causes DA neuron degeneration via the production of mitochondrial derived reactive oxygen species (ROS) which causes oxidative stress that leads to cell death. Paraquat selectivity to DA neurons is questionable since some have

found it to be selective (McCormack *et al.*, 2002) while others have not or have but only when paraquat is conjugated with other chemicals (Thiruchelvam *et al.*, 2000).

There have been a range of neurotoxin-based animal models generated throughout the years; however, rodents and non-human primates (NHP) are the most used and the use of MPTP is considered to be the gold standard due to its ability to demonstrate almost all of the PD hallmarks (Jackson-Lewis *et al.*, 2012, Pingale and Gupta, 2020).

1.3.2.2 Genetic models

Although the majority of PD cases are idiopathic, they share many characteristics with the familial ones. Thus, genetic models offer great opportunity to understanding the pathogenesis of the disease and enable therapeutic screening. Just like in neurotoxin-based models, there isn't a perfect genetic model that would demonstrate all PD hallmarks. Among many genes that have been linked to PD, five have been mostly studied in different animal models and these are *SNCA*, *LRRK2*, *PINK1*, *PRKN*, and *DJ-1*. These models have been developed by either generating knockouts, transgenic animals or injecting viral vectors carrying the gene of interest or preformed fibrils into the brain (Konnova and Swanberg, 2018).

Overexpression of *SNCA* in rodents and NHPs causes α -synuclein aggregates but the motor deficits and DA neurodegeneration can be variable depending on the route of administration. In transgenic rodents when *SNCA* is overexpressed, some motor deficits were observed with no DA neurodegeneration (Cannon *et al.*, 2013, Fleming *et al.*, 2005, Recasens *et al.*, 2014, Van der Perren *et al.*, 2015, Volpicelli-Daley *et al.*, 2016, Wakamatsu *et al.*, 2008).

The large size of *LRRK2* gene has limited its use in viral vector models (Van der Perren *et al.*, 2015); however, some attempts to express LRRK in mice and rats were able to induce some motor deficit with mild or no DA neurodegeneration (Dusonchet *et al.*, 2011, Lee *et al.*, 2010, Li *et al.*, 2009). Interestingly, injecting helper-dependent canine adenovirus type 2 (HD CAV-2) with *LRRK2*-G2019S in the striatum of *Microcebus murinus*, a NHP model, has induced clinical and histological symptoms similar to PD (Mestre-Francés *et al.*, 2018). The majority of transgenic mouse and rat models of *LRRK2* have little effect on DA neurodegeneration and most lack motor dysfunction (Blesa and Przedborski, 2014, Dawson *et al.*, 2010).

The nature of mutations in *PINK1*, *PRKN*, and *DJ-1* genes (autosomal recessive loss of function) have resulted in developing knockout models. Unfortunately, most did not to display motor deficits or DA neurodegeneration (Dawson *et al.*, 2010). Inactivation of *PINK1* and *PRKN* did not produce better models in mice but the DA neurons were more sensitive to subsequent insult by MPTP (Haque *et al.*, 2012, Van der Perren *et al.*, 2015).

Interestingly, one key observation that remains to be explained due to its unknown physiological significance and potential contribution to the pathogenesis of the disease is the loss of neuromelanin (NM) pigmentation normally produced by DA neurons in the brain, specifically in the *SNpc*. The intensity of this pigmentation in the substantia nigra is the greatest in humans where it can be examined macroscopically (Marsden, 1961). This key observation couldn't be replicated in any laboratory animals commonly used in PD research because it seems unique only to humans. However, (Carballo-Carbajal *et al.*, 2019) were able to generate a rat model that is able to produce human-like intensity of NM by overexpressing human tyrosinase in rat *SNpc*. This model was able to produce age dependent neurodegeneration associated with neuronal dysfunction and formed PD-like neuronal inclusions similar to that found in PD. The pathology presented in this model sounds promising, however, no report of motor deficit was revealed.

Rodents and NHPs comprise the majority of animal models in PD research. This is undeniably due to their close similarity to human biology in terms of genes and symptomatic and pre-symptomatic phenotypes that can be observed and measured (Konnova and Swanberg, 2018). Having said that, the variability in cellular and physical phenotypes opens the door for other animal models to be developed to better understand the full picture of the disease. Non-mammalian models such as *C. elegans*, zebrafish and *D. melanogaster* have well-defined neuropathology and behaviour, low maintenance costs, rapid life cycle and a genome easy to manipulate. Many models have been generated in *C. elegans* and zebrafish that displayed variable phenotypes similar to rodents. The number of animals produced and the rapid life cycle of *C. elegans* and zebrafish is an advantage in terms of drug screening and discovery (Cooper and Van Raamsdonk, 2018, Vaz *et al.*, 2018). As for *D. melanogaster*, a more detailed dive into its contribution in PD research can be found in the next section.

Finally, the attempts, so far, to generate a comprehensive model for PD that would recapitulate all hallmarks of the disease have not been successful; however, these

variance in models might be a reflection of the heterogeneity of the disease. Therefore, studying a combination of models or choosing one that would best recapitulate an aspect of the disease, I think, would be an optimal approach to understanding and studying PD pathology.

1.4 *Drosophila* as a powerful model organism

Among many models available to use, the common fruit fly (*Drosophila melanogaster*) has emerged as a powerful candidate for PD modelling. The use of fly as a model started at the beginning of the 20th century with the work of William E. Castle and his students at Harvard University (Castle *et al.*, 1906). Influenced by his work, Thomas Hunt Morgan worked further on *Drosophila* to establish it as a robust model, especially in understanding the basis of genetics. His pioneering works led to the discovery of the *white* (*w*) mutation, which resulted from a natural mutation occurring on the X chromosome that change the colour of a wild type fly eye from red to white (Kenney and Borisy, 2009). Using *Drosophila* in research labs is easy and cheap. Its size allows it to be maintained in high numbers with small space used and the relatively less complex structure enables the ease of experimental manipulations. It has a short lifespan (~90 days) with a rapid life cycle (it takes ~10 days to generate adult flies at 25°C). The low redundancy of its genome and the wide range of genetic tools available allow forward and reverse genetics to be made with efficiency (Roote and Prokop, 2013). In addition, the sequencing and publication of the whole genome of the *Drosophila* was a breakthrough in demonstrating similarities to the human genome. *Drosophila* has around 13,600 genes spread across four chromosomes (one sex chromosome, the first one, and three autosomes). Surprisingly, more than 75% of human-associated disease genes have orthologues in *Drosophila* (Adams *et al.*, 2000, Reiter *et al.*, 2001).

Using *Drosophila* as a model is still proving strong in a sense that six Noble prizes have been awarded to ground-breaking works based on fruit fly and the most recent one was awarded in 2017.

1.4.1 The genetic toolbox of *Drosophila*

The genetic toolbox in *Drosophila* sets it apart from other model organisms. Prior to its genome sequencing, unbiased randomly generated forward genetics were used to achieve genetic manipulations. This type of genetics works by introducing random mutations into the genome and then identifying or observing the effect on the

phenotypes. Such mutations can occur naturally or be generated artificially using chemicals, radiation, or insertional mutagens e.g., transposable elements. Chemically, flies can be fed ethyl methane sulphonate (EMS) that can introduce point mutations via alkylation (Sega, 1984). Ionising radiation e.g., X-ray has been known to be mutagenic and can introduce chromosomal rearrangements and deletions (Pastink *et al.*, 1987). Insertional mutagens utilise the ability of mobile genetic elements such as *P*-elements to jump randomly around the genome to cause mutations. These elements are not as strong as the previous two in term of introducing a wide range of mutations; however, the mutated genes can be rapidly and easily identified using the element as a genomic tag (St Johnston, 2002). In reverse genetics, on the other hand, there is no screening for mutations because the target is a known gene and changes to a phenotype can be observed when that particular gene is manipulated. Many methods have been developed to alter the gene of interest. *P*-elements can be modified and inserted within or near the gene of interest to cause mutations. Transgenic RNAi and CRISPR/Cas9 can be used for a more targeted way of altering the function of a gene (Adams and Sekelsky, 2002, Fire *et al.*, 1998, Gratz *et al.*, 2013). These tools, in combination with Gal4/UAS system and balancer chromosomes (see next sections), help *Drosophila* recapitulate human biology.

1.4.1.1 The Gal4/UAS system

One significant advantage of using *Drosophila* as a model organism is the Gal4/UAS system (Brand and Perrimon, 1993). It is originally based on an enhancer-trap method where the ability to express a gene of interest in specific cells or tissues is achieved. The system consists of two elements, a transcriptional activator derived from *Saccharomyces cerevisiae* (Gal4) placed under the control of a cell or tissue-specific promoter and a transgene placed under the control of the upstream activator sequence (UAS), which Gal4 binds to. These individual elements are made separately in two different flies and can only be expressed in the desired way when flies are mated to produce a progeny that carries both (Figure 1.8). Throughout the years, many flies have been produced to drive expression in different parts of the fly, e.g., *GMR*-Gal4 (eye), *elav*-Gal4 (neurons), and *TH*-Gal4 (DA neurons), as well as many flies have been produced to express different genes of interest.

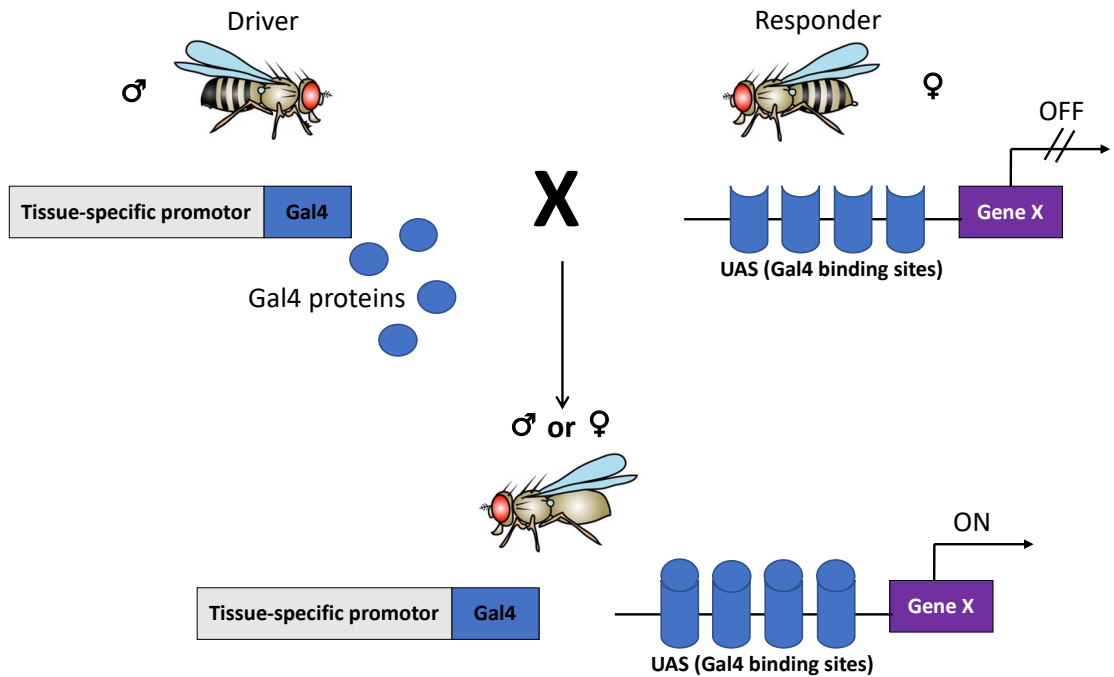


Figure 1.8. The Gal4/UAS system in *Drosophila*

The Gal4/UAS system allows ectopic expression of the gene of interest in specific tissues or cells when its two components are present in a fly. This figure illustrates the ability of the progeny to express gene X in a tissue-specific fashion. This occurred as result of a crossing scheme between a tissue specific Gal4 activator fly (Driver) and a UAS fly that has Gal4 binding sites (Responder).

The system has undertaken many modifications since its inception. The generation of Gal4-hormone receptor (GeneSwitch) elements allows temporal gene expression control (Osterwalder *et al.*, 2001). This temporal expression is achieved due to the ability of these lines to be activated only in the presence of the appropriate ligand such as mifepristone (RU486) that can be administered when required (Figure 1.9). Other modifications include, the addition of extra elements, such as FLP recombinase and Gal80, that add an extra level of regulation and the addition of RNA-mediated interference (RNAi), making the system capable of targeted gene knockdowns (Duffy, 2002).

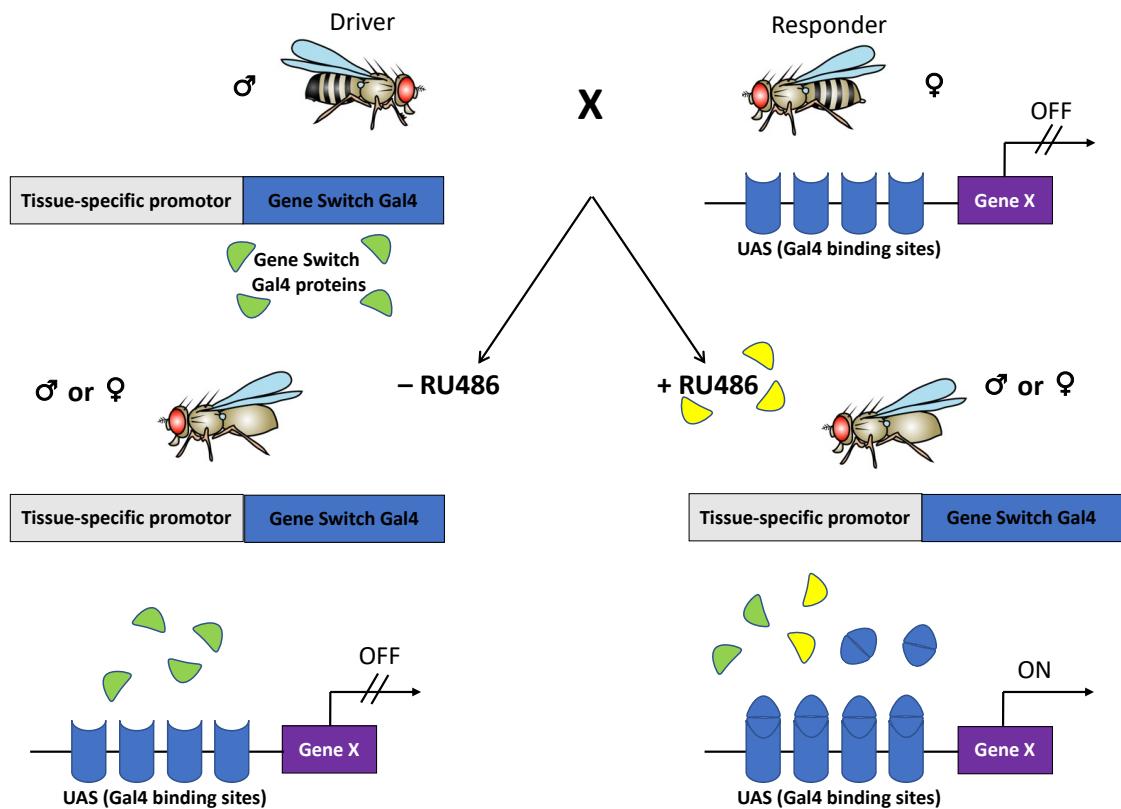


Figure 1.9. The Gal4/UAS system (GeneSwitch) in *Drosophila*

This modification to the conventional Gal4/UAS system (described previously) allows temporal expression of the gene of interest. This figure illustrates gene expression is dependent upon the presence of RU486.

1.4.1.2 Balancer chromosomes

The existence of balancer chromosomes makes fly genetics extremely versatile. Throughout the years, many balancer chromosomes have been developed for the main three chromosomes (the 4th chromosome is effectively ignored for these purposes being too small to undergo regular recombination events). These chromosomes are structurally rearranged with multiple aneuploid chromosomal inversions that inhibit homologous recombination during meiosis. If recombination does occur, the deletion of genomic regions or duplication of genomic regions will result in lethality. In addition, balancer chromosomes carry dominant markers that produce a distinct observable phenotype (Figure 1.10). All these properties aid in maintaining fly stocks, particularly those with deleterious mutations, and tracking mutations when designing crossing schemes (Kaufman, 2017).

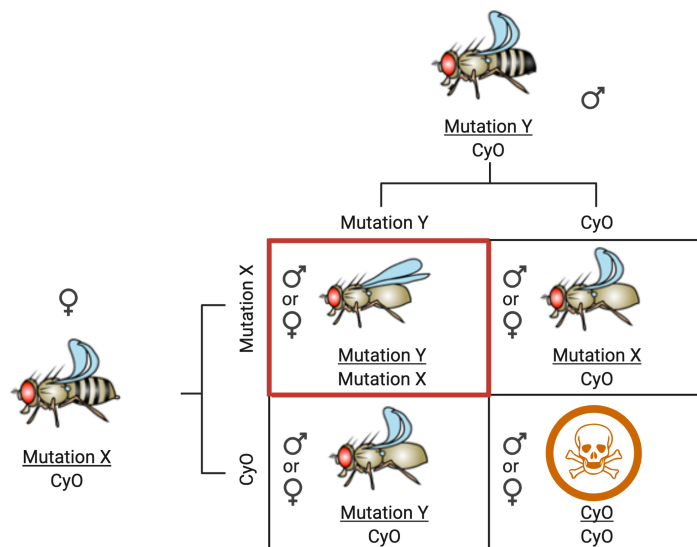


Figure 1.10. An illustration of a balancer chromosome used in a crossing scheme

Balancer chromosomes aid in fly selection of the desired genotype during crossing schemes. In this example, the desired genotype is the one carrying mutations X and Y. In order to acquire this, parent flies each carrying one of the desired mutations on one copy of the chromosome and the balancer one (the dominant marker for CyO is curly wings) on the other copy of the chromosome are crossed together. The results are two flies similar to the parents and one that would be the desired fly (red square). Of note, the fourth possible option won't appear in the offspring due to homozygous lethality caused by the balancer chromosomes.

1.4.2 *Drosophila* as a model for neurodegenerative disease

Neurodegenerative diseases are the result of neuronal death in the nervous system which leads to disruption in cognition, motor functions and eventually death. The nervous system is one of the most, if not the most, complex system in humans. Therefore, studying these disorders in human poses technical and ethical challenges. Human genetics and genomic studies have helped linked many of these disorders to candidate genes e.g. *apolipoprotein E (APOE)* to Alzheimer disease (AD) (Harold *et al.*, 2009), *LRRK2* to PD (Funayama *et al.*, 2002), and *Huntingtin (HD) gene* to Huntington's disease (Gusella *et al.*, 1983). However, identifying the pathological mechanism and progression of the disease is still difficult because the diagnosis usually occurs post-mortem or late when most of the initially affected neurons are dead. These challenges are best tackled with animal models and *Drosophila* has been shown to be very useful for modelling neurodegenerative diseases (McGurk *et al.*, 2015).

Technically, the short lifespan and the large isogenic number of flies it can produce are valuable in studying human ailments that are age-related (Hirth, 2010). Additionally, basic aspects of cell biology are quite similar in humans and flies, including regulation of gene expression, membrane trafficking, neural connectivity, cell signalling, and cell death. Many genes and pathways have been later discovered in mammals that were originally studied in flies. For example, Wnt protein that is crucial in many aspects of mammalian cell biology was studied first identified and studied in mutant wingless flies. This phenotype is caused by loss of the *Drosophila wingless* gene, an orthologue of the *Wnt* gene in mammals (Sang and Jackson, 2005).

There are very few ethical and safety issues in using *Drosophila* in scientific research compared to other animals such as mice. For example, using *Drosophila* doesn't require certain licensing from governments.

Drosophila have already proven highly successful in the study of neurodegenerative disorders including AD, PD, HD, Amyotrophic Lateral Sclerosis (ALS), and many others (Afsari *et al.*, 2014, Cao *et al.*, 2008, Watson *et al.*, 2008, Weiss *et al.*, 2012).

1.4.3 *Drosophila* models of PD

As mentioned earlier, a comprehensive one model that would recapitulate all hallmarks of PD is not yet available. Therefore, choosing the best model that fit the researcher needs is crucial. Most *Drosophila* models of PD have shown selective age dependent DA neurodegeneration that mimic what is found in humans which make them a great candidate to uncover the mechanism of this degeneration (Xiong and Yu, 2018). This is interesting because transgenic mice models, apart from viral mediated ones, have failed to replicate this aspect of the disease. A different dopamine metabolism and the expression of intrinsic protective factors or other genetic modifications that prevent the toxic effects of these PD-related mutations could explain this failure in mice (Burbulla *et al.*, 2017, Dawson *et al.*, 2010). Additionally, a large-scale drug screening and discovery is much more rapid and cost-effective in *Drosophila* compared to mice.

Despite lacking the homologous gene, expressing human α -synuclein in *Drosophila* was revealed to be successful in generating a PD disease model. In 2000, (Feany and Bender, 2000) managed to generate a fly model that expresses α -synuclein in neurons which then displayed age dependent DA neurodegeneration, neuronal inclusions and locomotor dysfunction. These phenotypes were replicated by others with varying

degrees of similarity (Chen and Feany, 2005, Periquet *et al.*, 2007). It is worth re-stating that the *Drosophila* genome contains no apparent ortholog of *SCNA* which would contribute to the generation of LBs.

PRKN and *PINK1* have been shown to be involved in mitochondrial abnormalities, which is one of the key observations found in PD. Mutations in both genes in flies exhibited similar phenotypes of mitochondrial abnormalities, reduced lifespan and locomotive impairment. Moreover, the overexpression of *human PINK1* in mutant *PINK1* flies have managed to restore normal mitochondrial morphology which suggest a conserved functionality. Also, both genes seem to be essential in regulating mitochondrial function (Clark *et al.*, 2006, Greene *et al.*, 2003).

Two orthologs of the *DJ-1* gene, that when mutant can cause PD in humans, exist in flies, *DJ-1 α* and *DJ-1 β* . The expression of *DJ-1 β* is more wide-spread than *DJ-1 α* which is mostly expressed in male testis. Flies with double knockout genes looked fairly normal in terms of viability, fertility and lifespan; however, when exposed to oxidative stress such as H₂O₂ and paraquat they displayed sensitivity that was rescued by re-introducing the genes into the flies (Meulener *et al.*, 2005). In another model, (Menzies *et al.*, 2005) were able to demonstrate that overexpression of *DJ- α* protected DA neurons from the insult of paraquat. These results suggested a possible role of *fly DJ-1* in protection against environmental and oxidative stress that can be seen in PD.

1.4.3.1 *LRRK2 Drosophila* models of PD

By producing and analysing LRRK transgenic alleles and loss of function mutants in *Drosophila*, (Lee *et al.*, 2007) developed a fly model for the fly homolog of *LRRK2* (*dLRRK*) and convincingly established an endogenous role for *LRRK2* in preventing the degeneration of DA neurons. No DA neurons loss or impairments in locomotive function were seen in this investigation. Pathogenic mutants and wild-type *dLRRK* transgenic expression did not demonstrate any noticeable abnormalities, whereas *dLRRK* loss-of-function mutants have significantly reduced locomotor activity. Additionally, the morphology and significant loss in tyrosine hydroxylase (TH) immunostaining of DA neurons in *dLRRK* mutants suggested a neurodegeneration in the mutants (Lee *et al.*, 2007).

The human *LRRK2-WT* and the mutant form *LRRK2-G2019S* were overexpressed to construct a gain-of-function *LRRK2 Drosophila* model by (Liu *et al.*, 2008). Expression

of both forms of *LRRK2* resulted in premature mortality, locomotor impairment, retinal degeneration, and selective loss of DA neurons in the brain. Furthermore, compared to *LRRK2-WT*, *LRRK2-G2019S* induced a more severe parkinsonism-like phenotype. L-DOPA treatment alleviated the *LRRK2-G2019S* induced locomotor impairment but did not prevent the loss of TH-positive neurons (Liu *et al.*, 2008).

(Imai *et al.*, 2008) employed *Drosophila* to study how LRRK2 functions normally in the body and how its dysfunction results in DA neurodegeneration. They showed genetic and biochemical data that *dLRRK* controls protein synthesis in order to maintain DA neurons. In addition, they observed that LRRK2 primes 4E-BP phosphorylation, and that action plays a significant role in mediating the pathogenic consequences of mutant *dLRRK*. Lastly, they found that behavioural abnormalities are accompanied with dopamine and dopaminergic cell death (Imai *et al.*, 2008).

The expression of the transgenics *G2019S*, *Y1699C*, and *G2385R* variant in flies showed late-onset loss of DA neurons in specific clusters and exhibited locomotor abnormalities compared to the *LRRK2-WT* (Ng *et al.*, 2009). Additionally, no retinal degeneration was observed in flies aged 20 or 60 day old. This discovery is in line with the findings of (Imai *et al.*, 2008, Lee *et al.*, 2007) where transgenic flies expressing *LRRK2-WT* are protected from this age-associated phenotype, whereas mutant *LRRK2*-mediated degeneration appeared to be late-onset and is limited to specific clusters of DA neurons. However, the findings in (Liu *et al.*, 2008) were in contrast to (Ng *et al.*, 2009) where degeneration in *Drosophila* expressing either *LRRK2-WT* or *LRRK2-G2019S* was observed to occur non-selectively across all the DA neuronal clusters and a significant retinal degeneration at as early as 3 week old flies.

Using *Drosophila* electroretinograms (ERGs), (Hindle *et al.*, 2013) examined the impact of *LRRK2* mutations. They reported that in flies expressing *LRRK2-G2019S* mutation in the DA neurons, the photoreceptor function was gradually deteriorating. After 28 days, it was found that there had been a loss of vision and that the photoreceptors had high levels of autophagy, apoptosis, and mitochondrial disorganisation. Furthermore, even in areas not directly innervated by DA neurons, fly head dissections showed widespread neurodegeneration across the visual system. Other mutations tested didn't show any photoreceptors degeneration or loss of vision. Lastly, they manipulated the levels of *dLRRK* expression simultaneously with expressing

LRRK2-G2019S in DA neurons and came to the conclusion that the *LRRK2-G2019S* mutation is a gain of function rather than dominant negative (Hindle *et al.*, 2013).

In summary, *Drosophila* is one of the most powerful organisms to use as a model in PD and neurodegenerative diseases in general due to its relatively cheap cost, short and rapid lifespan, having less ethical issues, ease of handling and keeping, similarity to humans in many biological aspects and wide experimentation for over 100 years. However, as in all animal models, there are some drawbacks in using *Drosophila*. It has to be transferred into fresh media on a regular basis to keep stocks viable i.e., it can't be frozen for long term storage. Moreover, the small size of *Drosophila* may introduce some difficulty in terms of handling and experiment design.

1.5 Investigating PD through *Drosophila* eyes

When modelling PD in animals, one might wonder how eye and vision relates to PD. In the next sections, the case for using *Drosophila*'s visual system to investigate PD will be discussed.

1.5.1 The retina

The retina is the neural part of the eye responsible for receiving the outside light and processing it into signals that are transmitted via the optical nerves to the brain where these signals are converted into perceived images. This processing is mediated by different types of neural cells, namely photoreceptors, horizontal cells, bipolar cells, amacrine cells and ganglion cells with metabolic and homeostatic support provided by different glial cells and retinal pigment epithelial cells. These retinal cells are organised in distinctive histological layers and starting from where light comes in i.e., outside to inside, there are the ganglion cell layer (GCL), inner plexiform layer (IPL), inner nuclear layer (INL), outer plexiform layer (OPL), and outer nuclear layer (ONL). These layers are sandwiched between a nerve fibre layer and a retinal pigment epithelium (RPE) layer (Sung and Chuang, 2010) (Figure 1.11) demonstrates the structure of the retina. ONL contains photoreceptors which are responsible for sensing light and transmitting it as an electrical signal to the next order of neurons. Photoreceptors are dominated by rods comprising 95% of all photoreceptors compared to 5% of cones that are concentrated in the foveola. Rods are responsible for low-light (scotopic) vision while cones are specialized for bright-light (photopic) colour vision (Lamb, 2016). The location of these photoreceptors (at the back of the retina) might seem counterintuitive at first but RPE

that set in proximity to photoreceptors help to absorb any scattered light that would cause image distortion (Archibald *et al.*, 2009). OPL contains horizontal cells which feedback and feedforward signals from photoreceptors and bipolar cells (Masland, 2012a). Bipolar cells somas are found in INL and are responsible for receiving information from the photoreceptors and projecting it to the retina ganglion cells (RGCs). Depending on the signal received from photoreceptors, bipolar cells can be divided into ON-bipolar cells (depolarize in response to light) or OFF-bipolar cells (hyperpolarize in response to light). Cones can be connected to either ON or OFF types of bipolar cells while rods are only connected to ON ones (Euler *et al.*, 2014). The next layer (IPL) contains amacrine cells and the synapses of bipolar cells and RGCs. Like horizontal cells, amacrine cells modulate the information transfer between bipolar cells and RGC and they are extremely diverse in function and level of axon stratifications (Masland, 2012b). The last layer (GCL) as the name suggests contains RGCs. These cells are the last stop of information modulation before it travels to the brain through the optic nerve. The GCL transmit image and non-image forming signals that help in the function of circadian rhythm, melatonin release modulation, and pupil size regulation (Mahabadi and Al Khalili, 2020).

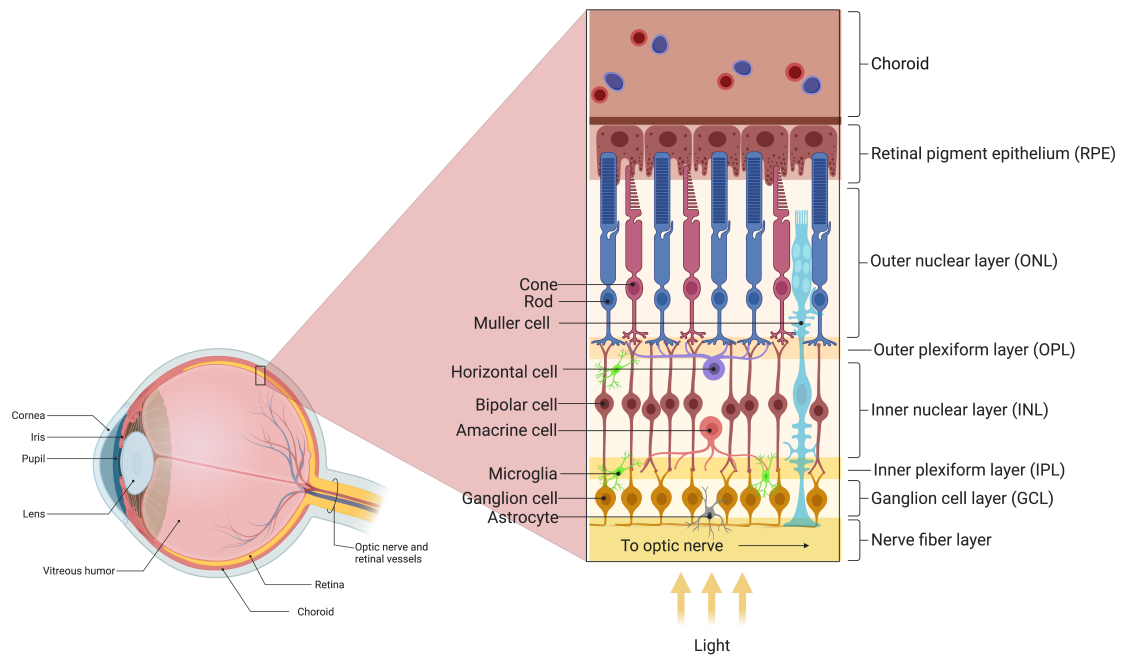


Figure 1.11. The structure of the eye and retina

Schematic sagittal section of the eye with the different histological layers and neural cells of the retina highlighted.

1.5.2 Visual dysfunctions in PD

Visual dysfunction is one of the non-motor symptoms reported by PD patients. The reported symptoms include visual hallucination, double vision, difficulty in reading, and deficit in colour discrimination and contrast sensitivity (Price *et al.*, 1992, Urwyler *et al.*, 2014). Using assays to evaluate the visual function such as electroretinogram (ERG), visual dysfunctions have been reported in patients (Bodis-Wollner *et al.*, 1987) and animal models (Hindle *et al.*, 2013, Onofrij and Bodis-Wollner, 1982). The cause for this dysfunction is not clear but likely involves the degeneration of DA neurons, just like in the *SNpc*, could be one. Among the different types of retinal cells, A18 amacrine cells have been identified as DA neurons and are located in the INL (Frederick *et al.*, 1982). Studies have shown that the INL was significantly thinner in PD patients (Hajee *et al.*, 2009) and the DA innervation was reduced (Nguyen-Legros, 1988). Additionally, post-mortem analysis has revealed a significant reduction of retinal DA neurons in PD patients. Interestingly, this reduction was comparable to non-PD patients for patients who received L-DOPA treatment (Harnois and Di Paolo, 1990). Similar results have been observed in animals as well. For example, a decrease in DA amacrine cells in mice (Marrocco *et al.*, 2020), a reduction in dopamine level in rats (Meng *et al.*, 2012), and

neurodegeneration in the retina of flies (Hindle *et al.*, 2013). These results suggest a crucial role for dopamine in maintaining the normal function of the retina. In addition to the DA degeneration, α -synuclein aggregates have been identified in the retina of PD patients and could explain the visual abnormalities (Ortuño-Lizarán *et al.*, 2018). Visual dysfunction can result from abnormalities beyond the retina such as abnormalities in the visual cortex (Weil *et al.*, 2016).

1.5.3 The structure of the *Drosophila* visual system

The visual system in *Drosophila* consists of the retina and the optic lobe. The retina, or the compound eye, is made up of about 800 individual units known as ommatidia that are organised in hexagonal crystalline array. Each ommatidium is insulated by pigment cells that prevent light passing between ommatidia. The core of the ommatidium contains 8 photoreceptor (R) cells with 6 in the outer region (R1-R6) while the other two (R7-R8) in the inner one. These cells are arranged in an asymmetrical trapezoid and only 7 can be seen (R1-R7) because R8 is located below R7 (Kumar, 2012) (Figure 1.12). Each R cell contains a microvillar structure known as rhabdomeres which express a light absorbing molecule called rhodopsin (Rh). On the one hand, R1-R6 express Rh1 and are similar to the mammalian rods in that they are involved in dim light vision and motion perception. On the other hand, R7 and R8 are similar to the mammalian cones in that they involved in colour vision and express different types of Rh. R7 expresses UV-sensitive Rh3 and Rh4 while R8 expresses blue-sensitive Rh5 and green-sensitive Rh6 (Behnia and Desplan, 2015). Rh2 is an UV-sensitive Rh that is expressed in the ocelli which is a simple eye found in the upper part of the fly head responsible for light detection rather than image formation and will not be discussed any further here (Montell, 2012, Salcedo *et al.*, 1999).

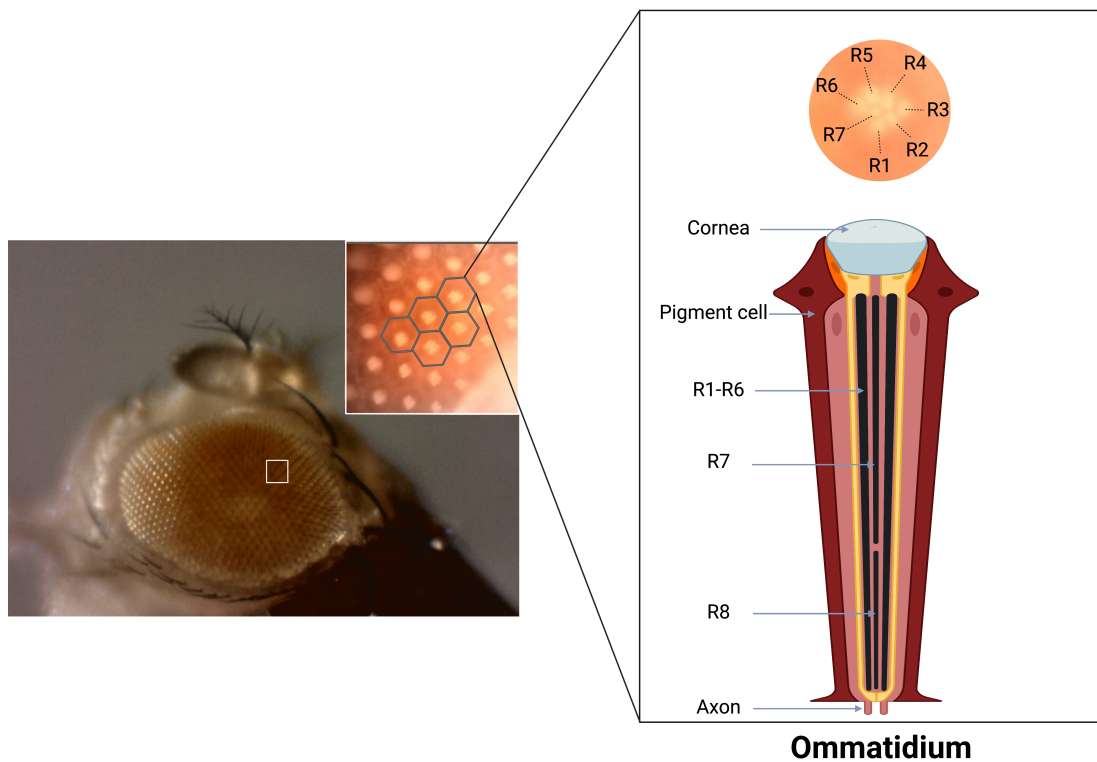


Figure 1.12. *Drosophila* eye with a schematic structure of the ommatidium.

The left image shows a *Drosophila* eye with the white square focusing on a group of ommatidia that are arranged in hexagonal crystalline array. The right image shows a schematic structure of a single ommatidium with the asymmetrical trapezoid arrangement of the photoreceptors above it.

The retina projects its synapses to the optic lobe which consists of the lamina, the medulla, and the lobula complex (lobula and lobula plate) (Figure 1.13). The modular organisation of the retina is maintained in the lamina where around 750 independent units called cartridges receive signals from the outer photoreceptors (R1-R6) that are involved in motion processing (Paulk *et al.*, 2013). The lamina contains five types of monopolar neurons that connect the retina to the medulla and amacrine cells that have connection within the lamina. The inner photoreceptors (R7 and R8) project directly to the medulla passing the lamina. The medulla is arranged in 10 layers (M1-M10) with the regions from M1 to M6 called the distal medulla and the regions from M7-M10 called proximal medulla. The distal medulla receives signals from the retina and the lamina while the proximal one receives information from the distal medulla. The medulla is the largest part of the optic lobe with around 40,000 neurons (Neriec and Desplan, 2016). The lobula complex is the last stop for visual information to go through before going to the central brain for further processing.

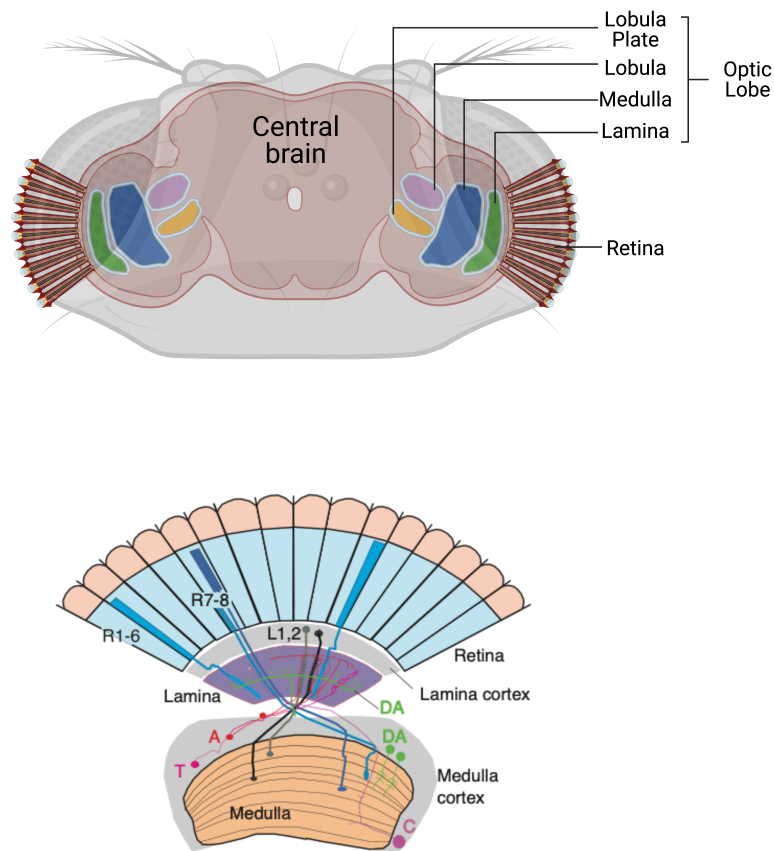


Figure 1.13. The anatomy of *Drosophila* visual system

The upper image shows a schematic structure of *Drosophila* visual system as described in (Nericc and Desplan, 2016). The lower image is adapted from (Afsari *et al.*, 2014) and shows photoreceptors (R1–R8), second-order lamina neurons (L1 and L2), amacrine neurons (A), and two kinds of third-order medulla neurons (C and T). The figure also highlights dopaminergic neurons (DA) that are intrinsic to the medulla and others that branch into the lamina.

1.5.4 Similarities between the *Drosophila* and human visual systems

In a quest to find a simpler neural circuitry than the retina of vertebrate, Santiago Ramón y Cajal and his colleagues turned to the fly visual system. To their surprise, they found cellular diversity and complexity similar to that observed in the vertebrate retina (Ramon y Cajal and Sanchez, 1915). Even though it is more than a century ago (Figure

1.14), their detailed drawing is still relevant in illustrating the similarities between the two systems.

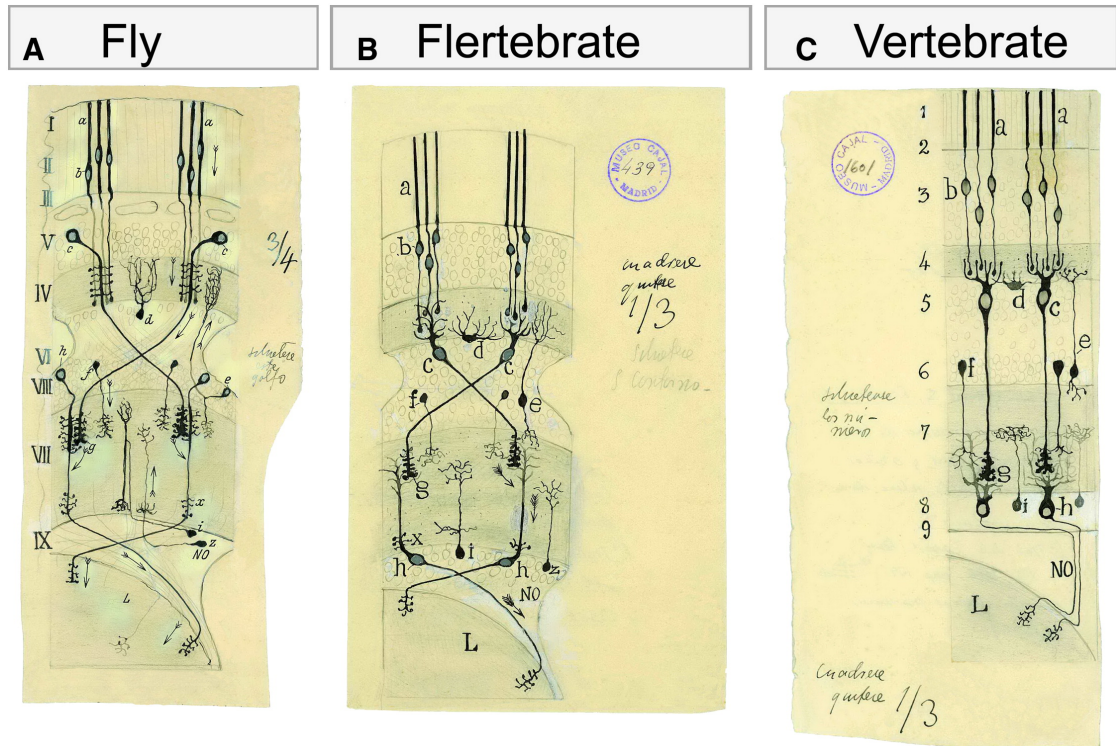


Figure 1.14. Cajal's drawing of fly and vertebrate visual systems

A) A drawing of the fly visual system with the different types of neurons and layers indicated with letters and Roman numerals, respectively. B) A drawing of fly visual system with the neurons cells bodies moved to correspond to their position in vertebrates. C) A drawing of vertebrate visual system with the different types of neurons and layers indicated with letters and Arabic numerals, respectively, that correspond with the fly system. Adapted from (Sanes and Zipursky, 2010)

The similarities between the two systems are interior rather than exterior. These similarities include the arrangement of neurons in distinctive layers, the small number of main neuronal types (5 in vertebrate and 6 in fly), the presence of multiple contact synapses with a single presynaptic terminal in close contact to multiple postsynaptic elements, and the arrangement of neurons in orderly mapping from one level to the next (review by (Sanes and Zipursky, 2010)'s Figure 1.15). Furthermore, like humans, *Drosophila* has DA neurons that innervate the visual system (Hindle *et al.*, 2013).

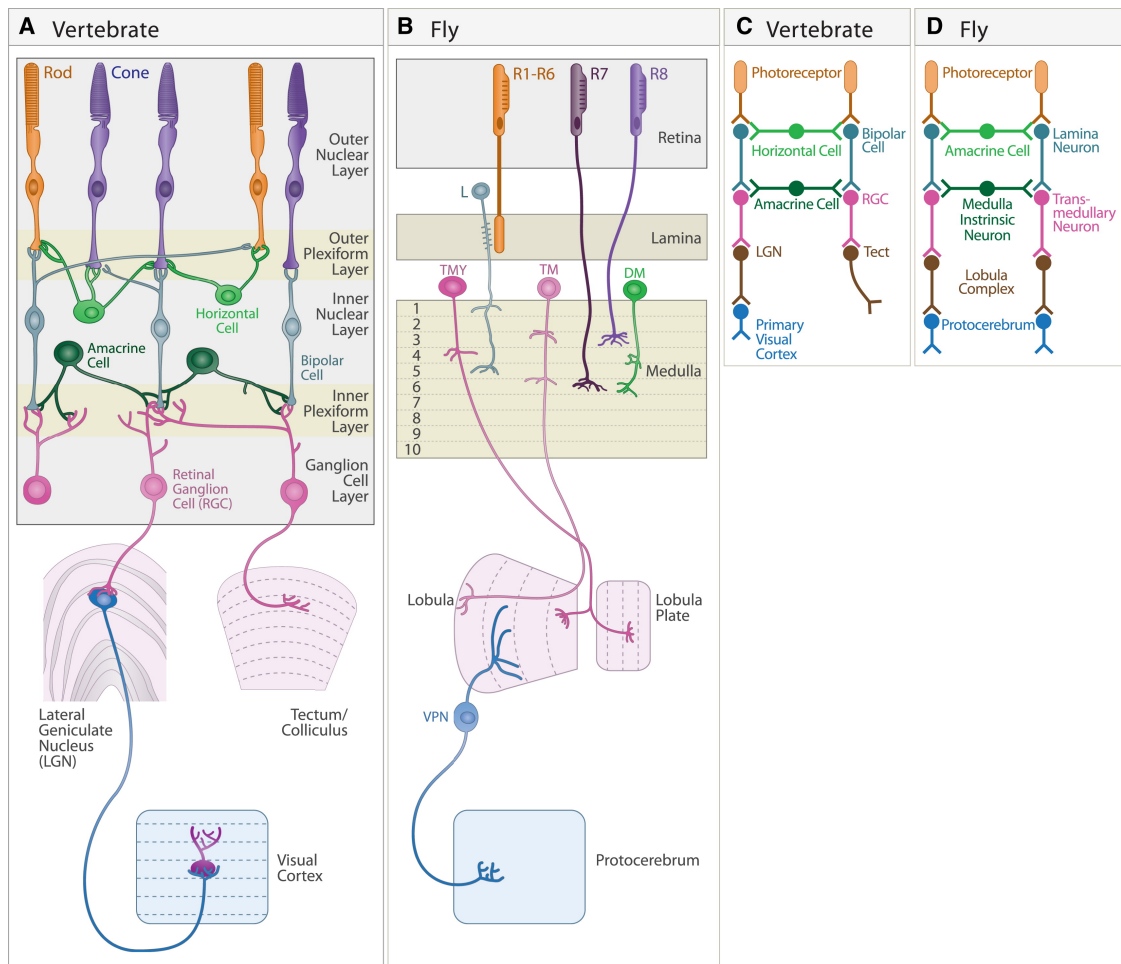


Figure 1.15. Similarities between vertebrate and fly visual systems

A and B show the similar neurons and layers between the two systems in colour coded manner. C and D show the similar steps in information transfer through the visual system. Adapted from (Sanes and Zipursky, 2010)

The similarities between the two systems can be observed in the phototransduction which is the process of converting light into electrical signals. Both vertebrates and invertebrates carry out phototransduction via a specialised form of a G protein-coupled receptor cascade (Figure 1.16). When a photon is absorbed by a molecule of visual pigments, it causes the isomerisation of the light-sensitive vitamin A derivative 11-cis 3-hydroxyretinal to all-trans 3-hydroxyretinal; in vertebrates, the isomerisation of the chromophore 2-dehydroretinal is needed instead of 3-hydroxyretinal. In both cases, this isomerisation results in the activation of rhodopsin, which forms metarhodopsin. In flies, metarhodopsin binds to the alpha subunit of a heterotrimeric G-protein (Gq), causing GDP to be exchanged for GTP and the G-alpha subunit to be activated. Phospholipase C (PLC) is activated by the active G-alpha subunit, which cleaves

phosphatidyl inositol 4,5 bisphosphate into inositol triphosphate (InsP₃) and diacyl glycerol (DAG). There is a calcium influx into the photoreceptors, and two hypotheses have been proposed to explain how this influx happens. According to one of these hypotheses, when InsP₃ binds to the InsP₃-receptors found in intracellular Ca²⁺ storage, the cation channels TRP and TRPL are activated. As a result, Ca²⁺ is released via a store-operated process. According to the second concept, DAG indirectly gates the TRP and TRPL channels, resulting in an influx of Ca²⁺ and Na⁺ into the photoreceptors. The influx of Ca²⁺ leads photoreceptors to depolarize, resulting in histamine release at the synapse. This subsequently causes downstream neurons to hyperpolarize. In contrast to *Drosophila*, vertebrate phototransduction does not make use of the inositol phospholipid signalling pathway. Instead, the G-protein effector is a phosphodiesterase that converts 3'-5' cyclic guanosine monophosphate (cGMP) to 5' GMP. This causes cGMP-gated channels to close and hyperpolarisation to occur (Hardie and Juusola, 2015, Hardie and Raghu, 2001).

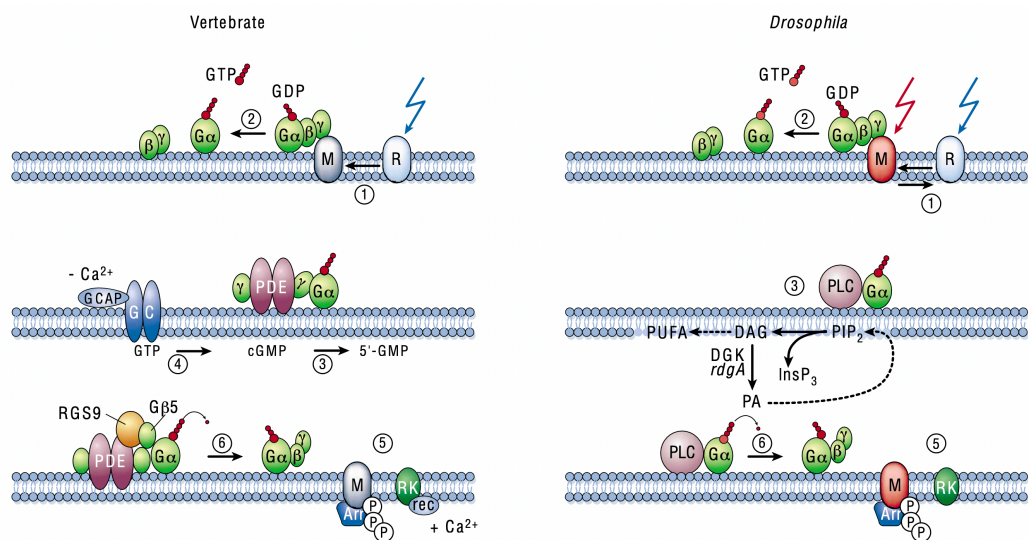


Figure 1.16 Phototransduction cascades in vertebrates and *Drosophila*

Numbers in circles (1-6) refer to the following steps: (1) Photoisomerisation; rhodopsin (R) is photoisomerised to metarhodopsin (M). Long-wavelength light can convert M back to R in *Drosophila*; in vertebrate, M releases the bound chromophore *all-trans* retinal. (2) GTP/GDP exchange; On the heterotrimeric G-protein (transducin in vertebrate rods, Gq in *Drosophila*), M catalyses the exchange of GDP for GTP, leading to the dissociation of the active GTP-bound α -subunit. (3) Activation; G α binds to and activates the effector enzyme (PDE in vertebrate rods, PLC in *Drosophila*). (4) Substrate resynthesis; in vertebrates, cGMP is resynthesised by guanylate cyclase (GC) and GC-activating protein (GCAP), which is inhibited by Ca²⁺. In *Drosophila*, DAG is converted to phosphatidic acid (PA) by DAG kinase (DGK). PA is converted to PIP₂ via a multienzymatic pathway. (5) Metarhodopsin inactivation; rhodopsin kinase (RK) phosphorylates M, which is then capped by arrestin (A). In the presence of Ca²⁺,

recoverin (Rec) inhibits RK in vertebrates. (6) Inactivation of G protein and effector; The GTPase activity of the G protein inactivates the effector enzyme and $G\alpha$, resulting in reassociation with $G\beta$, γ . This is accelerated by the activity of RGS9, G β 5 and PDE in vertebrate rods, and by PLC in *Drosophila* (Hardie and Raghu, 2001).

In conclusion, the retina is highly organised tissue and shares key neurons and features with the brain. It provides an accessible platform to study the CNS and this accessibility led to the development of many experimental non-invasive tools. Using the fly visual system to model PD can help shed some light on visual dysfunction and DA neurons loss found in PD.

1.6 Aims

Since the discovery of LRRK2 association to PD in the early 2000s, many studies have been undertaken to investigate the cellular basis of this link. No precise mechanism has been identified and studies are still on going to elucidate how mutations in *LRRK2* leads to PD pathology. This project aims to further our knowledge on the mechanism of action of LRRK2 and how mutations in this gene may lead to neurodegeneration. *Drosophila melanogaster* will be used mainly as the animal model. Loss-of-function (LOF) and gain-of-function approaches will be used to examine the effect of LRRK2 in the visual response of flies. Examining the visual response of flies provides results that can be quantifiable and help us understand the consequences of producing too little or too much LRRK2 in dopaminergic neurons in a functioning nervous system. Additionally, this project will aim to establish the stability and half-life of LRRK2 protein. This will help us understand the functional window over which the protein functions. The specific contributing aims of this investigation are outlined below:

1. To test the autonomy of LRRK2 activity by assessing the ability of *dLRRK*, the *Drosophila* orthologue of human *LRRK2*, to act in neuronal tissues when expressed in non-neuronal tissues to rescue visual dysfunction in old flies. This study will be linked an examination of the genetic interaction between eye colour genes and *dLRRK* where previously a synthetic lethality has been observed.
2. To determine the effect of increased *LRRK2-G2019S* activity on eye anatomy and physiology.
3. To test the stability of LRRK2 protein *in vitro* and *vivo* and the effect of mutations and kinase inhibitors on its stability.

2 Materials and Methods

2.1 *Drosophila* husbandry and genetics

2.1.1 *Drosophila* stocks

Drosophila stocks used in this project were purchased from Bloomington *Drosophila* Stock Centre (BDSC, Indiana University, Bloomington, USA), or were kindly donated from members of the *Drosophila* community. Rebalancing or recombination stocks also generated additional stocks. A summary of primary stocks used in this project are listed in Table 2.1. Stocks were quarantined before first use for at least 2 generations to confirm that they were mite free.

Stocks were raised at either 18°C or 25°C and were transferred to fresh media every 4 or 2 weeks, respectively. Experimental crosses performed were raised at either 25°C or 29°C, giving a generation time of about 10-12 days.

Table 2.1 Fly Stocks

Stock (referred to as)	Description	Source
Wild type		
<i>Canton-S</i> (+)	Wild-type, red eyes	Elliott/Sweeney Lab Stock
<i>w¹¹¹⁸</i> (<i>w</i>)	Wild-type, white eyes	Elliott/Sweeney Lab Stock
<i>w^{apricot}</i> (<i>w^a</i>)	Wild-type, orange eyes	BDSC #148
Balancer Stocks		
<i>w⁻</i> ; +/+; TM3/TM6B	Third Chromosome Balancer	Elliott/Sweeney Lab Stock
<i>W⁻</i> ; <i>CyO/If</i> ; TM6B/MKRS (DB)	Second and Third Chromosome Balancer	Elliott/Sweeney Lab Stock
Mutant Stocks		
<i>w⁻</i> ; +/+; <i>dLRRK^{e03680}</i> (<i>dLRRK^{LOF}</i>)	PBac(Burbulla <i>et al.</i>) <i>PiggyBac</i> -element disruption of <i>dLRRK</i> , generation of <i>dLRRK</i> loss of function mutant	(Wang <i>et al.</i> , 2008a)
<i>cn^{35k}</i>	<i>cinnabar</i> hypomorphic allele mutant	BDSC #268
<i>pr¹</i>	<i>purple</i> mutant	BDSC #370
Gal4 Stocks		
P(Gal4)56C (Pigment cell)	Eye pigment cells specific driver.	BDSC #27328
P(GawB)c564 (Repo tract)	Adult male accessory gland, seminal vesicle, ejaculatory duct, testis sheath, cyst cells and spermatocytes driver.	BDSC #6982
<i>Lsp2</i> -Gal4 (Fat body)	Fat body specific driver.	BDSC #6357

<i>rhl-Gal4/CyO</i>	Rhodopsin 1 promoter; photoreceptor specific driver	(Gonzalez-Bellido <i>et al.</i> , 2009)
<i>TH-Gal4</i>	Tyrosine hydroxylase; DA neuron specific driver	(Friggi-Grelin <i>et al.</i> , 2003)
<i>elav^{GS}-Gal4</i>	Embryonic lethal abnormal vision; pan-neuronal driver (gene switch)	BDSC #8760 (Osterwalder <i>et al.</i> , 2001)
<i>elav-Gal4</i>	Embryonic lethal abnormal vision; pan-neuronal driver	BDSC #43642
<i>GMR-Gal4</i>	Glass multimer reporter; eye specific driver	Elliott/Sweeney Lab Stock
UAS Stocks		
<i>UAS-hLRRK2/CyO</i>	Human <i>LRRK2</i> transgene	H. Lundbeck A/S, Denmark
<i>UAS-hLRRK2</i>	Human <i>LRRK2</i> transgene	(Liu <i>et al.</i> , 2008)
<i>UAS-hLRRK2-G2019S</i>	Human <i>LRRK2-G2019S</i> mutant transgene	
<i>UAS-hLRRK2-G2019S-K1906M</i>	Human <i>LRRK2-G2019S-K1906M</i> mutant transgene (kinase dead)	(Lin <i>et al.</i> , 2010)
<i>UAS-hLRRK2-R1441C</i>	Human <i>LRRK2-R1441C</i> mutant transgene	
<i>UAS-hLRRK2-G2385R</i>	Human <i>LRRK2-G2385R</i> mutant transgene	
<i>UAS-hLRRK2-I2020T</i>	Human <i>LRRK2-I2020T</i> mutant transgene	(Venderova <i>et al.</i> , 2009)
<i>UAS-hLRRK2-I1122V</i>	Human <i>LRRK2-I1122V</i> mutant transgene	
<i>UAS-dLRRK/CyO; dLRRK^{e03680}/TM6B</i>	<i>Drosophila LRRK</i> transgene; heterozygote <i>dLRRK</i> mutant	Elliott/Sweeney Lab Stock
<i>UAS-Sptr</i>	Second chromosome <i>sepiapterin reductase</i> insertion	(Kim <i>et al.</i> , 2017)
<i>UAS-se</i>	Second chromosome <i>sepia</i> insertion	
<i>UAS-pu</i>	Third chromosome <i>punch</i> insertion	

2.1.2 *Drosophila* media

Stocks were maintained in 25x95 mm plastic vials (Dutscher Scientific, UK) plugged with cotton wool (Fisher Scientific, UK) containing about 7 ml standard yeast-sucrose-agar media: (25 g/l sucrose, 3.75 g/l agar, 0.125 g/l CaCl₂, 0.125 g/l FeSO₄, 0.125 g/l MnCl₂, 0.125 g/l NaCl, 2 g/l KNaC₄H₄O₆.4H₂O); following boiling and cooling for 1 hr to about 45°C, the antifungal agents Bavistin (1.5 mg/l in 100% ethanol [EtOH]; BASF, Auckland, New Zealand) and Nipagin (0.7 mg/l in 100% EtOH; Sigma, UK) were added. Experimental flies kept on this media were transferred to fresh vials every 3-4 days.

For drug experiments, 4-24[®] instant *Drosophila* medium (Carolina Biological Supply Company, USA) was utilised. The instant media was prepared by mixing 50:50 with dH₂O. Stocks solutions of pharmaceuticals (10 mg/ml) were prepared by dissolving the drugs into 100% ethanol or dH₂O with subsequent storage at 4°C or -20°C. The appropriate volumes of these stocks were added to dH₂O to give the desired concentration according to the experiment before it was mixed with the instant food media.

In some instances, dried yeast is added to the medium to encourage flies to lay eggs. Experimental flies were aged at 29°C in complete darkness. When required in large numbers, stocks were raised in 1/3 pint bottles.

2.1.3 *Drosophila* anaesthesia

Adult flies were anaesthetised on a porous gas pad with continuous CO₂ administration to identify gender and genotype. Anaesthetised flies were observed using a dissecting microscope (Zeiss Stemi-2000, Carl Zeiss AG, Germany).

2.1.4 *Drosophila* crossing techniques

A crucial step in performing *Drosophila* crosses is to isolate virgin females in order to have a controlled genetic cross. *Drosophila* males and females are easily distinguished. Males have blackened tip to their abdomen and a patch of bristles on their foreleg, known as sex combs, compared to the females. Newly eclosed flies exhibit a pale pigmentation, unexpanded wings and the presence of a meconium, visible through the abdominal cuticle (Figure 2.1). At 25°C, female flies will not mate within 8 hours of eclosion. Based on this criterion, virgin females were collected in the morning through completely emptying vials and isolating obvious virgins based on the presence of the meconium and lack of cuticle tanning and then collecting any further females that eclosed within the following 8 hrs. Adult males and female virgins were then crossed in a fresh food vial. The parent flies were then removed after 7 days and transferred into a new vial/bottle or discarded in order to prevent over-crowding and allow specific selection of first generation for further crosses or experiments. All the experimental crosses performed were raised at either 25°C or 29°C, giving a generation time of 10-12 days (egg to adult).

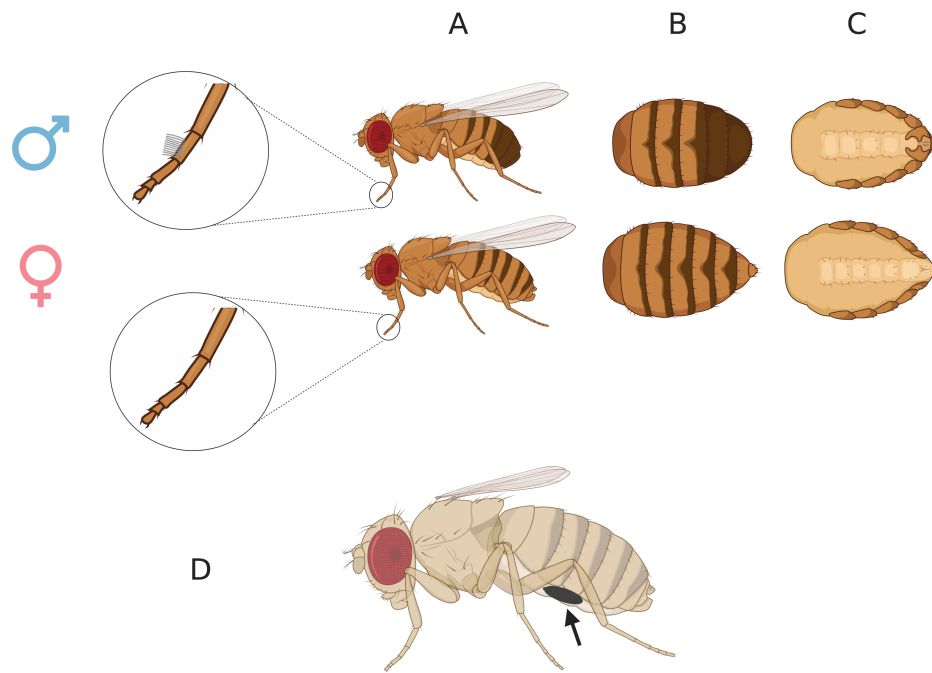


Figure 2.1 Selection criteria for *Drosophila* crossing

A-C Views of male (top) and female (bottom) *Drosophila*. A) Lateral whole body view with a magnified view of the front legs showing the presence of sex combs in male. B) Dorsal abdomen view showing a slightly larger female with dark separated stripes at the posterior tip that is merged in male C) Ventral abdomen view showing a male with darker and more complex anal plates than the pin-like extension in females D) Lateral whole body view of a virgin female showing pale pigmentation and unexpanded wings. The arrow indicates the presence of a meconium (larval food remains) which is visible in the early hours after eclosure.

2.1.5 Recombination

To allow the use of two or more genetic components on a single chromosome, Homologous chromosomal recombination in female flies was utilised to generate stocks in which two genetic components were present on the same chromosomal arm. For example, this approach was used to recombine the $dLRRK^{e03680}$ *piggyBac* mutation with both *Lsp2-Gal4* (fat body driver) (Figure 2.2). Recombination is achieved through mating individual stocks with each other and selecting against balancers to identify male offspring that carry the two desired genetic components. Chromosomal recombination does not occur in male flies, so identified males can be then crossed to appropriate balancer stocks to capture the required synthetic chromosome containing the desired elements. Individual flies that carry two transgenic elements often have a darker eye colour due to the presence of two copies of the mW^+ (*mini-White*) eye colour cassette,

one being present on each element. These flies can be easily recognised and selected. These offspring were then crossed to virgin females from balancer stocks for the relevant chromosome and potential recombinant offspring were selected. Where possible, these selections were made based on eye colour as well as other characteristic phenotypes. The presence of the desired genetic components was confirmed via PCR for *dLRRK^{e03680}* (see Figure 2.7) and the expression of GFP for *Lsp2-Gal4* which was carried out by crossing the Gal4 fly to a UAS-GFP fly and then observing the expression in the progeny.

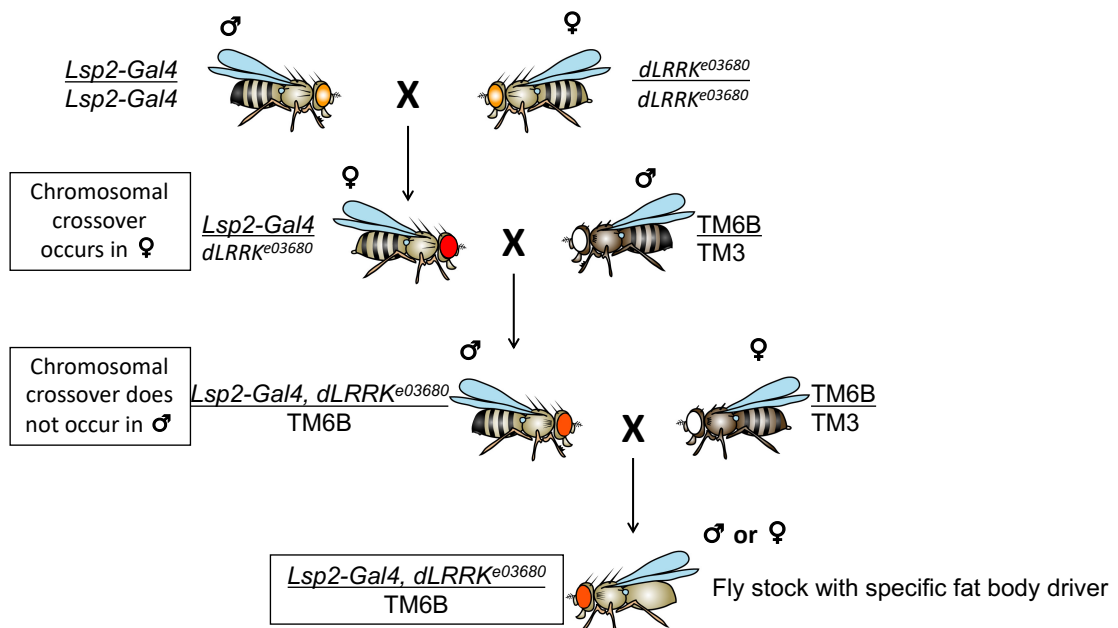


Figure 2.2. Recombination scheme in a *Drosophila* to allow the use of 2 desired elements on the same chromosome

The first cross is carried out to produce a fly that carry the 2 elements of interest (*Lsp2-GAL4* and *dLRRK^{e03680}*) on the same chromosome. Then, only female flies are crossed with a balancer fly to aid in appropriate offspring selection of flies with recombined chromosomes (darker eye, 2x *mW⁺*, and extra hairs on the thorax, *Hu* for *TM6B*). The final cross is carried out with only male flies to balancer flies to produce the stock and experimental flies.

2.2 Cell culture

2.2.1 Cell lines

Cell lines used in this investigation are Flp-In T-REx 293 cells that stably express different *LRRK2* mutations (*G2019S*, *D2017A*-Kinase dead) and the WT in inducible

and controlled fashion. These cells were obtained from Dario Alessi's lab (Dundee) and were made by transfecting HEK293 cells with plasmids and vector containing *LRRK2* gene (Nichols *et al.*, 2010). This fashion of expression is achieved due to the presence of tetracycline repressor that prevent *LRRK2* expression unless tetracycline (TC) or doxycycline (Doxy) is added (Figure 2.3).

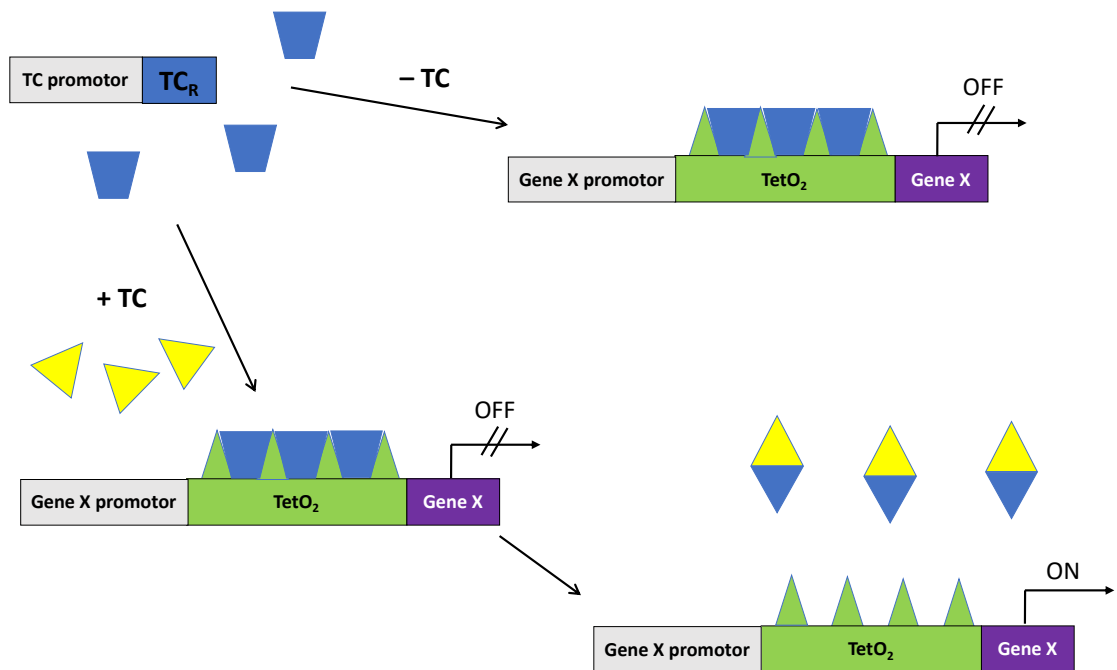


Figure 2.3. Flp-In T-REx system mechanism

Tetracycline repressor (TC_R) protein is expressed and binds to tetracycline operator 2 (TetO₂) sequence resulting in suppression of gene X expression. When tetracycline (TC) is added, it binds to TC_R and causes a conformational change that leads to its release from TetO₂ and de-suppression of gene X expression.

2.2.2 Growth and maintenance of cells

Cells were cultured in 1X Dulbecco's Modified Eagle Media (DMEM) (gibco, Invitrogen; + 4.5g/L D-Glucose, L-Glutamine, + Pyruvate) supplemented with 10% Foetal Bovine serum (FBS), 1:100 Penicillin/Streptomycin, 15 µg/ml blastocidin, and 100 µg/ml hygromycin.

To maintain cells for experiments, they were passaged every 3-4 days with a ratio of 1:5 in a 25cm culture flask. When cells reached around 90% in confluence, they were passaged by removing the media and then washing the flask with sterile Phosphate-

Buffered Saline (PBS). Cells were detached from the surface of the flask using either pre-warmed 1X trypsin/EDTA solution (Sigma; 0.5g porcine trypsin, 0.2g EDTA 4Na/L Hanks) (37°C for 3-5 mins) or a cell scraper. When using trypsin, the flask was hit on the sides firmly to dislodge cells after the incubation. After that, medium was added to neutralize trypsin and the cell mix transferred into 15 ml falcon tube. The tube was centrifuged at 1000 rpm for 5 mins and the supernatant is discarded. A pellet was left at the bottom of the tube that was resuspended in 1ml of media and passaged into new flasks according to appropriate ratios.

2.2.3 Counting and plating of cells

From the 1 ml resuspended pellet (see previous section), about 15 μ l is pipetted and added under a coverslip in a haemocytometer. Using a 10X objective in inverted microscope, cells were counted in one of the 4 large corner squares (4 X 4 grid, Figure 2.4). If there was fewer than 50 cells counted, another couple of squares were counted and an average is taken. The number of cells per ml was calculated by the number of cells in a 4 X 4 square multiplied by 10,000 e.g., a count of 100 = 1 X 10⁶ cells/ml. Cells will be diluted according to the typical plating densities (5-50,000 cells/well for a 24 well plate, 100,000-250,000 cells/well for a 6 well plate and 1-2 million cells/well for a 10 cm dish).

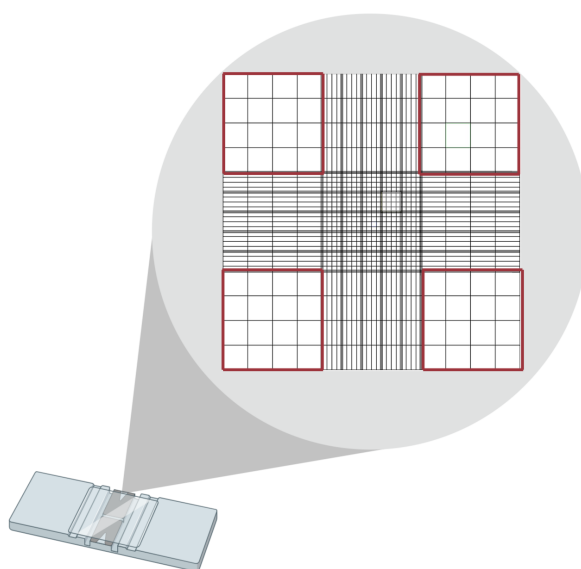


Figure 2.4. Haemocytometer gridlines

A haemocytometer with a zoomed-in image of the gridlines seen under the microscope to count cells. Cells were counted in any one of the 4 X 4 grid (red squares).

For LRRK2 stability and drug experiment, 6-well plates were used. After plating, cells were left for 24 hours to stick to the bottom of the flasks before doxycyclin was added (1 µg/ml) to induce the expression of LRRK2. It was then removed to stop the expression and the drug of choice was then added. Stocks solutions (10 mg/ml) were prepared by dissolving the drugs into DMSO (for MLI-2) or dH₂O (for B12) and were stored at 4°C or -20°C. The appropriate volumes of these stocks were added to the media to give the desired concentration according to the experiment.

2.3 Physiological and anatomical analyses

2.3.1 Flash Electroretinogram (fERG)

Unanaesthetised flies were pushed to the narrow end of a trimmed 200 µl yellow Gilson pipette tip so that just the head was left protruding. The fly then was fixed in place using nail varnish (La Femme, England, UK). In the ERG device, one glass electrode filled with simple *Drosophila* saline (130 mM NaCl, 4.7 mM KCl, 1.9 mM CaCl₂; Heisenberg, 1971) was placed on the surface of the eye for recording. Another glass electrode filled with the same saline is placed on the mouthparts was used as a reference. In one setup, flies were dark-adapted for 2 mins and then ERGs were recorded in response to five stimuli (10 seconds apart, 0.5 seconds long) of multiple channels blue LED light (Kingbright, KAF-5060PBESEEVGC, maximum emission wavelength 465 nm, Taipei, Taiwan) placed about 6 cm in front of the fly. The five stimuli were averaged for each fly. In another setup (eye adaptation experiment), a single LED channel was used to emit rapid flashes (100ms) of blue light at 5 seconds interval for 4 minutes in the dark. The amplitude of around 25 ERGs were averaged for each fly. An example of an ERG trace is shown in Figure 2.5.

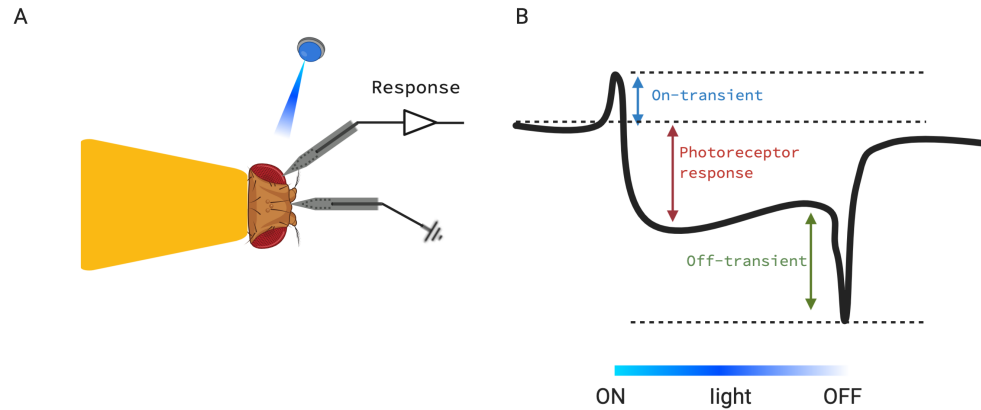


Figure 2.5. Recording the visual response of *Drosophila* using the flash ERG

A. Flies were restrained in shortened yellow pipette tips and exposed to light from the blue component of an LED light. An electrode filled with a simple saline solution was placed on the surface of the eye to record the response of the visual network, whilst a second electrode was placed within the mouthparts to act as a reference. B. A typical recording from a WT fly with the three main ERG components indicated. The on-transient was determined as the potential difference between the starting potential and the maximum value of the ERG trace. The photoreceptor response was determined as the potential difference between the starting level and the potential about halfway along the recording. The off-transient was determined as the potential difference between the end of the photoreceptor response and the minimum value of the ERG trace.

2.3.2 Deep Pseudopupil (DPP) and Pseudopupil Analysis (PPA)

For DPP, flies were prepared as described in the previous section (section 2.3.1) with an external white light positioned at an angle that would produce DPP (antidromic) in the eye of the fly. Footage was taken by an eyepiece camera (Dino-Eye Digital Eye Piece Camera, Dino-Lite, USA) fitted onto a dissecting microscope (Zeiss Stemi-2000 Carl Zeiss AG, Germany). For PPA, fly heads were decapitated on CO₂ pad and mounted onto a microscope slide using clear nail polish to fix the heads in place. Decapitated heads were held carefully from the proboscis using a tweezer to keep the eyes intact and heads should be fixed on the edges of the clear nail polish (Figure 2.6). When nail polish was dry, slides were examined under glycerol or oil 40X objective lens (Nikon) to analyse individual ommatidium and its rhabdomeres.

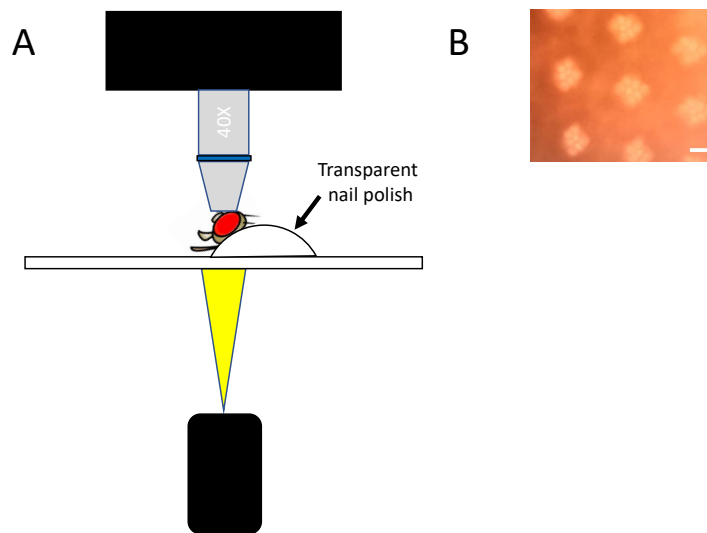


Figure 2.6. Schematic of the microscope setup for PPA

A. Fly head is fixed on a slide with transparent nail polish and the eye is positioned for visualization under a 40X objective immersion oil with a strong light illuminating the eye from below. B. Representative zoomed in image of an eye where multiple ommatidia can be visible. Scale bar = 50 μm

2.4 Molecular Biology

2.4.1 Genomic DNA isolation

Genomic DNA was isolated from single adult flies by homogenisation in 50 μl of extraction buffer (25 mM NaCl, 10 mM Tris-HCL pH 8.2, 1 mM EDTA) with the addition of Proteinase K (200 $\mu\text{g}/\text{ml}$). Proteinase K was added fresh on the day of the extraction. The homogenate was incubated at 37°C for 30 mins, followed by an incubation at 85°C for 10 mins in order to inactivate the proteinase K. To allow separation of particulates, the homogenate was centrifuged at 13000 rpm for 3 mins. 1-2 μl of supernatant was used as a PCR template. To increase the amount of isolated DNA, more than one fly was used.

2.4.2 Polymerase Chain Reaction (PCR)

The total volume of a PCR reaction was 20 μl and was run using 10 μl PCR mastermix (Promega, UK; 25 U/ml Taq DNA polymerase, Taq Reaction buffer, 200 μM of each dNTP, 1.5 mM MgCl_2), 1 μl of Forward primer and 1 μl of Reverse primer, 1-2 μl of genomic DNA and 6-7 μl of nuclease free water. A list of primers used in this investigation can be found in Table 2.2. Primers were ordered from Sigma-Aldrich, UK.

Table 2.2. Primer sequences

Primer	Sequence (5' – 3')
UAS- <i>pu</i>	Forward TCTACGGAGCGACAATTCAATTC
	Reverse CAGTGGTGTTTTTCGGTTGTG
UAS- <i>dLRRK</i>	Forward TCTACGGAGCGACAATTCAA
	Reverse AGAAGGGTGTTTGCTCCTGA
<i>dLRRK</i> ^{<i>e03680</i>}	Forward CGATAAAACACATGCGTC
	Reverse GGCTAACCGATGCAGAGGAA

Reactions were run in a Techne PRIME PCR thermocycler for 30 cycles. The PCR program was run as 95°C for 5 mins for an initial denaturation followed by 30 cycles of denaturation at 95°C for 30 sec, annealing temperature was calculated as 5°C lower than the lowest primers melting temperature I for 30-40 sec, and extension at 72°C for 1 min per kb. A final step of extension at 72°C for 10 mins was performed before the reaction was cooled down to 4°C to prevent DNA decomposition.

2.4.3 DNA agarose gel electrophoresis

To analyse the product of PCR, agarose gel electrophoresis was utilised. 1 g of agarose was heated using a microwave oven in 100 ml of 1X TAE buffer to produce 1% agarose gel. The distance travelled by a PCR fragment in agarose in a gel is inversely related to the size of PCR product. To visualise DNA in the gel using a blue light transilluminator, SYBR[®] safe (Invitrogen, UK; 10 µl/100 ml) was added to the gel when it was sufficiently cool prior to pouring 6X DNA loading dye (0.25% bromophenol blue (w/v) and 30% glycerol (v/v)) was added to PCR product in order to assist in loading the samples into the wells of the gel. A 1 kb or 100 bp DNA ladder (0.5 ug/lane; NEB, UK) was run alongside the DNA products in order to visualize the DNA band sizes. All gels were run at 100V for 30-45 mins.

PCR followed by gel electrophoresis was used to screen stocks for the presence of the *dLRRK*^{*e03680*} *piggyBac* P-element following a recombination. An example gel with wild-type (*w*^{*1118*}), homozygous *dLRRK*^{*e03680*} and successfully recombined *Lsp2*-GAL4, *dLRRK*^{*e03680*}/*dLRRK*^{*e03680*} stocks is shown in Figure 2.7.

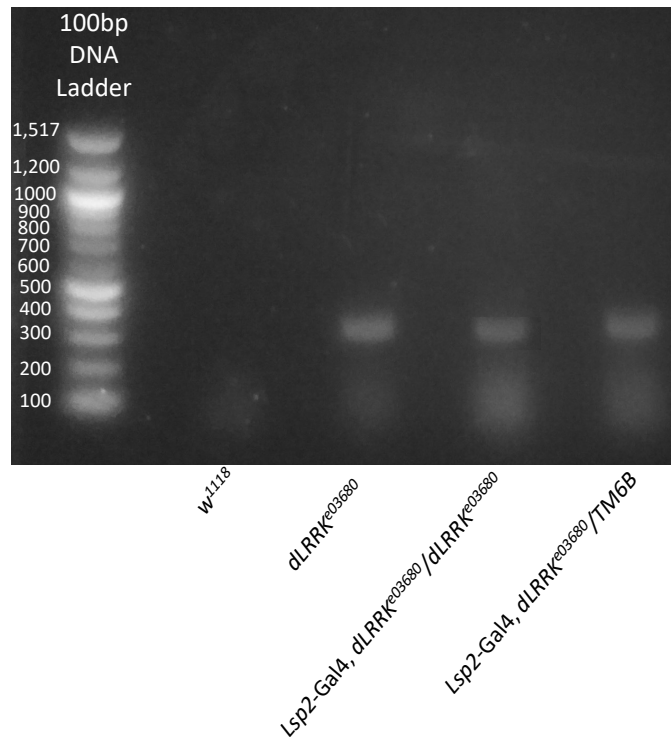


Figure 2.7. PCR of Mutant $dLRRK^{e03680}$ recombinants

Primers were designed to detect the presence of $dLRRK^{e03680}$. The gel shows a successful recombination of $dLRRK^{e03680}$ with $Lsp2$ -Gal4. The first lane is w^{1118} (negative control), the second lane is the homozygous $dLRRK^{e03680}$ (positive control), and the third and fourth lanes are the successful recombinants in the homozygous and heterozygous forms. The presence of $Lsp2$ -Gal4 was confirmed by GFP expression.

2.5 Western blotting

The method used for western blotting was adapted from Abcam (2016).

2.5.1 Protein extraction

Protein was extracted from adult fly heads. Flies were collected in 1.5 ml Eppendorf tubes and snap frozen on dry ice or liquid nitrogen. To separate the heads from the rest of the body, the 1.5 ml Eppendorf tube was placed inside a 50 ml falcon tube containing dry ice and vortexed 2-3 times for 30-60 secs. Fly heads were then collected into a new 1.5 ml Eppendorf and kept on dry ice or stored in -20°C till ready for extraction. RIPA buffer (150mM NaCl, 1.0% IGEPAL[®] CA-630, 0.5% sodium deoxycholate, 0.1% SDS, 50 mM Tris, pH 8.0; Sigma, UK) was used for protein extraction with the addition of protease inhibitor cocktail tablets (cOmplete tablet, Mini EDTA-free, *EASYpack*;

Roche). 1 µl of buffer per head was added to the heads and they were homogenized by a sterile plastic pestle and left on ice for 30 mins. After the incubation, tubes were centrifuged at 14000 rpm for 15 mins at 4°C. The extracted protein in the supernatant was removed into a new tube.

For haemolymph extraction of adult flies, an adapted protocol from [protocol.io \(https://www.protocols.io/view/Haemolymph-extraction-of-adult-Drosophila-dkn4vd\)](https://www.protocols.io/view/Haemolymph-extraction-of-adult-Drosophila-dkn4vd) was used. A hole was made at the bottom of a 0.5 ml Eppendorf tube and put into a 1.5 ml Eppendorf tube with the lid removed. Flies were anesthetised on a CO₂ pad and their thorax were speared with a needle. 40 speared flies were collected into the 0.5 ml Eppendorf tube on ice and then centrifuged for 1 min at 5000 rpm at 4°C. Around 1 µl of haemolymph was collected.

For cell culture, the same RIPA buffer used in fly protein extraction was used here as well. Cells were washed with ice cold PBS and then RIPA buffer was added. For a 6-well plate, 60 µl of RIPA was used and cells were scraped off of the plate using cell scraper. Then, lysates were transferred into 1.5 ml Eppendorf and incubated for 30 mins on ice. After the incubation, tubes were centrifuged at 14000 rpm for 5 mins at 4°C. The extracted protein in the supernatant was removed into a new tube. The concentration of the protein was quantified using bicinchoninic acid (BCA) assay (see section 2.5.2).

2.5.2 Quantification of protein concentration

Protein concentration was calculated using BCA kit (Pierce, Fisher Thermo Scientific, UK). A standard curve of bovine serum albumin (BSA) was produced by diluting a known BSA concentration (2 µg/ml) serially (2, 1, 0.5, 0.25, 0.125, 0.0625, 0.03125, 0 µg/ml) in RIPA buffer. To increase the quantification accuracy, lysates were diluted 2X and 10X and the average is taken. The assay was performed in a 96-well plate according to the manufacturer instructions. Absorption values were measured at 562 nm using a spectrophotometer (BMG Labtech Clariostar Plate Reader, Ortenberg, Germany). Absorption spectra values were used to determine protein concentration of samples in µg/µl.

2.5.3 Sodium Dodecyl Sulphate Polyacrylamide Gel Electrophoresis (SDS-PAGE)

Samples were mixed with 5X laemmli buffer (0.25M Tris-HCL, 10% SDS w/v, 50% glycerol v/v, 25% β-mercaptoethanol v/v, and 0.02% bromophenol blue w/v of 6.8 pH)

to a working concentration of 1X and boiled for 5 min at 85°C to denature protein. Protein samples (20 µl in a loading concentration of 7.5-10 µg/µl) and a protein ladder (6 µl PageRuler™ Plus Protein Ladder, Thermo Fisher Scientific, UK) were loaded into a handcasted gel of 7.5% resolving gel and 4% stacking gel. Gels were run in Criterion™ Vertical Electrophoresis Cell (Bio-Rad, UK) connected to a PowerPac™ Basic Power Supply (Bio-Rad, UK) filled with running buffer (25 mM Tris, 192 mM glycine, 0.1% SDS pH 8.3) for 30 min at 80V followed by ~ 1.5 hrs at 100V in cold conditions.

2.5.4 Protein transfer to polyvinylidene fluoride (PVDF) membrane

After protein separation in SDS-PAGE, a Mini-Trans-Blot Cell (Bio-Rad) was used to transfer proteins from the gel to a PVDF membrane (Amersham Hybond 0.45 µm PVDF; GE Healthcare, UK). Foam pads, Whatman gel blot paper and the SDS-PAGE gel were soaked in transfer buffer (25 mM Tris, 192 mM glycine, 20% methanol v/v). PVDF membrane was cut according to the gel size and then activated in 100% methanol for 30-60 secs followed by a quick dip into the transfer buffer. In the Mini Gel Holder Cassette, one foam pad is placed on the negative (black) side followed by a one Whatman gel blot paper and then the gel. On top of that, the activated PVDF membrane with a one Whatman gel blot paper and one foam pad. Avoiding any bubbles trapped between the gel and the PVDF membrane, the cassette is closed carefully and placed into the transfer tank filled with the transfer buffer. Proteins were transferred by applying 30V overnight increasing this to 60V the next morning for 30 mins or applying 80-100V for 1-2 hrs in cold conditions.

2.5.5 Probing of PVDF membrane

After protein transfer to the PVDF membrane, the membrane was washed in Tris buffered saline-Tween (TBS-T; 10 mM Tris, pH 7.6, 150 mM NaCl supplemented with 0.1% (v/v) Tween® 20) 2 times for 5 min at RT followed by the addition of a blocking solution, either 5% (w/v) BSA or skimmed milk in TBS-T, for 1 hr to prevent any non-specific binding. This was followed by an overnight incubation at 4°C of the primary antibody in 5% (w/v) BSA in TBS-T. Excess antibody was removed via washing the membrane 3 times for 10 min at RT. The suitable species of secondary antibody (conjugated to HRP) was added in either 5% (w/v) BSA or skimmed milk in TBS-T for 1-2 hrs at RT followed by removing excess antibody via washing the membrane in TBS-T 3 times for 10 min at RT. All washes and antibody incubation were performed on a rocking platform. The signal was visualised with chemiluminescent substrate

(Amersham ECL Prime Western Blotting Detection Reagent, GE Healthcare, Germany) according to the manufacturer instructions and was imaged either by exposing the blot in the dark to UltraCruz® X-Ray autoradiography films (Santa Cruz Biotechnology, Germany) or visualised using iBright™ FL1000 imaging system (Invitrogen, Thermo Fisher Scientific, UK). The list of antibodies used in this investigation can be found in Table 2.3.

Table 2.3. List of antibodies used in western blot

Antibody	Species	Dilution	Source
Primary			
hLRRK2	Mouse	1:1000	NeuroMab
hLRRK2	Rabbit	1:10,000	Abcam
dSynaptotagmin1	Rabbit	1:1000	(West <i>et al.</i> , 2015b)
β-Tubulin	Mouse	1:1000	Proteintech
GAPDH	Mouse	1:10,000	Abcam
pRab10	Rabbit	1:1000	
panRab10	Mouse	1:1000	
Secondary			
Mouse IgG HRP linked	Goat	1:10,000 – 20,000	Jackson ImmunoResearch
Rabbit IgG HRP linked	Goat	1:10,000 – 20,000	

2.6 Statistical analysis and bioinformatics

All statistical analyses were carried out in GraphPad Prism. Student's t-test was performed to test for statistical significance between two groups; univariate ANOVA followed by a post-hoc Tukey comparison was performed when comparing genotypes to control. Statistical significance was defined as $p < 0.05$ throughout. Error bars are either SD (\pm SD) or SEM (\pm SEM). P values are indicated graphically with **** $p < 0.00001$ *** $p < 0.0001$, ** $p < 0.001$, * $p < 0.05$, ns (no significant difference). The half-life ($t_{1/2}$) calculation for protein degradation was carried out in GraphPad Prism using non-linear regression analysis (curve fit) one phase decay model. The fitting method used was (Least square regression) with plateau = 0. Confidence Intervals (CI) of parameters are either 95% or 90%.

During the course of this investigation the following software and online resources were used. Unless otherwise stated default settings, assumptions and parameters were used.

For data management, analysis, and graphs plotting:

- Microsoft Excel
- GraphPad Prism v9.

For graphic design and image processing:

- Microsoft PowerPoint
- Photoshop (template from Roote and Prokop, 2013 Genotype Builder)
- BioRender.com
- Fiji
- DinoXcope software

For primer design:

- Primer3 (<http://bioinfo.ut.ee/primer3-0.4.0>)

For western blots quantification:

- Image Studio Lite

For ERG data processing:

- MATLAB (full code can be found at <https://github.com/wadelab/flyCode>)
- *DASYLab* for ERG recording
- *DASYView* for ERG analysis (customised software, C. J. H. Elliott, University of York).

3 The effects of *dLRRK*^{e03680} on eye physiology and eye pigment

3.1 Introduction

3.1.1 *Drosophila* LRRK (*dLRRK*)

The *Drosophila* genome has one orthologue to human *LRRK1/LRRK2* which is *dLRRK*. (*CG5483*) found on the right arm of chromosome 3. The *dLRRK* protein is around 2400 amino acids in length and structurally appears more similar to *LRRK1* than *LRRK2* as *dLRRK* does not have the ANK and WD40 domains (Figure 3.1). The GTPase domain of *dLRRK* shows 33% and 30% identity to the GTPase domain of *hLRRK2* and *hLRRK1*, respectively, and the *dLRRK* kinase domain shows 36% and 38% identity to the respective kinase domains of *hLRRK2* and *hLRRK1*. Like *LRRK2*, *dLRRK* is ubiquitously expressed in *Drosophila* tissues and has been found largely in the cytoplasm associated with membranous structures such as lysosomes, endosomes, and synaptic vesicles (Langston *et al.*, 2016).

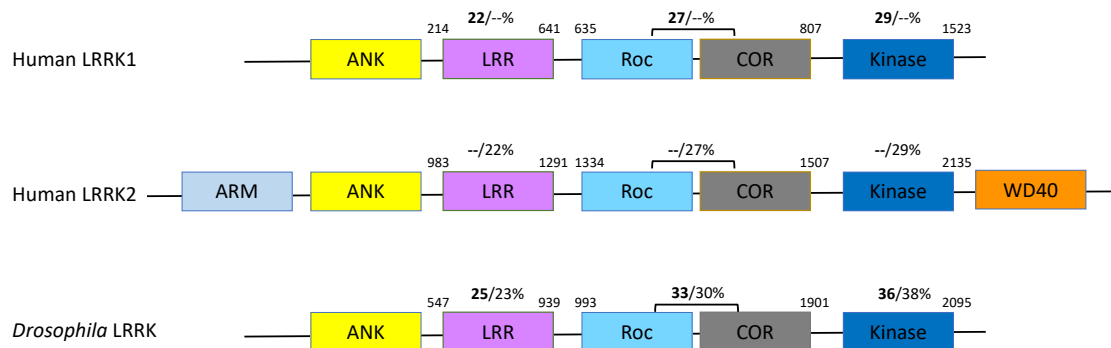


Figure 3.1 Comparison of the domain structure of LRRK proteins in human and *Drosophila*.

The predicted domains are indicated by labelled boxes. Percentage identities based on a Clustal 2.1 multiple sequence alignment are given relative to human *LRRK2* (left, bolded) and relative to human *LRRK1* (right) for LRR, Roc-COR and kinase domains. Adapted from (Langston *et al.*, 2016).

As the structural homology implies, *dLRRK* is functionally an active kinase capable of autophosphorylation (Imai *et al.*, 2008) and phosphorylation of many substrates. These diverse substrates may include 4E-BP, Futsch, endophilin A and ribosomal protein S15

(Lee *et al.*, 2010, Martin *et al.*, 2014b, Matta *et al.*, 2012, Xiong and Yu, 2018). In addition, dLRRK has been shown to interact with different membrane traffic-regulating Rab proteins in *Drosophila* follicle cells (Dodson *et al.*, 2012). The similarities between *dLRRK* and *hLRRK2* can also be observed in the similar effects they produce when manipulating their expression. The transgenic expression of mutant *dLRRK* in *Drosophila* DA neurons has shown a severe age dependent cell loss when expressed with *dLRRK-Y1383C* (equivalent to *LRRK2-Y1699C*) or *dLRRK-I1915T* (equivalent to *LRRK2-I2020T*) are expressed compared to the wild type *dLRRK* expression (Gehrke *et al.*, 2010, Imai *et al.*, 2008). The systemic loss of function mutant *dLRRK^{e03680}* or the overexpression of *hLRRK2-G2019S* in neuronal cells of the *Drosophila* have previously been shown to have caused an age dependent loss of visual function (Furmston, 2016, Hindle *et al.*, 2013). Although these results have shown a close resemblance between *dLRRK* and *hLRRK2* function, other reports showed irreproducible or conflicting outcomes. For example, the DA neurodegeneration was not reported in all studies (Wang *et al.*, 2008a) and the synaptic transmission in *dLRRK* mutant flies was found to be significantly depleted in one study (Lee *et al.*, 2010) while in another one no significant change was reported (Matta *et al.*, 2012). These results show the conservation between *dLRRK* and human *LRRK2* which makes investigating *dLRRK* even further for PD modelling a valuable tool.

3.1.2 Vision and *dLRRK*

Of non-motor symptoms reported by PD patients, a common one is disturbances in the visual function. This could be due in part to the loss of retinal DA neurons (Harnois and Di Paolo, 1990) such as the DA amacrine and inter-plexiform cells (Zhang *et al.*, 2021) that eventually affects the normal neural circuitry of the eye. Moreover, an age dependant visual dysfunction was observed in flies expressing human *LRRK2-G2019S* in DA neurons (Hindle *et al.*, 2013) and flies carrying the loss of function mutation *dLRRK^{e03680}* (Furmston, 2016). This visual dysfunction was assessed using an electroretinogram (ERG) technique which measures field potentials from the neuronal activity from the photoreceptors and the underlying second-order lamina neurons in response to pulses of light (see Figure 3.2). The visual dysfunction observed in these two *Drosophila* models might look similar, however, it is well to note that the decline of visual function was observed in all elements of the ERG (on-transient, photoreceptors, and off-transient) in *LRRK2-G2019S* model while in the loss of function *dLRRK*, it was mostly observed in the off-transient element.

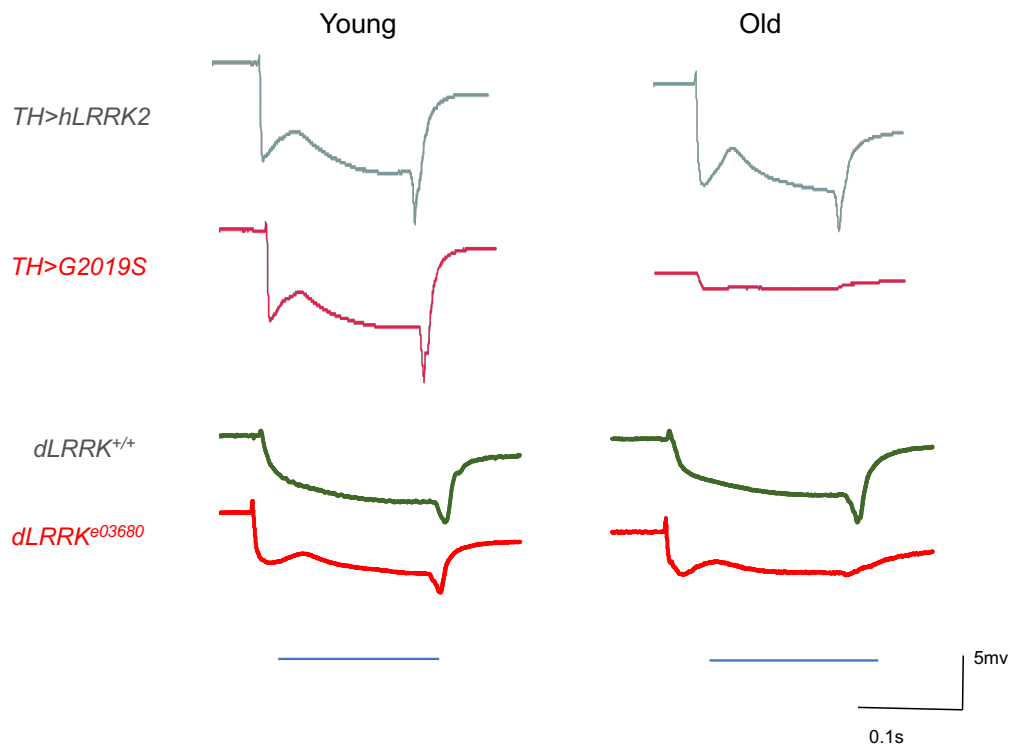


Figure 3.2 Age dependant loss of visual function in flies expressing human *LRRK2-G2019S* in DA neurons and *dLRRK^{e03680}* flies.

Representative ERG traces from young (left, 3 days) and old (right, 28 or 21 days) flies expressing human *LRRK2* in DA neurons (*TH>hLRRK2*), *LRRK2-G2019S* in DA neurons (*TH>G2019S*), wild-type (*dLRRK*), and *dLRRK* loss of function (*dLRRK^{e03680}*) flies. ERGs are recorded in response to 0.5 second blue light pulses. The blue lines drawn below the bottom ERG traces represent the duration of the light pulse. Scale bars for time (seconds) and potential (mV) are shown. Adapted and modified from (Furmston, 2016, Hindle *et al.*, 2013).

Interestingly, the loss of visual function observed in *dLRRK^{e03680}* flies was rescued with the expression of the native gene (*dLRRK*) autonomously in CNS (Furmston, 2016). The ability of the wildtype *dLRRK* transgene to rescue loss-of-function *dLRRK* mutants was tested in the lamina neurons, DA neurons and photoreceptors (Figure 3.3).

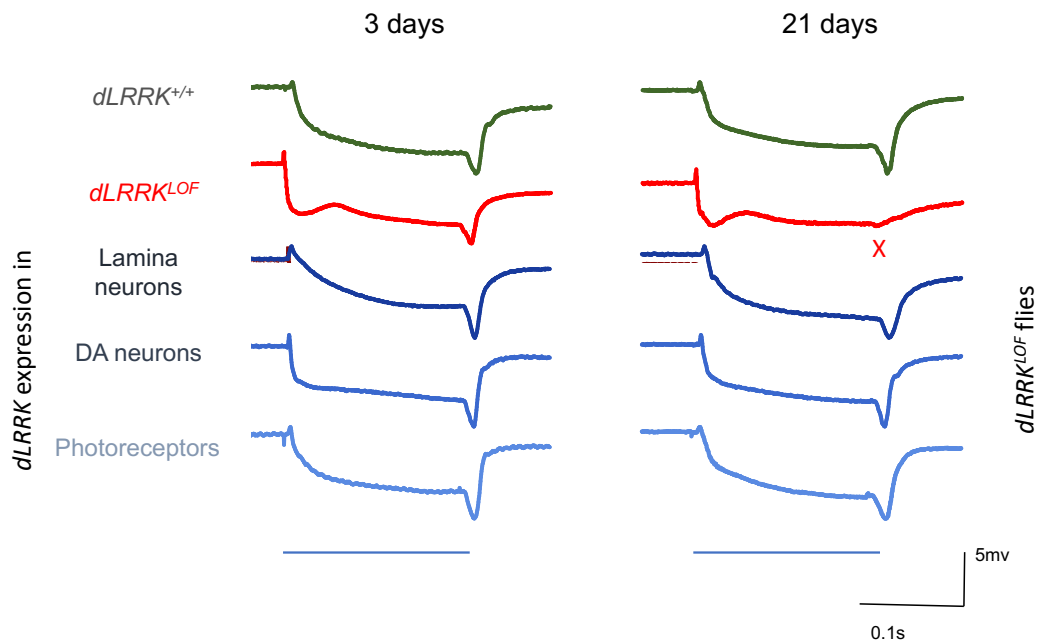


Figure 3.3 *dLRRK* expression in the lamina neurons, DA neurons or photoreceptors in *dLRRK*^{LOF} background rescues the age-dependant loss of visual function.

Representative ERG traces from 3 days (left) and 21 days (right) of wild-type (*dLRRK*; green), *dLRRK*^{LOF} mutant (red) and flies expressing *dLRRK* specifically in the lamina neurons, DA neurons or photoreceptors in a *dLRRK*^{LOF} background (shades of blue). ERGs are recorded in response to 0.5 second blue light pulses. The blue lines drawn below the bottom ERG traces represent the duration of the light pulse. Scale bars for time (seconds) and potential (mV) are shown. Each trace is the average of the fly's response to at least three flashes of light. Adapted and modified from (Furmston, 2016).

This previous data in addition to subsequent analysis from others like (Afsari *et al.*, 2014) demonstrate the essential role of *dLRRK*/*hLRRK2* for the maintenance of normal visual function.

3.1.3 *Drosophila* eye pigments biosynthesis

Genes regulating eye pigmentation have been linked to neurodegeneration including PD and Huntington's Disease (Campesan *et al.*, 2011, Cunningham *et al.*, 2018, Maddison and Giorgini, 2015, Tan and Guillemin, 2019). Observing the effects of manipulating the different genes involved in the synthesis of these pigments is a valuable tool to uncover the link between PD and pigmentation regulation. It is of interest to note that the substantia nigra pars compacta, where the PD sensitive population of DA neurons is

found, is a pigmented neuronal structure containing neuromelanin (Nagatsu *et al.*, 2022).

Wild type flies have red-brown eye colour due to a combination of two classes of pigments found in their pigment cells. These pigments are ommochromes (brown) and pteridines (red) and their production goes through distinct pathways with different enzymes for each. Figure 3.4 outlines the different eye colour genes involved in the kynurenine, pteridine and granule pathways.

Ommochromes are produced via a pathway known as kynurenine synthesis. It involves a series of oxidations that starts with tryptophan and end with the production of the brown pigment xanthommatin (a type of ommochromes found in most insects). Formylkynurenine, kynurenine and 3-hydroxykynurenine (3-HK) are intermediates of this synthesis pathway. The *Vermilion* (*v*) gene encodes tryptophan oxygenase (Searles and Voelker, 1986) which convert tryptophan into formylkynurenine and the *cinnabar* (*cn*) gene encodes kynurenine-3-hydroxylase (Warren *et al.*, 1996) which convert kynurenine into 3-hydroxykynurenine. *Scarlet* (*s*) and *white* (*w*) genes are localised at the membrane of the pigment granules and are involved in the transportation of 3-HK to the inside of the pigment granules (Mackenzie *et al.*, 1999). Once in the granule, phenoxazinone synthetase converts 3-HK to xanthommatin (Summers *et al.*, 1982).

The pathway of synthesising pteridines (or drosopterin) is more complex and less well understood than the synthesis of ommochromes. There are five types of pteridines produced in the fly, drosopterin and isodrosopterin are the major species. A series of enzymatic and non-enzymatic reactions are involved in the biosynthesis of pteridines derived from guanosine triphosphate (GTP). The *Punch* (*p*) gene encodes GTP cyclohydrolase I (GTPCH I) (McLean *et al.*, 1993) which converts GTP to 7,8-dihydroneopterin triphosphate (H₂-NTP). H₂-NTP is then converted by 6-pyruvoyltetrahydropterin (6-PTP) synthase, which is encoded by *purple* (*pr*) gene, into 6-PTP (Park *et al.*, 1990, Yim *et al.*, 1977). The *Sepia* (*se*) gene encodes pyrimidodiazepine (PDA) synthase (Kim *et al.*, 2006) that converts 6-PTP into PDA (a type of pteridines) which then would be transported into pigment granules (Kim *et al.*, 2013a). In addition to the *white* (*w*) gene, the *brown* (*bw*) gene is responsible for transporting pteridine precursors into pigment granules (Borycz *et al.*, 2008, Dreesen *et al.*, 1988). Interestingly, the biosynthesis of tetrahydrobiopterin (BH₄), which is an essential cofactor in the synthesis of the rate-limiting enzyme for dopamine tyrosine

hydroxylase (TH) (Homma *et al.*, 2013), is shared with pteridines synthesis and include three consecutive enzymatic reactions catalyzed by GTPCH I, PTPS, and sepiapterin reductase (Kim *et al.*, 2013a). Heterozygous mutations in the *GTPCHI* gene in humans causes an L-DOPA responsive dystonia, and is a known risk-factor in the inheritance of PD (Ichinose *et al.*, 1994, Nalls *et al.*, 2014).

The colour of a fly eye depends on its ability to synthesis the two pigments. For example, a bright red eye colour in *v* mutants is due to their inability to synthesis ommochromes (Searles and Voelker, 1986) and a dark brown in *se* mutants is due to their inability to synthesis pteridines (Kim *et al.*, 2006). In case of *white* flies, no pigments are being transported into pigment granules resulting in lack of any colour (Mackenzie *et al.*, 1999).

Eye colour genes are also involved in vesicular trafficking and pigment granules synthesis. Pigment granules are a type of lysosome-related organelle. Ommochromes are carried into type I pigment granules, a process which occur in primary and secondary pigment cells of ommatidia while pteridines are carried into type II pigment granules which occur exclusively in secondary pigment cells (Shoup, 1966). Among many genes, *Ruby (rb)*, *garnet (g)*, *carmine (cm)* and *orange (or)* genes are involved in lysosome-related organelle synthesis (Grant *et al.*, 2016). Intriguingly, *dLRRK* has been suggested to have a role in trafficking cargo to the pigment granules. A genetic interaction between *dLRRK* and some pigments colour genes in the kynurenine and pteridine pathways lead to synthetic lethality that might be due to *dLRRK* interference (Furmston, 2016). Many stages of eye pigment synthesis occur in other, non-neuronal tissues such as the Malpighian tubule (the *Drosophila* equivalent of the kidney) and how different tissues and pigment movement from tissue to tissue contribute to the final eye colour are not completely known.

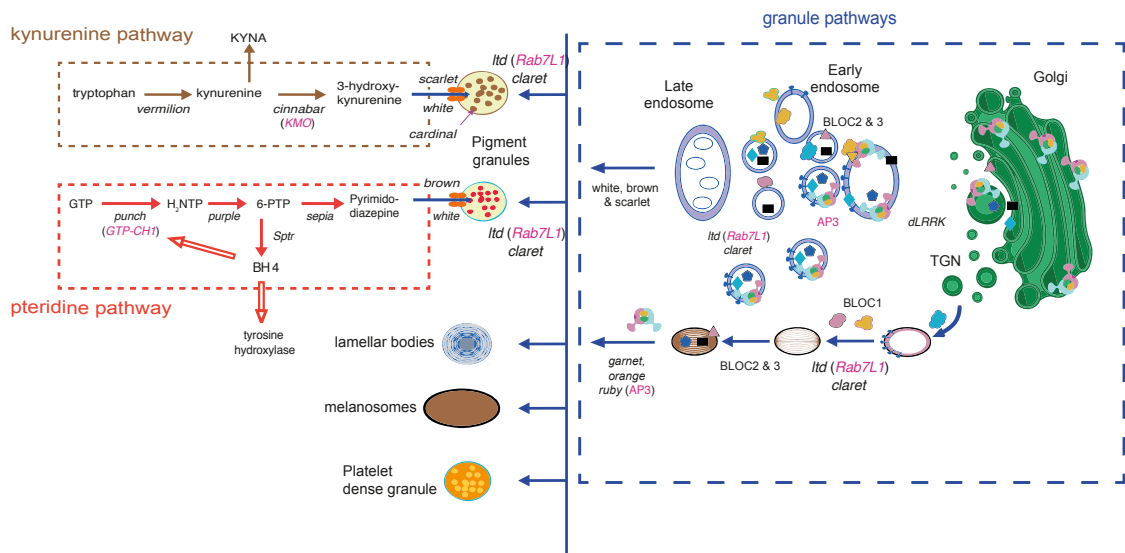


Figure 3.4 An illustration of the pathways involved in the biosynthesis of pigment granules

The biosynthesis of pigment granules involves the interaction of kynurenine, pteridine and granule pathways. Some pigment colour genes have been found to be synthetically lethal in $dLRRK^{LOF}$ flies suggesting that dLRRK might play a crucial role in this interaction. Taken from (Furmston, 2016).

3.2 Aims

1. Test if expressing $dLRRK$ in non-neuronal tissues could rescue the loss of visual function observed in $dLRRK^{LOF}$ flies via ERG recording.
2. Test the effect of manipulating eye pigment genes on their interaction with $dLRRK$ through genetic and physiological approaches.

3.3 Results

3.3.1 Investigating the ability of $dLRRK$ to rescue the visual dysfunction in $dLRRK^{LOF}$ old flies when expressed in non-neuronal tissues

It is thought that dLRRK/hLRRK2 can move from cell to cell and act in a non-cell autonomous manner (Wang *et al.*, 2017). We therefore wished to test if the visual dysfunction observed in $dLRRK^{LOF}$ flies could be rescued via expression of a $dLRRK$ transgene in non-neuronal tissue. Prior to testing the rescue ability of $dLRRK$ expression in non-neuronal tissues, an ERG test was used to confirm the finding from (Furmston, 2016) of reduced off-transient signal in old $dLRRK^{LOF}$ flies. This was carried out because the amplifier used in this investigation is different in terms of having an AC-

coupling, instead of DC, which would enhance transient signals and improve the signal to noise ratio. My data confirm the severe decline in the off-transient element of the ERG in old $dLRRK^{LOF}$ flies. However, I also observed a severe decline to the on-transient element of the ERG as well (Figure 3.5).

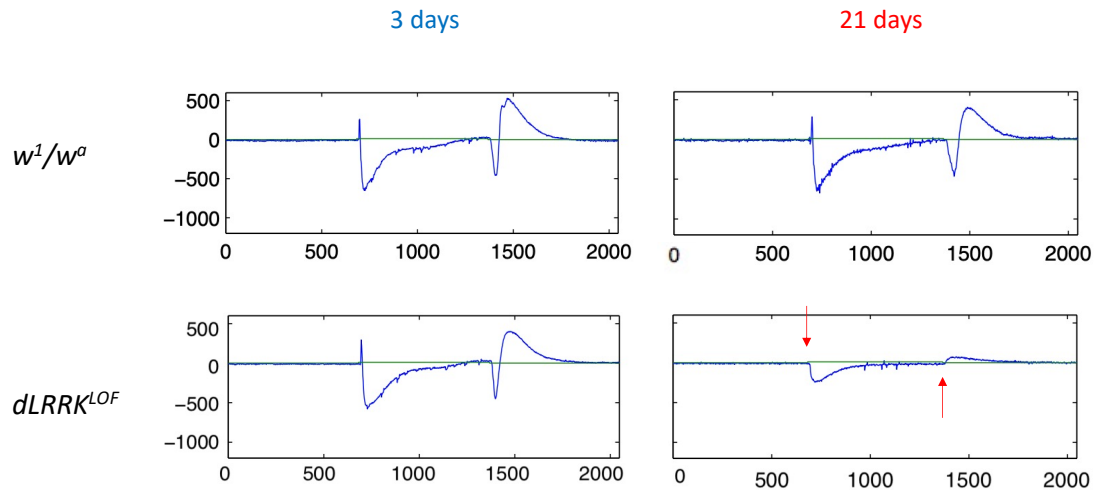


Figure 3.5 A reduction in ERG amplitude in $dLRRK^{LOF}$ old flies (21 days) compared to control.

Representative ERG traces from 3 days (left) and 21 days (right) of control flies (w^l/w^a) and $dLRRK$ loss of function mutant ($dLRRK^{e03680}$). The red arrows indicate the observed reduction in the on transient and off-transient elements of the ERG in old mutant flies compared to control. ERGs are recorded in response to 0.5 second blue light pulses. Each trace is the average of the fly's response to five flashes of blue light. ERG potential is measured in millivolt (mV) per milliseconds (ms).

3.3.1.1 A possible rescue of visual function in $dLRRK^{LOF}$ flies when $dLRRK$ is expressed in non-neuronal tissues

Next, the ability of restoring the age-dependant visual dysfunction observed in $dLRRK^{LOF}$ old flies (21 days) was tested by expressing the native gene ($dLRRK$) in non-neuronal tissues using the Gal4/UAS system. Three Gal4 constructs that drive expression in different tissues have been used to express the native $dLRRK$ in fat body ($Lsp2$ -Gal4; subsequently referred to as Fat body), pigment cells (P(GAL4)54C; subsequently referred to as Pigment cell), and male reproductive system (P(GawB)c564; subsequently referred to as Repro tract). These lines were chosen based on the expression pattern of LRRK detected in fat body by (Lazareva *et al.*, 2007), pigment cells by (Nagaraj and Banerjee, 2007), and male reproductive tract by (Hrdlicka *et al.*, 2002) and they were

chosen based on their distal location from the visual system (pigment cell are the closest while the reproductive tract is the farthest).

In order to express *dLRRK* in these locations, a multi-step fly crosses supported by balancer chromosomes have been performed and the summary of the crosses can be found in Figure 3.6.

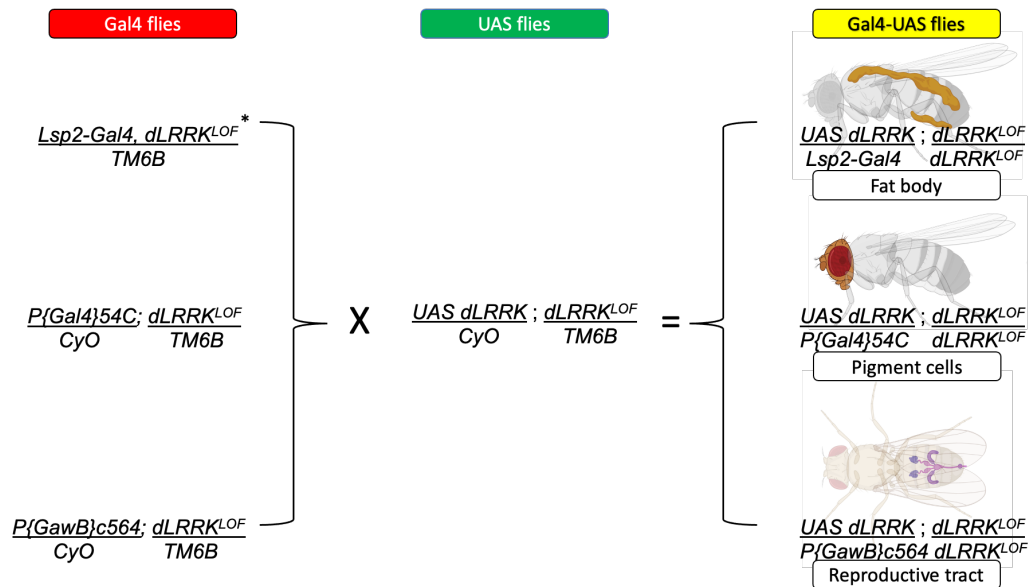


Figure 3.6 Crossing summary of flies expressing *dLRRK* gene in non-neural tissues using Gal4/UAS system for the assessment of visual system rescue.

The left side shows the different Gal4 lines used to cross with flies (in the middle) expressing *dLRRK* to produce flies expressing *dLRRK* in non-neuronal tissues (the right side). * The *Lsp2-Gal4* line was produced using recombination by the method described in section 2.1.5.

Examining the ERG traces in flies expressing the native gene (*dLRRK*) in non-neuronal tissues in *dLRRK*^{LOF} background revealed no reduction in amplitude (fat body and pigment cells rescues) or a modest reduction (Repro tract rescue) in old flies compared to the young flies (Figure 3.7A). The quantification of the components of ERG (on transient, photoreceptors, and off transient) showed a significant difference between young and old flies in Repro tract rescue flies similar to that seen in *dLRRK*^{LOF} flies. This difference is not seen in fat body rescue or pigment cell rescue flies (Figure 3.7 B). The initial visual response (on-transient) observed in the tested young flies (fat body, pigment cells, and repro tract rescues) appeared to be lower than the WT which might be due to the darker eye colours in these transgenes. These data suggest the possibility

that *dLRRK* has the ability to rescue the age-dependent loss of visual function in *dLRRK^{LOF}* old flies when expressed in fat body or pigment cells, but this ability is limited when the rescue is attempted from the reproductive tract. On-transient and off-transient data of the ERG are reflective of the lamina neuron response which contains DA neurons. Focusing on these data revealed a possible rescue for the age-dependant visual loss based on dLRRK function in fat body and pigment cells (Figure 3.7 C).

Figure 3.7 *dLRRK* expression in the fat body or pigment cells in *dLRRK^{LOF}* background revealed a possible rescues of the age-dependent loss of visual function.

A. Representative ERG traces from 3 days (left) and 21 days (right) of wild-type (w^1/w^a), *dLRRK^{LOF}* mutant and flies expressing *dLRRK* specifically in fat body, pigment cells, or reproductive tract in a *dLRRK^{LOF}* background. The red arrows indicate the observed reduction in the on-transient and off-transient elements of the ERG in the old mutant flies. ERGs are recorded in response to 0.5 second blue light pulses. Each trace is the mean of the fly's response to five flashes of blue light. ERG potential is measured in millivolt (mV) per milliseconds (ms). B. Quantification of the individual ERG components. The ERG of on-transient (top), photoreceptors (middle), and off-transient (bottom) responses were quantified for WT flies (w^1/w^a), *dLRRK^{LOF}*, and flies expressing *dLRRK* in fat body, pigment cells, or reproductive tract at 3 days (blue bars) and 21 days (red bars). C. Quantification of 21 day old flies on-transient (top) and off-transient (bottom) components of ERG. The ERG response was quantified for WT flies (w^1/w^a , orange bar), *dLRRK^{LOF}* (grey bar), and flies expressing *dLRRK* in fat body, pigment cells, and reproductive tract (green bars). A significant difference was found between *dLRRK^{LOF}* flies and flies expressing *dLRRK* in fat body and pigment cells which suggest the ability of *dLRRK* to rescue the visual dysfunction when expressed in these tissues. All statistical values are ANOVA with post-hoc Tukey: **** $p < 0.00001$, *** $p < 0.0001$, ** $p < 0.001$, * $p < 0.05$, ns (no significant difference). Data presented are mean \pm SD bars; n numbers are displayed inside bars. N.B. The presence of the *mW⁺* cassette in the Gal4 and UAS transgenes increase eye colour to a deep red which might lead to lower visual response.

3.3.1.2 Does *dLRRK* leak to other tissues?

UAS-transgenes can sometimes be expressed in low levels or leak to other tissues in the absence of Gal4 protein. We also wished to see if Gal4 expression alone in the absence of the UAS-*dLRRK* transgene could contribute to the rescue of the *dLRRK* mutant phenotype. Therefore, an experiment was carried out to record ERGs of flies carrying only a single component of the UAS/Gal4 system in *dLRRK^{LOF}* background. An age-dependent loss of visual function in old flies should indicate no leak of *dLRRK* from UAS-transgene. The data obtained showed a reduction in ERG amplitude in old flies of the *dLRRK^{LOF};UAS-dLRRK* genotype, however, the reduction was not as significant as the one found in the *dLRRK^{LOF}* mutant flies alone (Figure 3.8 A). The quantification of the components of ERG (on transient, photoreceptors, and off transient), on the other hand, showed a possible leak of *dLRRK* when the UAS-*dLRRK* transgene is present, leading to a rescue of the off-transient response in 21 day old flies. Similarly, when the pigment cells-Gal4 construct is present there is not a statistical significance difference found in the on-transient and off-transient responses (Figure 3.8 B-C). In addition to the ERG experiment, a western blot was performed to test for secreted hLRRK2 for extracted proteins from the haemolymph in flies expressing the hLRRK2 transgene

using fat body Gal4 driver to assess the presence of the protein of interest (anti-hLRRK2 was used due to the availability of this antibody in the lab) which might indicate a leak of protein from the haemolymph to the CNS. Unfortunately, the experiment was not successful due to the inability to find a loading control protein and possibly the ineffective technique of protein extraction (see section 2.4.1). The genetic and physiological data indicate a possible leak of dLRRK from the rescue transgene while the result found in the presence of the pigment cell-Gal4 construct suggests that eye colour may contribute to a protection of the eye function over time.

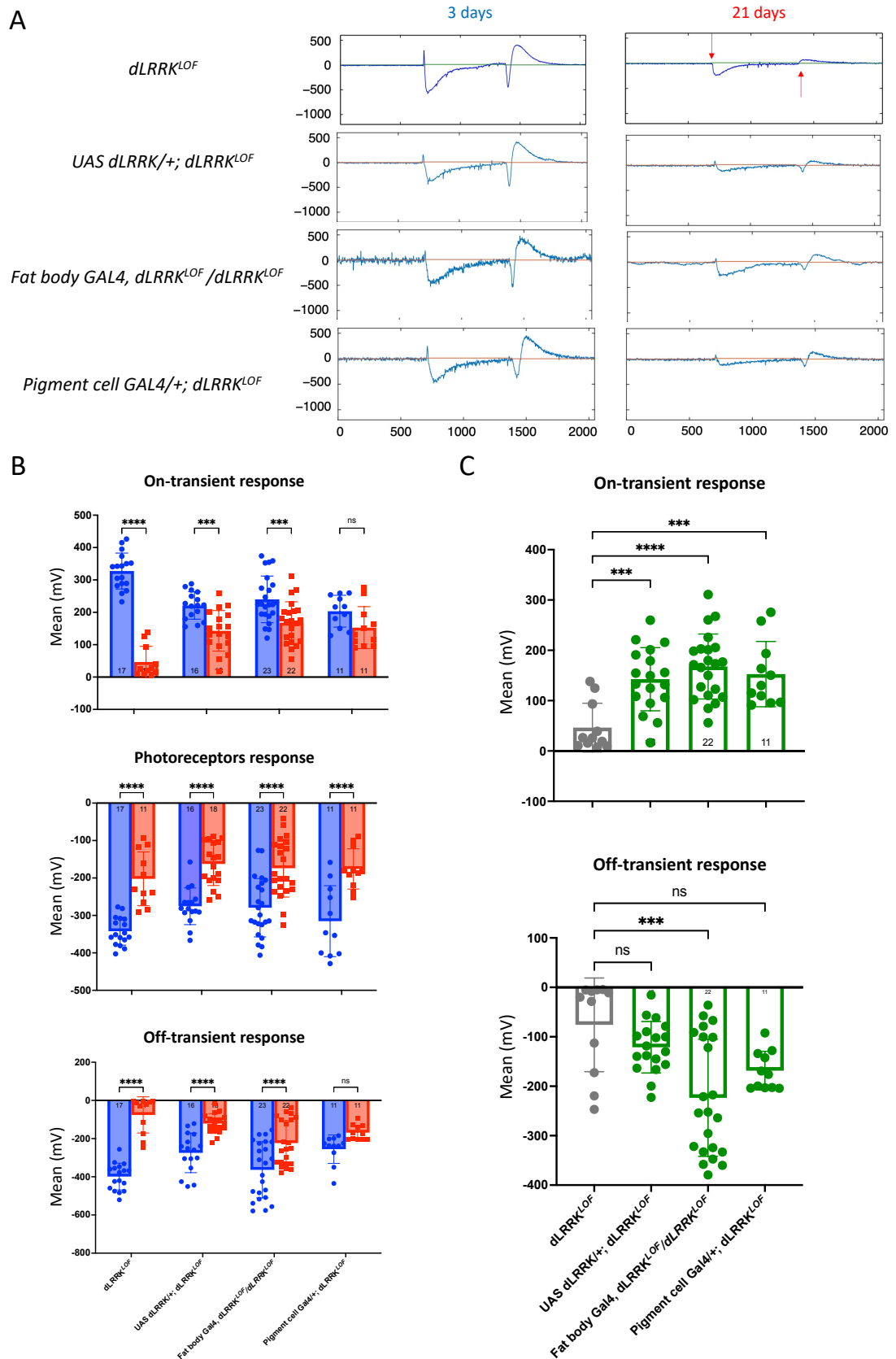


Figure 3.8 A possible leak of dLRRK is detected in pigment cells Gal4 flies when only one component of the UAS/GAL4 system is expressed in *dLRRK^{LOF}* flies background

A. Representative ERG traces from 3 days (left) and 21 days (right) of *dLRRK^{LOF}* mutant, flies with the UAS *dLRRK* component only in a *dLRRK^{LOF}* background, and flies with the GAL4 component only (Fat body and pigment cell). ERGs are recorded in response to 0.5 second blue light pulses. Each trace is the mean of the fly's response to five flashes of blue light. ERG potential is measured in millivolt (mV) per milliseconds (ms). B. Quantification of the individual ERG components. The ERG of on-transient (top), photoreceptors (middle), and off-transient (bottom) responses were quantified for *dLRRK^{LOF}* mutant, flies with the UAS *dLRRK* component only in a *dLRRK^{LOF}* background, and flies with the Gal4 component only (Fat body and pigment cell). C. Quantification of 21 day old flies on-transient (top) and off-transient (bottom) components of ERG. All statistical values are ANOVA with post-hoc Tukey: *****p*<0.00001 ****p*<0.0001, ***p*<0.001, **p*<0.05, ns (no significant difference). Data presented are mean ± SD bars; n numbers are displayed inside bars.

3.3.2 *dLRRK^{LOF}* interaction with eye pigments

Many flies bearing eye pigment mutations have been crossed with *dLRRK^{LOF}* to test for the presence of synthetic lethality. This synthetic lethality indicates a crucial role of the tested genes in the viability of the fly and a possible genetic interaction between eye pigment genes and *dLRRK*. To date, it has been found that loss-of-function mutations in *cinnabar*, *brown*, *scarlet*, *vermillion*, and *punch* are synthetically lethal with *dLRRK^{LOF}* (Cording & Furmston, unpublished). In this investigation, additional eye pigment genes have been tested to establish a better understanding of the possible interaction between *dLRRK* and eye pigments gene function in flies. Genetically, additional eye pigment mutations were examined to determine their potential synthetic lethality with *dLRRK^{LOF}*. We initially tested a *cinnabar* hypomorph (*cn^{35k}*) (Warren *et al.*, 1996) which works in the kynurenine pathway and *purple* hypomorph (*pr^l*) (Kim *et al.*, 1996) which works in the pteridine pathway. Physiologically, additional eye pigment genes were examined to determine their ability to rescue the age dependent visual loss in *dLRRK^{LOF}* flies. These eye pigment genes include *sepia* (*se*), *sepiapterin reductase* (*sptr*) and *punch* (*pu*).

3.3.2.1 The combination of *dLRRK^{LOF}* with *pr^l* showed no synthetic lethality.

To test for any genetic interaction between *dLRRK^{LOF}* and *pr^l* we performed the following cross outlined in (Figure 3.9). All possible progenies were viable from the experimental cross of *dLRRK^{LOF}* with *pr^l* indicating the absence of synthetic lethality. However, the viability for the desired genotype (homozygous for *pr^l* and *dLRRK^{LOF}*) was noticeably affected obstructing further experiment on them such as ERG and

survivability suggesting an evident physiological effect caused by the combined loss of *dLRRK* and *pr*.

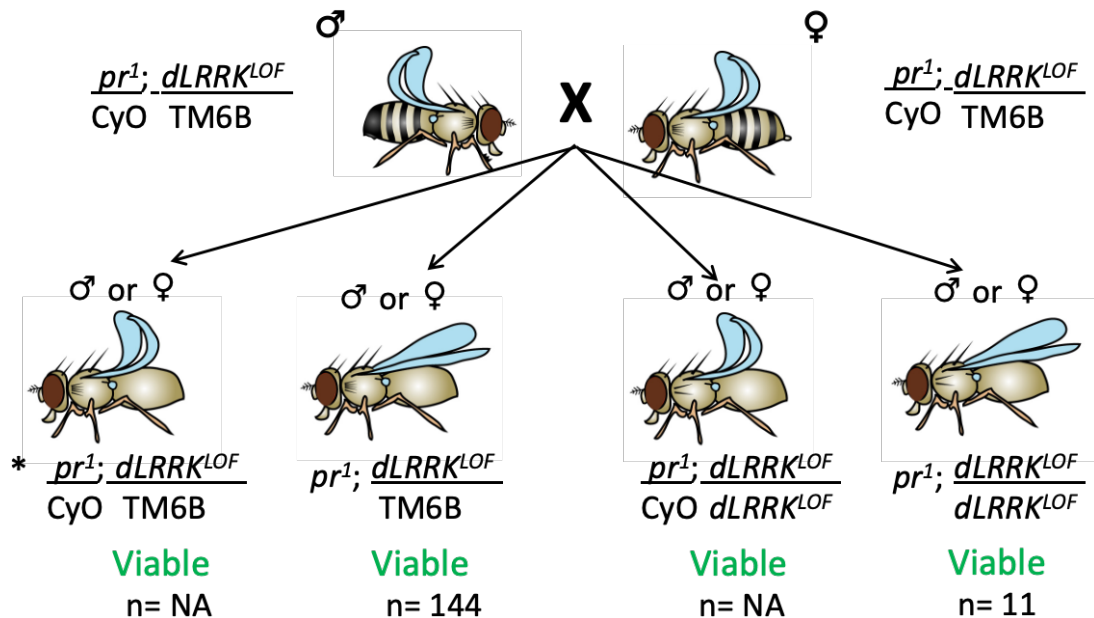


Figure 3.9 Homozygous or heterozygous pr^l mutation is NOT synthetically lethal with homozygous $dLRRK^{LOF}$ mutation

An experimental cross with adult virgin male and female flies that have the genotype $pr^l/CyO; dLRRK^{LOF}/TM6B$ was established. The possible progenies are shown with the associated balancer chromosome markers (curly wings for CyO and extra hairs on the thorax for TM6B). The desired genotypes are the two from the right, in particular, the first one from the right (homozygous for pr^l and $dLRRK^{LOF}$). The desired genotypes have shown to be viable indicating an absence of synthetic lethality. The viability was recorded in the first generation, but the number produced was later recorded from later generations that had the same genotype indicated by the asterisk (*). However, overtime the flies started to lose CyO marker which made counting flies with curly wings not possible, hence, the absence number in these genotypes. NA= not available.

3.3.2.2 The combination of $dLRRK^{LOF}$ with cn^{35k} showed no synthetic lethality.

To test for any genetic interaction between $dLRRK^{LOF}$ and cn^{35k} we performed the following cross outlined in (Figure 3.10). Like pr^l , cn^{35k} produced all possible progenies from the experimental cross with $dLRRK^{LOF}$ indicating the absence of synthetic lethality. However, unlike pr^l , the viability was severely affected for all genotypes including the desired one (homozygous for cn^{35k} and $dLRRK^{LOF}$) restricting further experiment on

them such as ERG and survivability. This also suggests a physiological effect caused by the combined loss of *dLRRK* and *cn*.

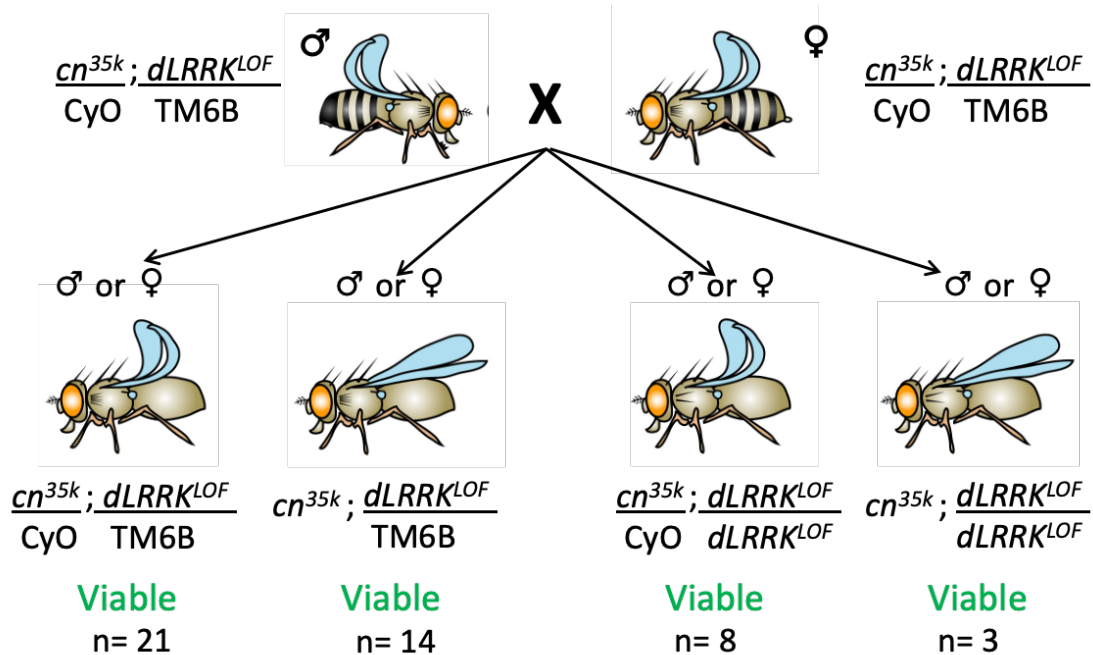


Figure 3.10 Homozygous or heterozygous cn^{35k} mutation is NOT synthetically lethal with homozygous $dLRRK^{LOF}$ mutation

An experimental cross with adult virgin male and female flies that have the genotype $cn^{35k}/CyO; dLRRK^{LOF}/TM6B$ was established. The possible progenies are shown with the associated balancer chromosome markers (curly wings for CyO and extra hairs on the thorax for TM6B). The desired genotypes are the two from the right, in particular, the first one from the right (homozygous for cn^{35k} and $dLRRK^{LOF}$). The desired genotypes have shown to be viable indicating an absence of synthetic lethality.

3.3.2.3 The effect of overexpressing of *se*, *sptr*, and *pu* in the DA neurons on visual function

It has previously been found that overexpression of *cinnabar* (*cn*) and *brown* (*bw*) in DA neurons and glial cells can rescue the loss of visual function in $dLRRK^{LOF}$ flies (Furmston, 2016). These rescues suggested that *cn* and *bw* work within the same pathways as *dLRRK*, and by increasing *cn* or *bw* in a $dLRRK^{LOF}$ background a restoration of the age-dependent loss of synaptic signaling is achieved. Here, we examined the expression of three additional pigment genes in DA neurons to look for a rescue of the $dLRRK^{LOF}$ loss of visual function and a possible interaction with *dLRRK*. These genes are *sepia* (*se*), *sepiapterin reductase* (*sptr*) and *punch* (*pu*), which encode enzymes

necessary for the pteridine pathway of pigment formation. A summary of experimental crosses can be found in Figure 3.11.

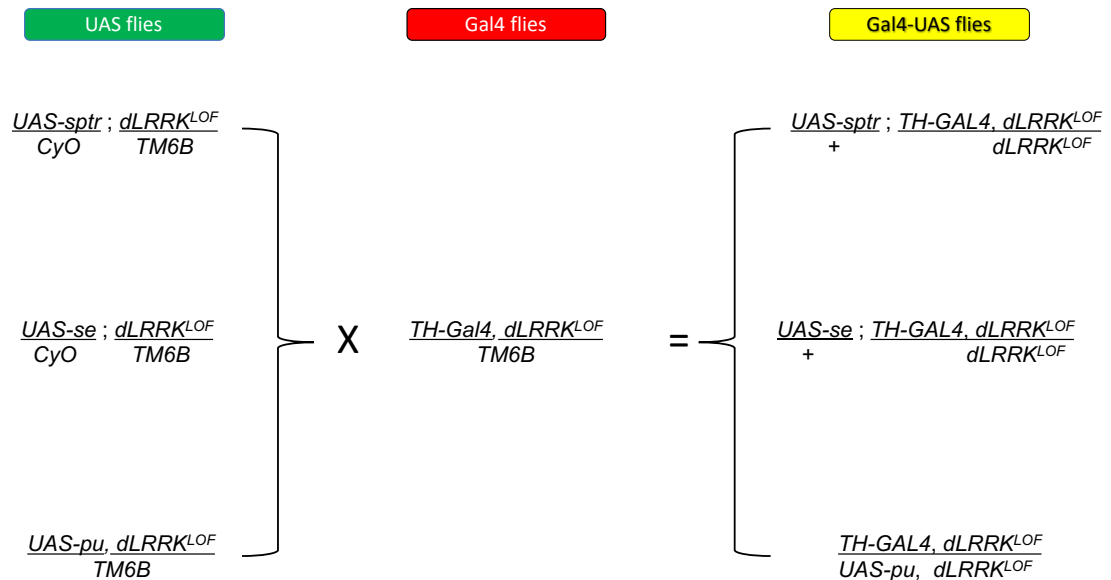


Figure 3.11 Crossing summary of flies over-expressing *sptr*, *se*, and *pu* in DA neurons in *dLRRK*^{LOF} background

The left side shows the different UAS lines used to cross with flies (in the middle) carrying Gal4 specific for DA neurons to produce flies expressing *sptr*, *se*, and *pu* in DA neurons in *dLRRK*^{LOF} background (the right side).

Examining the ERG traces of *sptr*, *se* and *pu* expression in combination with *dLRRK*^{LOF} showed a reduction in amplitude for old flies (Figure 3.12 A) and the quantification of ERG components (on transient, photoreceptors, and off transient) confirm this reduction by showing a significant age dependant decline in all genotypes tested indicating an inability to restore the visual dysfunction to the levels of young flies except in the off-transient element for *sptr* expression flies which shows no significant difference from the wild type control (Figure 3.12 B). Looking into the on-transient and off-transient data in old flies revealed no statistically significant difference is observed between tested and *dLRRK*^{LOF} mutant flies except in the on-transient element in *sptr* and *se* flies (Figure 3.12 C). The majority of the data from this experiment suggest that *sptr*, *se*, and *pu* expression were unable to rescue the age-dependent loss of visual function which indicate that they may not function within the same pathways as *dLRRK*.

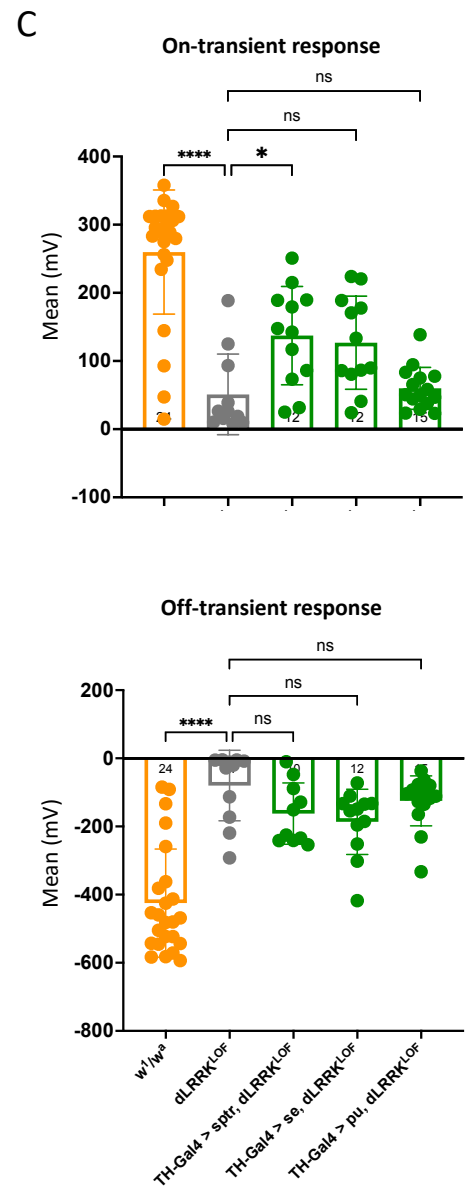
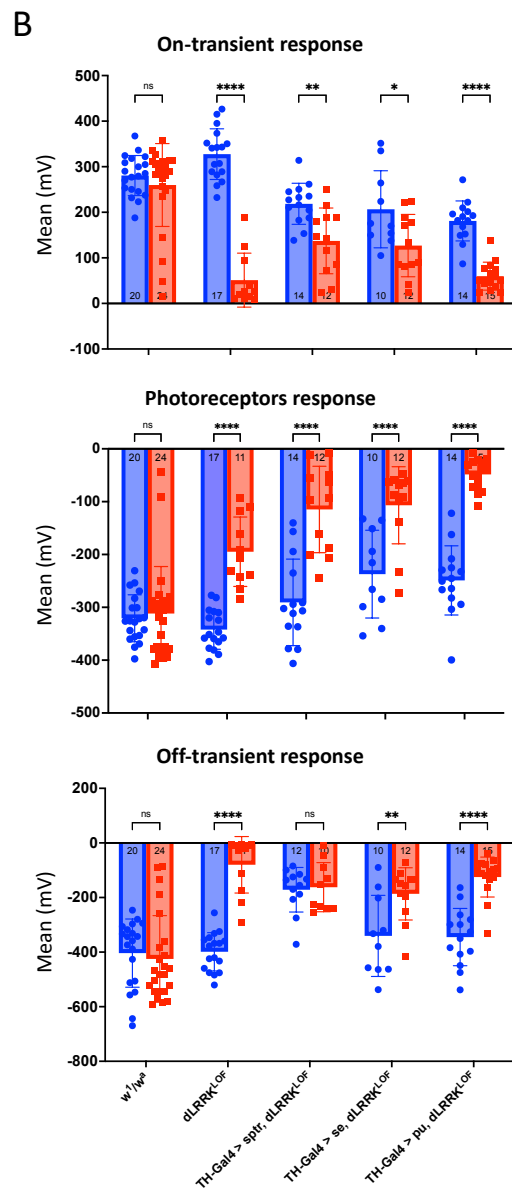
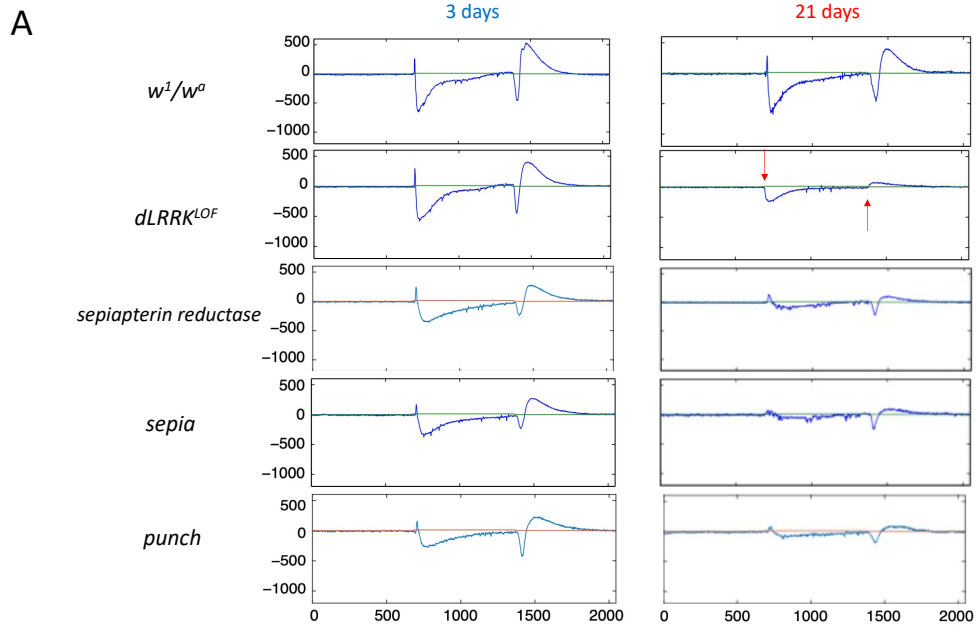


Figure 3.12 Over-expression of *sptr*, *se*, and *pu* had no effect on restoring normal ERG in old flies

A. Representative ERG traces from 3 days (left) and 21 days (right) of wild-type (w^1/w^a), $dLRRK^{LOF}$ mutant and flies over-expressing *sptr*, *se*, and *pu* in DA neurons in a $dLRRK^{LOF}$ background. ERGs are recorded in response to 0.5 second blue light pulses. Each trace is the mean of the fly's response to five flashes of blue light. ERG potential is measured in millivolt (mV) per milliseconds (ms). B. Quantification of the individual ERG components. The ERG of on-transient (top), photoreceptors (middle), and off-transient (bottom) responses were quantified for WT flies (w^1/w^a), $dLRRK^{LOF}$, and flies over-expressing *sptr*, *se*, and *pu* in DA neurons in a $dLRRK^{LOF}$ background. C. Quantification of 21 day old flies on-transient (top) and off-transient (bottom) components of ERG. All statistical values are ANOVA with post-hoc Tukey: **** $p < 0.00001$ *** $p < 0.0001$, ** $p < 0.001$, * $p < 0.05$, ns (no significant difference). Data presented are mean \pm SD bars; n numbers are displayed inside bars.

3.4 Discussion

In this investigation, we attempted to determine if the presence of dLRRK in other tissues could rescue the synaptic deficits observed in visual function of $dLRRK^{LOF}$ mutant flies. We tested expression of dLRRK in fat bodies, reproductive tract and pigment cells for ability to rescue elements of the ERG in the $dLRRK^{LOF}$ mutant. The expression of $dLRRK$ in non-neuronal tissues (pigment cells or fat body) was potentially able to rescue the age dependent loss of visual function in $dLRRK^{LOF}$ old flies.

The observation that the visual deficits in $dLRRK^{LOF}$ can be rescued by non-neuronal dLRRK raises the question of how the cells signal to each other - is it by cell-cell transfer of dLRRK or a downstream mechanism (e.g., TGF- β signalling)? The precise action of LRRK2 is still uncertain and has been linked to different organelles and cellular mechanisms (see section 1.2.4). A subset of late endosomal pathway extracellular vesicles known as exosomes are of particular interest because of their role in spreading misfolded proteins associated with neurodegenerative diseases. These exosomes contain materials such as DNA, RNA, or proteins, that are not normally secreted or are not stable extracellularly and can travel throughout the body and pass specialised compartments including the blood brain barrier (BBB) (Coleman and Hill, 2015). The findings in this investigation potentially support the notion of the ability of LRRK2 ability to travel throughout the body. The LRRK2 orthologue in the flies (dLRRK) when expressed outside the fly's visual system (a neuronal tissue) was able to rescue the age dependant loss of visual function found in $dLRRK^{LOF}$ old flies. The rescue was seen in flies expressing the native gene in pigment cells and fat body (non-neuronal tissue). Although

the quantification of ERG elements revealed no rescue was observed when *dLRRK* is expressed in male reproductive accessory organs, I would argue that it was because no gender selection was made and if the experiment were to be repeated just with male flies, I suspect a different result would come out.

Furthermore, the assertion that the severe reduction in the off-transient element of the ERG observed by (Furmston, 2016) in the *dLRRK^{LOF}* old flies was proposed to be due to the dysfunction in lower order neurons of the visual system (lamina neurons) is supported by the observation of a severe reduction in both the on-transient and off-transient found in this investigation. This is because the on-transient and off-transient elements of the ERG reflect the function of the lamina neurons that lie beneath the photoreceptors.

Mutations and imbalances in the levels of metabolites in the kynurenine and pteridine pathways have been linked to neurodegenerative disorders including PD. For example, in the kynurenine pathway, the levels of kynurenine and 3-HK have been shown to be higher in the CNS of PD patients (Iwaoka *et al.*, 2020). In addition, mutation in *cinnabar* (*cn³*) mutant flies have shown to affect the dynamic of mitochondria (Maddison *et al.*, 2020), which is a recurring theme in PD (Moon and Paek, 2015, Mortiboys *et al.*, 2015, Pickrell and Youle, 2015, Schapira *et al.*, 1990). Also, mutations in *scarlet* (*st¹*) mutant flies have revealed progressive loss of DA neurons, shortened lifespan, locomotor dysfunction and elevated levels of ROS. Furthermore, over-expression of *st* in the DA neurons of a PD fly model showed a neuroprotective effect (Cunningham *et al.*, 2018). In the pteridine pathway, BH₄ is produced from GTP by the action of *GTPCH I* (fly orthologue of *punch*) and *sepiapterin reductase* (fly orthologue of *sptr*). BH₄ is an essential cofactor for TH which regulates the biosynthesis of dopamine (Daubner *et al.*, 2011). A mutation in *punch* or *sepiapterin reductase* could have a cascading effect on BH₄ and therefore on dopamine levels. In fact, BH₄ levels have been found to be low in the CSF of PD patients and MPTP-treated monkeys (Ichinose *et al.*, 2018). That being said, the interaction mechanism between the different eye pigment genes in these pathways with *dLRRK* and the cause of synthetic lethality that it produces is still unknown. Although the crosses in this investigation (*cn^{35k}* and *pr¹*) didn't produce any lethality, the severe reduction in number and viability still indicate an interaction affecting physiology. Interestingly, the *cn^{35k}* mutation is a hypomorph mutation and has probably produced some protein that affected viability rather than lethality compared to the null mutation (*cn¹*) used in (Furmston, 2016) which led to a lethal interaction. In

addition, the overexpression of three eye pigment genes *punch*, *sepiapterin reductase*, and *sepia* in *dLRRK^{LOF}* old flies were not able to rescue the loss of visual function. This inability might indicate no interaction with the *dLRRK* mutation in the visual system or these genes function upstream of *dLRRK*. However, in the case of *punch*, data from the Elliott lab has demonstrated that *pu^{R1}* is synthetically lethal in combination with *dLRRK^{LOF}* (Cording and Elliott, unpublished) which might indicate an interaction is occurring but outside the visual system. Outside of the kynurenine and pteridine pathways, pigment genes can be involved in the trafficking and biosynthesis of pigment granules. They are involved with other sorting complexes proteins such as AP-3 and BLOC (Cheli *et al.*, 2010, Lloyd *et al.*, 1998) and RAB GTPase (Fukuda, 2021) in the movement of membrane bound vesicles carrying cargo. It is believed that *dLRRK/LRRK2* might function in this pathway and any dysfunction in the protein might lead to a negative effect on the granule pigment function which may lead to cell dysfunction and subsequent death. This idea is supported by the documented interaction of *LRRK2* with RAB proteins (Kuwahara and Iwatsubo, 2020) and the role of *dLRRK* and *LRRK2* in regulating the secretory dynamic of the trans Golgi network (Bonet-Ponce and Cookson, 2021, Lin *et al.*, 2015).

The pigment granules in the fly eye are a type of cell specific organelle known as lysosome-related organelles (LROs) generated by retinal cells. These LROs are derived from the endosomal system and their content varies based on the cell type where they originated from. In humans, LROs include melanosomes (produced by melanocytes in the skin), lamellar bodies (produced by alveolar type II cells in the lung), and alpha granules (produced by platelets cells in the blood) just to name a few (Bowman *et al.*, 2019). PD patients have high prevalence of melanoma than the general population (Bertoni *et al.*, 2010). Despite the association between PD and melanoma being well established, the mechanism underlying this association is still to be elucidated. For some time, it has been suggested that levodopa, the most effective treatment for PD, was the culprit (Sandyk, 1992). But recent studies such as (Dalvin *et al.*, 2017) found that the chance of developing melanoma for PD patients is almost the same as developing PD for melanoma patients which suggested no role for levodopa. *LRRK2-G2019S* patients have high cancers risk (Agalliu *et al.*, 2015) including an association with melanoma among others (Inzelberg *et al.*, 2016). Moreover, DA neurons and melanocytes are both pigmented and share common pathways that include L-dopa. If *LRRK2* plays a role in

regulating LROs such as melanosomes, then the increased risk of developing melanoma in LRRK2-PD patients could be attributed to LRRK2 dysfunction.

Another interesting type of LRO that might be affected in LRRK2-PD is lamellar bodies. These are produced by alveolar type II epithelial cells in the lungs which are responsible for synthesis and secretion of pulmonary surfactants that are required for normal lung function (Schmitz and Müller, 1991). It has been found that using LRRK2 inhibitors such as PFE-360 and MLI-2 induced abnormal changes to lamellar bodies *in vivo* or *in vitro* (Baptista *et al.*, 2020, Harney *et al.*, 2021). However, these changes were reversible and didn't affect lung function suggesting a safe and on target efficacy for these inhibitors. Interestingly, a recent study by (Lebovitz *et al.*, 2021) could tell a different story. Instead of using LRRK2 inhibitors, they used LRRK2 knockout mice to reduce the expression of the gene. They have found that reduction in LRRK2 promoted tumorigenesis in the lung which was associated with dysfunctional surfactant metabolism. These reports suggest an interaction between LRRK2 and lamellar bodies, however, the mechanism of that interaction is still to be elucidated. Our findings of genetic interactions between *pr*, *cn* and *dLRRK^{LOF}* further indicate and expand a potential role of dLRRK/LRRK2 in the regulation of membrane traffic and pigment synthesis in neurons.

4 The effect of dopaminergic *LRRK2-G2019S* expression on eye adaptation to light

4.1 Introduction

As mentioned in Chapter 1, visual dysfunction is one of the non-motor symptoms reported by PD patients. Although this dysfunction manifests mostly in the retina, PD-related neurological dysfunction can also be observed in the visual circuits beyond the retina e.g., in the visual cortex (Weil *et al.*, 2016). Investigating these visual symptoms is crucial because of their prevalence, as observed in one report by (Davidsdottir *et al.*, 2005) found 78% of PD patients showed at least one visual dysfunction, suggesting the possibility of using this system as a marker for early diagnosis (Diederich *et al.*, 2010).

The ability of the eyes to adjust to different light intensity depends on the feedback coming from the photoreceptors. In dark conditions, photoreceptors are very sensitive to light. This sensitivity decreases when illumination increases to avoid photoreceptors being saturated and extend their ability to detect a range of light intensity (Purves *et al.*, 2001). The process of converting light into neural signal is called phototransduction which involves a series of molecular reactions occurring within photoreceptors. These reactions start with activating the G-protein coupled receptor rhodopsin and working through multiple steps eventually leading to (in mammals) the closing of the ion channels in the photoreceptors membrane which leads to neurotransmitter being released and the initiation of neural signal to the next neurons. For more details on phototransduction see review by (Lamb and Pugh, 2006). This feedback will lead to eye adaptation which include change in pupil sizes.

Flies, just like humans, must adapt to light in order to respond to the variation of light levels that come from their environment. In fact, they adapt to changes in light intensity in a circadian fashion (Nippe *et al.*, 2017) where axons have been found to change in size and shape at the start of the day and the start of the night (Damulewicz *et al.*, 2020, Pyza and Meinertzhagen, 1999). In addition, they adapt to light over a shorter period of time (100 ms) (Juusola and Hardie, 2001), 10-100 times faster than vertebrates (Hardie and Juusola, 2015).

We investigate abnormalities in eye adaptation to light is investigated here as a model of visual symptoms observed in PD. Similar dysfunction has been reported in PD patients where after a period of light adaptation, PD patients demonstrated a

significantly larger pupil diameters with unequal pupil sizes (anisocoria) compared to controls (Micieli *et al.*, 1991). Moreover, irregular pupil reflexes to light (Giza *et al.*, 2011, Stergiou *et al.*, 2009) and supersensitivity to eye-drop test were observed as well (Yamashita *et al.*, 2010). Similarly, in our PD mimic flies, expressing *LRRK2-G2019S* in dopaminergic neurons produces abnormalities in the neural response of the eye: young flies showed higher neural responses, but old flies had lost their photoreceptors responses (Afsari *et al.*, 2014). This is a sign of failure of the eye to adapt. It was suggested that this was due to the high energy demand at an early age followed by an increased apoptosis and degradation of photoreceptors and their mitochondria (Afsari *et al.*, 2014, West *et al.*, 2015a). This led to the hypothesis that the overresponsive Steady State Visually Evoked Potential (SSVEP), which is an assay to evaluate visual function, in young flies expressing *LRRK2-G2019S* in the dopaminergic neurons might be due to a failure of adaptation.

In this investigation, eye adaptation will be tested in flies expressing *LRRK2-G2019S* in multiple neuronal cell types. Adaptation will be evaluated physiologically and anatomically. The physiological evaluation will utilize ERG (see section 2.3.1) to detect abnormalities in eyes neural response. In this approach, the neural response of the eye to brief flashes of dim light before and after a prolonged bright light is investigated.

Anatomically, deep pseudopupil (DPP) formation will be used to assess the integrity of the eye structure. DPP acts in a similar way to the change in pupil size in humans during light adaptation and was first observed in flies by (Franceschini and Kirschfeld, 1971). When the eye of a WT fly is illuminated from above, the DPP manifests as a dark spot where around 6 ommatidia absorb light. If the eye is illuminated from below, the DPP manifests as a bright spot where light travels along the 6 ommatidia towards the observer. The size of the DPP decreases with increased illumination. This is due to the pigment granule migration from the photoreceptor cell body towards the rhabdomeres which facilitates the reduction of the amount of light coming into the eyes to prevent harmful effects. When illumination is reduced, pigment granules migrate back to the cell (Fellgett *et al.*, 2021, Stavenga *et al.*, 2017).

In addition to the DPP which looks at the entire eye, pseudopupil analysis (PPA) is also used to look at the retinal anatomy in more detail. This is This technique has been used by different research groups (Campesan *et al.*, 2011, Song *et al.*, 2013) to examine individual ommatidia and their 7 visible rhabdomeres to assess any damage to them.

4.2 Aim

The aim of this chapter is to test if expressing *LRRK2-G2019S* in different parts of the fly's eye (photoreceptors, DA neurons, or pigment cells) has an effect on eye adaptation to light and this will be done

1. Physiologically using ERG to detect any abnormalities in eye neural response and
2. Anatomically using DPP and PPA to detect any structural abnormalities in the eye.

4.3 Results

4.3.1 Investigating the effect of expressing *LRRK2-G2019S* in components of the visual circuit on eye adaptation using ERG

The effect of expressing *LRRK2-G2019S* in sub-structures of the visual circuit on eye adaptation to light is assayed physiologically using ERG. Flies will be subjected to flashes of dim light in the dark before and after a period of prolonged bright light. The mean ERG amplitude before (referred to as dark adapted) and after (referred to as light adapted) will be quantified and compared to look for any differences that might suggest dysfunction of eye adaptation to light. As shown in Figure 4.1. The fly was acclimatised to the rapidly flashing blue light for 4 minutes and then exposed to bright white light for 6 minutes, before the rapid blue flashes were resumed. In some cases, the DC offset of the trace had to be adjusted to keep the recording on the screen – as shown by the red arrow.

In addition to *LRRK2-G2019S* (a hyperactive kinase) expression, *LRRK2-WT* and *LRRK2-G2019S-K1906M* (kinase dead, KD) were tested as controls. Ideally, *WT* flies (*CS* or *w*) and flies with only one component of the Gal4/UAS should have been tested as well. The measurement for these flies is at young (4 hours and 3 days) and old ages (21 days) and these time points were selected based on the work of (Afsari *et al.*, 2014, Hindle *et al.*, 2013) which showed abnormal ERG for *TH>G2019S* flies at these ages.

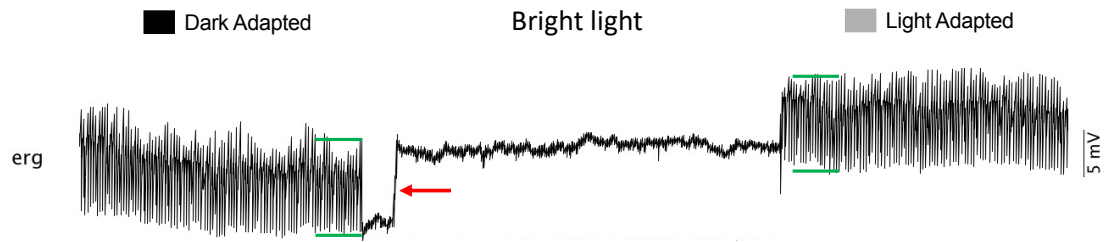


Figure 4.1 An example of a recorded ERG for eye adaptation to light test

Rapid blue flashes of 100ms were given at 5 seconds intervals and the ERG recorded as in section 2.3.1. The peak-peak amplitude of the ERG was measured before and after the bright light (green bars). To keep the trace within range, the DC offset was adjusted as required, as in this example (red arrow).

4.3.1.1 The effect of expressing *LRRK2-G2019S* in the photoreceptors

The first tissue to be tested for the effect of *LRRK2-G2019S* expression on visual responses was the photoreceptor. To facilitate this expression, the Gal4 driver to be utilised is *rh1-Gal4*, which drives expression in the first layer of the fly retina, the photoreceptors. This transgene is specific for the R1-6 photoreceptors. Across all the different ages and genotypes of tested flies, no change in ERG amplitude has been observed in the ERG traces (Figure 4.2 A) and their quantifications (Figure 4.2 B).

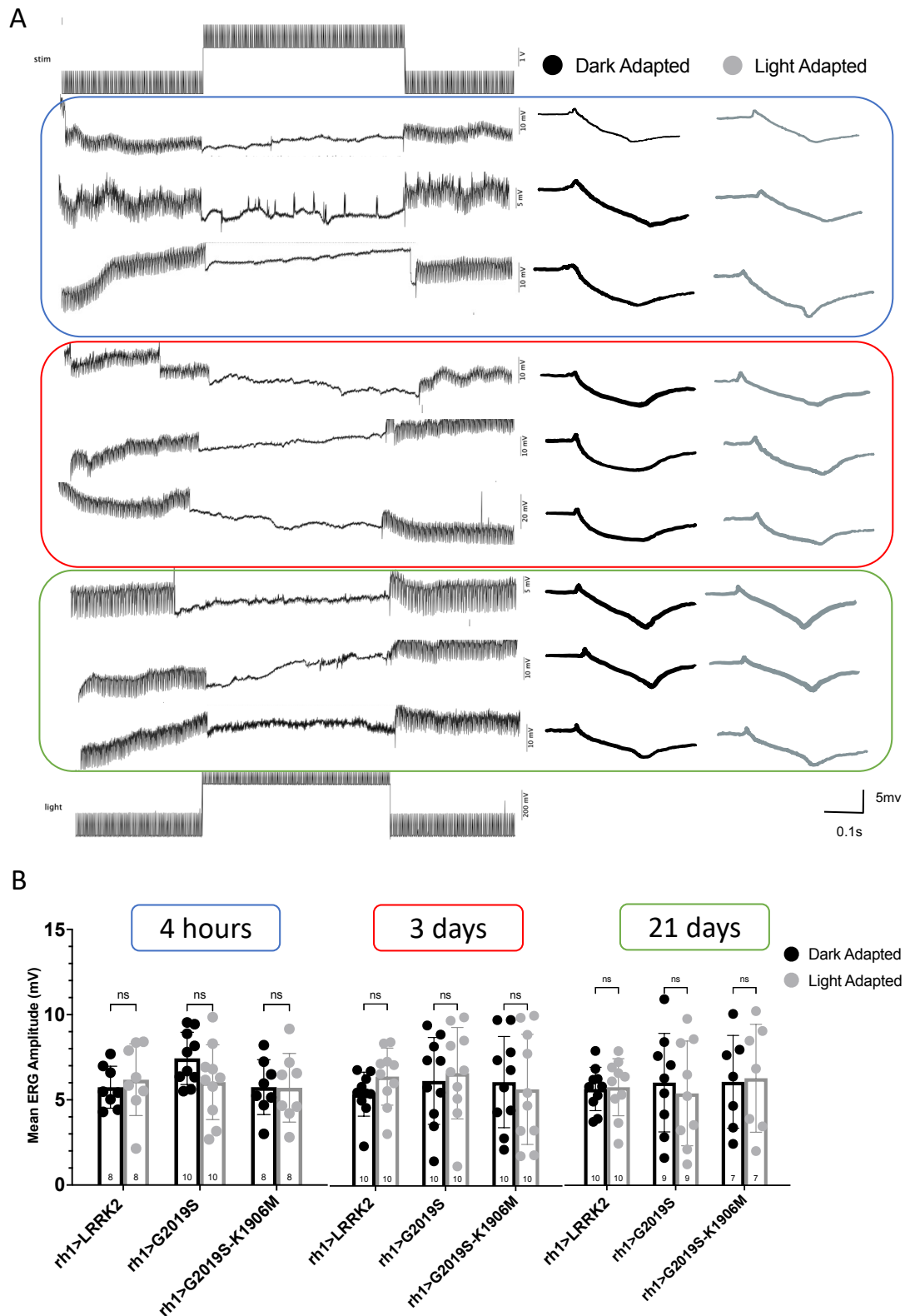


Figure 4.2 No changes in ERG amplitude is observed in flies expressing *LRRK2-G2019S* in the photoreceptors

A. Representatives ERG traces with their dark (in black) and light (in grey) adapted means next to them of flies expressing *LRRK2-WT*, *LRRK2-G2019S*, and *LRRK2-G2019S-K1906M* respectively in photoreceptors. The blue, red, and green boxes indicate the representative ages when the ERG was recorded which is 4 hours, 3 days,

and 21 days respectively. B. The quantification of ERG amplitude of 8-10 flies from each genotype in 4 hours, 3 days, and 21 days respectively. All statistical values are ANOVA with post-hoc Tukey: **** $p < 0.00001$ *** $p < 0.0001$, ** $p < 0.001$, * $p < 0.05$, ns (no significant difference). Data presented are mean \pm SD bars; n numbers are displayed inside bars.

4.3.1.2 The effect of expressing *LRRK2-G2019S* in DA neurons

Since no changes were observed in visual responses when *LRRK2-G2019S* was expressed in the photoreceptors, *TH-Gal4* was next used to drive the expression of *LRRK2-G2019S* in DA neurons. These DA neurons are found in the CNS and they can also be found in the lamina cortex which is the second layer of neurons found beneath the photoreceptors. In addition, the expression of *LRRK2-G2019S* in DA neurons has already been found to have an effect on fly visual function in aged flies (Hindle *et al.*, 2013). In this investigation, the expression of *LRRK2-WT*, *LRRK2-G2019S*, or *LRRK2-G2019S-K1906M (KD)* in DA neurons induced a significant difference in ERG amplitude before and after exposure to bright light in young flies (4 hours). The dark adapted flies had much larger ERGs than the light-adapted flies. By day 3, this difference was only seen in flies expressing *LRRK2-G2019S*. This is likely because in the *LRRK2-G2019S* expressing flies the dark adapted response was kept at almost the same level as the 4 hours one. By 21 days, the difference in ERG amplitude has disappeared but a decline in the overall amplitude for all genotypes is observed (Figure 4.3). This is interesting because a failure in light adaption was expected to be at an old age rather than at young one.

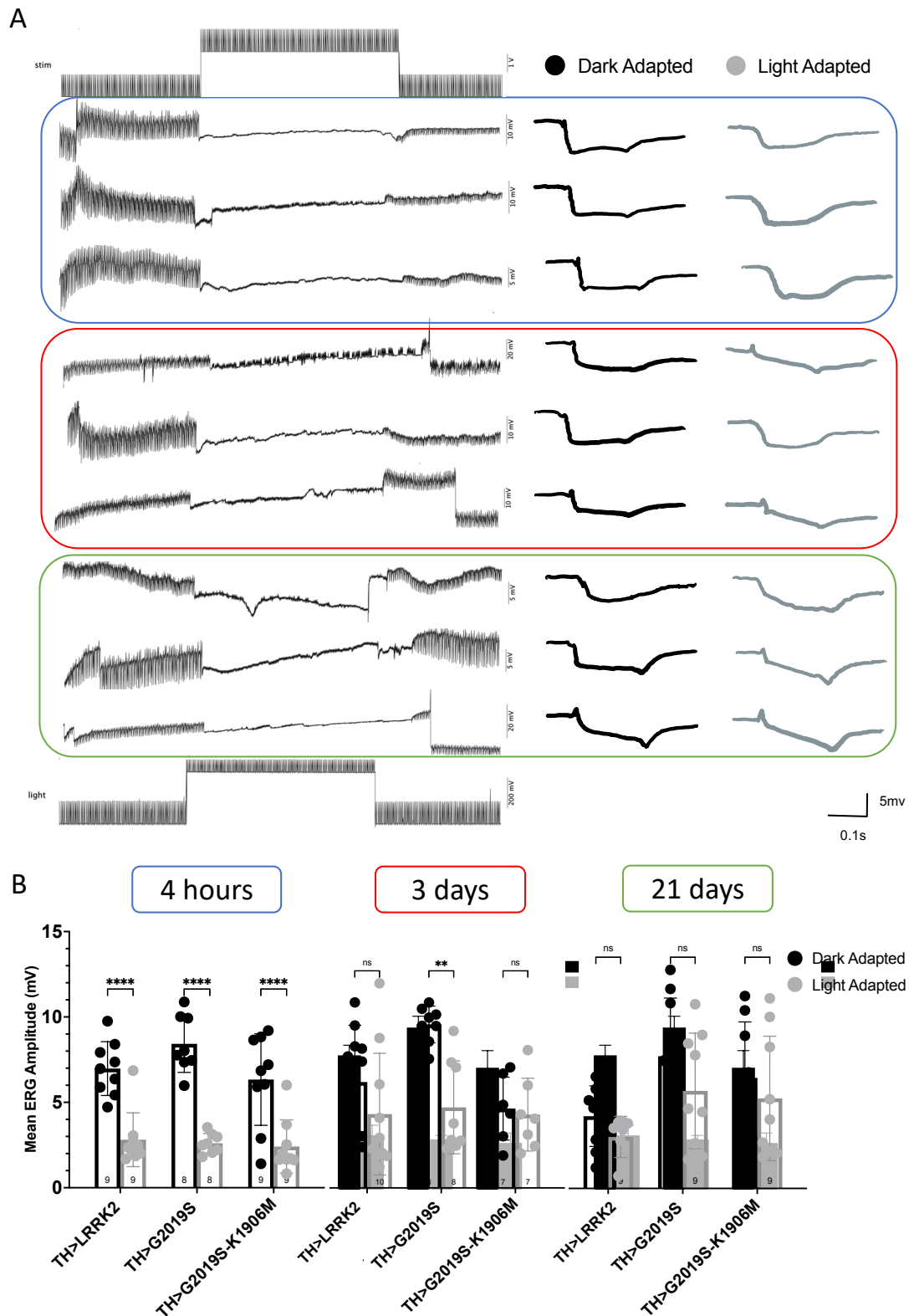


Figure 4.3 A failure in adaptation is observed in ERG amplitude in young flies expressing *G2019S* in DA neurons indicated by the decline in ERG amplitude in light adapted condition

A. Representatives ERG traces with their dark (in black) and light (in grey) adapted means next to them of flies expressing *LRRK2-WT*, *LRRK2-G2019S*, and *LRRK2-G2019S-K1906M* respectively in DA neurons. The blue, red, and green boxes indicate

the representative ages when the ERG was recorded which is 4 hours, 3 days, and 21 days respectively. B. The quantification of ERG amplitude of 8-10 flies from each genotype in 4 hours, 3 days, and 21 days respectively. All statistical values are ANOVA with post-hoc Tukey: **** $p < 0.00001$ *** $p < 0.0001$, ** $p < 0.001$, * $p < 0.05$, ns (no significant difference). Data presented are mean \pm SD bars; n numbers are displayed inside bars.

4.3.1.3 The effect on visual responses of expressing *LRRK2-G2019S* in pigment cells

The process of eye adaptation to light involves changes in phototransduction and migration of pigment granules toward or away from rhabdomere. Expressing *LRRK2-G2019S* in photoreceptors and DA neurons tested the changes in phototransduction effect on adaptation while expressing the protein in the pigment cells would test the pigment migration effect on adaptation. Expressing *LRRK2-G2019S* in pigment cells (P(Gal4)56C) in the 4 hour old flies demonstrated a decline in ERG amplitude from the dark adapted state to the light adapted state, however; only the *LRRK2-G2019S* expressing flies show statistical significance (Figure 4.4). In the 3 day old flies, the decline is again only seen in the *LRRK2-G2019S* expressing flies. Lastly, in the 21 day old, there is no effect, though the data suggests a larger sample might reveal a difference.

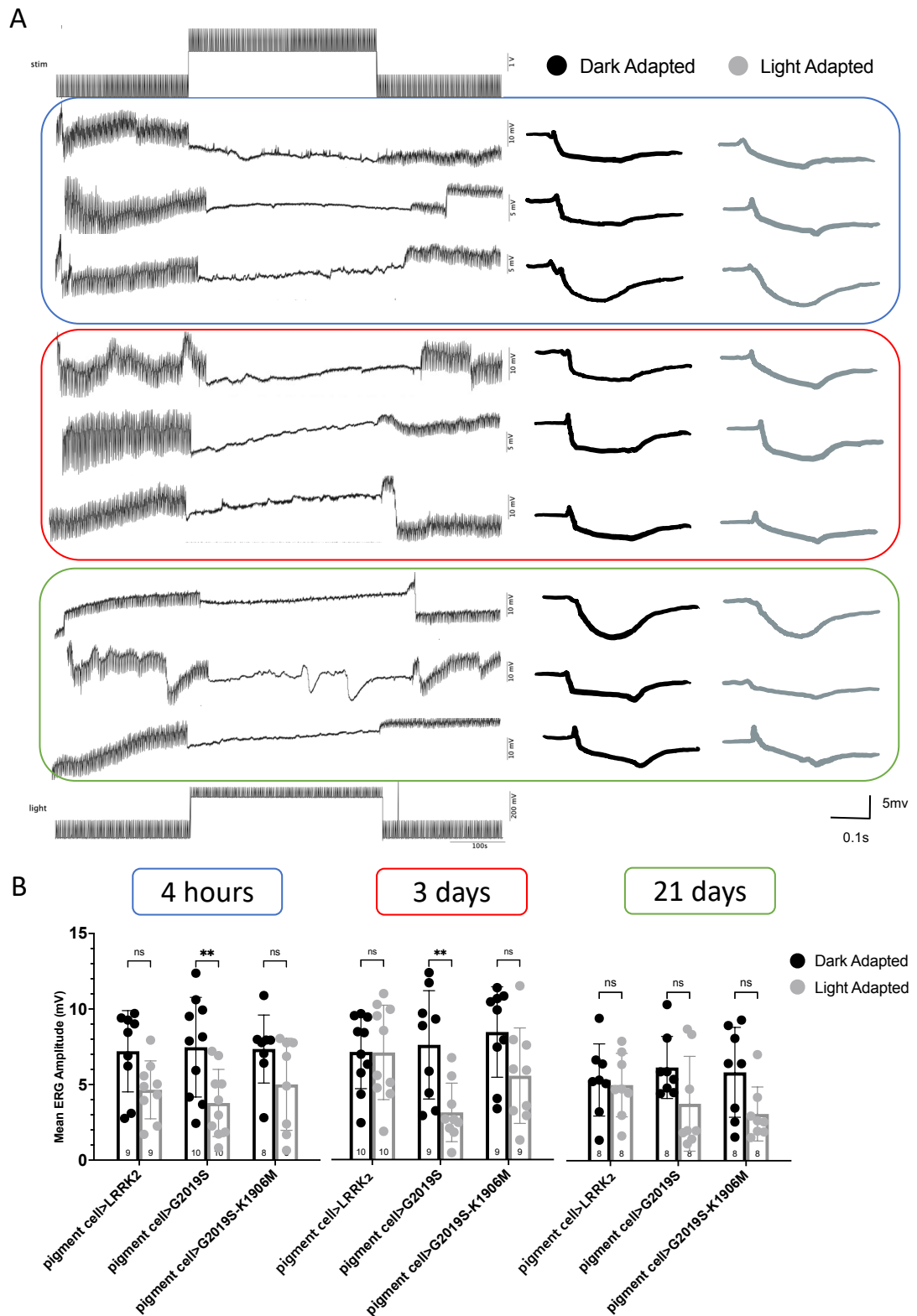


Figure 4.4 A failure in adaptation is observed in young flies expressing *LRRK2-G2019S* in pigment cells indicated by the decline in ERG amplitude in light adapted condition

A. Representatives ERG traces with their dark (in black) and light (in grey) adapted means next to them of flies expressing *LRRK2-WT*, *LRRK2-G2019S*, and *LRRK2-G2019S-K1906M* respectively in pigment cells. The blue, red, and green boxes indicate

the representative ages when the ERG was recorded which is 4 hours, 3 days, and 21 days respectively. B. The quantification of ERG amplitude of 8-10 flies from each genotype in 4 hours, 3 days, and 21 days respectively. All statistical values are ANOVA with post-hoc Tukey: **** $p < 0.00001$ *** $p < 0.0001$, ** $p < 0.001$, * $p < 0.05$, ns (no significant difference). Data presented are mean \pm SD bars; n numbers are displayed inside bars.

Focusing on the data from the young flies, particularly the 3 days old data, an ANOVA test for the different genotypes showed that the expressing of *LRRK2-G2019S* in DA neurons and pigment cells seems to affect significantly flies ability to adapt to light (Figure 4.5).

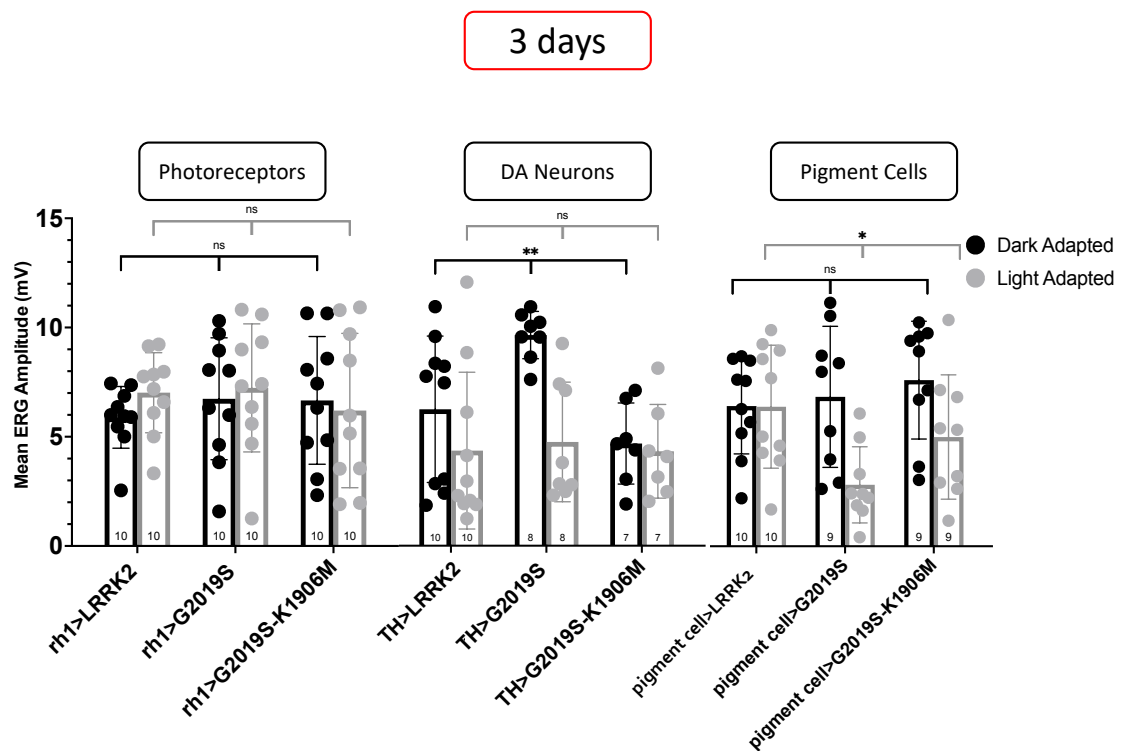


Figure 4.5 A significant difference in ERG amplitude is observed when *LRRK2-G2019S* is expressed in DA neurons and pigment cells in 3 days old flies

The quantification of ERG amplitude from 8-10 flies of *LRRK2-WT*, *LRRK2-G2019S*, and *LRRK2-G2019S-K1906M* in photoreceptors, DA neurons, and pigment cells respectively. All statistical values are one way ANOVA: **** $p < 0.00001$ *** $p < 0.0001$, ** $p < 0.001$, * $p < 0.05$, ns (no significant difference). Data presented are mean \pm SD bars; n numbers are displayed inside bars.

4.3.2 Investigating the effect of expressing *LRRK2-G2019S* on eye adaptation using Deep Pseudo-Pupil (DPP) analysis

In addition to investigating the effect of expressing *LRRK2-G2019S* expression on eye adaptation physiologically using ERG, DPP was utilised to examine any effect on the eye anatomy that may be development or degenerative. Flies are again subjected to a bright light before and after a period of prolonged darkness. The mean sizes of DPP of the before period (referred to as light adapted) and the after period (referred to as dark adapted) will be quantified and compared to look for any differences that might suggest dysfunction of eye adaptation to light. The same ages and genotypes from the ERG experimental analysis will be applied here as will.

4.3.2.1 The effect of expressing *LRRK2-G2019S* in photoreceptors on DPP development

We analysed DPP size and presence in flies expressing *LRRK2-G2019S* in photoreceptors. Overall, the mean size of the DPP in light adapted was $0.33 \text{ mm}^2 \pm 0.08 \text{ SD}$ and $0.32 \text{ mm}^2 \pm 0.07 \text{ SD}$ in dark adapted which corresponds to the area of 8-12 ommatidia. Assessing the formation of DPP in flies expressing *LRRK2-WT*, *LRRK2-G2019S*, and *LRRK2-G2019S-K1906M* in photoreceptors using *rh1-Gal4* revealed no structural differences observed between light adapted and dark adapted states of any age or genotypes. Furthermore, the quantification of DPP sizes confirm this observation where no significant statistical differences were found within the same genotype. Interestingly, however, an analysis of variance performed showed a significant difference among the different genotypes across all ages (Figure 4.6). At 4 hours and 21 days, *LRRK2-G2019S* expressing flies had an increased DPP of approximately 30% - 50% from either *LRRK2-WT* or *LRRK2-G2019S-K1906M* flies. At 3 days, DPP in *LRRK2-G2019S* expressing flies was around 35% more than *LRRK2-G2019S-K1906M* flies. Approaching this result was the observation that DPP in *LRRK2-WT* expressing flies was nearly the same size as the effect in *LRRK2-G2019S* expressing flies.

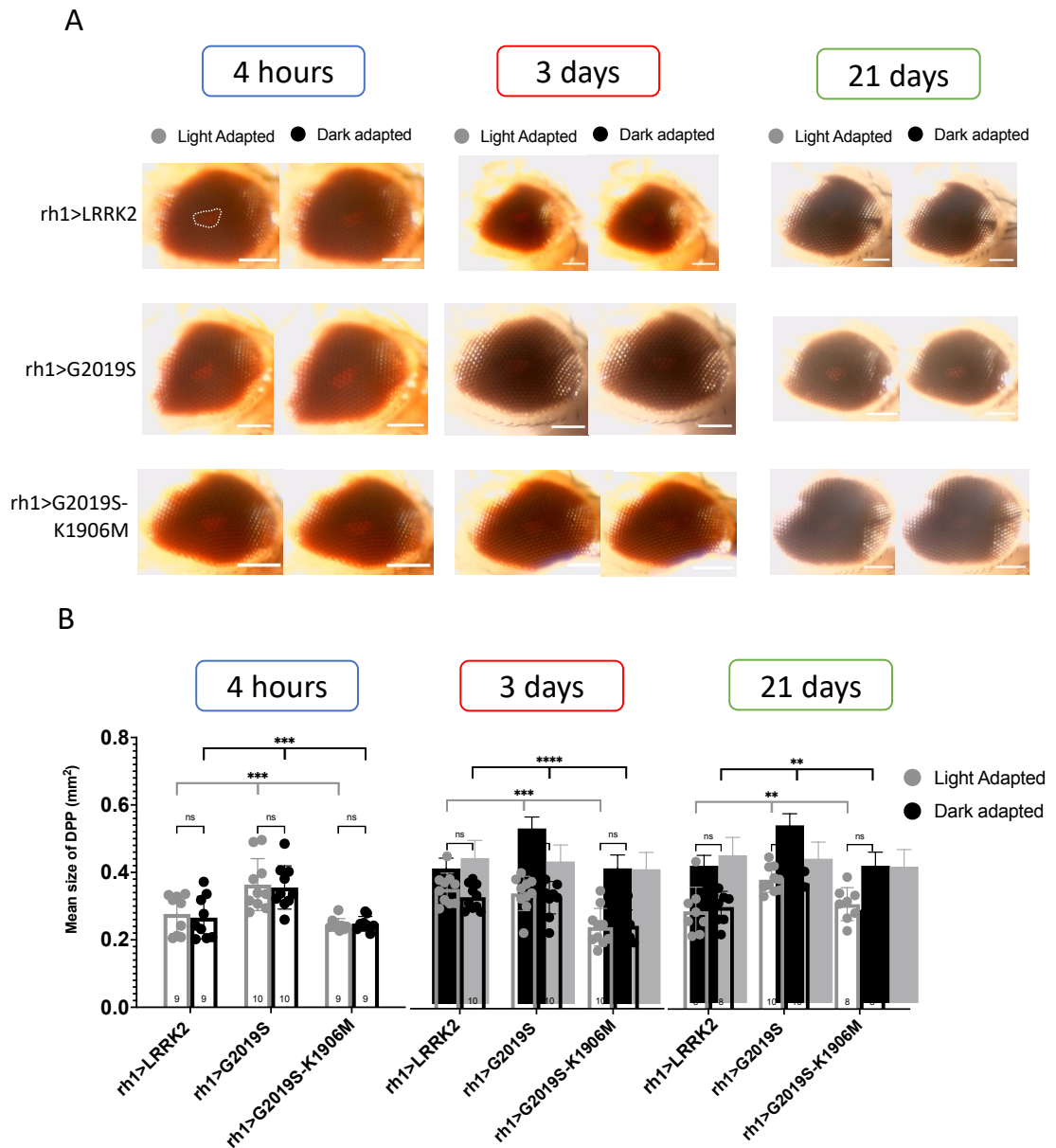


Figure 4.6 A larger DPP is formed in flies expressing *LRRK2-G2019S* in photoreceptors

A. Representative images of DPP formation in flies expressing *LRRK2-WT*, *LRRK2-G2019S*, and *LRRK2-G2019S-K1906M* in photoreceptors. B. The quantification of the size of DPP for 8-10 flies from each genotype in 4 hours, 3 days, and 21 days respectively. Abbreviations WT (*LRRK2* wild type), GS (*G2019S*), and KD (kinase dead). The white dotted line in light adapted WT flies indicate a sample of the DPP area of measurement. Scale bar 1 mm. All statistical values are ANOVA with post-hoc Tukey: **** $p < 0.00001$ *** $p < 0.0001$, ** $p < 0.01$, * $p < 0.05$, ns (no significant difference). Data presented are mean \pm SD bars; n numbers are displayed inside bars.

To add an extra layer in investigating the effect of expressing *LRRK2-G2019S* in sub-components of the fly eye on DPP, PPA was utilised to visualise the rhabdomeric

structure and arrangement in the ommatidium. Unfortunately, the analysis for these flies (*rh1-Gal4*) was unsuccessful in acquiring any clear images. This failure, most likely, was not due to abnormalities in the structure of the ommatidia but rather to the unoptimized settings of the microscope used to perform the task and the dark red nature of these flies' eyes because a WT fly with red eye colour showed similar results.

4.3.2.2 The effect on DPP of expressing *LRRK2-G2019S* in DA neurons

The assessment of DPP formation in flies expressing *LRRK2-G2019S* in DA neurons (*TH-Gal4*) was unsuccessful. The very pale-pigmented nature of their eyes made it very difficult to tell whether they are forming DPP or not, especially in young flies. Figure 4.7 demonstrates the best samples obtained from these flies where older flies seems to have some DPP formed as their eye pigments intensify with age. Moreover, it is possible that the camera used in this experiment was not sensitive enough to capture DPP in these pale-pigmented flies. Therefore, the quantification of DPP was not performed.

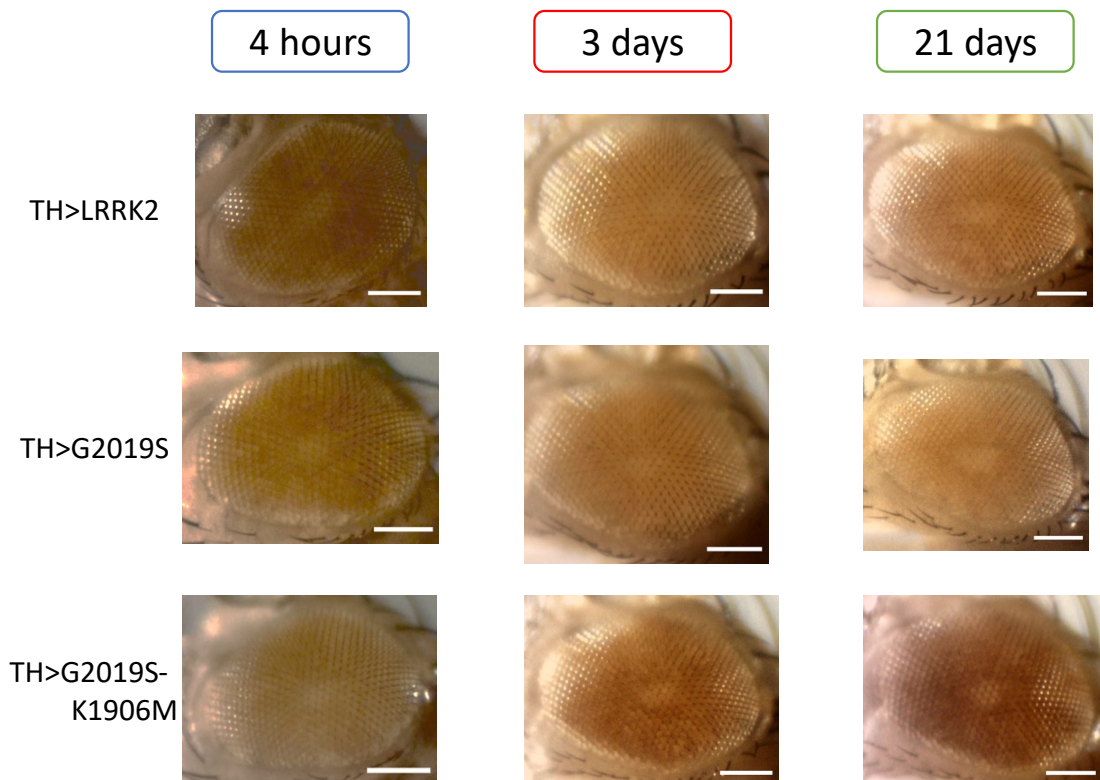


Figure 4.7 Inconclusive results for DPP formation in flies expressing *LRRK2-G2019S* in DA neurons

Representative images of DPP formation in flies expressing *LRRK2-WT*, *LRRK2-G2019S*, and *LRRK2-G2019S-K1906M* in DA neurons.. Scale bar 1 mm. n=8-10.

On the other hand, PPA of the *TH*-Gal4 was more successful than for the *rh1*-Gal4 flies, because the eyes were orange rather than dark red. The PPA of all three crosses showed a regular structure and clustering. There were no abnormalities in rhabdomere numbers (in each case 7 cells were counted) and the hexagonal pattern was preserved (Figure 4.8) indicating no anatomical damage brought by expressing *LRRK2-G2019S* in DA neurons.



Figure 4.8 No degeneration of ommatidia observed in flies expressing *LRRK2-G2019S* in DA neurons

Representative images of pseudopupil analysis in flies expressing *LRRK2-WT*, *LRRK2-G2019S*, and *LRRK2-G2019S-K1906M* in DA neurons. A 25-30 ommatidia were examined per fly. Scale bar 50 μm .

4.3.2.3 The effect on DPP of expressing *LRRK2-G2019S* in pigment cells

Similar to expressing *LRRK2-G2019S* in photoreceptors, expressing *LRRK2-G2019S* in pigment cell didn't reveal any structural differences between light adapted and dark adapted states for the DPP formation for any age or genotype. However, the

quantification of the size of the DPP formed revealed a significant difference among the different genotypes in mostly the young flies (4 hours and 3 days) compared to all ages in the photoreceptors of expressing flies. In addition, the size of DPP in the 4 hour old flies expressing *LRRK2-G2019S* was around 40% and 70% more than the WT and KD respectively. At 3 days, DPP in flies expressing *LRRK2-G2019S* was around 20% and 60% more than the wild type and kinase dead respectively. This increase was almost lost at 21 days (Figure 4.9).

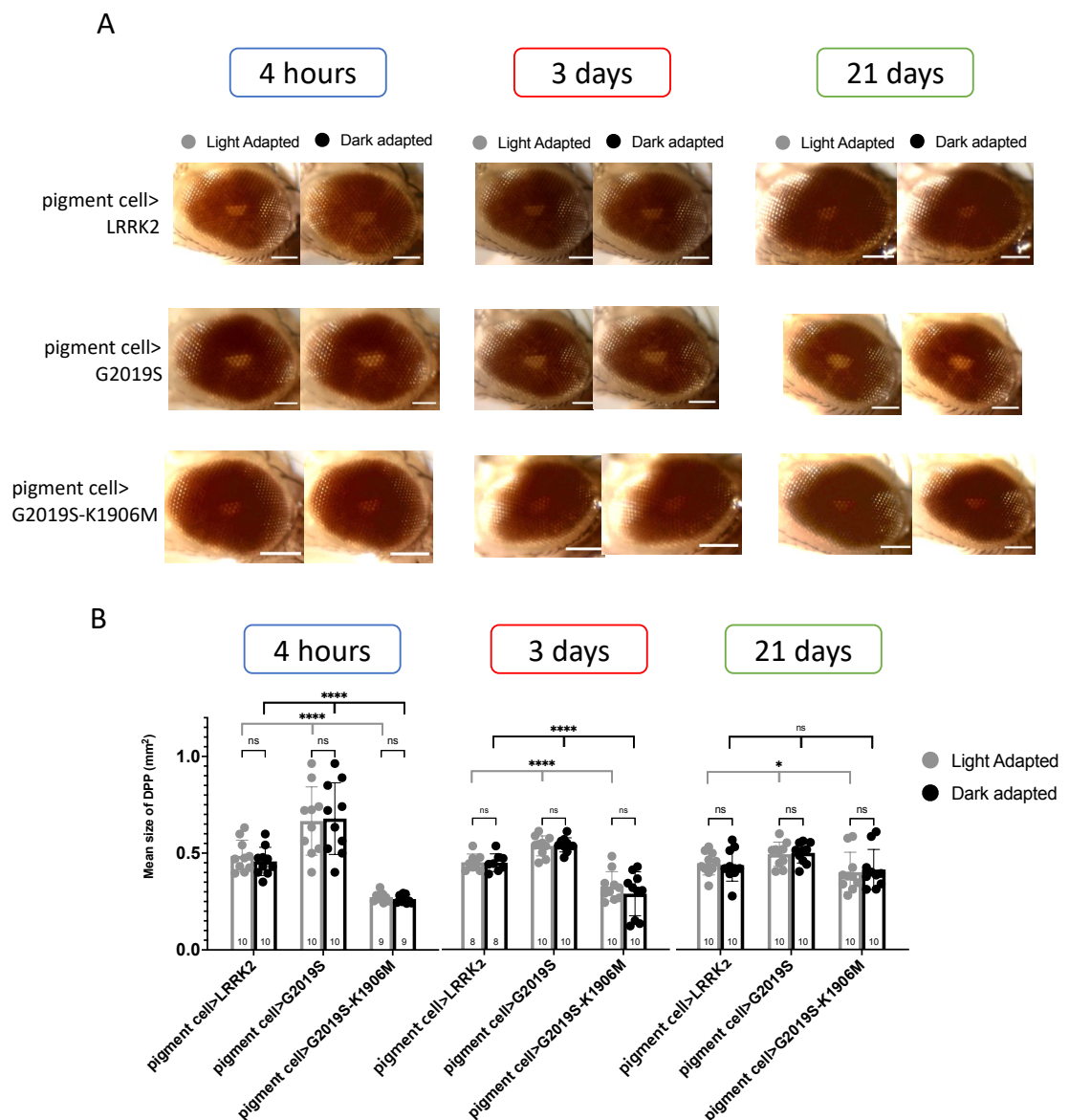


Figure 4.9 A larger DPP formed in young flies expressing *LRRK2-G2019S* in pigment cells

A. Representative images of DPP formation in flies expressing *LRRK2-WT*, *LRRK2-G2019S*, and *LRRK2-G2019S-K1906M* in pigment cells. B. The quantification of the size of DPP for 8-10 flies from each genotype in 4 hours, 3 days, and 21 days

respectively. Abbreviations WT (LRRK2 wild type), GS (G2019S), and KD (kinase dead). Scale bar 1 mm. All statistical values are ANOVA with post-hoc Tukey: **** $p < 0.00001$ *** $p < 0.0001$, ** $p < 0.001$, * $p < 0.05$, ns (no significant difference). Data presented are mean \pm SD bars; n numbers are displayed inside bars.

In regard to PPA of the for flies expressing *LRRK2-G2019S* in pigment cells, the data showed similar results to flies expressing LRRK2 variants in the the DA neurons flies i.e., no abnormalities in rhabdomeres numbers and structure have been observed (Figure 4.10).

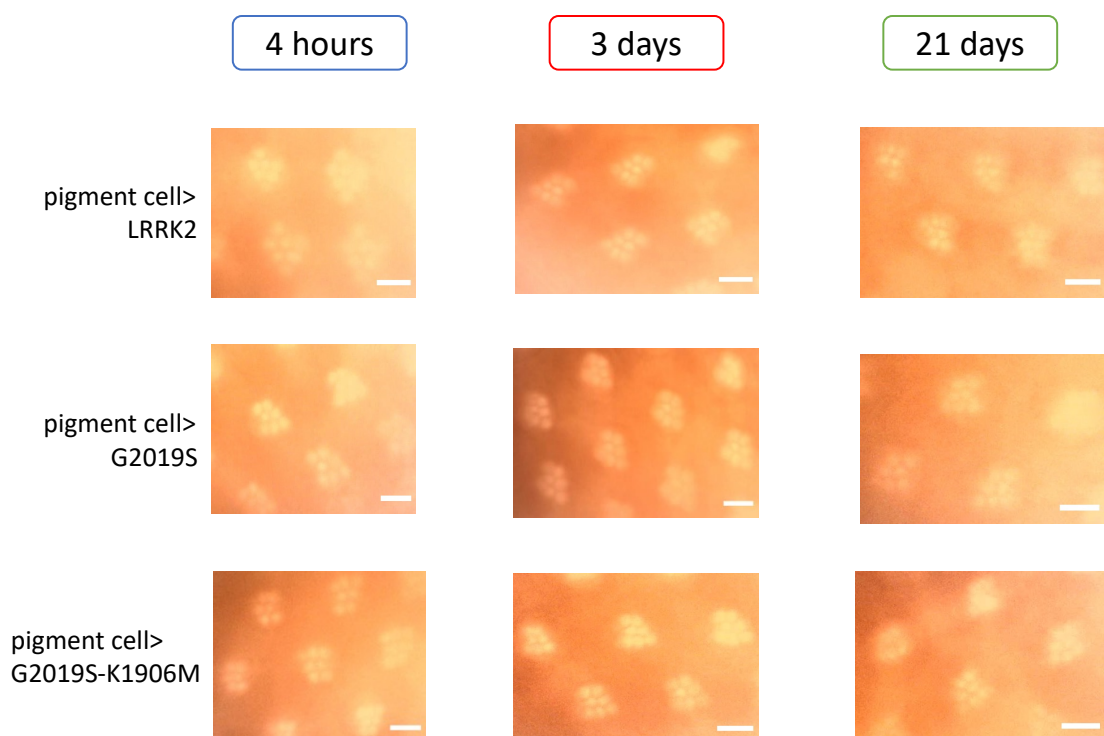


Figure 4.10 No degeneration of ommatidia observed in flies expressing *LRRK2-G2019S* in pigment cells

Representative images of pseudopupil analysis in flies expressing *LRRK2-WT*, *LRRK2-G2019S*, and *LRRK2-G2019S-K1906M* in pigment cells. A 25-30 ommatidia were examined per fly. Scale bar 50 μm .

4.4 Discussion

In this investigation, adaptation was assessed physiologically by comparing the amplitude of the ERG before and after a period of intense bright light. The key observation is that young flies (3 day old) expressing *LRRK2-G2019S* in DA neurons or

pigment cells fail to adapt to the dark, as indicated by their relatively larger ERGs before exposure to bright light. This was partially complemented by anatomical assessment where the DPP in flies with *LRRK2-G2019S* expressed in pigment cells was larger than the DPP of flies expressing *WT* or *KD* forms of *LRRK2* (Figure 4.7). This raises the question of the mechanism(s) behind this observation. First, as *LRRK2-G2019S* expression in fly DA neurons reduces dopamine release (Cording *et al.*, 2017) and this will affect the shape of the photoreceptor response in the ERG as flies treated with octopamine or dopamine had reduced photoreceptors signals (Chyb *et al.*, 1999), this may lead to aberrant ERGs. Secondly, I have shown earlier in chapter 3 that *dLRRK* (the *Drosophila* orthologue of *LRRK2*) mutants genetically interacts with mutations in genes regulating the formation of the pigment granules, therefore *LRRK2-G2019S* expression might result in disruption to the ERG and DPP through regulation of pigment granule formation and function. Both dopamine function and pigment granule migration affect the detection of light on the photoreceptor, so that, in either case *LRRK2-G2019S* expression leads to hyperactivity. The aberrant, oversized ERGs would indicate an excessive ionic flux, and resulting demand for ATP during each light flash. Synthesis of the extra ATP will potentially incur mitochondrial damage and start a degenerative cascade (Hindle *et al.*, 2013). It is reassuring that the *LRRK2-G2019S* expression in DA neurons and pigment cells have similar effects - as both of these processes control the adaptation of the eye, though probably by different mechanisms. Here, failure to adapt to light was observed in young flies (3 days) expressing *LRRK2-G2019S* in DA neurons. This observed physiological abnormality might be due to the degeneration of DA neurons which was reported in humans (Nguyen-Legros, 1988) and animal models (Marrocco *et al.*, 2020, Meng *et al.*, 2012). The larger neural response seen in young flies is similar to those observed by (Afsari *et al.*, 2014) which support the hypothesis of increased ATP demand in young flies because the neural response in old flies was unaffected but smaller than the young ones. The DPP-related anatomical assessment for these flies was unattainable due to low pigment content in their eyes. Thus, crossing them out with flies that have dark pigment might be a reasonable solution. Furthermore, using a different method for assessing the development of DPP than the one used in this project i.e., measuring the size of the DPP, might help obtaining quantifiable results. Examples of these methods include measuring light temperature from light scattering and absorption through DPP (Lo and Pak, 1981), counting the number of glowing ommatidia in the DPP (Fellgett *et al.*, 2021), or using slow motion camera to measure the time taken to form DPP (Katz and Minke, 2009).

In contrast, expressing *LRRK2-G2019S* in fly photoreceptors has no observed physiological effects on their ability to adapt to light. One possible explanation for this is that photoreceptors in flies are histaminergic neurons (Hardie, 1987) rather than dopaminergic which are the main type of neurons affected in PD. Anatomically, no structural damage was observed in the eye of the *rh1>G2019S* flies indicated by the formation of DPP but the DPP was larger than the controls in which other forms of *LRRK2* were expressed (Figure 4.6). This observation is in contrast with multiple studies that demonstrated signs of eye degeneration in the presence of Parkinson's related manipulations (Feany and Bender, 2000, Hindle *et al.*, 2013, Liu *et al.*, 2008, Venderova *et al.*, 2009). However, it is crucial to note that these reports were in flies expressing PD-related genes (*α -synuclein*, *parkin* and several *LRRK2* transgenes) in the eye using the *GMR-Gal4*, which expresses in all retinal cells, rather than just in photoreceptors. Moreover, the degree of pigmentation in these *rh1>G2019S* flies might have affected their adaptation to light as (Miller *et al.*, 1981) has reported different sensitivity to light between red-eyed and white-eyed flies.

On a longer timescale, disruption of adaptation in the eye may also affect other physiological processes. One of these is sleep dysfunction, which affects up to 60% of PD patients (De Cock *et al.*, 2008) and the aetiology of this dysfunction is still under investigation. Sleep-wake cycle is controlled by the circadian system which is regulated by endogenous processes that respond to environmental cues and the most important one is light (Ashbrook *et al.*, 2020). Disturbance in light exposure has been associated with alteration in sleep-cycle such as increased evening fatigue and low sleep quality (Figueiro *et al.*, 2017, Viola *et al.*, 2008). Abnormalities to circadian rhythm in PD have been reported by multiple studies (Ahsan Ejaz *et al.*, 2006, Placidi *et al.*, 2008, Videnovic and Golombek, 2013). That being said, eye adaptation to light works in a circadian fashion (Damulewicz *et al.*, 2020) which raise the question whether an impairment in light adaptation, as seen in this investigation, would have an effect on the circadian system and in turn affect the sleep-cycle and give us further insight into the pathophysiology of sleep disorders observed in PD.

5 Stability of LRRK2 Mutants Proteins *in vitro* and *in vivo*

5.1 Introduction

As set in detail in Chapter 1, Parkinson's disease (PD) is the second most common neurodegenerative disorder caused by the loss of dopaminergic (DA) neurons. Mutations in the *LRRK2* gene are genetic factors that have been associated with the autosomal dominant form of the disease. Many allelic variants associated with PD have been found throughout the gene; some are pathogenic (e.g., *LRRK2-R1441C/H*, *LRRK2-G2019S* and *LRRK2-I2020T*), others are risk factors (*LRRK2-G2385R*) (Kumari and Tan, 2009) and some may be neuroprotective (*LRRK2-N551K* and *LRRK2-R1398H*) (Gopalai *et al.*, 2019). The pathogenic mutations mostly affect the kinase or GTPase functions of LRRK2. Although there is little consensus about which other proteins are phosphorylated by LRRK2, novel therapies are being developed based on inhibition of LRRK2 kinase. For example, DNL-151 and DNL-201 are kinase inhibitors developed by Denali Therapeutics have shown promising results in clinical trials (GlobeNewswire).

In this context, knowing the stability and half-life of LRRK2 is crucial to help understand the functional window over which the protein functions. This is particularly important as (in cell culture) the breakdown of LRRK2 is affected by both mutations and kinase inhibitors (De Wit *et al.*, 2018). Steady state measurement of protein amount using western blot from cell transfection experiments indicate less LRRK2-R1441C and LRRK2-G2385R than LRRK2-WT protein, interpreted as an increase in the rate of degradation (Greene *et al.*, 2014, Rudenko *et al.*, 2017). *In vivo*, namely in *Drosophila*, less LRRK2-R1441C protein was also detected (Cording *et al.*, 2017). However, this reduction in protein could also be due to the differences in protein synthesis. Effects of LRRK2 expression on overall cellular protein synthesis have been demonstrated by (Martin *et al.*, 2014a). To determine if there are differences in LRRK2 stability, a pulse chase protocol is more appropriate. In a pulse chase experiment, the synthesis of LRRK2 can be controlled by a drug which is then washed away, and the decay of LRRK2 is followed. Only one mutant of LRRK2, LRRK2-G2385R has been tested in a pulse-chase experiment. This suggested that the mutant protein decayed faster than the wild type (Rudenko *et al.*, 2017). The availability of cell lines in which the LRRK2-WT and mutant proteins can be induced by the addition of a drug facilitates this approach.

Additionally, it is important to test if results from cell culture are reflected *in vivo*. The availability of inducible Gal4 constructs and Geneswitch technology (Osterwalder *et al.*, 2001) permits the design of pulse-chase experiments in *Drosophila*. Here the inducible GAL4 is used to drive expression of *hLRRK2-WT* and of mutant forms.

In line with the suggestion that LRRK2 autophosphorylation controls the rate of breakdown, kinase inhibitors also affect the level of protein recorded in steady state assays (Lobbestael *et al.*, 2016). However, it is sometimes difficult to mechanistically reconcile the effects of the pathogenic mutation and kinase inhibitors due to the different level of phosphorylation observed at different sites of the protein (De Wit *et al.*, 2018), and it is not known if these cell culture overexpression assay data conducted in heterologous cells are typical for neurons *in vivo*.

Since observing that toxic effects of increased kinase activity in *LRRK2* mutants causes toxic effects, inhibiting this activity has been a therapeutic target. Many kinase inhibitors have been tested to look for a potent and selective LRRK2 kinase inhibitor (Taymans and Greggio, 2016). Cis-2,6-dimethyl-4-(6-(5-(1-methylcyclopropoxy)-1H-indazol-3-yl) pyrimidin-4-yl) morpholine (MLi-2) is a highly potent and selective kinase inhibitor with CNS activity and well tolerated in PD mice (Fell *et al.*, 2015). These characteristics make it an attractive candidate for further investigation. However, as the case in many kinase inhibitors, MLI-2 works in a non-allosteric manner i.e., it is an ATP competitive compound. Interestingly, in a screening of 2080 FDA-approved compounds for their ability to reduce LRRK2 activity, an enzymatically active form of vitamin B₁₂ (5'-deoxy-adenosylcobalamin or AdoCbl) was found to modulate LRRK2-G2019S kinase activity in an allosteric fashion (Schaffner *et al.*, 2019). This is interesting because vitamin B₁₂ has been associated with PD (Shen, 2015) and can be found naturally in foodstuffs based on animal products.

In this investigation, LRRK2 stability will be tested in a pulse-chase approach. HEK293 Flp-In T-REx cells (for more information see section 2.2.1) will be used to examine *in vitro* effects of LRRK2 mutations on protein stability. These cells have already been transfected with different *LRRK2* mutations (*LRRK2-G2019S*, *LRRK2-R1441C*, and *LRRK2-D2017A*) or the *LRRK2-WT* gene. These cells have the advantage that the *LRRK2*-construct is always landed at the same site, minimizing discrepancies between the mutant lines. Cells will be induced to express *LRRK2* by the addition of doxycycline (Doxy). *In vivo*, the Gal4 Geneswitch/UAS technique (for more information see section

1.4.1.1) will be used in *Drosophila melanogaster* to express different human LRRK2 mutations (*LRRK2-G2019S*, *LRRK2-G2019S-K1906M*, *LRRK2-I2020T*, *LRRK2-R1441C*, *LRRK2-I1122V*, and *LRRK2-G2385R*) or the *LRRK2-WT* pan-neuronally (*elav^{GS}*-Gal4). These genes will be induced by the addition of Mifepristone (RU486) in the food. Unfortunately for these flies, the LRRK2 transgene landing site is not the same for each mutant which might introduce some observed differences.

Moreover, the effect of kinase inhibition on the stability of LRRK2 mutants will be tested. The active form of vitamin B₁₂ (5'-deoxy-adenosylcobalamin) will be utilised as an allosteric compound (the term vitamin B₁₂ will be used subsequently) and MLi-2 will be utilised as a non-allosteric compound. The stability of the protein will be examined using western blot (WB) and Image Studio Lite software will be used to quantify protein density.

5.2 Aims

1. To test the effect of multiple *LRRK2* mutations on the stability of the protein, using a pulse-chase approach.
2. To test the effect of kinase inhibition on LRRK2 stability using vitamin B₁₂ (allosteric inhibition) and MLi-2 (non-allosteric inhibition).

5.3 Results

We attempted to determine the half-life of LRRK2 and PD associated variants in mammalian cell culture and in *Drosophila* neurons. In our cell culture experiments, we used the Human Embryonic Kidney 293 (HEK293) cell line containing the Flp-In T-REx system to express *LRRK2* and PD associated variants in a Doxycyclin inducible manner (see Figure 2.3). In *Drosophila*, we used inducible Gal4 constructs and Geneswitch technology (see Figure 1.9). The timeline of the experiment (Figure 5.1) includes the induction of cells or flies with doxycyclin or RU486 respectively and quantifying the amount of protein using WB for 6 days. However, for half-life determination, the starting point (designated as day 0) of comparison for LRRK2 stability between the different mutations and treatments (untreated, B₁₂, or MLi-2) was set to be 1 day post media change and removal of inducing agents. Moreover, cells and flies which had not been exposed to the inducing agents were tested in WB for any possible leakage from the expression construct in the absence of the inducer.

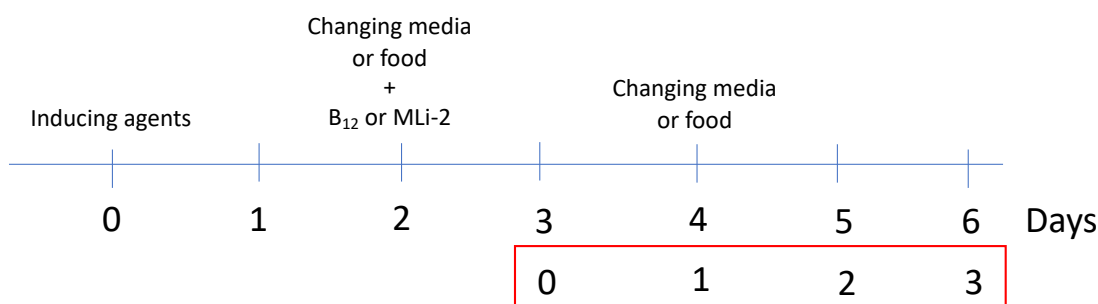


Figure 5.1 The timeline of LRRK2 stability experiment

The inducing agents (Doxy for cells or RU486 for flies) were added for 2 days to induce the expression of LRRK2. At the end of day 2, media or food was changed and B₁₂ or MLI-2 were added. The next day and for 4 days, proteins were quantified using WB for each treatment. The numbers within the red rectangle represents the set days of quantification and comparison between the different treatment.

5.3.1 *In vitro* evaluation of LRRK2 stability

5.3.1.1 No evident leak of expression was detected in the tested cell lines

Immunoblotting for LRRK2 abundance in Flp-In T-REx HEK293 uninduced cells revealed no leak of expression which is demonstrated by the absence of the LRRK2 band (Figure 5.2). The LRRK2 mutations to be evaluated in cells here were *LRRK2-WT*, *LRRK2-G2019S*, *LRRK2-D2017A* (kinase dead), and *LRRK2-R1441C*.

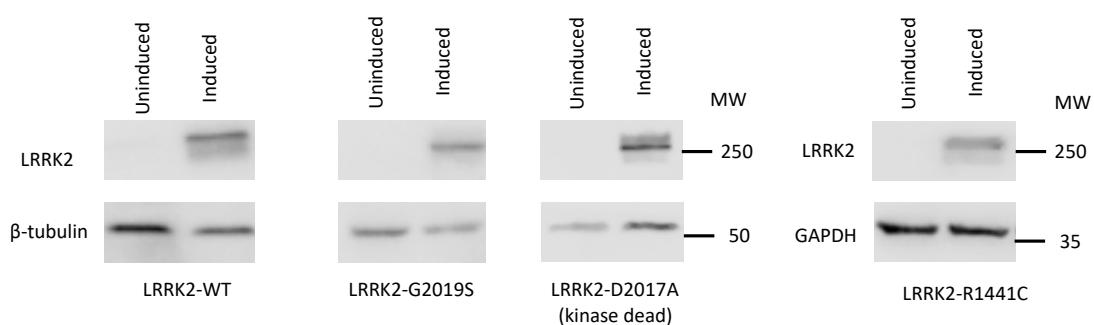


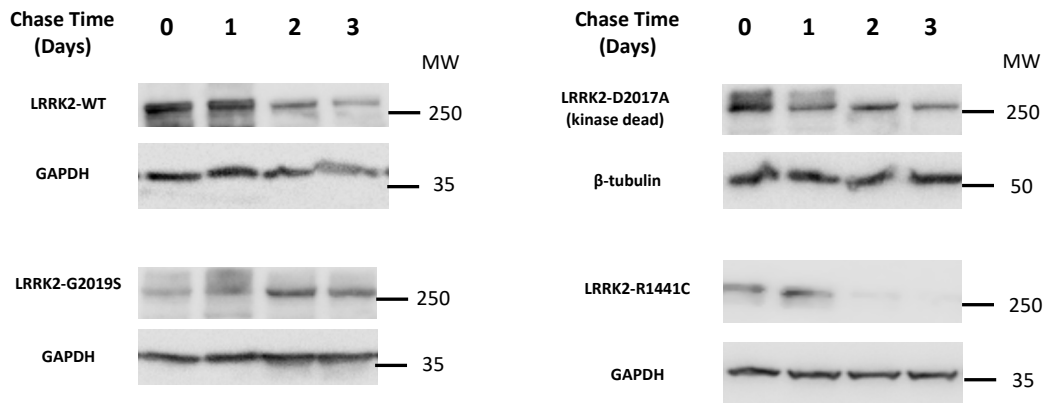
Figure 5.2 In the absence of inducing agent, no LRRK2 protein is expressed by the FLP-In T-REx system

Representative blots for LRRK2-WT, LRRK2-G2019S, LRRK2-D2017A (kinase dead), and LRRK2-R1441C in Flp-In T-REx HEK293 cells when induced or not with Doxy (1 μg/ml). β-tubulin/GAPDH lane represents the housekeeping loading protein. MW = Molecular Weight

5.3.1.2 Stability of LRRK2 protein in *vitro*

Examination of pulse-chased LRRK2 protein variants in cells revealed a shorter half-life ($t_{1/2}$) for LRRK2-WT than LRRK2-G2019S and LRRK2-D2017A (kinase dead) ($t_{1/2}$ -WT of 2.257 days, 95% CI of 1.714 to 3.181 days vs $t_{1/2}$ -G2019S of 3.377 days, 95% CI of 2.089 to 7.884 days and $t_{1/2}$ -D2017A of 3.335 days, 95% CI of 2.007 to 8.506 days) while LRRK2-R1441C appeared to have the shortest half-life ($t_{1/2}$ -R1441C of 0.9 days, 95% CI of 0.5734 to 1.438 days). Interestingly, it appeared that *LRRK2-R1441C* is the only mutation to have lost most of the protein by the last day of measurement while the rest are still maintaining some protein (Figure 5.3). The loading control changed from β -tubulin to GAPDH between experiments due to antibody availability. However since protein amounts of GAPDH or tubulin do not change throughout each experiment the results are reasonably internally controlled.

A



B

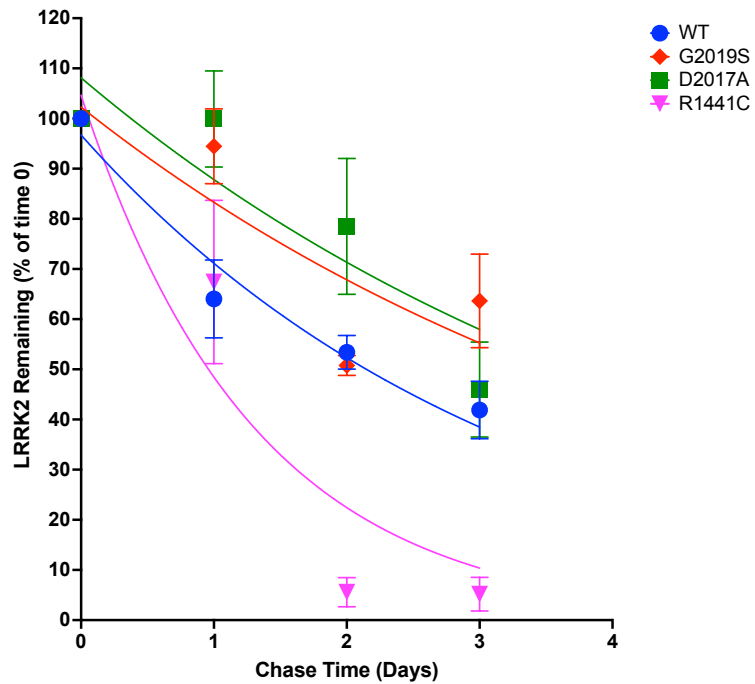


Figure 5.3 LRRK-R1441C appears to be potentially the least stable PD associated LRRK2 protein variant when expressed in cell culture

A. Representative blots and B. the time courses of the decay of LRRK2-WT, LRRK2-G2019S, LRRK2-D2017A (kinase dead), and LRRK2-R1441C in Flp-In T-REx HEK293 cells when induced with Doxy. Error bars indicate SEM with N = 3.

5.3.1.3 Kinase inhibitors effects on protein stability in *vitro*

After determining relative protein for LRRK2 and PD associated variants in untreated conditions, cells were treated with kinase inhibitors (vitamin B₁₂ and MLI-2) to investigate their effects on LRRK2 protein stability. Inhibitors were added after the removal of inducing agents. When vitamin B₁₂ was added to cells (1.9 µg/ml), the stability of LRRK2-WT ($t_{1/2-WT+B_{12}}$ of 2.194 days, 90% CI of 1.299 to 5.168 days vs $t_{1/2-WT}$ of 2.257 days), LRRK2-G2019S ($t_{1/2-G2019S+B_{12}}$ of 3.66 days, 90% CI of 1.923 to 19.86 days vs $t_{1/2-G2019S}$ of 3.377 days), and LRRK2-R1441C ($t_{1/2-R1441C+B_{12}}$ of 0.7179 days, 90% CI of 0.586 to 0.8736 days vs $t_{1/2-R1441C}$ of 0.9 days) were comparable to untreated cells. Interestingly, vitamin B₁₂ appear to statistically reduce the stability of LRRK2-D2017A (kinase dead) by almost 2 days ($t_{1/2-D2017A+B_{12}}$ of 1.398 days, 90% CI of 0.7684 to 3.217 vs $t_{1/2-D2017}$ of 3.335 days), however, the protein doesn't appear to decay totally with time but there is less abundance than the untreated cells (Figure 5.4).

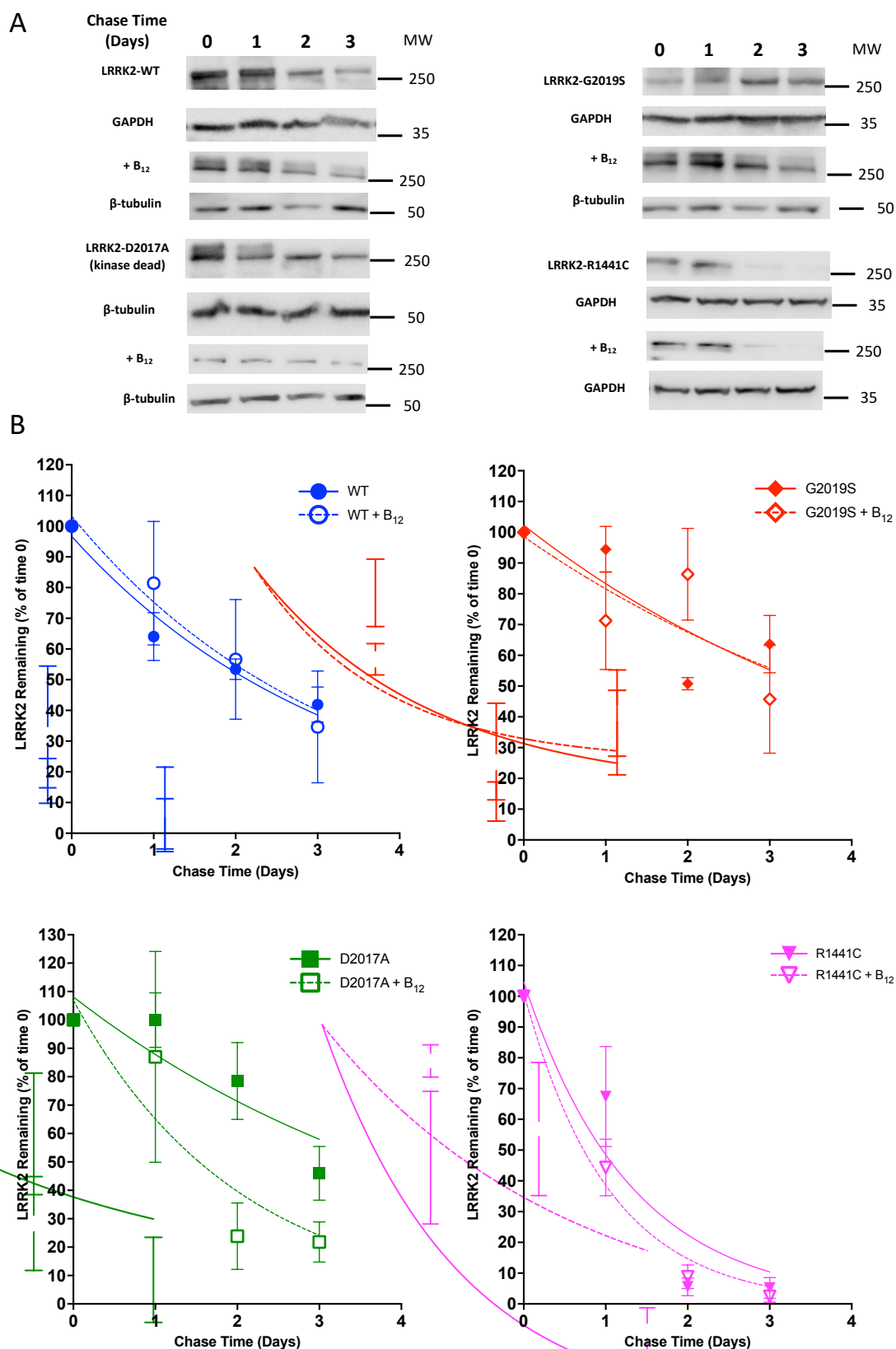


Figure 5.4 Vitamin B₁₂ appears to affect LRRK2-D2017A protein stability

A. Representative blots and B. the time courses of the decay of LRRK2-WT, LRRK2-G2019S, LRRK2-D2017A (kinase dead), and LRRK2-R1441C in Flp-In T-REx HEK293 cells when treated with or without vitamin B₁₂. Error bars indicate SEM with N = 3.

When the LRRK2 inhibitor MLi-2 is added to cells (1.3ng/ml), the stability of LRRK2-WT ($t_{1/2-WT+MLi-2}$ of 2.149 days, 95% CI of 1.166 to 6.777 days vs $t_{1/2-WT}$ of 2.257 days), LRRK2-D2017A ($t_{1/2-D2019A+MLi-2}$ of 3.676 days, 95% CI of 1.736 to 325.2 days vs $t_{1/2-D2019A}$ of 3.335 days), and LRRK2-R1441C ($t_{1/2-R1441C+MLi-2}$ of 1.102 days, 95% CI of 0.688 to 1.895 days vs $t_{1/2-R1441C}$ of 0.9 days) were comparable to untreated cells. The case for LRRK2-G2019S is similar to that of LRRK2-D2017A and vitamin B₁₂ where MLi-2 appear to statistically reduce the stability of the protein by almost a day ($t_{1/2-G2019S+MLi-2}$ of 2.565 days, 95% CI of 1.6 to 5.504 vs $t_{1/2-G2019S}$ of 3.377 days), however, the amount of protein appeared in blot to be very similar to the untreated cells and the effect is subtle. (Figure 5.5).

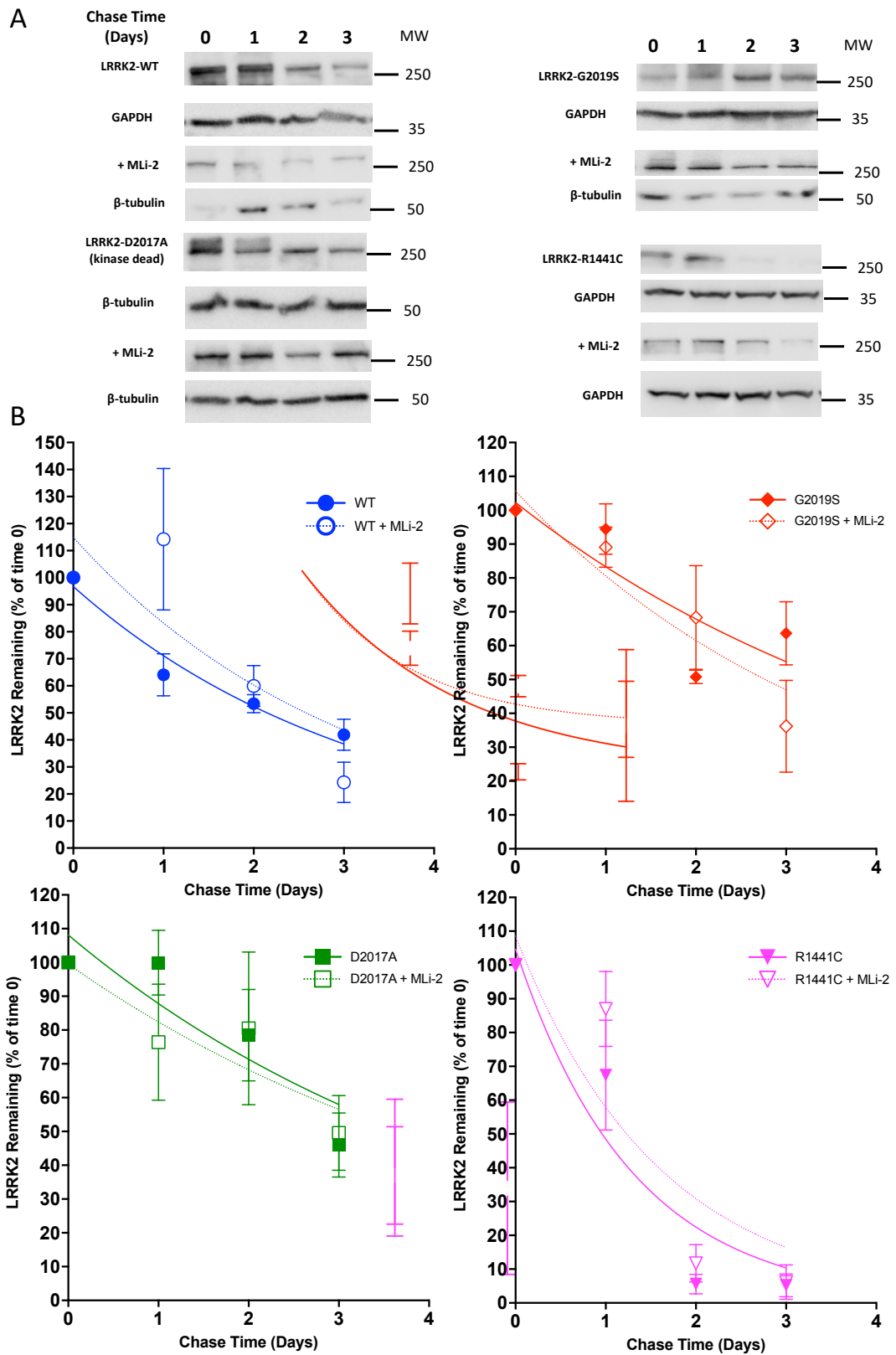


Figure 5.5 MLI-2 appears to have no effect on LRRK2 stability

A. Representative blots and B. the time courses of the decay of LRRK2-WT, LRRK2-G2019S, LRRK2-D2017A (kinase dead), and LRRK2-R1441C in Flp-In T-REx HEK293 cells when treated with or without vitamin MLI-2. Error bars indicate SEM with N = 3

5.3.2 *In vivo* evaluation of LRRK2 stability

5.3.2.1 Testing for leak of expression of LRRK2 in uninduced transgenic flies

To test for LRRK2 and PD associated LRRK2 variant stability in an *in vivo* system we employed the *Drosophila* Geneswitch system where the Gal4 expression of LRRK2 and PD associated variants are induced by the addition of RU486 to the diet of the experimental flies. We initially tested for protein leakage expression in the absence of inducing agent we tested animals for LRRK2 expression in the absence of RU486. WB for transgenic uninduced flies revealed no leak of expression which is demonstrated by the absence of the LRRK2 band except for the *LRRK2-I2020T* mutation (Figure 5.6). Therefore, the available mutations in flies that can be evaluated here were *LRRK2-WT*, *LRRK2-G2019S*, *LRRK2-G2019S-K1906M* (kinase dead), *LRRK2-R1441C*, *LRRK2-I1122V*, and *LRRK2-G2385R*.

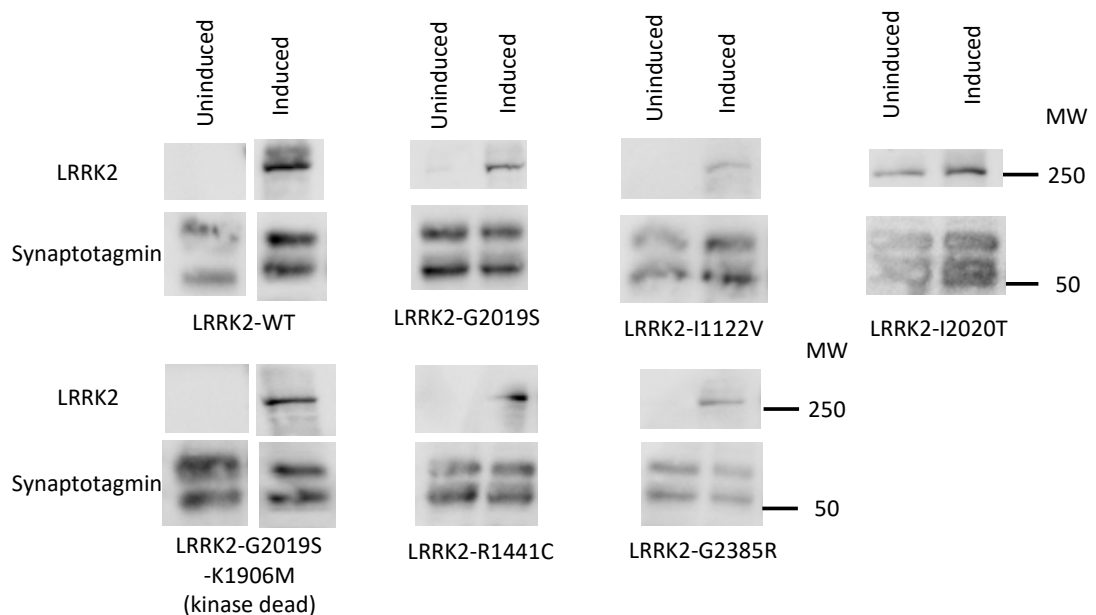


Figure 5.6 No *LRRK2* expression from transgenes is observed in uninduced animals indicating absence of expression except for the *LRRK2-I2020T* transgene.

Representative blots for *LRRK2-WT*, *LRRK2-G2019S*, *LRRK2-G2019S-K1906M* (kinase dead), *LRRK2-R1441C*, *LRRK2-I1122V*, and *LRRK2-G2385R* in *Drosophila melanogaster* when induced or not with RU486 (10 $\mu\text{g/ml}$). Synaptotagmin lane represents the housekeeping loading protein. Error bars indicate SEM with $N = 3$. MW, Molecular Weight.

5.3.2.2 Stability of LRRK2 protein in *in vivo*

We carried out a full pulse-chase analysis for the LRRK2 protein and the LRRK2 PD associated variants to test for LRRK2 protein stability in *in vivo* flies. WB analysis of pulse chase expressed LRRK2 and PD-associated variants revealed comparable stability level for LRRK2-WT, LRRK2-G2019S-K1906M (kinase dead), LRRK2-G2019S, and LRRK2-I1122V ($t_{1/2}$ -WT of 0.905 days, 95% CI of 0.569 to 1.431 vs $t_{1/2}$ -G2019S-K1906M of 0.746, 95% CI of 0.523 to 1.044 days, $t_{1/2}$ -G2019S of 1.049 days, 95% CI of 0.6343 to 1.773 and $t_{1/2}$ -I1122V of 0.851 days, 95% CI of 0.578 to 1.241). The stability for LRRK2-R1441C appeared to be reduced by half a day than the LRRK2-WT ($t_{1/2}$ -R1441C of 0.563 days, 95% CI of 0.4811 to 0.6520 vs $t_{1/2}$ -WT of 0.905 days). While LRRK2-G2385R appeared statistically to be more stable than the WT by half a day ($t_{1/2}$ -G2385R of 1.606 days, 95% CI of 0.7581 to 5.424 vs $t_{1/2}$ -WT of 0.905 days), this stability looks questionable because the calculation started from a low level of protein to a very low level pointing to a limited reliability in this result. It is good to note that it looks like LRRK2-R1441C and LRRK2-G2385R are the only two to have lost all of the protein by the second to last day of measurement (Figure 5.7).

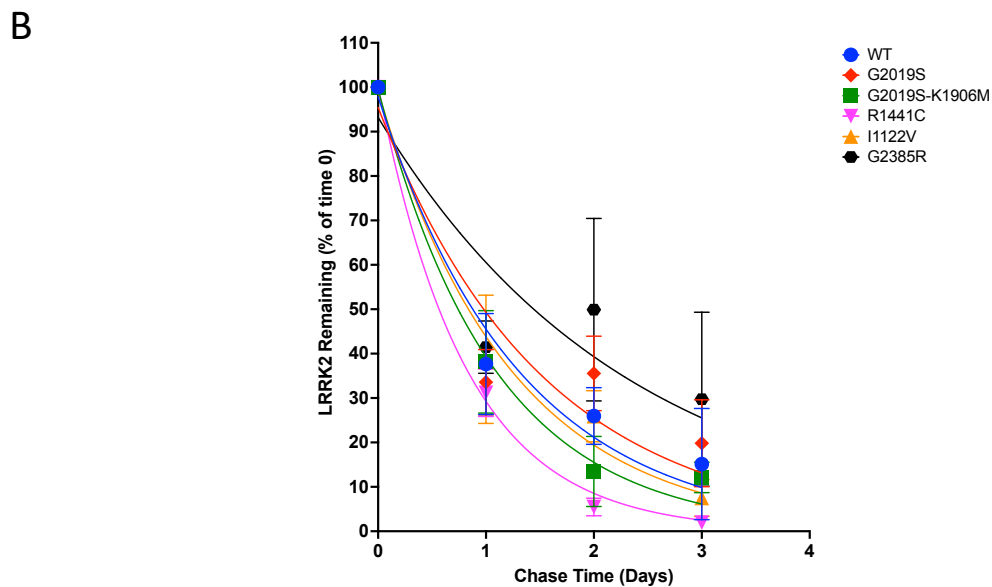
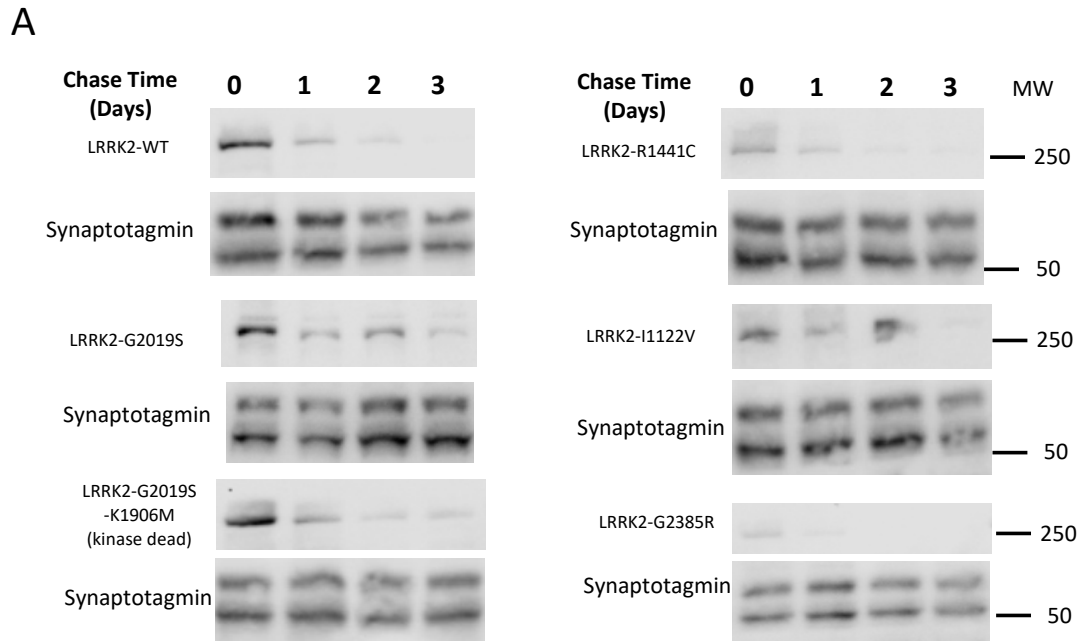


Figure 5.7 R1441C is potentially the least stable of LRRK2 protein variants

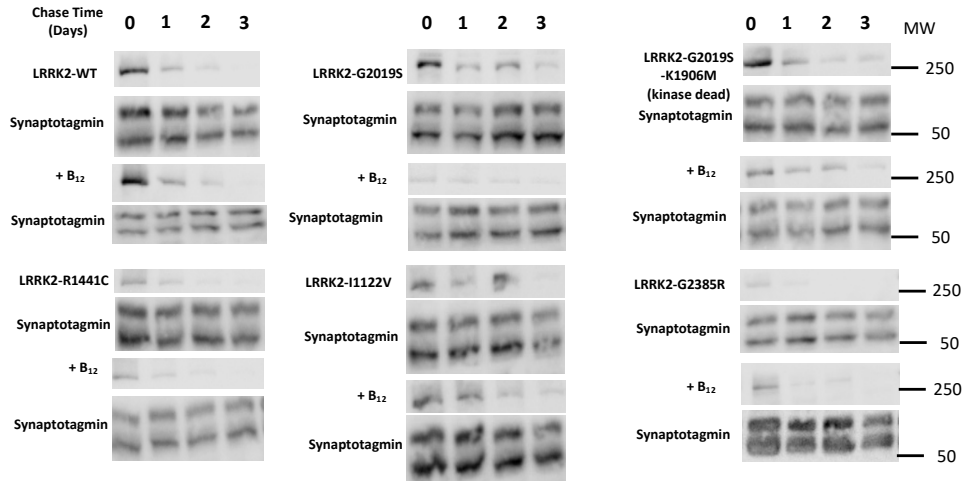
A. Representative blots and B. the time courses of the decay of LRRK2-WT, LRRK2-G2019S, LRRK2-G2019S-K1906M (kinase dead), LRRK2-R1441C, LRRK2-I1122V, and LRRK2-G2385R in *Drosophila melanogaster* when induced with RU486. Error bars indicate SEM with N = 3.

5.3.2.3 Kinase inhibitors effects on protein stability in vivo

To test for LRRK2 protein stability in the presence of kinase inhibitors in vivo vitamin B₁₂ and MLi-2 were added to the diet of experimental flies. When vitamin B₁₂ was added

(4 $\mu\text{g/ml}$), the stability of LRRK2 for LRRK2-WT ($t_{1/2\text{-WT+B}_{12}}$ of 0.727 days, 90% CI of 0.606 to 0.869 vs $t_{1/2\text{-WT}}$ of 0.905 days), LRRK2-G2019S ($t_{1/2\text{-G2019S+B}_{12}}$ of 1.421 days, 90% CI of 1.073 to 1.954 days vs $t_{1/2\text{-G2019S}}$ of 1.049 days), LRRK2-G2019S-K1906M ($t_{1/2\text{-G2019S-K1906M+B}_{12}}$ of 0.614 days, 90% CI of 0.433 to 0.835 days vs $t_{1/2\text{-G2019S-K1906M}}$ of 0.746 days), and LRRK2-R1441C ($t_{1/2\text{-R1441C+B}_{12}}$ of 0.714 days, 90% CI of 0.531 to 0.943 vs $t_{1/2\text{-R1441C}}$ of 0.563 days) are comparable to the untreated flies. The LRRK2-I1122V stability appeared to be improved by a day ($t_{1/2\text{-I1122V+B}_{12}}$ of 2.106 days, 90% CI of 1.118 to 6.821 vs $t_{1/2\text{-I1122V}}$ of 0.851 days) when vitamin B₁₂ is added. Although the stability of LRRK2-G2385R appeared to be reduced by vitamin B₁₂ ($t_{1/2\text{-G2385R+B}_{12}}$ of 0.325 days, 90% CI 0.164 to 0.457 vs $t_{1/2\text{-G2385R}}$ of 1.606 days), this reduction compared to the untreated flies is questionable because the $t_{1/2}$ calculation of the latter ones was not accurate (Figure 5.8).

A



B

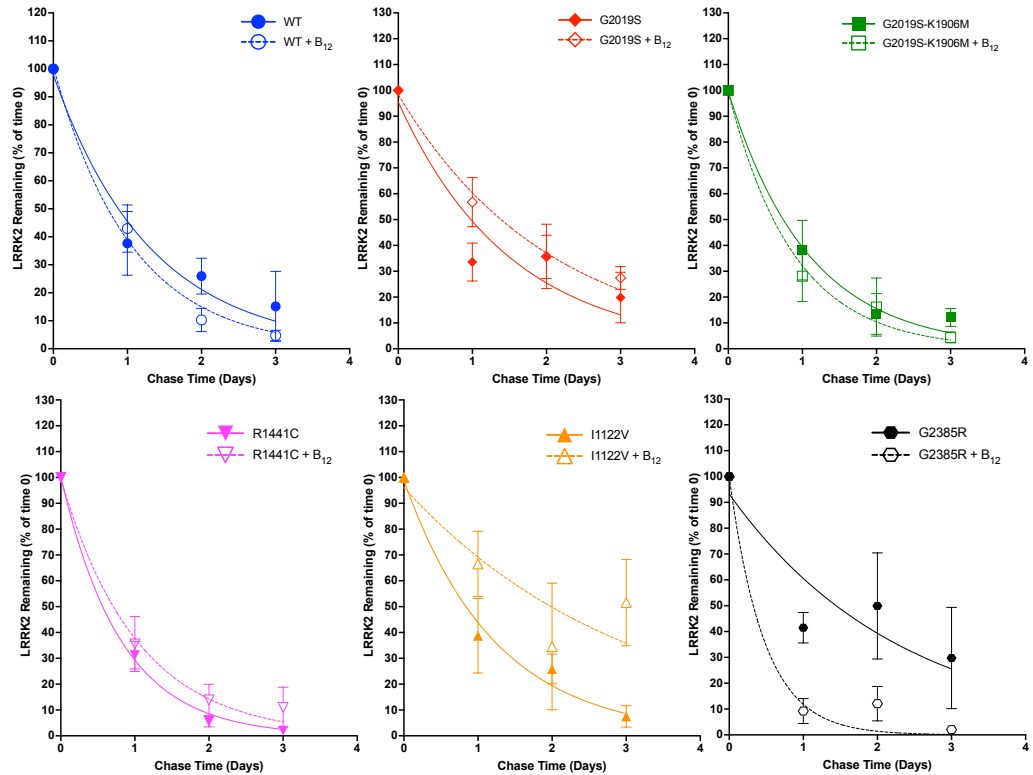


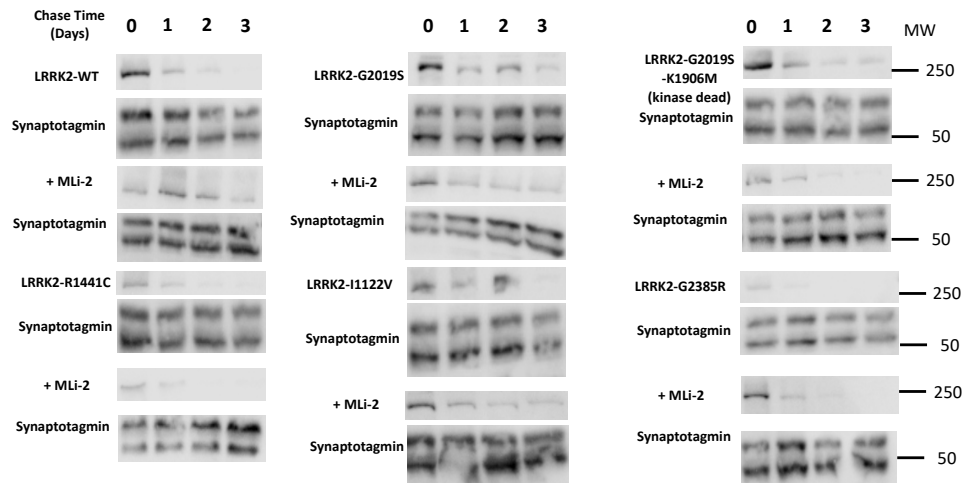
Figure 5.8 Vitamin B₁₂ might affect LRRK2 stability of LRRK2-I1122V

A. Representative blots and B. the time courses of the decay of LRRK2-WT, LRRK2-G2019S, LRRK2-G2019S-K1906M (kinase dead), LRRK2-R1441C, LRRK2-I1122V, and LRRK2-G2385R in *Drosophila melanogaster* when treated with or without vitamin B₁₂. Error bars indicate SEM with N = 3.

When MLi-2 is added (1 μ g/ml), compared to uninduced flies, the stability of LRRK2-G2019S ($t_{1/2}$ -G2019S+MLi-2 of 1.173 days, 95% CI of 0.773 to 1.894 vs $t_{1/2}$ -G2019S of 1.049 days), LRRK2-G2019S-K1906M ($t_{1/2}$ -G2019S-K1906M+MLi-2 of 1.03 days, 95% CI 0.56 to

2.043 vs $t_{1/2}$ -G2019S-K1906M of 0.746 days), and LRRK2-R1441C ($t_{1/2}$ -R1441C+MLi-2 of 0.801 days, 95% CI of 0.577 to 1.106 vs $t_{1/2}$ -R1441C of 0.563 days) are fairly comparable to untreated flies. The stability of LRRK2-WT ($t_{1/2}$ -WT+MLi-2 of 1.495 days, 95% CI of 0.871 to 3.165 vs $t_{1/2}$ -WT of 0.905 days) and LRRK2-I1122V ($t_{1/2}$ -I1122V+MLi-2 of 1.259 days vs $t_{1/2}$ -I1122V of 0.851 days) are improved by almost half a day. Lastly, the reduced stability of LRRK2-G2385R ($t_{1/2}$ -G2385R+MLi-2 of 0.397 days, 95% CI 0.174 to 0.619 vs $t_{1/2}$ -G2385R of 1.606 days) is still questionable similar to results observed with vitamin B₁₂ (Figure 5.9).

A



B

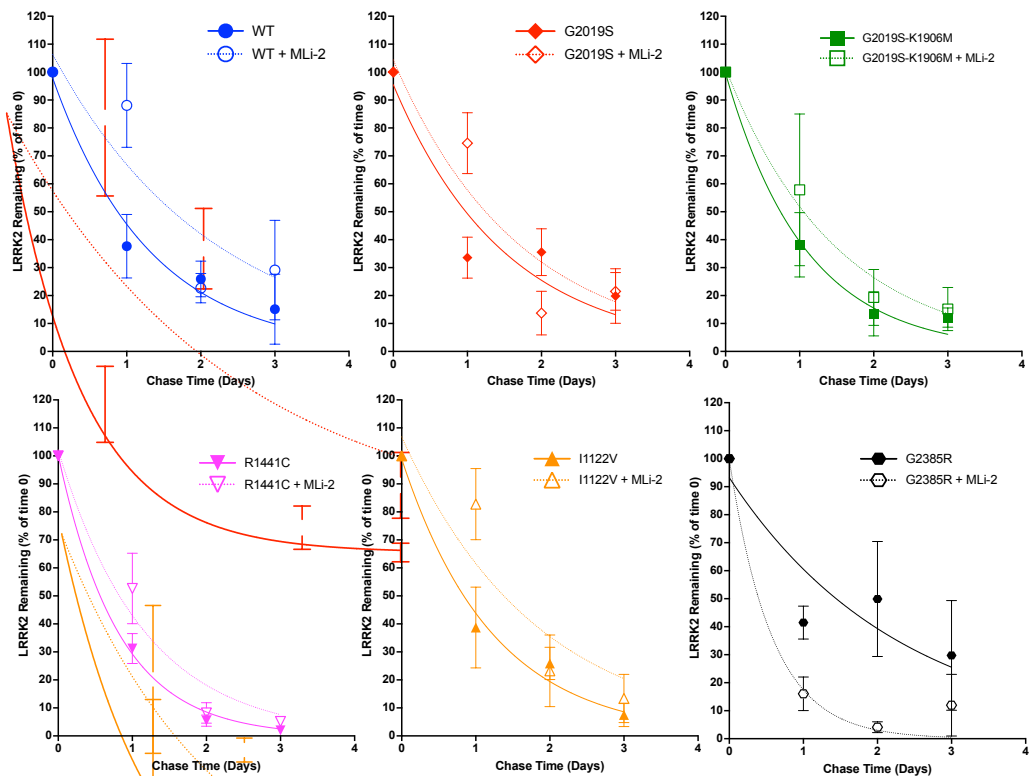


Figure 5.9 MLi-2 might effect LRRK2 stability for LRRK2-WT and LRRK2-I1122V

A. Representative blots and B. the time courses of the decay of LRRK2-WT, LRRK2-G2019S, LRRK2-G2019S-K1906M (kinase dead), LRRK2-R1441C, LRRK2-I1122V, and LRRK2-G2385R in *Drosophila melanogaster* when treated with or without MLi-2. Error bars indicate SEM with N = 3.

5.3.3 Examining LRRK2 stability via Rab10 and phosphorylated Rab10 expression

Rab10 is a protein that belongs to the Ras family of small GTPases that regulate intracellular vesicle trafficking. It has been found to be a direct target for phosphorylation by LRRK2 (Steger *et al.*, 2016) which, therefore, makes it an attractive downstream target for further investigation. Recently, the Elliott lab has published papers demonstrating a functional association between LRRK2-G2019S and Rab10 in DA neurons (Fellgett *et al.*, 2021, Petridi *et al.*, 2020). In line with this suggestion, the stability of Rab10 and phosphorylated Rab10 should be disrupted if LRRK2 stability is disrupted as well. Due to the ongoing pandemic, the work on these experiments were cut short and unfortunately only one replicate of WB assay was performed which prevented any useful interpretations or conclusions.

5.4 Discussion

In this investigation, the effect of *LRRK2* PD-associated mutations and kinase inhibitors on LRRK2 protein stability was tested in cell culture (*in vitro*) and *Drosophila melanogaster* (*in vivo*). In both situations, pulse-chase experiments potentially showed that *LRRK2* mutations had differences in the rate of degradation, and that this stability might be impacted by both inhibitors tested. *In vitro*, the order of stability (most stable to least stable) was LRRK2-D2017A (kinase dead), LRRK2-G2019S, LRRK2-WT, and LRRK2-R1441C. *In vivo*, the order of stability was similar for LRRK2-WT, LRRK2-G2019S-K1906M (kinase dead), LRRK2-I1122V, and LRRK2-G2019S then LRRK2-R1441C. Vitamin B₁₂ potentially improved the stability of LRRK2-I1122V in flies while it potentially reduced the stability of LRRK2-D2019A (kinase dead) in cells. MLi-2 had no effect on cells while it potentially improved the stability of LRRK2-WT and LRRK2-I1122V in flies.

The findings in this investigation suggest the notion that mutations and the presence of kinase inhibitors have an impact on LRRK2 stability. The half-life of LRRK2-WT found here was 0.9 days in flies which converts to around 21 hours. These findings are within the range found in other reports (Ohta *et al.*, 2009, Rudenko *et al.*, 2017, Wang *et al.*, 2008b) that have used tagging methods in pulse-chasing the protein degradation. LRRK2 degradation has been linked to lysosomal and proteasomal pathways. In the lysosomal pathway, Chaperone Mediated Autophagy (CMA) has been found to regulate LRRK2 abundance and mutations to the protein (*LRRK2-G2019S*, *LRRK2-D1994A*, and *LRRK2-R1441C*) compromised the ability of this mechanism to degrade the protein (Orenstein *et al.*, 2013). For degradation via the proteasomal pathway, the C-terminus of Hsp70-Interacting Protein (CHIP) has been found to mediate LRRK2 degradation and like in CMA mutations (*LRRK2-G2019S*, *LRRK2-D1994A*, and *LRRK2-R1441C*) affected the ability of this system to degrade the protein. CHIP regulates this degradation via ubiquitination of LRRK2 and it has been found to bind to different LRRK2 domains (ARM, ANK, ROC, LRR, WD40) (Ding and Goldberg, 2009, Ko *et al.*, 2009, Rudenko *et al.*, 2017). The presence of the mutations potentially alters the ability of CHIP to mediate ubiquitination of LRRK2. Some of the results obtained in this investigation agree with these previous findings while other do not. For instance, *LRRK2-R1441C* degradation curve suggests a less stable protein in cells and flies while the kinase dead was found to be less stable just in flies. These discrepancies might simply be due to the different models used (cells vs flies) and the different type of mutations e.g., the kinase dead used here is *LRRK2-D2017A* compared to *LRRK2-D1994A* (Orenstein *et al.*, 2013). It is possible the effect of difference in models used can be seen clearly in the amount of LRRK2 protein measured at last day of measurement where in cells all transgene except *R1441C* have still some proteins left compared to flies (see Figure 5.3). In addition, in our cell-based experiment, all LRRK2 constructs are inserted at the same loci in cells while this is not the case in flies.

In addition to PD-associated mutations, kinase inhibition has been reported to affect LRRK2 stability. Here, MLi-2, a highly potent and selective kinase inhibitors, was found to reduce LRRK2-WT stability significantly in cells and slightly in flies which is similar to observations reported by (Lobbestael *et al.*, 2016) in cells, (Kelly *et al.*, 2018) in rats, and (Baptista *et al.*, 2020) in primates. In terms of LRRK2 mutations, *G2019S* was shown to be resilient to inhibition by MLi-2 in rats (Kelly *et al.*, 2018), similar to what has been observed in flies in this investigation.

MLi-2 and many other kinase inhibitors developed for LRRK2 works in a non-allosteric manner i.e., they are ATP competitive compounds. Although very effective, they have to be highly specific to overcome the high degree of similarities in other ATP binding kinase in cells and to be able to compete with the high amount of ATP found in cells without being toxic. Vitamin B₁₂ is a very interesting compound that inhibits LRRK2 kinase activity by blocking its dimerization (Schaffner *et al.*, 2019). The different levels of stabilization by vitamin B₁₂ effects on different LRRK2 mutations found in this investigation further our understanding on the mechanism of action of this compound. This is interesting because (Schaffner *et al.*, 2019) reported that vitamin B₁₂ interacts with the kinase domain of LRRK2 while we see a vitamin B₁₂ stabilization effect LRRK2 bearing mutations in other domains e.g., LRRK2-R1441C in ROC domain and LRRK2-G2385R in WD40 domain. Another interesting allosteric approach that has shown promising results in modulating LRRK2 kinase activity and abundance is the use of small and stable single-domain fragments derived from camelid heavy chain-only antibodies called nanobodies. Expression of nanobodies that bind LRRK2 have been shown to inhibit LRRK2 from phosphorylating Rabs while leaving autophosphorylation intact. Moreover, they can target multiple domains of LRRK2 to potentially modulate activity (Singh *et al.*, 2022).

Investigating kinase inhibition on LRRK2 stability has implications on other forms of familial PD. *GBA1*, which encodes the lysosomal enzyme glucocerebrosidase (GCase) activity, has been associated with an increased risk of developing PD (Avenali *et al.*, 2020). PD patients carrying *LRRK2-R1441C* or *LRRK2-R1441G* mutations have shown increased accumulation of oxidized dopamine, decreased lysosomal GCase activity, and increased α -synuclein protein levels in their iPSC-derived DA neurons (Nguyen and Krainc, 2018, Ysselstein *et al.*, 2019). Likewise, knockdown of Rab10, reduces lysosomal GCase activity in human fibroblasts and iPSC-derived DA neurons (Steger *et al.*, 2016). Surprisingly, overexpression of Rab10-WT was sufficient to restore lysosomal GCase activity in iPSC-derived DA neurons *LRRK2* mutations (*LRRK2-G2019S* or *LRRK2-R1441C*) or *GBA* (*GBA-N370S* or *GBA-E326K*) mutations of iPSC-derived DA neurons. Also, pharmacological LRRK2 kinase inhibition can restore lysosomal GCase activity, and reduce oxidized dopamine and phosphorylated α -synuclein levels, in iPSC-derived DA neurons carrying *GBA* mutations (N370S or E326K) and primary astrocytes derived from *D409V GBA* knock-in mice (Sanyal *et al.*, 2020, Ysselstein *et al.*, 2019). While the previous observations clearly suggest an impact

of LRRK2 and its inhibitions on lysosomal abnormalities in PD, the precise mechanism has still to be elucidated.

6 General discussion and future works

6.1 Introduction

The overall aim of this research was to further our understanding on the mechanism of action of *LRRK2* mutations and how they may lead to neurodegeneration using the fruit fly as an animal model. In order to achieve this, the following questions were investigated:

1. Can we test for non-autonomy of LRRK2 function by expressing *dLRRK* in non-neuronal tissues to rescue the visual dysfunction observed in *dLRRK^{LOF}* old flies? Related to this, given a synthetic lethal genetic interaction between eye colour mutations and *dLRRK* we wished to investigate the viability of the flies mutant for combinations of eye colour genes and *dLRRK*.
2. Does dopaminergic *LRRK2-G2019S* expression have an effect on the ability of the eye's ability to adapt to light?
3. Do LRRK2 mutations and kinase inhibition affects protein stability *in vivo* as well as *in vitro*?

This chapter reviews our answers to these questions, offering a comprehensive, and concise overview of the key data generated from this investigation. It sets the findings in the general context of LRRK2 biology and also raises further questions and topics for further investigation.

6.2 dLRRK/LRRK2 mode of action

The outcomes from this thesis builds on previous findings from (Furmston, 2016) which found a specific early loss of the ERG off-transient component in a *dLRRK^{LOF}* model. The findings in this thesis strengthen this observation by adding the loss of the ERG on-transient component which strongly supports that the defect was in the adaptation of lower-order visual neurons (lamina neurons) rather than in the photoreceptors. Moreover, the expression of *dLRRK* in different neuronal tissues led to the rescue of visual response in *dLRRK^{LOF}* flies (Furmston, 2016). In addition, the extensive neurodegeneration observed throughout the visual system caused by DA expression of *LRRK2-G2019S* in flies (Hindle *et al.*, 2013) indicated a transcellular signalling of unknown mechanism. The possibilities for this cell-cell transfer could be alterations in the release of dopamine or another neurotransmitter, changes in secretion of growth factors, secretion of endosomal intermediates such as exosomes or diffusion of free

radicals. However, due to dLRRK/LRRK2 close association with the endocytic pathway, it is more likely to presume that dLRRK/LRRK2 is secreted by exosomes perhaps in a mis-folded manner. The findings in this thesis strongly support the exosomes theory because non-neuronal (pigment cells and fat body) expression of *dLRRK* was able to rescue the visual deficit in *dLRRK^{LOF}* flies which is not surprising since they can travel throughout the body and pass specialised compartment including the BBB. Indeed, this is made more likely by the position of the pigment cells and fatty tissue near to the retina. The exosomes theory is supported even further by LRRK2 interaction with different membrane proteins critical in the biosynthesis and traffic of pigment granules found in this thesis and previously (Furmston, 2016, Petridi, 2017). The role of dLRRK in the pigment granules (a type of lysosomal related organelle) regulation supports the idea that LRRK2 interacts with and regulates the lysosome rather than the mitochondria. For example, (Sanyal *et al.*, 2020) have found that LRRK2 inhibition can restore some of the impaired lysosome function observed in *GBA* heterozygous iPSC neurons. This interaction between LRRK2 and lysosomes was also observed by (Bonet-Ponce *et al.*, 2020, Kluss *et al.*, 2021) where LRRK2 sequesters Rab8a to damaged lysosomes and vesicle sorting from lysosomes.

Intriguingly, another approach that might explain the non-autonomous action of LRRK2 is the link found between inflammatory diseases and LRRK2. Inflammatory bowel disease (IBD) including Crohn's disease (CD) have been linked to increased risk of developing PD (Park *et al.*, 2019, Wan *et al.*, 2020) and LRRK2 has been shown to play a crucial role in the gut immune cells (Santos *et al.*, 2019) which when affected could in turn lead to neuroinflammation. Neuroinflammation causes the build-up of cytokines and ROS in the brain, which are particularly harmful to DA neurons in the *SNpc* that is known for having the highest density of microglia (Cabezudo *et al.*, 2020). This idea is not new to PD since Braak described the staging of PD (see section 1.1.4) by the level of α -synuclein spreading (Braak *et al.*, 2003). Our data points to another mechanism of spreading in addition to the non-autonomy of α -synuclein driving PD progression, we suggest that PD may also spread via LRRK2 function, potentially via exosomes. The findings in this thesis and others may provide novel therapeutic targets for preventing disease progression e.g., in the lysosomal pathway or immune cells.

6.3 LRRK2 and non-motor deficits in PD

The findings in chapter 4 support even further the theory of LRRK2 spreading from cell to cell since the aberrant ERG was found in flies expressing *LRRK2-G2019S* in pigment cells that do not contribute to the ERG trace, as well when *LRRK2-G2019S* is expressed in DA neurons. During each light flash, the initial larger ERGs observed when *LRRK2-G2019S* is expressed generate an excessive ionic flow and resulting in increased demand for ATP (Hindle *et al.*, 2013). The excess ATP production will potentially cause mitochondrial damage, triggering a degenerative cascade of photoreceptors indicated by the smaller ERG amplitude observed in old flies. Mitochondrial damage is a theme in PD however it appears to be an indirect consequence in case of *LRRK2* mutations. The involvement of LRRK2 in lysosomal function may point to dysfunction in lysosomes leading to failure to degrade damaged and senescent lysosomes, thus causing excessive ROS generation by degenerate mitochondria. This is not the case with *parkin* or *PINK1* linked PD which are known to be involved more directly in mitochondrial function (Quinn *et al.*, 2020). Therefore, therapies targeting mitochondria function in *LRRK2* mutations linked PD, such as using ursocholic acid (UCA) or ursodeoxycholic acid (UDCA) (Furmston, 2016), would not obviously be the favourable approach, but may have some benefits.

Failure of neuronal adaptation might also contribute to other PD deficits. For example, the reward system which is suggested to be altered in PD in a dopamine-dependant manner (Frank *et al.*, 2004). Reward and motivation in healthy individuals cause pupillary dilation, presumably due to effects of arousal and attention. Dopamine-induced dilation of the pupil may occur as a result of increased sympathetic outflow in the locus coeruleus, energising upcoming actions (Murphy *et al.*, 2011, Varazzani *et al.*, 2015). A reduced pupillary dilation has been observed in PD patients (Manohar and Husain, 2015, Muhammed *et al.*, 2016) similar to the light adaptation abnormalities in the fly eye found in this thesis. Assessment and treatment of the visual deficits in PD is often neglected probably because PD patients and their family members are often oblivious of the relationship between visual deficits and PD, the movement deficits being a primary observation and concern. Thus, development of portable ERG/SSVEP setups for human use would be helpful, both in assessing the progress of the disease, but also in monitoring any therapy.

6.4 LRRK2 stability and kinase inhibitors

A key finding in chapter 5 was that LRRK2 stability appeared to be affected by mutations and kinase inhibitors. The cause of this instability is still not clear but recent experiments with LRRK2 and ubiquitination might give us some clues. Ubiquitination is a common post-translational protein modification that involves the covalent attachment of a single (monoubiquitination or multi-monoubiquitination) or a chain of ubiquitin proteins (polyubiquitination). The link occurs between the carboxyl group of C-terminal residue of ubiquitin (G76) and the side chain amino group of a lysine (K) residue of the protein substrate (Buneeva and Medvedev, 2022). According to the Protein Lysine Modification Database (PLMD), 4 sites on LRRK2 have been identified as ubiquitination sites (K905, K906, K412, and K1132) so far. LRRK2 has been found to be promoted for proteasomal degradation by 2 ubiquitin ligases, CHIP and tripartite motif family 1 (TRIM1). The exact ubiquitination sites for these are still not clear. For TRIM1, it is reported to be between the ARM and LRR domains while CHIP is reported to act on multiple domains (Ding and Goldberg, 2009, Stormo *et al.*, 2022). In addition, dephosphorylation of LRRK2 can induce its ubiquitination by binding to PP2A phosphatase, eventually leading to degradation (Drouyer *et al.*, 2021). The previous reports give multiple targets to consider for more investigation and targeted novel therapies.

Investigating the effect of kinase inhibitors on LRRK2 stability can lead to potential therapeutic interventions for PD. The most common mutation, *LRRK2-G2019S* is proposed to have an increase in intrinsic kinase activity (Lee *et al.*, 2019). In this investigation, 2 kinase inhibitors of different mechanism of action on kinase activity and different potential effects on LRRK2 protein stability, MLi-2 (non-allosteric) and vitamin B₁₂ (allosteric) were tested for LRRK2 protein stability. The latter one is of interest because it is found naturally in many animal products but not in plant foods, therefore it is reasonable to imply that it is potentially safe as a therapeutic. Deficiency in B₁₂ either due to diet or inability to absorb the vitamin as observed in some cases of IBD can increase the risk of developing PD and other neurological symptoms among many (Hunt *et al.*, 2014, Shen, 2015). In this project, we have found that Vitamin B₁₂ was potentially able to improve the stability of LRRK2-I1122V in flies and LRRK2-D2019A (kinase dead) in cells. Vitamin B₁₂ in this investigation and in another study (Schaffner *et al.*, 2019) has shown promising results on LRRK2 linked PD but it has also been shown to affect other types of familial PD specifically *PINK1* linked PD.

Vitamin B₅ (a family member of vitamin B) has been shown to rescue the mitochondrial dysfunction found in *PINK1* loss of function flies (Huang *et al.*, 2022). Our results and previous results give a good platform to consider using vitamin B₁₂ in more research with regard to LRRK2 function.

6.5 Future works

In chapter 3, dLRRK has been suggested to be involved in the biosynthesis and function of pigment granules in addition to genetic interaction with different small molecule synthesis pathways (kynurenine, pteridine and granule pathways) that are important to neurotransmitter, antioxidant and tissue pigment generation. We have found in this project that expressing eye pigment genes *se*, *sptr*, and *pu* were not able to rescue the age-dependent loss of visual function in *dLRRK^{LOF}* old flies. In addition, we have found that no synthetic lethality was produced when *cn^{35k}* and *pr^l* individually were crossed with *dLRRK^{LOF}*. It would be useful to test the interaction of dLRRK with more eye colour genes to add the data we have generated here to form a clear picture for this interaction. Furthermore, to expand on the data of testing the genetic interaction in null or loss of function mutations, to test for interaction at the tissue and cellular level by knocking down eye pigment gene function using targeted RNAi in various tissues to locate the critical tissue where this interaction between these genes and LRRK2 occurs.

In chapter 4, a critical issue in the inability to obtain good results for DPP or PPA was due to the variation in eye colour pigmentation of flies. The degree of pigmentation of the eye is also known to affect the size of the ERG due to the absorbance of light by the pigment (Stark, 1973). Thus, testing ERGs in PD models would be optimal where eye colour pigmentation is uniform between the different genotypes. Flies expressing *LRRK2* in pigment cells have shades of orange and gave the best results in all three assays in this project. Incorporating *w^{apricot}*, which has an orange eye, into flies might be a good strategy to unify eye colour of flies into shades of orange. Moreover, some statistical significance might not appear in graphs even though they look significant due to the small sample size. This could be easily addressed by increasing the number of examined sample.

In chapter 5, we observed that mutations in LRRK2 was potentially affecting the protein stability, specifically LRRK2-R1441C where it appeared to be less stable than the wild type in cells and in flies. LRRK2 degradation in cells appeared to be still ongoing by the end of the measurement period for all genotypes except for LRRK2-R1441C

compared to the flies which LRRK2 appeared to be mostly degraded by the end of the measurement period which might not give a complete picture of the protein decay in cells. An extension of the measurement period could resolve this issue. However, in case of cell culture, when I began the project, the hypothesis that LRRK2 was associated with microtubules was not well supported and considered unlikely. But several recent papers have emphasised that LRRK2 can interact with microtubules. Evidence has been accumulating from structural studies which supports this interaction (Deniston *et al.*, 2020, Leschziner and Reck-Peterson, 2021). This potential interaction suggests that using GAPDH instead of β -tubulin for normalisation would be more appropriate. A different approach in examining LRRK2 stability is to investigate strong and direct interactors upstream (e.g., protein 14-3-3) or downstream (Rab10) of LRRK2 which for the latter I had some preliminary data that was cut short by Covid. In flies, it would be good to use a set of flies where the transgenes are all inserted in the same genomic landing sites, and an inducible *TH*-Gal4 so that the precise effects and timing of LRRK2 expression in DA neurons can be established.

6.6 Conclusion

Throughout this project, the function and dynamic of *dLRRK/LRRK2* have been tested in a *Drosophila* model of PD and in tissue culture. Multiple assays have been utilised to investigate the interaction of *LRRK2* and *dLRRK* with other mutations in pigment synthesis and pigment granule biogenesis on viability, effects on vision, and general stability of the protein in flies as well as in cells. The findings provided in this thesis supplement previously published LRRK2 data and raise new research concerns that may help us learn more about how mutations in this gene cause Parkinson's disease.

Summary of key findings:

1. Expressing *dLRRK* in non-neuronal tissue was able to rescue visual deficit found in *dLRRK^{LOF}* old flies.
2. Expressing eye pigment genes *se*, *sptr*, and *pu* were not able to rescue the age dependant loss of visual function in *dLRRK^{LOF}* old flies.
3. No synthetic lethality was observed for *cn^{35k}* and *pr¹* individually when crossed with *dLRRK^{LOF}*.
4. Young flies expressing *LRRK2-G2019S* in DA neurons or pigment cells failed to adapt to the light.

5. The potential order of LRRK2 stability in flies (most stable to least stable) was similar for LRRK2-WT, LRRK2-G2019S-K1906M (kinase dead), LRRK2-I1122V, and LRRK2-G2019S then LRRK2-R1441C while in cells it was LRRK2-D2017A (kinase dead), LRRK2-G2019S, LRRK2-WT, and LRRK2-R1441C.
6. The LRRK2 inhibitor Vitamin B₁₂ potentially improved the stability of LRRK2-I1122V in flies while it potentially reduced the stability of LRRK2-D2019A (kinase dead) in cells.
7. The LRRK2 inhibitor had no effect on the stability of LRRK2 while it potentially improved the stability of LRRK2-WT and LRRK2-I1122V in flies.

References

- Adams, M. D., S. E. Celniker, R. A. Holt, C. A. Evans, J. D. Gocayne, P. G. Amanatides, S. E. Scherer, P. W. Li, R. A. Hoskins, R. F. Galle, R. A. George, S. E. Lewis, S. Richards, M. Ashburner, S. N. Henderson, G. G. Sutton, J. R. Wortman, M. D. Yandell, Q. Zhang, L. X. Chen, R. C. Brandon, Y. H. Rogers, R. G. Blazej, M. Champe, B. D. Pfeiffer, K. H. Wan, C. Doyle, E. G. Baxter, G. Helt, C. R. Nelson, G. L. Gabor, J. F. Abril, A. Agbayani, H. J. An, C. Andrews-Pfannkoch, D. Baldwin, R. M. Ballew, A. Basu, J. Baxendale, L. Bayraktaroglu, E. M. Beasley, K. Y. Beeson, P. V. Benos, B. P. Berman, D. Bhandari, S. Bolshakov, D. Borkova, M. R. Botchan, J. Bouck, P. Brokstein, P. Brottier, K. C. Burtis, D. A. Busam, H. Butler, E. Cadieu, A. Center, I. Chandra, J. M. Cherry, S. Cawley, C. Dahlke, L. B. Davenport, P. Davies, B. de Pablos, A. Delcher, Z. Deng, A. D. Mays, I. Dew, S. M. Dietz, K. Dodson, L. E. Doup, M. Downes, S. Dugan-Rocha, B. C. Dunkov, P. Dunn, K. J. Durbin, C. C. Evangelista, C. Ferraz, S. Ferriera, W. Fleischmann, C. Fosler, A. E. Gabrielian, N. S. Garg, W. M. Gelbart, K. Glasser, A. Glodek, F. Gong, J. H. Gorrell, Z. Gu, P. Guan, M. Harris, N. L. Harris, D. Harvey, T. J. Heiman, J. R. Hernandez, J. Houck, D. Hostin, K. A. Houston, T. J. Howland, M. H. Wei, C. Ibegwam, M. Jalali, F. Kalush, G. H. Karpen, Z. Ke, J. A. Kennison, K. A. Ketchum, B. E. Kimmel, C. D. Kodira, C. Kraft, S. Kravitz, D. Kulp, Z. Lai, P. Lasko, Y. Lei, A. A. Levitsky, J. Li, Z. Li, Y. Liang, X. Lin, X. Liu, B. Mattei, T. C. McIntosh, M. P. McLeod, D. McPherson, G. Merkulov, N. V. Milshina, C. Mobarry, J. Morris, A. Moshrefi, S. M. Mount, M. Moy, B. Murphy, L. Murphy, D. M. Muzny, D. L. Nelson, D. R. Nelson, K. A. Nelson, K. Nixon, D. R. Nusskern, J. M. Pacleb, M. Palazzolo, G. S. Pittman, S. Pan, J. Pollard, V. Puri, M. G. Reese, K. Reinert, K. Remington, R. D. Saunders, F. Scheeler, H. Shen, B. C. Shue, I. Siden-Kiamos, M. Simpson, M. P. Skupski, T. Smith, E. Spier, A. C. Spradling, M. Stapleton, R. Strong, E. Sun, R. Svirskas, C. Tector, R. Turner, E. Venter, A. H. Wang, X. Wang, Z. Y. Wang, D. A. Wassarman, G. M. Weinstock, J. Weissenbach, S. M. Williams, WoodageT, K. C. Worley, D. Wu, S. Yang, Q. A. Yao, J. Ye, R. F. Yeh, J. S. Zaveri, M. Zhan, G. Zhang, Q. Zhao, L. Zheng, X. H. Zheng, F. N. Zhong, W. Zhong, X. Zhou, S. Zhu, X. Zhu, H. O. Smith, R. A. Gibbs, E. W. Myers, G. M. Rubin and J. C. Venter (2000). The genome sequence of *Drosophila melanogaster*. *Science* 287(5461) 2185-2195.
- Adams, M. D. and J. J. Sekelsky (2002). From sequence to phenotype: reverse genetics in *drosophila melanogaster*. *Nature Reviews Genetics* 3(3) 189-198.
- Afsari, F., K. V. Christensen, G. P. Smith, M. Hentzer, O. M. Nippe, C. J. H. Elliott and A. R. Wade (2014). Abnormal visual gain control in a Parkinson's disease model. *Human Molecular Genetics* 23(17) 4465-4478.
- Agalliu, I., M. San Luciano, A. Mirelman, N. Giladi, B. Waro, J. Aasly, R. Inzelberg, S. Hassin-Baer, E. Friedman, J. Ruiz-Martinez, J. F. Marti-Masso, A. Orr-Urtreger, S. Bressman and R. Saunders-Pullman (2015). Higher Frequency of Certain Cancers in LRRK2 G2019S Mutation Carriers With Parkinson Disease: A Pooled Analysis. *JAMA Neurology* 72(1) 58-65.
- Ahsan Ejaz, A., I. S. Sekhon and S. Munjal (2006). Characteristic findings on 24-h ambulatory blood pressure monitoring in a series of patients with Parkinson's disease. *European Journal of Internal Medicine* 17(6) 417-420.
- Aman, Y., T. Schmauck-Medina, M. Hansen, R. I. Morimoto, A. K. Simon, I. Bjedov, K. Palikaras, A. Simonsen, T. Johansen, N. Tavernarakis, D. C. Rubinsztein, L. Partridge, G. Kroemer, J. Labbadia and E. F. Fang (2021). Autophagy in healthy aging and disease. *Nature Aging* 1(8) 634-650.

- Angeles, D. C., B. H. Gan, L. Onstead, Y. Zhao, K. L. Lim, J. Dachsel, H. Melrose, M. Farrer, Z. K. Wszolek, D. W. Dickson and E. K. Tan (2011). Mutations in LRRK2 increase phosphorylation of peroxiredoxin 3 exacerbating oxidative stress-induced neuronal death. *Hum Mutat* 32(12) 1390-1397.
- Angeles, D. C., P. Ho, L. L. Chua, C. Wang, Y. W. Yap, C. Ng, Z. Zhou, K. L. Lim, Z. K. Wszolek, H. Y. Wang and E. K. Tan (2014). Thiol peroxidases ameliorate LRRK2 mutant-induced mitochondrial and dopaminergic neuronal degeneration in *Drosophila*. *Hum Mol Genet* 23(12) 3157-3165.
- Archibald, N. K., M. P. Clarke, U. P. Mosimann and D. J. Burn (2009). The retina in Parkinson's disease. *Brain* 132(Pt 5) 1128-1145.
- Ashbrook, L. H., A. D. Krystal, Y.-H. Fu and L. J. Ptáček (2020). Genetics of the human circadian clock and sleep homeostat. *Neuropsychopharmacology* 45(1) 45-54.
- Avazzadeh, S., J. M. Baena, C. Keighron, Y. Feller-Sanchez and L. R. Quinlan (2021). Modelling Parkinson's Disease: iPSCs towards Better Understanding of Human Pathology. *Brain Sciences* 11(3) 373.
- Avenali, M., F. Blandini and S. Cerri (2020). Glucocerebrosidase Defects as a Major Risk Factor for Parkinson's Disease. *Frontiers in Aging Neuroscience* 12.
- Baptista, M. A. S., K. Merchant, T. Barrett, S. Bhargava, D. K. Bryce, J. M. Ellis, A. A. Estrada, M. J. Fell, B. K. Fiske, R. N. Fuji, P. Galatsis, A. G. Henry, S. Hill, W. Hirst, C. Houle, M. E. Kennedy, X. Liu, M. L. Maddess, C. Markgraf, H. Mei, W. A. Meier, E. Needle, S. Ploch, C. Royer, K. Rudolph, A. K. Sharma, A. Stepan, S. Steyn, C. Trost, Z. Yin, H. Yu, X. Wang and T. B. Sherer (2020). LRRK2 inhibitors induce reversible changes in nonhuman primate lungs without measurable pulmonary deficits. *Science Translational Medicine* 12(540) eaav0820.
- Behnia, R. and C. Desplan (2015). Visual circuits in flies: beginning to see the whole picture. *Current Opinion in Neurobiology* 34 125-132.
- Beilina, A., I. N. Rudenko, A. Kaganovich, L. Civiero, H. Chau, S. K. Kalia, L. V. Kalia, E. Lobbestael, R. Chia, K. Ndukwe, J. Ding, M. A. Nalls, M. Olszewski, D. N. Hauser, R. Kumaran, A. M. Lozano, V. Baekelandt, L. E. Greene, J. M. Taymans, E. Greggio and M. R. Cookson (2014). Unbiased screen for interactors of leucine-rich repeat kinase 2 supports a common pathway for sporadic and familial Parkinson disease. *Proc Natl Acad Sci U S A* 111(7) 2626-2631.
- Bertoni, J. M., J. P. Arlette, H. H. Fernandez, C. Fitzer-Attas, K. Frei, M. N. Hassan, S. H. Isaacson, M. F. Lew, E. Molho, W. G. Ondo, T. J. Phillips, C. Singer, J. P. Sutton, J. E. Wolf and N. A. P. M. Sur (2010). Increased Melanoma Risk in Parkinson Disease A Prospective Clinicopathological Study. *Archives of Neurology* 67(3) 347-352.
- Berwick, D. C., G. R. Heaton, S. Azeggagh and K. Harvey (2019). LRRK2 Biology from structure to dysfunction: research progresses, but the themes remain the same. *Mol Neurodegener* 14(1) 49.
- Bishop, M. P., S. T. Elder and R. G. Heath (1963). Intracranial self-stimulation in man. *Science* 140(3565) 394-396.
- Biskup, S., D. J. Moore, F. Celsi, S. Higashi, A. B. West, S. A. Andrabi, K. Kurkinen, S. W. Yu, J. M. Savitt, H. J. Waldvogel, R. L. Faull, P. C. Emson, R. Torp, O. P. Ottersen, T. M. Dawson and V. L. Dawson (2006). Localization of LRRK2 to membranous and vesicular structures in mammalian brain. *Ann Neurol* 60(5) 557-569.
- Blesa, J. and S. Przedborski (2014). Parkinson's disease: animal models and dopaminergic cell vulnerability. *Front Neuroanat* 8 155.

- Bodis-Wollner, I., M. S. Marx, S. Mitra, P. Bobak, L. Mylin and M. Yahr (1987). Visual dysfunction in Parkinson's disease. Loss in spatiotemporal contrast sensitivity. *Brain* 110 (Pt 6) 1675-1698.
- Bolam, J. P. and E. K. Pissadaki (2012). Living on the edge with too many mouths to feed: why dopamine neurons die. *Mov Disord* 27(12) 1478-1483.
- Bonet-Ponce, L., A. Beilina, C. D. Williamson, E. Lindberg, J. H. Kluss, S. Saez-Atienzar, N. Landeck, R. Kumaran, A. Mamais, C. K. E. Bleck, Y. Li and M. R. Cookson (2020). LRRK2 mediates tubulation and vesicle sorting from lysosomes. *Science Advances* 6(46) eabb2454.
- Bonet-Ponce, L. and M. R. Cookson (2021). LRRK2 recruitment, activity, and function in organelles. *Febs j*.
- Borycz, J., J. A. Borycz, A. Kubów, V. Lloyd and I. A. Meinertzhagen (2008). Drosophila ABC transporter mutants white, brown and scarlet have altered contents and distribution of biogenic amines in the brain. *J Exp Biol* 211(Pt 21) 3454-3466.
- Bowman, S. L., J. Bi-Karchin, L. Le and M. S. Marks (2019). The road to lysosome-related organelles: Insights from Hermansky-Pudlak syndrome and other rare diseases. *Traffic (Copenhagen, Denmark)* 20(6) 404-435.
- Braak, H., K. D. Tredici, U. Rüb, R. A. I. de Vos, E. N. H. Jansen Steur and E. Braak (2003). Staging of brain pathology related to sporadic Parkinson's disease. *Neurobiology of Aging* 24(2) 197-211.
- Brand, A. H. and N. Perrimon (1993). TARGETED GENE-EXPRESSION AS A MEANS OF ALTERING CELL FATES AND GENERATING DOMINANT PHENOTYPES. *Development* 118(2) 401-415.
- Brighouse, A., J. B. Dacks and M. C. Field (2010). Rab protein evolution and the history of the eukaryotic endomembrane system. *Cellular and molecular life sciences : CMLS* 67(20) 3449-3465.
- Buneeva, O. and A. Medvedev (2022). Atypical Ubiquitination and Parkinson's Disease. *Int J Mol Sci* 23(7).
- Burbulla, L. F., P. Song, J. R. Mazzulli, E. Zampese, Y. C. Wong, S. Jeon, D. P. Santos, J. Blanz, C. D. Obermaier, C. Strojny, J. N. Savas, E. Kiskinis, X. Zhuang, R. Kruger, D. J. Surmeier and D. Krainc (2017). Dopamine oxidation mediates mitochondrial and lysosomal dysfunction in Parkinson's disease. *Science* 357(6357) 1255-1261.
- Burré, J., S. Vivona, J. Diao, M. Sharma, A. T. Brunger and T. C. Südhof (2013). Properties of native brain α -synuclein. *Nature* 498(7453) E4-E6.
- Cabezudo, D., V. Baekelandt and E. Lobbstaël (2020). Multiple-Hit Hypothesis in Parkinson's Disease: LRRK2 and Inflammation. *Frontiers in Neuroscience* 14.
- Campesan, S., E. W. Green, C. Breda, K. V. Sathyasaikumar, P. J. Muchowski, R. Schwarcz, C. P. Kyriacou and F. Giorgini (2011). The Kynurenine Pathway Modulates Neurodegeneration in a Drosophila Model of Huntington's Disease. *Current Biology* 21(11) 961-966.
- Cannon, J. R., K. D. Geghman, V. Tapias, T. Sew, M. K. Dail, C. Li and J. T. Greenamyre (2013). Expression of human E46K-mutated alpha-synuclein in BAC-transgenic rats replicates early-stage Parkinson's disease features and enhances vulnerability to mitochondrial impairment. *Exp Neurol* 240 44-56.

- Cao, W., H.-J. Song, T. Gangi, A. Kelkar, I. Antani, D. Garza and M. Konsolaki (2008). Identification of novel genes that modify phenotypes induced by Alzheimer's beta-amyloid overexpression in *Drosophila*. *Genetics* 178(3) 1457-1471.
- Carballo-Carbajal, I., A. Laguna, J. Romero-Gimenez, T. Cuadros, J. Bove, M. Martinez-Vicente, A. Parent, M. Gonzalez-Sepulveda, N. Penueles, A. Torra, B. Rodriguez-Galvan, A. Ballabio, T. Hasegawa, A. Bortolozzi, E. Gelpi and M. Vila (2019). Brain tyrosinase overexpression implicates age-dependent neuromelanin production in Parkinson's disease pathogenesis. *Nat Commun* 10(1) 973.
- Castle, W. E., F. W. Carpenter, A. H. Clark, S. O. Mast and W. M. Barrows (1906). The Effects of Inbreeding, Cross-Breeding, and Selection upon the Fertility and Variability of *Drosophila*. *Proceedings of the American Academy of Arts and Sciences* 41(33) 731-786.
- Cheli, V. T., R. W. Daniels, R. Godoy, D. J. Hoyle, V. Kandachar, M. Starcevic, J. A. Martinez-Agosto, S. Poole, A. DiAntonio, V. K. Lloyd, H. C. Chang, D. E. Krantz and E. C. Dell'Angelica (2010). Genetic modifiers of abnormal organelle biogenesis in a *Drosophila* model of BLOC-1 deficiency. *Human Molecular Genetics* 19(5) 861-878.
- Chen, L. and M. B. Feany (2005). Alpha-synuclein phosphorylation controls neurotoxicity and inclusion formation in a *Drosophila* model of Parkinson disease. *Nat Neurosci* 8(5) 657-663.
- Chia, R., S. Haddock, A. Beilina, I. N. Rudenko, A. Mamais, A. Kaganovich, Y. Li, R. Kumaran, M. A. Nalls and M. R. Cookson (2014). Phosphorylation of LRRK2 by casein kinase 1 α regulates trans-Golgi clustering via differential interaction with ARHGEF7. *Nature Communications* 5(1) 5827.
- Cho, H. J., J. Yu, C. Xie, P. Rudrabhatla, X. Chen, J. Wu, L. Parisiadou, G. Liu, L. Sun, B. Ma, J. Ding, Z. Liu and H. Cai (2014). Leucine-rich repeat kinase 2 regulates Sec16A at ER exit sites to allow ER-Golgi export. *Embo j* 33(20) 2314-2331.
- Chyb, S., W. Hevers, M. Forte, W. J. Wolfgang, Z. Selinger and R. C. Hardie (1999). Modulation of the Light Response by cAMP in *Drosophila* Photoreceptors. *The Journal of Neuroscience* 19(20) 8799-8807.
- Clark, I. E., M. W. Dodson, C. Jiang, J. H. Cao, J. R. Huh, J. H. Seol, S. J. Yoo, B. A. Hay and M. Guo (2006). *Drosophila pink1* is required for mitochondrial function and interacts genetically with parkin. *Nature* 441(7097) 1162-1166.
- Coleman, B. M. and A. F. Hill (2015). Extracellular vesicles – Their role in the packaging and spread of misfolded proteins associated with neurodegenerative diseases. *Seminars in Cell & Developmental Biology* 40 89-96.
- Cooper, J. F. and J. M. Van Raamsdonk (2018). Modeling Parkinson's Disease in *C. elegans*. *Journal of Parkinson's disease* 8 17-32.
- Cording, A. C., N. Shiaelis, S. Petridi, C. A. Middleton, L. G. Wilson and C. J. H. Elliott (2017). Targeted kinase inhibition relieves slowness and tremor in a *Drosophila* model of LRRK2 Parkinson's disease. *Npj Parkinsons Disease* 3.
- Corro, C., L. Novellademunt and V. S. W. Li (2020). A brief history of organoids. *Am J Physiol Cell Physiol* 319(1) C151-C165.
- Cunningham, P. C., K. Waldeck, B. Ganetzky and D. T. Babcock (2018). Neurodegeneration and locomotor dysfunction in *Drosophila* scarlet mutants. *Journal of Cell Science* 131(18).

- D'Adamo, P., M. Masetti, V. Bianchi, L. Morè, M. L. Mignogna, M. Giannandrea and S. Gatti (2014). RAB GTPases and RAB-interacting proteins and their role in the control of cognitive functions. *Neuroscience & Biobehavioral Reviews* 46 302-314.
- Dalvin, L. A., G. M. Damento, B. P. Yawn, B. A. Abbott, D. O. Hodge and J. S. Pulido (2017). Parkinson Disease and Melanoma: Confirming and Reexamining an Association. *Mayo Clinic Proceedings* 92(7) 1070-1079.
- Damulewicz, M., O. Woźnicka, M. Jasińska and E. Pyza (2020). CRY-dependent plasticity of tetrad presynaptic sites in the visual system of *Drosophila* at the morning peak of activity and sleep. *Scientific Reports* 10(1) 18161.
- Daubner, S. C., T. Le and S. Wang (2011). Tyrosine hydroxylase and regulation of dopamine synthesis. *Archives of biochemistry and biophysics* 508(1) 1-12.
- Dauer, W. and S. Przedborski (2003). Parkinson's Disease: Mechanisms and Models. *Neuron* 39(6) 889-909.
- Davidson, S., A. Cronin-Golomb and A. Lee (2005). Visual and spatial symptoms in Parkinson's disease. *Vision Research* 45(10) 1285-1296.
- Dawson, T. M., H. S. Ko and V. L. Dawson (2010). Genetic animal models of Parkinson's disease. *Neuron* 66(5) 646-661.
- De Cock, V. C., M. Vidailhet and I. Arnulf (2008). Sleep disturbances in patients with parkinsonism. *Nature Clinical Practice Neurology* 4(5) 254-266.
- de Lau, L. M. L. and M. M. B. Breteler (2006). Epidemiology of Parkinson's disease. *Lancet Neurology* 5(6) 525-535.
- De Wit, T., V. Baekelandt and E. Lobbstaël (2018). LRRK2 Phosphorylation: Behind the Scenes. *Neuroscientist* 24(5) 486-500.
- Deniston, C. K., J. Salogiannis, S. Mathea, D. M. Snead, I. Lahiri, M. Matyszewski, O. Donosa, R. Watanabe, J. Böhning, A. K. Shiao, S. Knapp, E. Villa, S. L. Reck-Peterson and A. E. Leschziner (2020). Structure of LRRK2 in Parkinson's disease and model for microtubule interaction. *Nature* 588(7837) 344-349.
- Di Fonzo, A., C. F. Rohe, J. Ferreira, H. F. Chien, L. Vacca, F. Stocchi, L. Guedes, E. Fabrizio, M. Manfredi, N. Vanacore, S. Goldwurm, G. Breedveld, C. Sampaio, G. Meco, E. Barbosa, B. A. Oostra, V. Bonifati and N. Italian Parkinson Genetics (2005). A frequent LRRK2 gene mutation associated with autosomal dominant Parkinson's disease. *Lancet* 365(9457) 412-415.
- Dickson, D. W., H. Braak, J. E. Duda, C. Duyckaerts, T. Gasser, G. M. Halliday, J. Hardy, J. B. Leverenz, K. Del Tredici, Z. K. Wszolek and I. Litvan (2009). Neuropathological assessment of Parkinson's disease: refining the diagnostic criteria. *The Lancet Neurology* 8(12) 1150-1157.
- Diederich, N. J., V. Pieri, G. Hipp, O. Rufra, S. Blyth and M. Vaillant (2010). Discriminative power of different nonmotor signs in early Parkinson's disease. A case-control study. *Mov Disord* 25(7) 882-887.
- Ding, X. and M. S. Goldberg (2009). Regulation of LRRK2 Stability by the E3 Ubiquitin Ligase CHIP. *PLoS One* 4(6) e5949.
- Dodson, M. W., T. Zhang, C. Jiang, S. Chen and M. Guo (2012). Roles of the *Drosophila* LRRK2 homolog in Rab7-dependent lysosomal positioning. *Hum Mol Genet* 21(6) 1350-1363.

- Dorsey, E. R., A. Elbaz, E. Nichols, F. Abd-Allah, A. Abdelalim, J. C. Adsuar, M. G. Ansha, C. Brayne, J.-Y. J. Choi, D. Collado-Mateo, N. Dahodwala, H. P. Do, D. Edessa, M. Endres, S.-M. Fereshtehnejad, K. J. Foreman, F. G. Gankpe, R. Gupta, G. J. Hankey, S. I. Hay, M. I. Hegazy, D. T. Hibstu, A. Kasaeian, Y. Khader, I. Khalil, Y.-H. Khang, Y. J. Kim, Y. Kokubo, G. Logroscino, J. Massano, N. Mohamed Ibrahim, M. A. Mohammed, A. Mohammadi, M. Moradi-Lakeh, M. Naghavi, B. T. Nguyen, Y. L. Nirayo, F. A. Ogbo, M. O. Owolabi, D. M. Pereira, M. J. Postma, M. Qorbani, M. A. Rahman, K. T. Roba, H. Safari, S. Safiri, M. Satpathy, M. Sawhney, A. Shafieesabet, M. S. Shiferaw, M. Smith, C. E. I. Szoeki, R. Tabarés-Seisdedos, N. T. Truong, K. N. Ukwaja, N. Venketasubramanian, S. Villafaina, K. g. weldegwergs, R. Westerman, T. Wijeratne, A. S. Winkler, B. T. Xuan, N. Yonemoto, V. L. Feigin, T. Vos and C. J. L. Murray (2018). Global, regional, and national burden of Parkinson's disease, 1990–2016: a systematic analysis for the Global Burden of Disease Study 2016. *The Lancet Neurology* 17(11) 939-953.
- Doty, R. L. (2012). Olfactory dysfunction in Parkinson disease. *Nature Reviews Neurology* 8(6) 329-339.
- Dreesen, T. D., D. H. Johnson and S. Henikoff (1988). The brown protein of *Drosophila melanogaster* is similar to the white protein and to components of active transport complexes. *Mol Cell Biol* 8(12) 5206-5215.
- Drouyer, M., M. F. Bolliger, E. Lobbstaël, C. Van den Haute, M. Emanuele, R. Lefebvre, W. Sibran, T. De Wit, C. Leghay, E. Mutez, N. Dzamko, G. M. Halliday, S. Murayama, A. Martoriati, K. Cailliau, J.-F. Bodart, M.-C. Chartier-Harlin, V. Baekelandt, R. J. Nichols and J.-M. Taymans (2021). Protein phosphatase 2A holoenzymes regulate leucine-rich repeat kinase 2 phosphorylation and accumulation. *Neurobiology of Disease* 157 105426.
- Duffy, J. B. (2002). GAL4 system in *Drosophila*: A fly geneticist's Swiss army knife. *Genesis* 34(1-2) 1-15.
- Dusonchet, J., O. Kochubey, K. Stafa, S. M. Young, R. Zufferey, D. J. Moore, B. L. Schneider and P. Aebischer (2011). A Rat Model of Progressive Nigral Neurodegeneration Induced by the Parkinson's Disease-Associated G2019S Mutation in LRRK2. *The Journal of Neuroscience* 31(3) 907-912.
- Dzamko, N., F. Inesta-Vaquera, J. Zhang, C. Xie, H. Cai, S. Arthur, L. Tan, H. Choi, N. Gray, P. Cohen, P. Pedrioli, K. Clark and D. R. Alessi (2012). The IκappaB kinase family phosphorylates the Parkinson's disease kinase LRRK2 at Ser935 and Ser910 during Toll-like receptor signaling. *PLoS One* 7(6) e39132.
- Eguchi, T., T. Kuwahara, M. Sakurai, T. Komori, T. Fujimoto, G. Ito, S. Yoshimura, A. Harada, M. Fukuda, M. Koike and T. Iwatsubo (2018). LRRK2 and its substrate Rab GTPases are sequentially targeted onto stressed lysosomes and maintain their homeostasis. *Proceedings of the National Academy of Sciences of the United States of America* 115(39) E9115-E9124.
- Esteves, A. R., R. H. Swerdlow and S. M. Cardoso (2014). LRRK2, a puzzling protein: insights into Parkinson's disease pathogenesis. *Exp Neurol* 261 206-216.
- Euler, T., S. Haverkamp, T. Schubert and T. Baden (2014). Retinal bipolar cells: elementary building blocks of vision. *Nature Reviews Neuroscience* 15(8) 507-519.
- Exner, N., A. K. Lutz, C. Haass and K. F. Winklhofer (2012). Mitochondrial dysfunction in Parkinson's disease: molecular mechanisms and pathophysiological consequences. *Embo j* 31(14) 3038-3062.

- Fasano, A., N. P. Visanji, L. W. C. Liu, A. E. Lang and R. F. Pfeiffer (2015). Gastrointestinal dysfunction in Parkinson's disease. *The Lancet Neurology* 14(6) 625-639.
- Feany, M. B. and W. W. Bender (2000). A Drosophila model of Parkinson's disease. *Nature* 404(6776) 394-398.
- Fell, M. J., C. Mirescu, K. Basu, B. Cheewatrakoolpong, D. E. DeMong, J. M. Ellis, L. A. Hyde, Y. Lin, C. G. Markgraf, H. Mei, M. Miller, F. M. Poulet, J. D. Scott, M. D. Smith, Z. Yin, X. Zhou, E. M. Parker, M. E. Kennedy and J. A. Morrow (2015). MLi-2, a Potent, Selective, and Centrally Active Compound for Exploring the Therapeutic Potential and Safety of LRRK2 Kinase Inhibition. *Journal of Pharmacology and Experimental Therapeutics* 355(3) 397-409.
- Fellgett, A., C. A. Middleton, J. Munns, C. Ugbo, D. Jaciuch, L. G. Wilson, S. Chawla and C. J. H. Elliott (2021). Multiple Pathways of LRRK2-G2019S/Rab10 Interaction in Dopaminergic Neurons. *Journal of Parkinson's disease* 11 1805-1820.
- Figueiro, M. G., B. Stevenson, J. Heerwagen, K. Kampschroer, C. M. Hunter, K. Gonzales, B. Plitnick and M. S. Rea (2017). The impact of daytime light exposures on sleep and mood in office workers. *Sleep Health* 3(3) 204-215.
- Fire, A., S. Q. Xu, M. K. Montgomery, S. A. Kostas, S. E. Driver and C. C. Mello (1998). Potent and specific genetic interference by double-stranded RNA in *Caenorhabditis elegans*. *Nature* 391(6669) 806-811.
- Fleming, S. M., P. O. Fernagut and M. F. Chesselet (2005). Genetic mouse models of parkinsonism: strengths and limitations. *NeuroRx : the journal of the American Society for Experimental NeuroTherapeutics* 2(3) 495-503.
- Fleming, S. M., C. Zhu, P. O. Fernagut, A. Mehta, C. D. DiCarlo, R. L. Seaman and M. F. Chesselet (2004). Behavioral and immunohistochemical effects of chronic intravenous and subcutaneous infusions of varying doses of rotenone. *Exp Neurol* 187(2) 418-429.
- Franceschini, N. and K. Kirschfeld (1971). [Pseudopupil phenomena in the compound eye of drosophila]. *Kybernetik* 9(5) 159-182.
- Frank, M. J., L. C. Seeberger and R. C. O'Reilly (2004). By Carrot or by Stick: Cognitive Reinforcement Learning in Parkinsonism. *Science* 306(5703) 1940-1943.
- Frederick, J. M., M. E. Rayborn, A. M. Laties, D. M. Lam and J. G. Hollyfield (1982). Dopaminergic neurons in the human retina. *J Comp Neurol* 210(1) 65-79.
- Friggi-Grelin, F., H. Coulom, M. Meller, D. Gomez, J. Hirsh and S. Birman (2003). Targeted gene expression in Drosophila dopaminergic cells using regulatory sequences from tyrosine hydroxylase. *J Neurobiol* 54(4) 618-627.
- Fukuda, M. (2021). Rab GTPases: Key players in melanosome biogenesis, transport, and transfer. *Pigment Cell & Melanoma Research* 34(2) 222-235.
- Funayama, M., K. Hasegawa, H. Kowa, M. Saito, S. Tsuji and F. Obata (2002). A new locus for Parkinson's disease (PARK8) maps to chromosome 12p11.2-q13.1. *Ann Neurol* 51(3) 296-301.
- Funayama, M., K. Hasegawa, E. Ohta, N. Kawashima, M. Komiyama, H. Kowa, S. Tsuji and F. Obata (2005). An LRRK2 mutation as a cause for the parkinsonism in the original PARK8 family. *Ann Neurol* 57(6) 918-921.
- Furmston, R. (2016). Investigating the Role of LRRK2 in the Visual System in a Drosophila Model of Parkinson's Disease. *Biology*. University of York. 291.

- Gad, H., N. Ringstad, P. Löw, O. Kjaerulff, J. Gustafsson, M. Wenk, G. Di Paolo, Y. Nemoto, J. Crun, M. H. Ellisman, P. De Camilli, O. Shupliakov and L. Brodin (2000). Fission and uncoating of synaptic clathrin-coated vesicles are perturbed by disruption of interactions with the SH3 domain of endophilin. *Neuron* 27(2) 301-312.
- Galet, B., H. Cheval and P. Ravassard (2020). Patient-Derived Midbrain Organoids to Explore the Molecular Basis of Parkinson's Disease. *Front Neurol* 11 1005.
- Gehrke, S., Y. Imai, N. Sokol and B. Lu (2010). Pathogenic LRRK2 negatively regulates microRNA-mediated translational repression. *Nature* 466(7306) 637-641.
- Giguère, N., S. Burke Nanni and L. E. Trudeau (2018). On Cell Loss and Selective Vulnerability of Neuronal Populations in Parkinson's Disease. *Front Neurol* 9 455.
- Gilks, W. P., P. M. Abou-Sleiman, S. Gandhi, S. Jain, A. Singleton, A. J. Lees, K. Shaw, K. P. Bhatia, V. Bonifati, N. P. Quinn, J. Lynch, D. G. Healy, J. L. Holton, T. Revesz and N. W. Wood (2005). A common LRRK2 mutation in idiopathic Parkinson's disease. *Lancet* 365(9457) 415-416.
- Giltsbach, B. K. and A. Kortholt (2014). Structural biology of the LRRK2 GTPase and kinase domains: implications for regulation. *Frontiers in Molecular Neuroscience* 7(32).
- Giza, E., D. Fotiou, S. Bostantjopoulou, Z. Katsarou and A. Karlovasitou (2011). Pupil Light Reflex in Parkinson's Disease: Evaluation With Pupillometry. *International Journal of Neuroscience* 121(1) 37-43.
- GlobeNewswire. Available at: <https://www.globenewswire.com/news-release/2020/01/14/1970308/0/en/Denali-Therapeutics-Announces-Broad-Pipeline-Progress-Including-Positive-Results-From-Its-LRRK2-Program-for-Parkinson-s-Disease.html>.
- Godena, V. K., N. Brookes-Hocking, A. Moller, G. Shaw, M. Oswald, R. M. Sancho, C. C. J. Miller, A. J. Whitworth and K. J. De Vos (2014). Increasing microtubule acetylation rescues axonal transport and locomotor deficits caused by LRRK2 Roc-COR domain mutations. *Nature Communications* 5(1) 5245.
- Goetz, C. G. (1986). Charcot on Parkinson's disease. *Mov Disord* 1(1) 27-32.
- Goldman, S. M. (2014). Environmental toxins and Parkinson's disease. *Annu Rev Pharmacol Toxicol* 54 141-164.
- Gonzalez-Bellido, P. T., T. J. Wardill, R. Kostyleva, I. A. Meinertzhagen and M. Jusuola (2009). Overexpressing temperature-sensitive dynamin decelerates phototransduction and bundles microtubules in *Drosophila* photoreceptors. *The Journal of neuroscience : the official journal of the Society for Neuroscience* 29(45) 14199-14210.
- Gopalai, A. A., J. L. Lim, H. H. Li, Y. Zhao, T. T. Lim, G. B. Eow, S. Puvanarajah, S. Viswanathan, M. I. Norlinah, Z. A. Aziz, S. K. Lim, C. T. Tan, A. H. Tan, S. Y. Lim, E. K. Tan and A. A. Annuar (2019). LRRK2 N551K and R1398H variants are protective in Malays and Chinese in Malaysia: A case-control association study for Parkinson's disease. *Molecular Genetics & Genomic Medicine*.
- Gorostidi, A., J. Ruiz-Martínez, A. Lopez de Munain, A. Alzualde and J. F. Martí Massó (2008). LRRK2 G2019S and R1441G mutations associated with Parkinson's disease are common in the Basque Country, but relative prevalence is determined by ethnicity. *Neurogenetics* 10(2) 157.

- Grant, P., T. Maga, A. Loshakov, R. Singhal, A. Wali, J. Nwankwo, K. Baron and D. Johnson (2016). An Eye on Trafficking Genes: Identification of Four Eye Color Mutations in *Drosophila*. *G3-Genes Genomes Genetics* 6(10) 3185-3196.
- Gratz, S. J., A. M. Cummings, J. N. Nguyen, D. C. Hamm, L. K. Donohue, M. M. Harrison, J. Wildonger and K. M. O'Connor-Giles (2013). Genome Engineering of *Drosophila* with the CRISPR RNA-Guided Cas9 Nuclease. *Genetics* 194(4) 1029-+.
- Greene, I. D., F. Mastaglia, B. P. Meloni, K. A. West, J. Chieng, C. J. Mitchell, W.-P. Gai and S. Boulos (2014). Evidence that the LRRK2 ROC domain Parkinson's disease-associated mutants A1442P and R1441C exhibit increased intracellular degradation. *Journal of Neuroscience Research* 92(4) 506-516.
- Greene, J. C., A. J. Whitworth, I. Kuo, L. A. Andrews, M. B. Feany and L. J. Pallanck (2003). Mitochondrial pathology and apoptotic muscle degeneration in *Drosophila* parkin mutants. *Proc Natl Acad Sci U S A* 100(7) 4078-4083.
- Gusella, J. F., N. S. Wexler, P. M. Conneally, S. L. Naylor, M. A. Anderson, R. E. Tanzi, P. C. Watkins, K. Ottina, M. R. Wallace, A. Y. Sakaguchi and et al. (1983). A polymorphic DNA marker genetically linked to Huntington's disease. *Nature* 306(5940) 234-238.
- Hajee, M. E., W. F. March, D. R. Lazzaro, A. H. Wolintz, E. M. Shrier, S. Glazman and I. G. Bodis-Wollner (2009). Inner retinal layer thinning in Parkinson disease. *Arch Ophthalmol* 127(6) 737-741.
- Halliday, G. M., J. L. Holton, T. Revesz and D. W. Dickson (2011). Neuropathology underlying clinical variability in patients with synucleinopathies. *Acta Neuropathol* 122(2) 187-204.
- Halperin, A., D. Elstein and A. Zimran (2006). Increased incidence of Parkinson disease among relatives of patients with Gaucher disease. *Blood Cells Mol Dis* 36(3) 426-428.
- Haque, M. E., M. P. Mount, F. Safarpour, E. Abdel-Messih, S. Callaghan, C. Mazerolle, T. Kitada, R. S. Slack, V. Wallace, J. Shen, H. Anisman and D. S. Park (2012). Inactivation of Pink1 Gene in Vivo Sensitizes Dopamine-producing Neurons to 1-Methyl-4-phenyl-1,2,3,6-tetrahydropyridine (MPTP) and Can Be Rescued by Autosomal Recessive Parkinson Disease Genes, Parkin or DJ-1. *Journal of Biological Chemistry* 287(27) 23162-23170.
- Hardie, R. C. (1987). Is histamine a neurotransmitter in insect photoreceptors? *J Comp Physiol A* 161(2) 201-213.
- Hardie, R. C. and M. Juusola (2015). Phototransduction in *Drosophila*. *Current Opinion in Neurobiology* 34 37-45.
- Hardie, R. C. and P. Raghu (2001). Visual transduction in *Drosophila*. *Nature* 413(6852) 186-193.
- Harney, J., P. Bajaj, J. E. Finley, A. K. Kopec, P. H. Koza-Taylor, G. G. Boucher, T. A. Lanz, C. M. Doshna, C. J. Soms, K. Adkins and C. Houle (2021). An in vitro alveolar epithelial cell model recapitulates LRRK2 inhibitor-induced increases in lamellar body size observed in preclinical models. *Toxicology in Vitro* 70 105012.
- Harnois, C. and T. Di Paolo (1990). Decreased dopamine in the retinas of patients with Parkinson's disease. *Invest Ophthalmol Vis Sci* 31(11) 2473-2475.
- Harold, D., R. Abraham, P. Hollingworth, R. Sims, A. Gerrish, M. L. Hamshere, J. S. Pahwa, V. Moskvina, K. Dowzell, A. Williams, N. Jones, C. Thomas, A. Stretton, A. R. Morgan, S. Lovestone, J. Powell, P. Proitsi, M. K. Lupton, C. Brayne, D. C.

- Rubinsztein, M. Gill, B. Lawlor, A. Lynch, K. Morgan, K. S. Brown, P. A. Passmore, D. Craig, B. McGuinness, S. Todd, C. Holmes, D. Mann, A. D. Smith, S. Love, P. G. Kehoe, J. Hardy, S. Mead, N. Fox, M. Rossor, J. Collinge, W. Maier, F. Jessen, B. Schürmann, R. Heun, H. van den Bussche, I. Heuser, J. Kornhuber, J. Wiltfang, M. Dichgans, L. Frölich, H. Hampel, M. Hüll, D. Rujescu, A. M. Goate, J. S. K. Kauwe, C. Cruchaga, P. Nowotny, J. C. Morris, K. Mayo, K. Sleegers, K. Bettens, S. Engelborghs, P. P. De Deyn, C. Van Broeckhoven, G. Livingston, N. J. Bass, H. Gurling, A. McQuillin, R. Gwilliam, P. Deloukas, A. Al-Chalabi, C. E. Shaw, M. Tsolaki, A. B. Singleton, R. Guerreiro, T. W. Mühleisen, M. M. Nöthen, S. Moebus, K.-H. Jöckel, N. Klopp, H. E. Wichmann, M. M. Carrasquillo, V. S. Pankratz, S. G. Younkin, P. A. Holmans, M. O'Donovan, M. J. Owen and J. Williams (2009). Genome-wide association study identifies variants at CLU and PICALM associated with Alzheimer's disease. *Nature genetics* 41(10) 1088-1093.
- Hatano, T., S.-i. Kubo, S. Imai, M. Maeda, K. Ishikawa, Y. Mizuno and N. Hattori (2007). Leucine-rich repeat kinase 2 associates with lipid rafts. *Human Molecular Genetics* 16(6) 678-690.
- Healy, D. G., M. Falchi, S. S. O'Sullivan, V. Bonifati, A. Durr, S. Bressman, A. Brice, J. Aasly, C. P. Zabetian, S. Goldwurm, J. J. Ferreira, E. Tolosa, D. M. Kay, C. Klein, D. R. Williams, C. Marras, A. E. Lang, Z. K. Wszolek, J. Berciano, A. H. V. Schapira, T. Lynch, K. P. Bhatia, T. Gasser, A. J. Lees and N. W. Wood (2008). Phenotype, genotype, and worldwide genetic penetrance of LRRK2-associated Parkinson's disease: a case-control study. *The Lancet Neurology* 7(7) 583-590.
- Hentati, F., J. Trinh, C. Thompson, E. Nosova, M. J. Farrer and J. O. Aasly (2014). LRRK2 parkinsonism in Tunisia and Norway: a comparative analysis of disease penetrance. *Neurology* 83(6) 568-569.
- Herbst, S., P. Campbell, J. Harvey, E. M. Bernard, V. Papayannopoulos, N. W. Wood, H. R. Morris and M. G. Gutierrez (2020). LRRK2 activation controls the repair of damaged endomembranes in macrophages. *Embo j* 39(18) e104494.
- Hernán, M. A., B. Takkouche, F. Caamaño-Isorna and J. J. Gestal-Otero (2002). A meta-analysis of coffee drinking, cigarette smoking, and the risk of Parkinson's disease. *Annals of Neurology* 52(3) 276-284.
- Hernandez-Baltazar, D., L. M. Zavala-Flores and A. Villanueva-Olivo (2017). The 6-hydroxydopamine model and parkinsonian pathophysiology: Novel findings in an older model. *Neurología (English Edition)* 32(8) 533-539.
- Higashi, S., S. Biskup, A. B. West, D. Trinkaus, V. L. Dawson, R. L. M. Faull, H. J. Waldvogel, H. Arai, T. M. Dawson, D. J. Moore and P. C. Emson (2007). Localization of Parkinson's disease-associated LRRK2 in normal and pathological human brain. *Brain Research* 1155 208-219.
- Hindle, S., F. Afsari, M. Stark, C. A. Middleton, G. J. O. Evans, S. T. Sweeney and C. J. H. Elliott (2013). Dopaminergic expression of the Parkinsonian gene LRRK2-G2019S leads to non-autonomous visual neurodegeneration, accelerated by increased neural demands for energy. *Human Molecular Genetics* 22(11) 2129-2140.
- Hirsch, E. C. and S. Hunot (2009). Neuroinflammation in Parkinson's disease: a target for neuroprotection? *The Lancet Neurology* 8(4) 382-397.
- Hirth, F. (2010). *Drosophila melanogaster* in the study of human neurodegeneration. *CNS & neurological disorders drug targets* 9(4) 504-523.
- Ho, P. W., C. T. Leung, H. Liu, S. Y. Pang, C. S. Lam, J. Xian, L. Li, M. H. Kung, D. B. Ramsden and S. L. Ho (2020). Age-dependent accumulation of oligomeric SNCA/ α -

synuclein from impaired degradation in mutant LRRK2 knockin mouse model of Parkinson disease: role for therapeutic activation of chaperone-mediated autophagy (CMA). *Autophagy* 16(2) 347-370.

Hoglinger, G. U., J. Feger, A. Prigent, P. P. Michel, K. Parain, P. Champy, M. Ruberg, W. H. Oertel and E. C. Hirsch (2003). Chronic systemic complex I inhibition induces a hypokinetic multisystem degeneration in rats. *J Neurochem* 84(3) 491-502.

Homma, D., S. Katoh, H. Tokuoka and H. Ichinose (2013). The role of tetrahydrobiopterin and catecholamines in the developmental regulation of tyrosine hydroxylase level in the brain. *J Neurochem* 126(1) 70-81.

Hrdlicka, L., M. Gibson, A. Kiger, C. Micchelli, M. Schober, F. Schöck and N. Perrimon (2002). Analysis of twenty-four Gal4 lines in *Drosophila melanogaster*. *Genesis* 34(1-2) 51-57.

Hsieh, C. H., A. Shaltouki, A. E. Gonzalez, A. Bettencourt da Cruz, L. F. Burbulla, E. St Lawrence, B. Schüle, D. Krainc, T. D. Palmer and X. Wang (2016). Functional Impairment in Miro Degradation and Mitophagy Is a Shared Feature in Familial and Sporadic Parkinson's Disease. *Cell Stem Cell* 19(6) 709-724.

Huang, Y., Z. Wan, Y. Tang, J. Xu, B. Laboret, S. Nallamotheu, C. Yang, B. Liu, R. O. Lu, B. Lu, J. Feng, J. Cao, S. Hayflick, Z. Wu and B. Zhou (2022). Pantothenate kinase 2 interacts with PINK1 to regulate mitochondrial quality control via acetyl-CoA metabolism. *Nature Communications* 13(1) 2412.

Hunt, A., D. Harrington and S. Robinson (2014). Vitamin B12 deficiency. *BMJ : British Medical Journal* 349 g5226.

Ichinose, H., K. Inoue, S. Arakawa, Y. Watanabe, H. Kurosaki, S. Koshiba, E. Hustad, M. Takada and J. O. Aasly (2018). Alterations in the reduced pteridine contents in the cerebrospinal fluids of LRRK2 mutation carriers and patients with Parkinson's disease. *Journal of Neural Transmission* 125(1) 45-52.

Ichinose, H., T. Ohye, E. Takahashi, N. Seki, T. Hori, M. Segawa, Y. Nomura, K. Endo, H. Tanaka, S. Tsuji and et al. (1994). Hereditary progressive dystonia with marked diurnal fluctuation caused by mutations in the GTP cyclohydrolase I gene. *Nature genetics* 8(3) 236-242.

Imai, Y., S. Gehrke, H. Q. Wang, R. Takahashi, K. Hasegawa, E. Oota and B. Lu (2008). Phosphorylation of 4E-BP by LRRK2 affects the maintenance of dopaminergic neurons in *Drosophila*. *Embo j* 27(18) 2432-2443.

Inzelberg, R., Y. Samuels, E. Azizi, N. Qutob, L. Inzelberg, E. Domany, E. Schechtman and E. Friedman (2016). Parkinson disease (PARK) genes are somatically mutated in cutaneous melanoma. *Neurol Genet* 2(3) e70.

Ito, G., T. Okai, G. Fujino, K. Takeda, H. Ichijo, T. Katada and T. Iwatsubo (2007). GTP Binding Is Essential to the Protein Kinase Activity of LRRK2, a Causative Gene Product for Familial Parkinson's Disease. *Biochemistry* 46(5) 1380-1388.

Iwaoka, K., C. Otsuka, T. Maeda, K. Yamahara, K. Kato, K. Takahashi, K. Takahashi and Y. Terayama (2020). Impaired metabolism of kynurenine and its metabolites in CSF of parkinson's disease. *Neuroscience Letters* 714 134576.

Jackson-Lewis, V., J. Blesa and S. Przedborski (2012). Animal models of Parkinson's disease. *Parkinsonism Relat Disord* 18 Suppl 1 S183-185.

Jaleel, M., R. J. Nichols, M. Deak, D. G. Campbell, F. Gillardon, A. Knebel and D. R. Alessi (2007). LRRK2 phosphorylates moesin at threonine-558: characterization of how

- Parkinson's disease mutants affect kinase activity. *The Biochemical journal* 405(2) 307-317.
- Jeong, G. R., E.-H. Jang, J. R. Bae, S. Jun, H. C. Kang, C.-H. Park, J.-H. Shin, Y. Yamamoto, K. Tanaka-Yamamoto, V. L. Dawson, T. M. Dawson, E.-M. Hur and B. D. Lee (2018). Dysregulated phosphorylation of Rab GTPases by LRRK2 induces neurodegeneration. *Molecular Neurodegeneration* 13(1) 8.
- Jeong, G. R. and B. D. Lee (2020). Pathological Functions of LRRK2 in Parkinson's Disease. *Cells* 9(12) 2565.
- Juusola, M. and R. C. Hardie (2001). Light adaptation in *Drosophila* photoreceptors: I. Response dynamics and signaling efficiency at 25 degrees C. *The Journal of general physiology* 117(1) 3-25.
- Kandel, E., J. Schwartz, T. Jessell, S. Siegelbaum, A. Hudspeth and S. Mack (2014). The Basal Ganglia. *Principles of Neural Science, Fifth Edition*. New York, NY, McGraw-Hill Education.
- Katz, B. and B. Minke (2009). *Drosophila* photoreceptors and signaling mechanisms. *Frontiers in Cellular Neuroscience* 3.
- Kaufman, T. C. (2017). A Short History and Description of *Drosophila melanogaster* Classical Genetics: Chromosome Aberrations, Forward Genetic Screens, and the Nature of Mutations. *Genetics* 206(2) 665-689.
- Ke, M., C.-M. Chong and H. Su (2019). Using induced pluripotent stem cells for modeling Parkinson's disease. *World journal of stem cells* 11(9) 634-649.
- Kelly, K., S. Wang, R. Boddu, Z. Liu, O. Moukha-Chafiq, C. Augelli-Szafran and A. B. West (2018). The G2019S mutation in LRRK2 imparts resiliency to kinase inhibition. *Experimental Neurology* 309 1-13.
- Kenney, D. E. and G. G. Borisy (2009). Thomas Hunt Morgan at the marine biological laboratory: naturalist and experimentalist. *Genetics* 181(3) 841-846.
- Kim, D.-H., M. Shin, S.-H. Jung, Y.-J. Kim and W. D. Jones (2017). A fat-derived metabolite regulates a peptidergic feeding circuit in *Drosophila*. *PLOS Biology* 15(3) e2000532.
- Kim, H., K. Kim and J. Yim (2013a). Biosynthesis of drosopterins, the red eye pigments of *Drosophila melanogaster*. *Iubmb Life* 65(4) 334-340.
- Kim, H.-S., S.-M. Cheon, J.-W. Seo, H.-J. Ryu, K.-W. Park and J. W. Kim (2013b). Nonmotor symptoms more closely related to Parkinson's disease: Comparison with normal elderly. *Journal of the Neurological Sciences* 324(1) 70-73.
- Kim, J., B. K. Koo and J. A. Knoblich (2020). Human organoids: model systems for human biology and medicine. *Nat Rev Mol Cell Biol* 21(10) 571-584.
- Kim, J., H. Suh, S. Kim, K. Kim, C. Ahn and J. Yim (2006). Identification and characteristics of the structural gene for the *Drosophila* eye colour mutant sepia, encoding PDA synthase, a member of the Omega class glutathione S-transferases. *Biochemical Journal* 398(3) 451-460.
- Kim, N., J. Kim, D. Park, C. Rosen, D. Dorsett and J. Yim (1996). Structure and expression of wild-type and suppressible alleles of the *Drosophila* purple gene. *Genetics* 142(4) 1157-1168.

- Kim, W. G., R. P. Mohny, B. Wilson, G. H. Jeohn, B. Liu and J. S. Hong (2000). Regional difference in susceptibility to lipopolysaccharide-induced neurotoxicity in the rat brain: role of microglia. *J Neurosci* 20(16) 6309-6316.
- Kluss, J. H., M. C. Mazza, Y. Li, C. Manzoni, P. A. Lewis, M. R. Cookson and A. Mamais (2021). Preclinical modeling of chronic inhibition of the Parkinson's disease associated kinase LRRK2 reveals altered function of the endolysosomal system in vivo. *Molecular Neurodegeneration* 16(1) 17.
- Ko, H. S., R. Bailey, W. W. Smith, Z. Liu, J.-H. Shin, Y.-I. Lee, Y.-J. Zhang, H. Jiang, C. A. Ross, D. J. Moore, C. Patterson, L. Petrucelli, T. M. Dawson and V. L. Dawson (2009). CHIP regulates leucine-rich repeat kinase-2 ubiquitination, degradation, and toxicity. *Proceedings of the National Academy of Sciences* 106(8) 2897-2902.
- Konnova, E. A. and M. Swanberg (2018). Animal Models of Parkinson's Disease. In T. B. Stoker and J. C. Greenland eds. *Parkinson's Disease: Pathogenesis and Clinical Aspects*. Brisbane (AU).
- Kouli, A., K. M. Torsney and W. L. Kuan (2018). Parkinson's Disease: Etiology, Neuropathology, and Pathogenesis. In T. B. Stoker and J. C. Greenland eds. *Parkinson's Disease: Pathogenesis and Clinical Aspects*. Brisbane (AU).
- Krishnan, S., G. Sarma, S. Sarma and A. Kishore (2011). Do nonmotor symptoms in Parkinson's disease differ from normal aging? *Movement Disorders* 26(11) 2110-2113.
- Kumar, A., E. Greggio, A. Beilina, A. Kaganovich, D. Chan, J. M. Taymans, B. Wolozin and M. R. Cookson (2010). The Parkinson's disease associated LRRK2 exhibits weaker in vitro phosphorylation of 4E-BP compared to autophosphorylation. *PLoS One* 5(1) e8730.
- Kumar, J. P. (2012). Building an ommatidium one cell at a time. *Developmental dynamics : an official publication of the American Association of Anatomists* 241(1) 136-149.
- Kumari, U. and E. K. Tan (2009). LRRK2 in Parkinson's disease: genetic and clinical studies from patients. *Febs Journal* 276(22) 6455-6463.
- Kuwahara, T. and T. Iwatsubo (2020). The Emerging Functions of LRRK2 and Rab GTPases in the Endolysosomal System. *Frontiers in Neuroscience* 14(227).
- Lamb, T. D. (2016). Why rods and cones? *Eye (London, England)* 30(2) 179-185.
- Lamb, T. D. and E. N. Pugh, Jr (2006). Phototransduction, Dark Adaptation, and Rhodopsin Regeneration The Proctor Lecture. *Investigative Ophthalmology & Visual Science* 47(12) 5138-5152.
- Langston, J. W. (2017). The MPTP Story. *Journal of Parkinson's disease* 7(s1) S11-S19.
- Langston, J. W., P. Ballard, J. W. Tetrud and I. Irwin (1983). Chronic Parkinsonism in humans due to a product of meperidine-analog synthesis. *Science* 219(4587) 979-980.
- Langston, R. G., I. N. Rudenko and M. R. Cookson (2016). The function of orthologues of the human Parkinson's disease gene LRRK2 across species: implications for disease modelling in preclinical research. *Biochemical Journal* 473 221-232.
- Lanning, N. J., C. VanOpstall, M. L. Goodall, J. P. MacKeigan and B. D. Looyenga (2018). LRRK2 deficiency impairs trans-Golgi to lysosome trafficking and endocytic cargo degradation in human renal proximal tubule epithelial cells. *Am J Physiol Renal Physiol* 315(5) F1465-f1477.

- Law, B. M. H., V. A. Spain, V. H. L. Leinster, R. Chia, A. Beilina, H. J. Cho, J.-M. Taymans, M. K. Urban, R. M. Sancho, M. B. Ramírez, S. Biskup, V. Baekelandt, H. Cai, M. R. Cookson, D. C. Berwick and K. Harvey (2014). A Direct Interaction between Leucine-rich Repeat Kinase 2 and Specific β -Tubulin Isoforms Regulates Tubulin Acetylation*. *Journal of Biological Chemistry* 289(2) 895-908.
- Lazareva, A. A., G. Roman, W. Mattox, P. E. Hardin and B. Dauwalder (2007). A role for the adult fat body in *Drosophila* male courtship behavior. *PLoS Genet* 3(1) e16.
- Lázaro, D. F., M. C. Dias, A. Carija, S. Navarro, C. S. Madaleno, S. Tenreiro, S. Ventura and T. F. Outeiro (2016). The effects of the novel A53E alpha-synuclein mutation on its oligomerization and aggregation. *Acta neuropathologica communications* 4(1) 128-128.
- Lazaro, D. F., M. A. S. Pavlou and T. F. Outeiro (2017). Cellular models as tools for the study of the role of alpha-synuclein in Parkinson's disease. *Exp Neurol* 298(Pt B) 162-171.
- Lazaro, D. F., E. F. Rodrigues, R. Langohr, H. Shahpasandzadeh, T. Ribeiro, P. Guerreiro, E. Gerhardt, K. Krohnert, J. Klucken, M. D. Pereira, B. Popova, N. Kruse, B. Mollenhauer, S. O. Rizzoli, G. H. Braus, K. M. Danzer and T. F. Outeiro (2014). Systematic comparison of the effects of alpha-synuclein mutations on its oligomerization and aggregation. *PLoS Genet* 10(11) e1004741.
- Lebovitz, C., N. Wretham, M. Osooly, K. Milne, T. Dash, S. Thornton, B. Tessier-Cloutier, P. Sathiyaseelan, S. Bortnik, N. E. Go, E. Halvorsen, R. A. Cederberg, N. Chow, N. Dos Santos, K. L. Bennewith, B. H. Nelson, M. B. Bally, W. L. Lam and S. M. Gorski (2021). Loss of Parkinson's susceptibility gene LRRK2 promotes carcinogen-induced lung tumorigenesis. *Scientific Reports* 11(1) 2097.
- Lee, H., R. Flynn, I. Sharma, E. Haberman, P. J. Carling, F. J. Nicholls, M. Stegmann, J. Vowles, W. Haenseler, R. Wade-Martins, W. S. James and S. A. Cowley (2020). LRRK2 Is Recruited to Phagosomes and Co-recruits RAB8 and RAB10 in Human Pluripotent Stem Cell-Derived Macrophages. *Stem Cell Reports* 14(5) 940-955.
- Lee, J. H., J.-h. Han, H. Kim, S. M. Park, E.-h. Joe and I. Jou (2019). Parkinson's disease-associated LRRK2-G2019S mutant acts through regulation of SERCA activity to control ER stress in astrocytes. *Acta neuropathologica communications* 7(1) 68.
- Lee, S., H. P. Liu, W. Y. Lin, H. F. Guo and B. W. Lu (2010). LRRK2 Kinase Regulates Synaptic Morphology through Distinct Substrates at the Presynaptic and Postsynaptic Compartments of the *Drosophila* Neuromuscular Junction. *Journal of Neuroscience* 30(50) 16959-16969.
- Lee, S. B., W. Kim, S. Lee and J. Chung (2007). Loss of LRRK2/PARK8 induces degeneration of dopaminergic neurons in *Drosophila*. *Biochemical and Biophysical Research Communications* 358(2) 534-539.
- Lesage, S., A. Dürr, M. Tazir, E. Lohmann, A.-L. Leutenegger, S. Janin, P. Pollak and A. Brice (2006). LRRK2 G2019S as a Cause of Parkinson's Disease in North African Arabs. *New England Journal of Medicine* 354(4) 422-423.
- Leschziner, A. E. and S. L. Reck-Peterson (2021). Structural Biology of LRRK2 and its Interaction with Microtubules. *Mov Disord* 36(11) 2494-2504.
- Li, X., Q. J. Wang, N. Pan, S. Lee, Y. Zhao, B. T. Chait and Z. Yue (2011). Phosphorylation-dependent 14-3-3 binding to LRRK2 is impaired by common mutations of familial Parkinson's disease. *PLoS One* 6(3) e17153.

- Li, Y., W. Liu, T. F. Oo, L. Wang, Y. Tang, V. Jackson-Lewis, C. Zhou, K. Geghman, M. Bogdanov, S. Przedborski, M. F. Beal, R. E. Burke and C. Li (2009). Mutant LRRK2R1441G BAC transgenic mice recapitulate cardinal features of Parkinson's disease. *Nature Neuroscience* 12(7) 826-828.
- Lin, C.-H., H. Li, Y.-N. Lee, Y.-J. Cheng, R.-M. Wu and C.-T. Chien (2015). Lrrk regulates the dynamic profile of dendritic Golgi outposts through the golgin Lava lamp. *The Journal of cell biology* 210(3) 471-483.
- Lin, C. H., P. I. Tsai, R. M. Wu and C. T. Chien (2010). LRRK2 G2019S mutation induces dendrite degeneration through mislocalization and phosphorylation of tau by recruiting autoactivated GSK3 β . *J Neurosci* 30(39) 13138-13149.
- Liu, Z., X. Y. Wang, Y. Yu, X. P. Li, T. Wang, H. B. Jiang, Q. T. Ren, Y. C. Jiao, A. Sawa, T. Moran, C. A. Ross, C. Montell and W. W. Smith (2008). A Drosophila model for LRRK2-linked parkinsonism. *Proceedings of the National Academy of Sciences of the United States of America* 105(7) 2693-2698.
- Lloyd, V., M. Ramaswami and H. Kramer (1998). Not just pretty eyes: Drosophila eye-colour mutations and lysosomal delivery. *Trends Cell Biol* 8(7) 257-259.
- Lo, M. V. and W. L. Pak (1981). Light-induced pigment granule migration in the reticular cells of Drosophila melanogaster. Comparison of wild type with ERG-defective mutants. *The Journal of general physiology* 77(2) 155-175.
- Lobbestael, E., L. Civiero, T. De Wit, J. M. Taymans, E. Greggio and V. Baekelandt (2016). Pharmacological LRRK2 kinase inhibition induces LRRK2 protein destabilization and proteasomal degradation. *Scientific Reports* 6.
- Lobbestael, E., J. Zhao, Iakov N. Rudenko, A. Beylina, F. Gao, J. Wetter, M. Beullens, M. Bollen, Mark R. Cookson, V. Baekelandt, R. J. Nichols and J.-M. Taymans (2013). Identification of protein phosphatase 1 as a regulator of the LRRK2 phosphorylation cycle. *Biochemical Journal* 456(1) 119-128.
- Lozano, A. M. and N. Lipsman (2013). Probing and regulating dysfunctional circuits using deep brain stimulation. *Neuron* 77(3) 406-424.
- Ma, J., J. Gao, J. Wang and A. Xie (2019). Prion-Like Mechanisms in Parkinson's Disease. *Frontiers in Neuroscience* 13(552).
- Mackenzie, S. M., M. R. Brooker, T. R. Gill, G. B. Cox, A. J. Howells and G. D. Ewart (1999). Mutations in the white gene of Drosophila melanogaster affecting ABC transporters that determine eye colouration. *Biochimica et Biophysica Acta (BBA) - Biomembranes* 1419(2) 173-185.
- MacLeod, D. A., H. Rhinn, T. Kuwahara, A. Zolin, G. Di Paolo, B. D. McCabe, K. S. Marder, L. S. Honig, L. N. Clark, S. A. Small and A. Abeliovich (2013). RAB7L1 interacts with LRRK2 to modify intraneuronal protein sorting and Parkinson's disease risk. *Neuron* 77(3) 425-439.
- Maddison, D. C., M. Alfonso-Núñez, A. M. Swaih, C. Breda, S. Campesan, N. Allcock, A. Straatman-Iwanowska, C. P. Kyriacou and F. Giorgini (2020). A novel role for kynurenine 3-monooxygenase in mitochondrial dynamics. *PLoS genetics* 16(11) e1009129-e1009129.
- Maddison, D. C. and F. Giorgini (2015). The kynurenine pathway and neurodegenerative disease. *Seminars in Cell & Developmental Biology* 40 134-141.
- Mahabadi, N. and Y. Al Khalili (2020). Neuroanatomy, Retina. StatPearls Publishing, Treasure Island (FL).

- Mamais, A., R. Chia, A. Beilina, D. N. Hauser, C. Hall, P. A. Lewis, M. R. Cookson and R. Bandopadhyay (2014). Arsenite Stress Down-regulates Phosphorylation and 14-3-3 Binding of Leucine-rich Repeat Kinase 2 (LRRK2), Promoting Self-association and Cellular Redistribution*. *Journal of Biological Chemistry* 289(31) 21386-21400.
- Mamais, A., C. Manzoni, I. Nazish, C. Arber, B. Sonustun, S. Wray, T. T. Warner, M. R. Cookson, P. A. Lewis and R. Bandopadhyay (2018). Analysis of macroautophagy related proteins in G2019S LRRK2 Parkinson's disease brains with Lewy body pathology. *Brain Res* 1701 75-84.
- Manohar, S. G. and M. Husain (2015). Reduced pupillary reward sensitivity in Parkinson's disease. *npj Parkinson's Disease* 1(1) 15026.
- Marchand, A., M. Drouyer, A. Sarchione, M.-C. Chartier-Harlin and J.-M. Taymans (2020). LRRK2 Phosphorylation, More Than an Epiphenomenon. *Frontiers in Neuroscience* 14(527).
- Marín, I., W. N. van Egmond and P. J. M. van Haastert (2008). The Roco protein family: a functional perspective. *The FASEB Journal* 22(9) 3103-3110.
- Marras, C., A. Lang, B. P. van de Warrenburg, C. M. Sue, S. J. Tabrizi, L. Bertram, S. Mercimek-Mahmutoglu, D. Ebrahimi-Fakhari, T. T. Warner, A. Durr, B. Assmann, K. Lohmann, V. Kostic and C. Klein (2016). Nomenclature of genetic movement disorders: Recommendations of the international Parkinson and movement disorder society task force. *Movement Disorders* 31(4) 436-457.
- Marrocco, E., A. Indrieri, F. Esposito, V. Tarallo, A. Carboncino, F. G. Alvino, S. De Falco, B. Franco, M. De Risi and E. De Leonibus (2020). α -synuclein overexpression in the retina leads to vision impairment and degeneration of dopaminergic amacrine cells. *Scientific Reports* 10(1) 9619-9619.
- Marsden, C. D. (1961). Pigmentation in the nucleus substantiae nigrae of mammals. *J Anat* 95 256-261.
- Martin, I., L. Abalde-Atristain, J. W. Kim, T. M. Dawson and V. L. Dawson (2014a). Abberant protein synthesis in G2019S LRRK2 Drosophila Parkinson disease-related phenotypes. *Fly* 8(3) 165-169.
- Martin, I., J. W. Kim, B. D. Lee, H. C. Kang, J. C. Xu, H. Jia, J. Stankowski, M. S. Kim, J. Zhong, M. Kumar, S. A. Andrabi, Y. Xiong, D. W. Dickson, Z. K. Wszolek, A. Pandey, T. M. Dawson and V. L. Dawson (2014b). Ribosomal protein s15 phosphorylation mediates LRRK2 neurodegeneration in Parkinson's disease. *Cell* 157(2) 472-485.
- Masland, R. H. (2012a). The neuronal organization of the retina. *Neuron* 76(2) 266-280.
- Masland, R. H. (2012b). The tasks of amacrine cells. *Visual neuroscience* 29(1) 3-9.
- Mata, I. F., J. M. Kachergus, J. P. Taylor, S. Lincoln, J. Aasly, T. Lynch, M. M. Hulihan, S. A. Cobb, R.-M. Wu, C.-S. Lu, C. Lahoz, Z. K. Wszolek and M. J. Farrer (2005). Lrrk2 pathogenic substitutions in Parkinson's disease. *Neurogenetics* 6(4) 171-177.
- Matsuda, W., T. Furuta, K. C. Nakamura, H. Hioki, F. Fujiyama, R. Arai and T. Kaneko (2009). Single nigrostriatal dopaminergic neurons form widely spread and highly dense axonal arborizations in the neostriatum. *J Neurosci* 29(2) 444-453.
- Matta, S., K. Van Kolen, R. da Cunha, G. van den Bogaart, W. Mandemakers, K. Miskiewicz, P. J. De Bock, V. A. Morais, S. Vilain, D. Haddad, L. Delbroek, J. Swerts, L. Chávez-Gutiérrez, G. Esposito, G. Daneels, E. Karran, M. Holt, K. Gevaert, D. W.

- Moechars, B. De Strooper and P. Verstreken (2012). LRRK2 controls an EndoA phosphorylation cycle in synaptic endocytosis. *Neuron* 75(6) 1008-1021.
- McCormack, A. L., M. Thiruchelvam, A. B. Manning-Bog, C. Thiffault, J. W. Langston, D. A. Cory-Slechta and D. A. Di Monte (2002). Environmental risk factors and Parkinson's disease: selective degeneration of nigral dopaminergic neurons caused by the herbicide paraquat. *Neurobiol Dis* 10(2) 119-127.
- McGurk, L., A. Berson and N. M. Bonini (2015). Drosophila as an In Vivo Model for Human Neurodegenerative Disease. *Genetics* 201(2) 377-402.
- McLean, J. R., S. Krishnakumar and J. M. O'Donnell (1993). Multiple mRNAs from the Punch locus of *Drosophila melanogaster* encode isoforms of GTP cyclohydrolase I with distinct N-terminal domains. *The Journal of biological chemistry* 268(36) 27191-27197.
- Meng, T., Z. H. Zheng, T. T. Liu and L. Lin (2012). Contralateral retinal dopamine decrease and melatonin increase in progression of hemiparkinsonium rat. *Neurochem Res* 37(5) 1050-1056.
- Menzies, F. M., S. C. Yenissetti and K. T. Min (2005). Roles of *Drosophila* DJ-1 in survival of dopaminergic neurons and oxidative stress. *Curr Biol* 15(17) 1578-1582.
- Mestre-Francés, N., N. Serratrice, A. Gennetier, G. Devau, S. Cobo, S. G. Trouche, P. Fontès, C. Zussy, P. De Deurwaerdere, S. Salinas, F. J. Mennechet, J. Dusonchet, B. L. Schneider, I. Saggio, V. Kalatzis, M. R. Luquin-Piudo, J.-M. Verdier and E. J. Kremer (2018). Exogenous LRRK2G2019S induces parkinsonian-like pathology in a nonhuman primate. *JCI insight* 3(14) e98202.
- Meulener, M., A. J. Whitworth, C. E. Armstrong-Gold, P. Rizzu, P. Heutink, P. D. Wes, L. J. Pallanck and N. M. Bonini (2005). *Drosophila* DJ-1 mutants are selectively sensitive to environmental toxins associated with Parkinson's disease. *Curr Biol* 15(17) 1572-1577.
- Micieli, G., C. Tassorelli, E. Martignoni, C. Pacchetti, P. Bruggi, M. Magri and G. Nappi (1991). Disordered pupil reactivity in Parkinson's disease. *Clin Auton Res* 1(1) 55-58.
- Miller, G. V., K. N. Hansen and W. S. Stark (1981). Phototaxis in *Drosophila*: R1-6 input and interaction among ocellar and compound eye receptors. *Journal of Insect Physiology* 27(11) 813-819.
- Montell, C. (2012). *Drosophila* visual transduction. *Trends in Neurosciences* 35(6) 356-363.
- Moon, H. E. and S. H. Paek (2015). Mitochondrial Dysfunction in Parkinson's Disease. *Experimental Neurobiology* 24(2) 103-116.
- Mortiboys, H., R. Furnston, G. Bronstad, J. Aasly, C. Elliott and O. Bandmann (2015). UDCA exerts beneficial effect on mitochondrial dysfunction in LRRK2(G2019S) carriers and in vivo. *Neurology* 85(10) 846-852.
- Muda, K., D. Bertinetti, F. Gesellchen, J. S. Hermann, F. von Zweyendorf, A. Geerlof, A. Jacob, M. Ueffing, C. J. Gloeckner and F. W. Herberg (2014). Parkinson-related LRRK2 mutation R1441C/G/H impairs PKA phosphorylation of LRRK2 and disrupts its interaction with 14-3-3. *Proceedings of the National Academy of Sciences* 111(1) E34-E43.
- Muhammed, K., S. Manohar, M. Ben Yehuda, T. T.-J. Chong, G. Tofaris, G. Lennox, M. Bogdanovic, M. Hu and M. Husain (2016). Reward sensitivity deficits modulated by dopamine are associated with apathy in Parkinson's disease. *Brain* 139(10) 2706-2721.

- Murphy, P. R., I. H. Robertson, J. H. Balsters and R. G. O'Connell (2011). Pupillometry and P3 index the locus coeruleus–noradrenergic arousal function in humans. *Psychophysiology* 48(11) 1532-1543.
- Nagaraj, R. and U. Banerjee (2007). Combinatorial signaling in the specification of primary pigment cells in the Drosophila eye. *Development* 134(5) 825-831.
- Nagatsu, T., A. Nakashima, H. Watanabe, S. Ito and K. Wakamatsu (2022). Neuromelanin in Parkinson's Disease: Tyrosine Hydroxylase and Tyrosinase. *Int J Mol Sci* 23(8).
- Nalls, M. A., N. Pankratz, C. M. Lill, C. B. Do, D. G. Hernandez, M. Saad, A. L. DeStefano, E. Kara, J. Bras, M. Sharma, C. Schulte, M. F. Keller, S. Arepalli, C. Letson, C. Edsall, H. Stefansson, X. Liu, H. Pliner, J. H. Lee, R. Cheng, M. A. Ikram, J. P. Ioannidis, G. M. Hadjigeorgiou, J. C. Bis, M. Martinez, J. S. Perlmutter, A. Goate, K. Marder, B. Fiske, M. Sutherland, G. Xiromerisiou, R. H. Myers, L. N. Clark, K. Stefansson, J. A. Hardy, P. Heutink, H. Chen, N. W. Wood, H. Houlden, H. Payami, A. Brice, W. K. Scott, T. Gasser, L. Bertram, N. Eriksson, T. Foroud and A. B. Singleton (2014). Large-scale meta-analysis of genome-wide association data identifies six new risk loci for Parkinson's disease. *Nature genetics* 46(9) 989-993.
- Neriec, N. and C. Desplan (2016). From the Eye to the Brain: Development of the Drosophila Visual System. *Essays on Developmental Biology, Pt A* 116 247-+.
- Ng, C. H., S. Z. Mok, C. Koh, X. Ouyang, M. L. Fivaz, E. K. Tan, V. L. Dawson, T. M. Dawson, F. Yu and K. L. Lim (2009). Parkin protects against LRRK2 G2019S mutant-induced dopaminergic neurodegeneration in Drosophila. *J Neurosci* 29(36) 11257-11262.
- Nguyen, M. and D. Krainc (2018). LRRK2 phosphorylation of auxilin mediates synaptic defects in dopaminergic neurons from patients with Parkinson's disease. *Proceedings of the National Academy of Sciences of the United States of America* 115(21) 5576-5581.
- Nguyen-Legros, J. (1988). Functional neuroarchitecture of the retina: hypothesis on the dysfunction of retinal dopaminergic circuitry in Parkinson's disease. *Surg Radiol Anat* 10(2) 137-144.
- Nichols, R. J., N. Dzamko, N. A. Morrice, D. G. Campbell, M. Deak, A. Ordureau, T. Macartney, Y. R. Tong, J. Shen, A. R. Prescott and D. R. Alessi (2010). 14-3-3 binding to LRRK2 is disrupted by multiple Parkinson's disease-associated mutations and regulates cytoplasmic localization. *Biochemical Journal* 430 393-404.
- Nichols, W. C., N. Pankratz, D. Hernandez, C. Paisan-Ruiz, S. Jain, C. A. Halter, V. E. Michaels, T. Reed, A. Rudolph, C. W. Shults, A. Singleton, T. Foroud and P. i. Parkinson Study Group (2005). Genetic screening for a single common LRRK2 mutation in familial Parkinson's disease. *Lancet* 365(9457) 410-412.
- Nippe, O. M., A. R. Wade, C. J. H. Elliott and S. Chawla (2017). Circadian Rhythms in Visual Responsiveness in the Behaviorally Arrhythmic Drosophila Clock Mutant Clk(Jrk). *Journal of biological rhythms* 32(6) 583-592.
- Noyce, A. J., J. P. Bestwick, L. Silveira-Moriyama, C. H. Hawkes, G. Giovannoni, A. J. Lees and A. Schrag (2012). Meta-analysis of early nonmotor features and risk factors for Parkinson disease. *Annals of Neurology* 72(6) 893-901.
- Obeso, J. A., M. Stamelou, C. G. Goetz, W. Poewe, A. E. Lang, D. Weintraub, D. Burn, G. M. Halliday, E. Bezard, S. Przedborski, S. Lehericy, D. J. Brooks, J. C. Rothwell, M. Hallett, M. R. DeLong, C. Marras, C. M. Tanner, G. W. Ross, J. W. Langston, C.

- Klein, V. Bonifati, J. Jankovic, A. M. Lozano, G. Deuschl, H. Bergman, E. Tolosa, M. Rodriguez-Violante, S. Fahn, R. B. Postuma, D. Berg, K. Marek, D. G. Standaert, D. J. Surmeier, C. W. Olanow, J. H. Kordower, P. Calabresi, A. H. V. Schapira and A. J. Stoessl (2017). Past, present, and future of Parkinson's disease: A special essay on the 200th Anniversary of the Shaking Palsy. *Mov Disord* 32(9) 1264-1310.
- Ohta, E., Y. Katayama, F. Kawakami, M. Yamamoto, K. Tajima, T. Maekawa, N. Iida, S. Hattori and F. Obata (2009). I2020T leucine-rich repeat kinase 2, the causative mutant molecule of familial Parkinson's disease, has a higher intracellular degradation rate than the wild-type molecule. *Biochemical and Biophysical Research Communications* 390(3) 710-715.
- Onofrj, M. and I. Bodis-Wollner (1982). Dopaminergic deficiency causes delayed visual evoked potentials in rats. *Ann Neurol* 11(5) 484-490.
- Orenstein, S. J., S.-H. Kuo, I. Tasset, E. Arias, H. Koga, I. Fernandez-Carasa, E. Cortes, L. S. Honig, W. Dauer, A. Consiglio, A. Raya, D. Sulzer and A. M. Cuervo (2013). Interplay of LRRK2 with chaperone-mediated autophagy. *Nature Neuroscience* 16(4) 394-406.
- Ortuño-Lizarán, I., T. G. Beach, G. E. Serrano, D. G. Walker, C. H. Adler and N. Cuenca (2018). Phosphorylated α -synuclein in the retina is a biomarker of Parkinson's disease pathology severity. *Mov Disord* 33(8) 1315-1324.
- Osterwalder, T., K. S. Yoon, B. H. White and H. Keshishian (2001). A conditional tissue-specific transgene expression system using inducible GAL4. *Proc Natl Acad Sci U S A* 98(22) 12596-12601.
- Ozelius, L. J., G. Senthil, R. Saunders-Pullman, E. Ohmann, A. Deligtisch, M. Tagliati, A. L. Hunt, C. Klein, B. Henick, S. M. Hailpern, R. B. Lipton, J. Soto-Valencia, N. Risch and S. B. Bressman (2006). LRRK2 G2019S as a Cause of Parkinson's Disease in Ashkenazi Jews. *New England Journal of Medicine* 354(4) 424-425.
- Pacelli, C., N. Giguère, M. J. Bourque, M. Lévesque, R. S. Slack and L. Trudeau (2015). Elevated Mitochondrial Bioenergetics and Axonal Arborization Size Are Key Contributors to the Vulnerability of Dopamine Neurons. *Curr Biol* 25(18) 2349-2360.
- Paisán-Ruíz, C., S. Jain, E. W. Evans, W. P. Gilks, J. Simón, M. van der Brug, A. López de Munain, S. Aparicio, A. M. Gil, N. Khan, J. Johnson, J. R. Martinez, D. Nicholl, I. Martí Carrera, A. S. Pena, R. de Silva, A. Lees, J. F. Martí-Massó, J. Pérez-Tur, N. W. Wood and A. B. Singleton (2004). Cloning of the gene containing mutations that cause PARK8-linked Parkinson's disease. *Neuron* 44(4) 595-600.
- Pan, P.-Y., X. Li, J. Wang, J. Powell, Q. Wang, Y. Zhang, Z. Chen, B. Wicinski, P. Hof, T. A. Ryan and Z. Yue (2017). Parkinson's Disease-Associated LRRK2 Hyperactive Kinase Mutant Disrupts Synaptic Vesicle Trafficking in Ventral Midbrain Neurons. *The Journal of neuroscience : the official journal of the Society for Neuroscience* 37(47) 11366-11376.
- Pankratz, N., G. W. Beecham, A. L. DeStefano, T. M. Dawson, K. F. Doheny, S. A. Factor, T. H. Hamza, A. Y. Hung, B. T. Hyman, A. J. Iverson, D. Krainc, J. C. Latourelle, L. N. Clark, K. Marder, E. R. Martin, R. Mayeux, O. A. Ross, C. R. Scherzer, D. K. Simon, C. Tanner, J. M. Vance, Z. K. Wszolek, C. P. Zabetian, R. H. Myers, H. Payami, W. K. Scott and T. Foroud (2012). Meta-analysis of Parkinson's disease: identification of a novel locus, RIT2. *Ann Neurol* 71(3) 370-384.
- Park, S., J. Kim, J. Chun, K. Han, H. Soh, E. A. Kang, H. J. Lee, J. P. Im and J. S. Kim (2019). Patients with Inflammatory Bowel Disease Are at an Increased Risk of

- Parkinson's Disease: A South Korean Nationwide Population-Based Study. *Journal of Clinical Medicine* 8(8) 1191.
- Park, Y. S., J. H. Kim, K. B. Jacobson and J. J. Yim (1990). Purification and characterization of 6-pyruvoyl-tetrahydropterin synthase from *Drosophila melanogaster*. *Biochimica et Biophysica Acta (BBA) - Protein Structure and Molecular Enzymology* 1038(2) 186-194.
- Parkinson'sUK. (2018). *The incidence and prevalence of Parkinson's in the UK report [online]*. Available at: www.parkinsons.org.uk.
- Pastink, A., A. P. Schalet, C. Vreeken, E. Paradi and J. C. Eeken (1987). The nature of radiation-induced mutations at the white locus of *Drosophila melanogaster*. *Mutat Res* 177(1) 101-115.
- Paulk, A., S. S. Millard and B. van Swinderen (2013). Vision in *Drosophila*: Seeing the World Through a Model's Eyes. *Annual Review of Entomology, Vol 58* 58 313-332.
- Pellegrini, L., D. N. Hauser, Y. Li, A. Mamais, A. Beilina, R. Kumaran, A. Wetzel, J. Nixon-Abell, G. Heaton, I. Rudenko, M. Alkaslasi, N. Ivanina, H. L. Melrose, M. R. Cookson and K. Harvey (2018). Proteomic analysis reveals co-ordinated alterations in protein synthesis and degradation pathways in LRRK2 knockout mice. *Human Molecular Genetics* 27(18) 3257-3271.
- Periquet, M., T. Fulga, L. Myllykangas, M. G. Schlossmacher and M. B. Feany (2007). Aggregated alpha-synuclein mediates dopaminergic neurotoxicity in vivo. *J Neurosci* 27(12) 3338-3346.
- Petridi, S. (2017). *The Role of LRRK2 in The Pathogenesis of Parkinson's Disease. Biology*. University of York. 259.
- Petridi, S., C. A. Middleton, C. Ugbo, A. Fellgett, L. Covill and C. J. H. Elliott (2020). In Vivo Visual Screen for Dopaminergic Rab ↔ LRRK2-G2019S Interactions in *Drosophila* Discriminates Rab10 from Rab3. *G3 Genes|Genomes|Genetics* 10(6) 1903-1914.
- Pfeiffer, R. F. (2016). Non-motor symptoms in Parkinson's disease. *Parkinsonism & Related Disorders* 22 S119-S122.
- Piao, J., S. Zabierowski, B. N. Dubose, E. J. Hill, M. Navare, N. Claros, S. Rosen, K. Ramnarine, C. Horn, C. Fredrickson, K. Wong, B. Safford, S. Kriks, A. El Maarouf, U. Rutishauser, C. Henchcliffe, Y. Wang, I. Riviere, S. Mann, V. Bermudez, S. Irion, L. Studer, M. Tomishima and V. Tabar (2021). Preclinical Efficacy and Safety of a Human Embryonic Stem Cell-Derived Midbrain Dopamine Progenitor Product, MSK-DA01. *Cell Stem Cell* 28(2) 217-229.e217.
- Pickrell, Alicia M. and Richard J. Youle (2015). The Roles of PINK1, Parkin, and Mitochondrial Fidelity in Parkinson's Disease. *Neuron* 85(2) 257-273.
- Pingale, T. and G. L. Gupta (2020). Classic and evolving animal models in Parkinson's disease. *Pharmacol Biochem Behav* 199 173060.
- Placidi, F., F. Izzi, A. Romigi, P. Stanzione, M. G. Marciani, L. Brusa, F. Sperli, S. Galati, P. Pasqualetti and M. Pierantozzi (2008). Sleep-wake cycle and effects of cabergoline monotherapy in de novo Parkinson's disease patients. *Journal of Neurology* 255(7) 1032-1037.
- Pollak, P., A. L. Benabid, C. Gross, D. M. Gao, A. Laurent, A. Benazzouz, D. Hoffmann, M. Gentil and J. Perret (1993). Effects of the stimulation of the subthalamic nucleus in Parkinson disease. *Rev Neurol (Paris)* 149(3) 175-176.

- Polymeropoulos, M. H., C. Lavedan, E. Leroy, S. E. Ide, A. Dehejia, A. Dutra, B. Pike, H. Root, J. Rubenstein, R. Boyer, E. S. Stenroos, S. Chandrasekharappa, A. Athanassiadou, T. Papapetropoulos, W. G. Johnson, A. M. Lazzarini, R. C. Duvoisin, G. Di Iorio, L. I. Golbe and R. L. Nussbaum (1997). Mutation in the alpha-synuclein gene identified in families with Parkinson's disease. *Science* 276(5321) 2045-2047.
- Price, M. J., R. G. Feldman, D. Adelberg and H. Kayne (1992). Abnormalities in color vision and contrast sensitivity in Parkinson's disease. *Neurology* 42(4) 887-890.
- Purves, D., G. Augustine, D. Fitzpatrick, L. Katz, A. LaMantia, J. McNamara and S. Williams (2001). Neuroscience. 2nd edition. Sunderland (MA): Sinauer Associates.
- Pyza, E. and I. A. Meinertzhagen (1999). Daily rhythmic changes of cell size and shape in the first optic neuropil in *Drosophila melanogaster*. *J Neurobiol* 40(1) 77-88.
- Quinn, P. M. J., P. I. Moreira, A. F. Ambrósio and C. H. Alves (2020). PINK1/PARKIN signalling in neurodegeneration and neuroinflammation. *Acta neuropathologica communications* 8(1) 189.
- Ramon y Cajal, S. and D. Sanchez (1915). Contribución al conocimiento de los centros nerviosos de los insectos. *Trab. Lab. Invest. Biol.* 13 1-68.
- Recasens, A., B. Dehay, J. Bove, I. Carballo-Carbajal, S. Dovero, A. Perez-Villalba, P. O. Fernagut, J. Blesa, A. Parent, C. Perier, I. Farinas, J. A. Obeso, E. Bezard and M. Vila (2014). Lewy body extracts from Parkinson disease brains trigger alpha-synuclein pathology and neurodegeneration in mice and monkeys. *Ann Neurol* 75(3) 351-362.
- Reiter, L. T., L. Potocki, S. Chien, M. Gribskov and E. Bier (2001). A systematic analysis of human disease-associated gene sequences in *Drosophila melanogaster*. *Genome research* 11(6) 1114-1125.
- Rideout, H. J., M.-C. Chartier-Harlin, M. J. Fell, W. D. Hirst, S. Huntwork-Rodriguez, C. E. G. Leyns, O. S. Mabrouk and J.-M. Taymans (2020). The Current State-of-the Art of LRRK2-Based Biomarker Assay Development in Parkinson's Disease. *Frontiers in Neuroscience* 14(865).
- Roote, J. and A. Prokop (2013). How to design a genetic mating scheme: a basic training package for *Drosophila* genetics. *G3 (Bethesda)* 3(2) 353-358.
- Ross, O. A., A. I. Soto-Ortolaza, M. G. Heckman, J. O. Aasly, N. Abahuni, G. Annesi, J. A. Bacon, S. Bardiën, M. Bozi, A. Brice, L. Brighina, C. Van Broeckhoven, J. Carr, M.-C. Chartier-Harlin, E. Dardiotis, D. W. Dickson, N. N. Diehl, A. Elbaz, C. Ferrarese, A. Ferraris, B. Fiske, J. M. Gibson, R. Gibson, G. M. Hadjigeorgiou, N. Hattori, J. P. A. Ioannidis, B. Jasinska-Myga, B. S. Jeon, Y. J. Kim, C. Klein, R. Kruger, E. Kyrtzi, S. Lesage, C.-H. Lin, T. Lynch, D. M. Maraganore, G. D. Mellick, E. Mutez, C. Nilsson, G. Opala, S. S. Park, A. Puschmann, A. Quattrone, M. Sharma, P. A. Silburn, Y. H. Sohn, L. Stefanis, V. Tadic, J. Theuns, H. Tomiyama, R. J. Uitti, E. M. Valente, S. van de Loo, D. K. Vassilatis, C. Vilariño-Güell, L. R. White, K. Wirdefeldt, Z. K. Wszolek, R.-M. Wu, M. J. Farrer and C. Genetic Epidemiology Of Parkinson's Disease (2011). Association of LRRK2 exonic variants with susceptibility to Parkinson's disease: a case-control study. *The Lancet. Neurology* 10(10) 898-908.
- Rudenko, I. N., A. Kaganovich, R. G. Langston, A. Beilina, K. Ndukwe, R. Kumaran, A. A. Dillman, R. Chia and M. R. Cookson (2017). The G2385R risk factor for Parkinson's disease enhances CHIP-dependent intracellular degradation of LRRK2. *Biochemical Journal* 474(9) 1547-1558.
- Ruiz-Martínez, J., A. Gorostidi, B. Ibañez, A. Alzualde, D. Otaegui, F. Moreno, A. López de Munain, A. Bergareche, J. C. Gómez-Esteban and J. F. Martí Massó (2010).

- Penetrance in Parkinson's disease related to the LRRK2 R1441G mutation in the Basque country (Spain). *Mov Disord* 25(14) 2340-2345.
- Salcedo, E., A. Huber, S. Henrich, L. V. Chadwell, W.-H. Chou, R. Paulsen and S. G. Britt (1999). Blue- and Green-Absorbing Visual Pigments of *Drosophila*: Ectopic Expression and Physiological Characterization of the R8 Photoreceptor Cell-Specific Rh5 and Rh6 Rhodopsins. *The Journal of Neuroscience* 19(24) 10716-10726.
- Sandyk, R. (1992). Accelerated growth of malignant melanoma by levodopa in Parkinson's disease and role of the pineal gland. *Int J Neurosci* 63(1-2) 137-140.
- Sanes, J. R. and S. L. Zipursky (2010). Design principles of insect and vertebrate visual systems. *Neuron* 66(1) 15-36.
- Sang, T.-K. and G. R. Jackson (2005). *Drosophila* models of neurodegenerative disease. *NeuroRx : the journal of the American Society for Experimental NeuroTherapeutics* 2(3) 438-446.
- Santos, S. F., H. L. de Oliveira, E. S. Yamada, B. C. Neves and A. Pereira (2019). The Gut and Parkinson's Disease—A Bidirectional Pathway. *Frontiers in Neurology* 10.
- Sanyal, A., M. P. DeAndrade, H. S. Novis, S. Lin, J. Chang, N. Lengacher, J. J. Tomlinson, M. G. Tansey and M. J. LaVoie (2020). Lysosome and Inflammatory Defects in GBA1-Mutant Astrocytes Are Normalized by LRRK2 Inhibition. *Mov Disord* 35(5) 760-773.
- Schaffner, A., X. Li, Y. Gomez-Llorente, E. Leandrou, A. Memou, N. Clemente, C. Yao, F. Afsari, L. Zhi, N. Pan, K. Morohashi, X. Hua, M. M. Zhou, C. Wang, H. Zhang, S. G. Chen, C. J. Elliott, H. Rideout, I. Ubarretxena-Belandia and Z. Yue (2019). Vitamin B(12) modulates Parkinson's disease LRRK2 kinase activity through allosteric regulation and confers neuroprotection. *Cell Res* 29(4) 313-329.
- Schapira, A. H., J. M. Cooper, D. Dexter, J. B. Clark, P. Jenner and C. D. Marsden (1990). Mitochondrial complex I deficiency in Parkinson's disease. *J Neurochem* 54(3) 823-827.
- Schmitz, G. and G. Müller (1991). Structure and function of lamellar bodies, lipid-protein complexes involved in storage and secretion of cellular lipids. *Journal of Lipid Research* 32(10) 1539-1570.
- Scholz, D., D. Pörtl, A. Genewsky, M. Weng, T. Waldmann, S. Schildknecht and M. Leist (2011). Rapid, complete and large-scale generation of post-mitotic neurons from the human LUHMES cell line. *Journal of Neurochemistry* 119(5) 957-971.
- Searles, L. L. and R. A. Voelker (1986). Molecular characterization of the *Drosophila* vermilion locus and its suppressible alleles. *Proceedings of the National Academy of Sciences of the United States of America* 83(2) 404-408.
- Sega, G. A. (1984). A review of the genetic effects of ethyl methanesulfonate. *Mutat Res* 134(2-3) 113-142.
- Shen, L. (2015). Associations between B Vitamins and Parkinson's Disease. *Nutrients* 7(9) 7197-7208.
- Shimada, T., A. E. Fournier and K. Yamagata (2013). Neuroprotective Function of 14-3-3 Proteins in Neurodegeneration. *BioMed Research International* 2013 564534.
- Shin, N., H. Jeong, J. Kwon, H. Y. Heo, J. J. Kwon, H. J. Yun, C. H. Kim, B. S. Han, Y. Tong, J. Shen, T. Hatano, N. Hattori, K. S. Kim, S. Chang and W. Seol (2008). LRRK2 regulates synaptic vesicle endocytosis. *Exp Cell Res* 314(10) 2055-2065.

- Shoup, J. R. (1966). The development of pigment granules in the eyes of wild type and mutant *Drosophila melanogaster*. *J Cell Biol* 29(2) 223-249.
- Simón-Sánchez, J., J.-F. Martí-Massó, J. V. Sánchez-Mut, C. Paisán-Ruiz, A. Martínez-Gil, J. Ruiz-Martínez, A. Sáenz, A. B. Singleton, A. López de Munain and J. Pérez-Tur (2006). Parkinson's disease due to the R1441G mutation in Dardarin: A founder effect in the basques. *Movement Disorders* 21(11) 1954-1959.
- Singh, R. K., A. Soliman, G. Guaitoli, E. Störmer, F. v. Zweyendorf, T. D. Maso, A. Oun, L. V. Rillaer, S. H. Schmidt, D. Chatterjee, J. A. David, E. Pardon, T. U. Schwartz, S. Knapp, E. J. Kennedy, J. Steyaert, F. W. Herberg, A. Kortholt, C. J. Gloeckner and W. Versées (2022). Nanobodies as allosteric modulators of Parkinson's disease associated LRRK2. *Proceedings of the National Academy of Sciences* 119(9) e2112712119.
- Skipper, L., K. Wilkes, M. Toft, M. Baker, S. Lincoln, M. Hulihan, O. A. Ross, M. Hutton, J. Aasly and M. Farrer (2004). Linkage disequilibrium and association of MAPT H1 in Parkinson disease. *Am J Hum Genet* 75(4) 669-677.
- Smith, G. A., J. Jansson, E. M. Rocha, T. Osborn, P. J. Hallett and O. Isacson (2016). Fibroblast Biomarkers of Sporadic Parkinson's Disease and LRRK2 Kinase Inhibition. *Mol Neurobiol* 53(8) 5161-5177.
- Soliman, A., F. N. Cankara and A. Kortholt (2020). Allosteric inhibition of LRRK2, where are we now. *Biochem Soc Trans* 48(5) 2185-2194.
- Song, W., M. R. Smith, A. Syed, T. Lukacovich, B. A. Barbaro, J. Purcell, D. J. Bornemann, J. Burke and J. L. Marsh (2013). Morphometric Analysis of Huntington's Disease Neurodegeneration in *Drosophila*. In D. M. Hatters and A. J. Hannan eds. *Tandem Repeats in Genes, Proteins, and Disease: Methods and Protocols*. Totowa, NJ, Humana Press. 41-57.
- St Johnston, D. (2002). The art and design of genetic screens: *Drosophila melanogaster*. *Nature Reviews Genetics* 3(3) 176-188.
- Stafa, K., E. Tsika, R. Moser, A. Musso, L. Glauser, A. Jones, S. Biskup, Y. Xiong, R. Bandopadhyay, V. L. Dawson, T. M. Dawson and D. J. Moore (2014). Functional interaction of Parkinson's disease-associated LRRK2 with members of the dynamin GTPase superfamily. *Human Molecular Genetics* 23(8) 2055-2077.
- Stark, W. S. (1973). The effect of eye colour pigments on the action spectrum of *Drosophila*. *Journal of Insect Physiology* 19(5) 999-1006.
- Stavenga, D. G., M. F. Wehling and G. Belusic (2017). Functional interplay of visual, sensitizing and screening pigments in the eyes of *Drosophila* and other red-eyed dipteran flies. *J Physiol* 595(16) 5481-5494.
- Steger, M., F. Diez, H. S. Dhekne, P. Lis, R. S. Nirujogi, O. Karayel, F. Tonelli, T. N. Martinez, E. Lorentzen, S. R. Pfeffer, D. R. Alessi and M. Mann (2017). Systematic proteomic analysis of LRRK2-mediated Rab GTPase phosphorylation establishes a connection to ciliogenesis. *Elife* 6.
- Steger, M., F. Tonelli, G. Ito, P. Davies, M. Trost, M. Vetter, S. Wachter, E. Lorentzen, G. Duddy, S. Wilson, M. A. Baptista, B. K. Fiske, M. J. Fell, J. A. Morrow, A. D. Reith, D. R. Alessi and M. Mann (2016). Phosphoproteomics reveals that Parkinson's disease kinase LRRK2 regulates a subset of Rab GTPases. *Elife* 5.
- Steinert, J. R., S. Campesan, P. Richards, C. P. Kyriacou, I. D. Forsythe and F. Giorgini (2012). Rab11 rescues synaptic dysfunction and behavioural deficits in a *Drosophila* model of Huntington's disease. *Hum Mol Genet* 21(13) 2912-2922.

- Stergiou, V., D. Fotiou, D. Tsiptsios, B. Haidich, M. Nakou, C. Giantselidis and A. Karlovasitou (2009). Pupillometric findings in patients with Parkinson's disease and cognitive disorder. *Int J Psychophysiol* 72(2) 97-101.
- Stormo, A. E. D., F. Shavarebi, M. FitzGibbon, E. M. Earley, H. Ahrendt, L. S. Lum, E. Verschueren, D. L. Swaney, G. Skibinski, A. Ravisankar, J. van Haren, E. J. Davis, J. R. Johnson, J. Von Dollen, C. Balen, J. Porath, C. Crosio, C. Mirescu, C. Iaccarino, W. T. Dauer, R. J. Nichols, T. Wittmann, T. C. Cox, S. Finkbeiner, N. J. Krogan, S. A. Oakes and A. Hiniker (2022). The E3 ligase TRIM1 ubiquitinates LRRK2 and controls its localization, degradation, and toxicity. *J Cell Biol* 221(4).
- Summers, K. M., A. J. Howells and N. A. Pyliotis (1982). Biology of Eye Pigmentation in Insects. In M. J. Berridge, J. E. Treherne and V. B. Wigglesworth eds. *Advances in Insect Physiology*. Academic Press. 119-166.
- Sung, C.-H. and J.-Z. Chuang (2010). The cell biology of vision. *The Journal of cell biology* 190(6) 953-963.
- Takahashi, K. and S. Yamanaka (2006). Induction of pluripotent stem cells from mouse embryonic and adult fibroblast cultures by defined factors. *Cell* 126(4) 663-676.
- Tan, E. K., R. Peng, Y. Y. Teo, L. C. Tan, D. Angeles, P. Ho, M. L. Chen, C. H. Lin, X. Y. Mao, X. L. Chang, K. M. Prakash, J. J. Liu, W. L. Au, W. D. Le, J. Jankovic, J. M. Burgunder, Y. Zhao and R. M. Wu (2010). Multiple LRRK2 variants modulate risk of Parkinson disease: a Chinese multicenter study. *Hum Mutat* 31(5) 561-568.
- Tan, V. X. and G. J. Guillemin (2019). Kynurenine Pathway Metabolites as Biomarkers for Amyotrophic Lateral Sclerosis. *Frontiers in Neuroscience* 13(1013).
- Tanner, C. M., F. Kamel, G. W. Ross, J. A. Hoppin, S. M. Goldman, M. Korell, C. Marras, G. S. Bhudhikanok, M. Kasten, A. R. Chade, K. Comyns, M. B. Richards, C. Meng, B. Priestley, H. H. Fernandez, F. Cambi, D. M. Umbach, A. Blair, D. P. Sandler and J. W. Langston (2011). Rotenone, paraquat, and Parkinson's disease. *Environ Health Perspect* 119(6) 866-872.
- Tansey, M. G. and M. S. Goldberg (2010). Neuroinflammation in Parkinson's disease: its role in neuronal death and implications for therapeutic intervention. *Neurobiol Dis* 37(3) 510-518.
- Tao, Y., S. C. Vermilyea, M. Zammit, J. Lu, M. Olsen, J. M. Metzger, L. Yao, Y. Chen, S. Phillips, J. E. Holden, V. Bondarenko, W. F. Block, T. E. Barnhart, N. Schultz-Darken, K. Brunner, H. Simmons, B. T. Christian, M. E. Emborg and S.-C. Zhang (2021). Autologous transplant therapy alleviates motor and depressive behaviors in parkinsonian monkeys. *Nature Medicine* 27(4) 632-639.
- Tayebi, N., M. Callahan, V. Madike, B. K. Stubblefield, E. Orvisky, D. Krasnewich, J. J. Fillano and E. Sidransky (2001). Gaucher disease and parkinsonism: a phenotypic and genotypic characterization. *Mol Genet Metab* 73(4) 313-321.
- Taylor, J. P., M. M. Hulihan, J. M. Kachergus, H. L. Melrose, S. J. Lincoln, K. M. Hinkle, J. T. Stone, O. A. Ross, R. Hauser, J. Aasly, T. Gasser, H. Payami, Z. K. Wszolek and M. J. Farrer (2007). Leucine-rich repeat kinase 1: a paralog of LRRK2 and a candidate gene for Parkinson's disease. *Neurogenetics* 8(2) 95-102.
- Taymans, J.-M. and E. Greggio (2016). LRRK2 Kinase Inhibition as a Therapeutic Strategy for Parkinson's Disease, Where Do We Stand? *Current neuropharmacology* 14(3) 214-225.
- Thiruchelvam, M., B. J. Brockel, E. K. Richfield, R. B. Baggs and D. A. Cory-Slechta (2000). Potentiated and preferential effects of combined paraquat and maneb on

- nigrostriatal dopamine systems: environmental risk factors for Parkinson's disease? *Brain Res* 873(2) 225-234.
- Thomas, B. and M. F. Beal (2007). Parkinson's disease. *Human Molecular Genetics* 16(R2) R183-R194.
- Thomas, J. M., T. Li, W. Yang, F. Xue, P. S. Fishman and W. W. Smith (2016). 68 and FX2149 Attenuate Mutant LRRK2-R1441C-Induced Neural Transport Impairment. *Front Aging Neurosci* 8 337.
- Tieng, V., L. Stoppini, S. Villy, M. Fathi, M. Dubois-Dauphin and K. H. Krause (2014). Engineering of midbrain organoids containing long-lived dopaminergic neurons. *Stem Cells Dev* 23(13) 1535-1547.
- Tong, Z.-B., H. Hogberg, D. Kuo, S. Sakamuru, M. Xia, L. Smirnova, T. Hartung and D. Gerhold (2017). Characterization of three human cell line models for high-throughput neuronal cytotoxicity screening. *Journal of Applied Toxicology* 37(2) 167-180.
- Touchot, N., P. Chardin and A. Tavitian (1987). Four additional members of the ras gene superfamily isolated by an oligonucleotide strategy: molecular cloning of YPT-related cDNAs from a rat brain library. *Proc Natl Acad Sci U S A* 84(23) 8210-8214.
- Trancikova, A., A. Mamais, P. J. Webber, K. Stafa, E. Tsika, L. Glauser, A. B. West, R. Bandopadhyay and D. J. Moore (2012). Phosphorylation of 4E-BP1 in the mammalian brain is not altered by LRRK2 expression or pathogenic mutations. *PLoS One* 7(10) e47784.
- Trinh, J. and M. Farrer (2013). Advances in the genetics of Parkinson disease. *Nature Reviews Neurology* 9(8) 445-454.
- Uhl, G. R., J. C. Hedreen and D. L. Price (1985). Parkinson's disease: loss of neurons from the ventral tegmental area contralateral to therapeutic surgical lesions. *Neurology* 35(8) 1215-1218.
- Ungerstedt, U. (1968). 6-hydroxy-dopamine induced degeneration of central monoamine neurons. *European Journal of Pharmacology* 5(1) 107-110.
- Urwyler, P., T. Nef, A. Killen, D. Collerton, A. Thomas, D. Burn, I. McKeith and U. P. Mosimann (2014). Visual complaints and visual hallucinations in Parkinson's disease. *Parkinsonism & Related Disorders* 20(3) 318-322.
- Van der Perren, A., C. Van den Haute and V. Baekelandt (2015). Viral vector-based models of Parkinson's disease. *Curr Top Behav Neurosci* 22 271-301.
- Varazzani, C., A. San-Galli, S. Gilardeau and S. Bouret (2015). Noradrenaline and Dopamine Neurons in the Reward/Effort Trade-Off: A Direct Electrophysiological Comparison in Behaving Monkeys. *The Journal of Neuroscience* 35(20) 7866-7877.
- Vaz, R. L., T. F. Outeiro and J. J. Ferreira (2018). Zebrafish as an Animal Model for Drug Discovery in Parkinson's Disease and Other Movement Disorders: A Systematic Review. *Frontiers in Neurology* 9(347).
- Venderova, K., G. Kabbach, E. Abdel-Messih, Y. Zhang, R. J. Parks, Y. Imai, S. Gehrke, J. Ngsee, M. J. Lavoie, R. S. Slack, Y. Rao, Z. Zhang, B. Lu, M. E. Haque and D. S. Park (2009). Leucine-Rich Repeat Kinase 2 interacts with Parkin, DJ-1 and PINK-1 in a *Drosophila melanogaster* model of Parkinson's disease. *Hum Mol Genet* 18(22) 4390-4404.
- Videnovic, A. and D. Golombek (2013). Circadian and sleep disorders in Parkinson's disease. *Experimental Neurology* 243 45-56.

- Viola, A. U., L. M. James, L. J. Schlangen and D. J. Dijk (2008). Blue-enriched white light in the workplace improves self-reported alertness, performance and sleep quality. *Scand J Work Environ Health* 34(4) 297-306.
- Volpicelli-Daley, L. A., D. Kirik, L. E. Stoyka, D. G. Standaert and A. S. Harms (2016). How can rAAV- α -synuclein and the fibril α -synuclein models advance our understanding of Parkinson's disease? *Journal of Neurochemistry* 139(S1) 131-155.
- Wakamatsu, M., A. Ishii, S. Iwata, J. Sakagami, Y. Ukai, M. Ono, D. Kanbe, S. Muramatsu, K. Kobayashi, T. Iwatsubo and M. Yoshimoto (2008). Selective loss of nigral dopamine neurons induced by overexpression of truncated human alpha-synuclein in mice. *Neurobiol Aging* 29(4) 574-585.
- Wan, Q.-Y., R. Zhao and X.-T. Wu (2020). Older patients with IBD might have higher risk of Parkinson's disease. *Gut* 69(1) 193-194.
- Wang, D., B. Tang, G. Zhao, Q. Pan, K. Xia, R. Bodmer and Z. Zhang (2008a). Dispensable role of Drosophila ortholog of LRRK2 kinase activity in survival of dopaminergic neurons. *Molecular Neurodegeneration* 3 3-3.
- Wang, L., C. Xie, E. Greggio, L. Parisiadou, H. Shim, L. Sun, J. Chandran, X. Lin, C. Lai, W.-J. Yang, D. J. Moore, T. M. Dawson, V. L. Dawson, G. Chiosis, M. R. Cookson and H. Cai (2008b). The Chaperone Activity of Heat Shock Protein 90 Is Critical for Maintaining the Stability of Leucine-Rich Repeat Kinase 2. *The Journal of Neuroscience* 28(13) 3384-3391.
- Wang, S., Z. Liu, T. Ye, O. S. Mabrouk, T. Maltbie, J. Aasly and A. B. West (2017). Elevated LRRK2 autophosphorylation in brain-derived and peripheral exosomes in LRRK2 mutation carriers. *Acta neuropathologica communications* 5(1) 86.
- Warren, W. D., S. Palmer and A. J. Howells (1996). Molecular characterization of the cinnabar region of Drosophila melanogaster: identification of the cinnabar transcription unit. *Genetica* 98(3) 249-262.
- Watson, M. R., R. D. Lagow, K. Xu, B. Zhang and N. M. Bonini (2008). A drosophila model for amyotrophic lateral sclerosis reveals motor neuron damage by human SOD1. *The Journal of biological chemistry* 283(36) 24972-24981.
- Waxman, E. A. and B. I. Giasson (2009). Molecular mechanisms of alpha-synuclein neurodegeneration. *Biochim Biophys Acta* 1792(7) 616-624.
- Weil, R. S., A. E. Schrag, J. D. Warren, S. J. Crutch, A. J. Lees and H. R. Morris (2016). Visual dysfunction in Parkinson's disease. *Brain* 139(11) 2827-2843.
- Weiss, K. R., Y. Kimura, W.-C. M. Lee and J. T. Littleton (2012). Huntingtin aggregation kinetics and their pathological role in a Drosophila Huntington's disease model. *Genetics* 190(2) 581-600.
- West, R. J. H., R. Furmston, C. A. C. Williams and C. J. H. Elliott (2015a). Neurophysiology of Drosophila models of Parkinson's disease. *Parkinson's disease* 2015 381281-381281.
- West, R. J. H., Y. Lu, B. Marie, F.-B. Gao and S. T. Sweeney (2015b). Rab8, POSH, and TAK1 regulate synaptic growth in a Drosophila model of frontotemporal dementia. *Journal of Cell Biology* 208(7) 931-947.
- Wilson, G. R., J. C. Sim, C. McLean, M. Giannandrea, C. A. Galea, J. R. Riseley, S. E. Stephenson, E. Fitzpatrick, S. A. Haas, K. Pope, K. J. Hogan, R. G. Gregg, C. J. Bromhead, D. S. Wargowski, C. H. Lawrence, P. A. James, A. Churchyard, Y. Gao, D. G. Phelan, G. Gillies, N. Salce, L. Stanford, A. P. Marsh, M. L. Mignogna, S. J.

- Hayflick, R. J. Leventer, M. B. Delatycki, G. D. Mellick, V. M. Kalscheuer, P. D'Adamo, M. Bahlo, D. J. Amor and P. J. Lockhart (2014). Mutations in RAB39B cause X-linked intellectual disability and early-onset Parkinson disease with α -synuclein pathology. *Am J Hum Genet* 95(6) 729-735.
- Xiang, W., J. C. Schlachetzki, S. Helling, J. C. Bussmann, M. Berlinghof, T. E. Schäffer, K. Marcus, J. Winkler, J. Klucken and C. M. Becker (2013). Oxidative stress-induced posttranslational modifications of alpha-synuclein: specific modification of alpha-synuclein by 4-hydroxy-2-nonenal increases dopaminergic toxicity. *Mol Cell Neurosci* 54 71-83.
- Xiong, Y. and J. Yu (2018). Modeling Parkinson's Disease in Drosophila: What Have We Learned for Dominant Traits? *Frontiers in Neurology* 9(228).
- Yamashita, F., M. Hirayama, T. Nakamura, M. Takamori, N. Hori, K. Uchida, T. Hama and G. Sobue (2010). Pupillary autonomic dysfunction in multiple system atrophy and Parkinson's disease: an assessment by eye-drop tests. *Clin Auton Res* 20(3) 191-197.
- Yim, J. J., E. H. Grell and K. B. Jacobson (1977). Mechanism of Suppression in Drosophila: Control of Sepiapterin Synthase at the Purple Locus. *Science* 198(4322) 1168-1170.
- Yim, Y. I., T. Sun, L. G. Wu, A. Raimondi, P. De Camilli, E. Eisenberg and L. E. Greene (2010). Endocytosis and clathrin-uncoating defects at synapses of auxilin knockout mice. *Proc Natl Acad Sci U S A* 107(9) 4412-4417.
- Ysselstein, D., M. Nguyen, T. J. Young, A. Severino, M. Schwake, K. Merchant and D. Krainc (2019). LRRK2 kinase activity regulates lysosomal glucocerebrosidase in neurons derived from Parkinson's disease patients. *Nature Communications* 10(1) 5570-5570.
- Yue, M., K. M. Hinkle, P. Davies, E. Trushina, F. C. Fiesel, T. A. Christenson, A. S. Schroeder, L. Zhang, E. Bowles, B. Behrouz, S. J. Lincoln, J. E. Beevers, A. J. Milnerwood, A. Kurti, P. J. McLean, J. D. Fryer, W. Springer, D. W. Dickson, M. J. Farrer and H. L. Melrose (2015). Progressive dopaminergic alterations and mitochondrial abnormalities in LRRK2 G2019S knock-in mice. *Neurobiol Dis* 78 172-195.
- Zahoor, I., A. Shafi and E. Haq (2018). Pharmacological Treatment of Parkinson's Disease. In T. B. Stoker and J. C. Greenland eds. *Parkinson's Disease: Pathogenesis and Clinical Aspects*. Brisbane (AU).
- Zhang, Y., X. Zhang, Y. Yue and T. Tian (2021). Retinal Degeneration: A Window to Understand the Origin and Progression of Parkinson's Disease? *Front Neurosci* 15 799526.
- Zharikov, A. D., J. R. Cannon, V. Tapias, Q. Bai, M. P. Horowitz, V. Shah, A. El Ayadi, T. G. Hastings, J. T. Greenamyre and E. A. Burton (2015). shRNA targeting α -synuclein prevents neurodegeneration in a Parkinson's disease model. *J Clin Invest* 125(7) 2721-2735.
- Zhou, F. M., C. J. Wilson and J. A. Dani (2002). Cholinergic interneuron characteristics and nicotinic properties in the striatum. *J Neurobiol* 53(4) 590-605.
- Zimprich, A., S. Biskup, P. Leitner, P. Lichtner, M. Farrer, S. Lincoln, J. Kachergus, M. Hulihan, R. J. Uitti, D. B. Calne, A. J. Stoessl, R. F. Pfeiffer, N. Patenge, I. C. Carbajal, P. Vieregge, F. Asmus, B. Muller-Myhsok, D. W. Dickson, T. Meitinger, T. M. Strom, Z. K. Wszolek and T. Gasser (2004a). Mutations in LRRK2 cause autosomal-dominant parkinsonism with pleomorphic pathology. *Neuron* 44(4) 601-607.

Zimprich, A., B. Müller-Myhsok, M. Farrer, P. Leitner, M. Sharma, M. Hulihan, P. Lockhart, A. Strongosky, J. Kachergus, D. B. Calne, J. Stoessl, R. J. Uitti, R. F. Pfeiffer, C. Trenkwalder, N. Homann, E. Ott, K. Wenzel, F. Asmus, J. Hardy, Z. Wszolek and T. Gasser (2004b). The PARK8 locus in autosomal dominant parkinsonism: confirmation of linkage and further delineation of the disease-containing interval. *American journal of human genetics* 74(1) 11-19.